Development and characterization of cell models of tau aggregation

Annalisa Cavallini[1,2]

A thesis submitted in partial fulfilment of the requirements for the degree of Doctor of Philosophy from University College London

[1] Eli Lilly & Company Ltd., Erl Wood Manor, Sunninghill Road, Windlesham, Surrey, GU20 6PH, UK

[2] UCL Institute of Neurology, Queen Square, London, WC1N 3BG, UK

Declaration

I, Annalisa Cavallini, confirm that the work presented in this thesis is my own. Where information has been derived from other sources, I confirm that this has been indicated in the thesis.

ABSTRACT

Abnormal folding and hyperphosporylation of tau protein leads to the generation of paired helical filaments (PHFs) and neurofibrillary tangles (NFTs), a key neuropathological hallmark of Alzheimer's disease and other tauopathies. Cellular models able to recapitulate tau pathology are useful for understanding disease mechanisms and screening and profiling compounds that interfere with tau aggregation. We have established a HEK T-REx cell culture model where the inducible expression of mutant tau, accompanied by the introduction of aggregated mutant tau extracted from transgenic mouse brain, leads to endogenous tau aggregation and filament assembly, suggesting a seeding process as a likely mechanism underlying NFT formation. We found that substantial aggregation of soluble tau into Triton X-100-insoluble tau can be induced by spontaneous uptake of mutant tau aggregates, which are internalised through an endocytic mechanism that is temperature-, time- and ATP-dependent, can be potentiated by transfection reagents and impaired by pharmacological agents inhibiting macropinocytosis, suggesting a potential mechanism for the propagation of tau pathology in tauopathy brains. We also found that seed-competent tau species are sarkosly-insoluble, tagged by AT8 and MC1 antibodies, and are present in conditioned media from seeded cells. Finally, we established a more physiologically relevant model of seeded tau aggregation in rodent neurons. In summary, our study establishes cell-based tauopathy models that not only provide mechanistic insights into the pathogenesis of tau aggregation, but also offer a robust system for identifying therapeutic strategies to prevent propagation and spreading of tau pathology.

Publications arising from this thesis

Cavallini, A., Jackson, S., Sanchez, J.M., Murray, T., Falcon, B., Isaacs, A., Goedert, M., O'Neill, M., Hutton, M. & Bose, S. 2014., "Characterisation of a co-culture cell-based model of Tau aggregation and propagation.", *Alzheimer's and Dementia,* vol. 10, pp. P646.

Ahmed, Z., Cooper, J., Murray, T.K., Garn, K., McNaughton, E., Clarke, H., Parhizkar, S., Ward, M.A., Cavallini, A., Jackson, S., Bose, S., Clavaguera, F., Tolnay, M., Lavenir, I., Goedert, M., Hutton, M.L. & O'Neill, M.J. 2014, "A novel in vivo model of tau propagation with rapid and progressive neurofibrillary tangle pathology: The pattern of spread is determined by connectivity, not proximity.", *Acta Neuropathologica,* vol. 127, no. 5, pp. 667-683.

Falcon, B., Cavallini, A., Angers, R., Glover, S., Murray, T.K., Barnham, L., Jackson, S., O'Neill M.J., Isaacs, A.M., Hutton, M.L., Szekeres, P.G., Goedert, M. & Bose, S. 2015, "Conformation determines the seeding potencies of native and recombinant tau aggregates.", *Journal of Biological Chemistry,* vol. 290, no. 2, pp. 1049-1065.

Jackson, S.J., Kerridge, C., Cooper, J., Cavallini, A., Falcon, B., Cella, C.V., Landi, A., Szekeres, P.G., Murray, T.K., Ahmed, Z., Goedert, M, Hutton, M., O'Neill, M.J., & Bose, S. 2016 "Short Fibrils Constitute the Major Species of Seed-Competent Tau in the Brains of Mice Transgenic for Human P301S Tau", The Journal of Neuroscience, vol. 36, no.2, pp. 762–772

Table of contents

List of figures

List of tables

List of abbreviations

Abbreviation:	Explanation:
AAV	Adeno-associated virus
Aβ	Amyloid-beta
AD	Alzheimer’s disease
AGD	Argyrophilic grain disease
APP	Amyloid precursor protein
AS	Alphascreen
BSA	Bovine serum albumin
BiFC	Bimolecular fluorescence complementation
CamKII	Ca2+/calmodulin kinase II
CBD	Corticobasal degeneration
CFP	Cyan fluorescent protein
CNS	Central nervous system
DIV	Days in vitro
DMEM	Dulbecco's Modified Eagle's Medium
DMSO	Dimethyl sulfoxide
DPBS	Dulbecco's phosphate-buffered saline
DTT	Dithiothreitol
EDTA	Ethylenediaminetetraacetic acid
EEA1	Early endosome antigen 1
EGTA	Ethylene glycol-bis(β-aminoethyl ether)-N,N,N',N'-tetraacetic acid
EIPA	5-(N-Ethyl-N-isopropyl) amiloride
FRET	Fluorescence resonance energy transfer
FTD	Frontotemporal dementia
FTDP-17	Frontotemporal dementia with parkinsonism linked to chromosome 17
GFAP	Glial fibrillary acidic protein
GFP	Green fluorescent protein
HBSS	Hank's balanced salt solution
HCI	High-content imaging
IF	Immunofluorescence
IHC	Immunohistochemistry
iPSC	Induced pluripotent stem cell
IVIG	Intravenous immunoglobulin
LAMP1	Lysosomal-associated membrane protein 1
LDH	Lactate dehydrogenase
m2′3′-3CNP	Mouse 2′,3′-cyclic nucleotide 3′-phosphodiesterase
MAPT	Microtubule associated protein tau
MoPrP	Mouse prion protein promoter
MT	Microtubule
MVB	Multivesicular body

ND	Not determined
NFTs	Neurofibrillary tangles
NPs	Neuropil threads
PAGE	Polyacrylamide gel electrophoresis
PART	Primary age-related tauopathy
PFA	Paraformaldehyde
PHFs	Paired helical filaments
PiD	Pick’s disease
PMSF	Phenylmethylsulphonyl fluoride
PSD95	Postsynaptic density protein 95
PSP	Progressive supranuclear palsy
RCNs	Rat cortical neurons
RD	Repeat domain
RT	Room temperature
SDS	sodium dodecyl sulphate
SFs	Straight filaments
SI	Sarkosyl-insoluble
SOD1	Superoxide dismutase 1
TBS	Tris buffer saline
TD	Tangle-only dementia
ThioS	Thioflavin S
ThioT	Thioflavin T
TL	Total lysate
TNTs	Tunneling nanotubes
TRIM21	Tripartite motif protein 21
tTA	Tetracycline-dependent transactivator system
WB	Western blot
WT	Wild type
YFP	Yellow fluorescent protein

1. INTRODUCTION

1.1 Tau

Tau is a microtubule (MT)-binding protein predominantly expressed in neurons, that stabilizes and promotes the assembly of MTs (Witman et al. 1976, Drechsel et al. 1992), and whose interactions with MTs are negatively regulated by phosphorylation (Biernat et al. 1993, Bramblett et al. 1993). Tau is encoded by the MAPT gene on chromosome 17q21 (Lewis et al. 2001, Neve et al. 1986), and in humans, alternative splicing of the mRNA at exons 2, 3, and 10 results in 6 tau isoforms (Figure 1.1). These isoforms differ by the presence or absence of none (0N), one (1N) or two (2N) 29 aminoacid N-terminal acidic inserts –projection domain- and three (3R) or four (4R) repeat domains (RD) at the C-terminal tubulin-binding motif, separated by a central proline-rich region. 4R tau has higher affinity for microtubules than 3R tau, and consequently higher efficiency at promoting microtubule assembly, but also higher propensity for self-aggregation (Goedert, Jakes 1990, Greenberg, Davies 1990, Greenberg et al. 1992, Gustke et al. 1994). The various isoforms are differentially expressed during development, nevertheless, the 3R and 4R tau isoforms are expressed in a one-to-one ratio in most regions of the adult brain, and deviations from this ratio are characteristic of neurodegenerative tauopathies (Hong et al. 1998); the 2N isoform is underrepresented compared to the 0N and 1N isoforms (~9%, 37%, 54% of total tau, respectively) (Goedert, Jakes 1990). The expression and splicing pattern of tau in the human brain also present regional variation, with protein levels two times higher in the neocortex than in white matter and cerebellum, and these variations may explain the differential vulnerability of brain regions to tau pathology (Trabzuni et al. 2012). A “big Tau” isoform with 695 aminoacids is expressed predominantly in the peripheral nervous system, likely due to larger diameter of axons, and it is equivalent to 2N4R plus 242 residues from exon 4a (Couchie et al. 1992, Goedert, Spillantini & Crowther 1992). Tau is a naturally unfolded soluble protein, lacking significant amounts of secondary structure under normal conditions, with a preference for adopting a paperclip-like shape in which the N-terminal, C-terminal and repeat domains are in close proximity (Jeganathan et al. 2006), which may protect tau from aggregation, as events that prevent formation of the hairpin structure, i.e. truncation, can facilitate tau aggregation (Wang et al. 2007). Tau conformation changes from random coil to highly ordered β-pleated sheet structures as it assembles into insoluble, hyperphosphorylated paired helical filaments (PHFs) as well as less frequent straight filaments (SFs) that constitute neurofibrillary tangles (NFTs) in AD and related tauopathies (Kidd 1963, Berriman et al. 2003). In PHFs, the repeat domains constitute the beta-sheet core, whereas the short C-terminal and the long N-terminal domain form a “fuzzy coat” which supposedly stabilises the PHFs. Tau is the most commonly associated misfolded protein in human neurodegenerative diseases, based on the predominance of disorders involving tau neuropathology.

Clone	Inserts/repeats	Number of aminoacids	MW (KDa)
htau40	2N4R	441	45.9
htau39	2N3R	410	42.6
htau34	1N4R	412	43.0
htau37	1N3R	381	39.7
htau24	0N4R	383	40.0
htau23	0N3R	352	36.7
big tau	2N4R + exon 4a	695	72.7

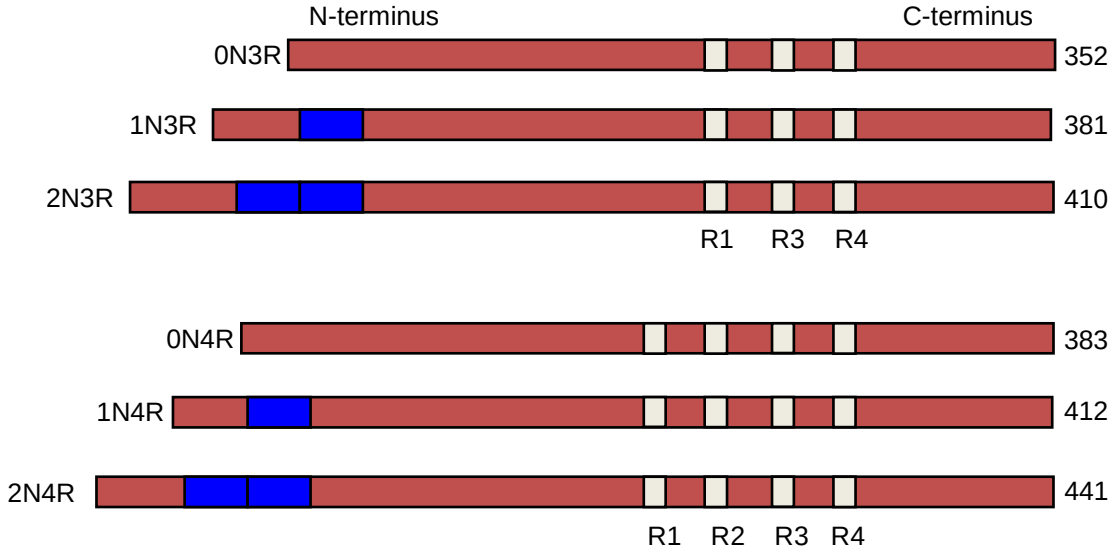

Figure 1.1: Domain structure of the tau isoforms expressed in the adult human brain. Tau isoforms differ in the number of tubulin-binding domains (three or four C-terminus repeats, R1-R4, grey); the presence or absence of none, one or two 29-amino acid long acidic inserts (N-terminus, blue) and a proline rich region in between these two. Adapted from (Ballatore, Lee & Trojanowski 2007).

1.2 Tauopathies

1.2.1 Classification of tauopathies

Tauopathies are characterized by intracellular aggregation of abnormally phosphorylated tau (Kosik, Joachim & Selkoe 1986, Pollock, Mirra & Binder 1986, Goedert et al. 1988, Lee et al. 1991). They include Alzheimer's disease (AD), argyrophilic grain disease (AGD), progressive supranuclear palsy (PSP), corticobasal degeneration (CBD), Pick's disease (PiD), primary age-related tauopathy (PART), formerly known as tangle-only dementia (TD), and frontotemporal dementia and parkinsonism linked to chromosome 17 (FTDP-17*T*), the latter being caused by mutations in MAPT (Hutton et al. 1998, Spillantini et al. 1998, Rizzu et al. 1999, Goedert, Jakes 2005). The causal link between tau abnormality and neuronal dysfunction is underscored by the significant correlation between total NFT burden and cognitive decline observed in AD patients (Wilcock, Esiri 1982, Arriagada, Marzloff & Hyman 1992) and also by the existence of an increasing number of dominantly inherited mutations in the *MAPT* gene in frontotemporal dementia with parkinsonism linked to chromosome 17 (FTDP-17) (Hutton et al. 1998, Spillantini et al. 1998, Rizzu et al. 1999, Goedert, Jakes 2005). For a full up-to-date database, see http://www.molgen.vib-ua.be/FTDMutations/. Tauopathies share a common molecular

mechanism and have lesions in common, such as gross brain atrophy, nerve cell loss, gliosis, superficial spongiosis and ballooned neurons, but the tau isoforms involved, the morphology of the inclusions, the cell type involved, the cellular tau pathology, the selective vulnerability of anatomic systems and the clinical presentations significantly vary across disease types (Clavaguera et al. 2013, Murray et al. 2014) (Table 1).

Table 1: Neurodegenerative diseases with tau inclusions. Adapted from (Murray et al. 2014).

Pathologic diagnosis	**Histologic tau findings**
Alzheimer's disease	NFTs found in neocortex and limbic regions. Intracellular NFTs are found to be both 3R and 4R tau-positive with a preferential shift to 3R immunoreactivity in extracellular NFTs.
Amyotrophic lateral sclerosis of Guam	NFTs positive for 3R and 4R found in neocortex and limbic areas with a predilection for cortical layer II.
Argyrophilic grain disease	Spindle-shaped, 4R tau-positive lesions accumulate in neuronal processes. Grains are typically found in the neuropil of limbic areas, but can be found diffusely deposited in cortex. Coiled bodies in oligodendrocytes and tau-positive pretangles can be abundantly found.
Chronic traumatic encephalopathy	Widespread NFTs, tau-immunoreactive astrocytic inclusions, and neuritic pathology can be found with a predilection for superficial cortical layers and sulcal depths. Irregular, patchy tau pathology observed in cortex.
Corticobasal degeneration	4R tau-positive ballooned neurons, astrocytic plaques, and neuropil threads are found in both gray and white matter of cortical and striatal regions. Diffuse neurofibrillary tangles with calcification NFTs and neuropil threads found diffusely deposited in frontal and temporal cortex, as well as limbic areas.
Down's syndrome	NFTs and granulovaculoar degeneration can be found in the hippocampus.
Familial British dementia	NFTs and neuropil threads found relatively restricted to limbic regions.
Familial Danish dementia	NFTs and neuropil threads found in limbic with abnormal neurites limited to amyloid-laden blood vessels and variable involvement of cortical regions.
Frontotemporal dementia and parkinsonism linked to chromosome 17 (caused by MAPT mutations)	Widespread neuronal and glial cytoplasmic inclusions immunopositive for 3R, 3+4R, or 4R tau. Morphology of lesions varies with reportedly observed coiled bodies, tufted astrocytes, and astrocytic plaques.

Frontotemporal lobar degeneration (some cases caused by C9ORF72 mutations)	NFT pathology can be found in a similar Alzheimer's-like limbic and cortical distribution.
Gerstmann–Sträussler–Scheinker disease	Tau pathology can be absent, not reported, or inconsistently reported as widespread neurofibrillary pathology depending on the PRNP mutation.
Guadeloupean parkinsonism	Widespread neurofibrillary pathology can be found as NFTs, neuropil threads, and astrocytic tufts. Myotonic dystrophy NFTs in limbic and brainstem regions.
Neurodegeneration with brain iron accumulation	Diffuse neuritic pathology in cortex, but rare NFT pathology.
Niemann–Pick disease, type C	NFTs, neuropil threads, and oligodendroglial coiled bodies range from transentorhinal confinement to widespread limbic and cortical involvement.
Non-Guamanian motor neuron disease with neurofibrillary tangles	NFTs can be found in limbic structures, midbrain, and pontine nuclei.
Parkinsonism–dementia complex of Guam	NFTs positive for 3R and 4R found in cortical areas with a predilection for cortical layers II and III. Tau pathology is also found in limbic, basal ganglia, brainstem, and spinal cord. Granular hazy tau inclusions are found in motor cortex, amygdala, and inferior olivary nucleus.
Pick's disease	Widespread spherical cytoplasmic 3R tau-positive inclusions (Pick bodies) can be found in hippocampus, basal ganglia, brainstem nuclei, and especially cortex.
Postencephalitic parkinsonism	Widespread tau-positive neuronal and glial lesions. Globose NFTs are a prominent feature in brainstem nuclei, especially substantia nigra and locus coeruleus. NFTs are more common in limbic structures than cortex, and have a predilection for layers II and III.
Progressive supranuclear palsy	4R tau-positive globose NFTs, tufted astrocytes, and coiled bodies are often found in the subthalamic nucleus, globus pallidus, ventral thalamus, cerebellar dentate nucleus, and variable involvement of cortex.
SLC9A6-related mental retardation	Glial tau pathology, resembling coiled bodies, can be found in brainstem and cerebellar white matter tracts. Astrocytic plaques can also be found in brainstem, thalamus, and cerebral white matter. NFT-like inclusions can be found in brainstem and thalamic nuclei, hippocampus, and cortex.
Subacute sclerosing	Glial fibrillary tangles can be found in oligodendroglia. NFTs

panencephalitis	can be found differentially distributed in hippocampus and/or cerebral cortex.
Tangle predominant dementia	4R predominant NFT accumulation relatively combined to limbic regions.
White matter tauopathy with globular glial inclusions	Widespread globular oliogdendroglial inclusions, less so in astroglial, immunoreactive for 4R-tau

Thus, the neuronal inclusions found in AD and TD are composed of both 3R and 4R tau isoforms (Goedert et al. 1992, Noda et al. 2006), whereas in PiD tau, isoforms with 3 repeats predominate in the neuronal deposits (Delacourte et al. 1996), and PSP, CBD and AGD (Flament et al. 1991, Ksiezak-Reding et al. 1994, Togo et al. 2002, Tolnay et al. 2002) are characterised by assembly of 4-repeat tau into filaments. PSP and CBD are 4-repeat tauopathies, but their tau cleavage products vary in size. Detergent-insoluble cleaved tau from PSP migrates as a single band of 33 kDa, whereas that of CBD migrates as a doublet of 37 kDa (Arai et al. 2004). FTDP-17T inclusions are composed predominantly of 3 repeats, 4 repeats or a mixture of all 6 brain tau isoforms, depending on the underlying *MAPT* mutations (Ghetti et al. 2011). The distinct migration of the full length tau species aids the classification of tauopathies: in AD, the 6 brain tau isoforms are detected by immunoblotting as a major tau triplet (tau 60, 64 and 69); in CBD and PSP, mainly 4R tau isoforms form aggregates, and they appear as a major tau doublet (tau 64 and 69); in PiD the doublet tau 60 and 64 represents filamentous tau deposits predominantly made of 3R isoforms (Tolnay et al. 2002). As regards to the morphology of the filaments, in AD and TD tau inclusions occur in the form of neurofibrillary tangles (NFTs) located in the somatodendritic compartment, and neuropil threads (NTs) found in distal axons and dendrites. In AGD, argyrophilic grains in neuronal processes, pre-tangle neurons in limbic areas and glial tau inclusions in astrocytes and oligodendrocytes make up the hallmark lesions (Botez et al. 1999, Tolnay, Clavaguera 2004). Neuropathologically, PSP brains present neuronal tau inclusions known as globose-type NFTs and NTs (Probst et al. 1988), as well as by glial changes in the form of tufted astrocytes and oligodendroglial coiled bodies (Nishimura et al. 1992, Yamada, McGeer & McGeer 1992). In CBD brains, intracytoplasmic pathological tau in NTs, pre-tangle neurons or small NFTs, as well as astrocytic plaques and coiled bodies are found (Feany et al. 1995, Komori et al. 1998, Tolnay, Probst 2002). In PiD, Pick bodies are mainly present in neocortical, hippocampal and subcortical nerve cells (Probst et al. 1996). FTDP-17T brains are characterised by severe nerve cell loss, astrocytic gliosis and spongiosis, with filamentous tau inclusions in nerve cells and/or glial cells. A recent breakthrough in understanding the conformation of amyloid fibrils in AD came from cryo-EM studies by Fitzpatrick et al., who produced an atomic model of PHFs and SFs from the brain of an individual with AD. While the core of both PHFs and SFs consists of two identical C-shaped protofilaments comprising tau R3 and R4 domains (residues 306–378), the inter-protofilament packing is different between the 2 types of filaments; the rest of the protein forms a “fuzzy coat” around the 3R-4R core; the model included a putative binding site for the PET tracer AV1451/flortaucipir; this is the first molecular-level structure of tau fibrils from AD brain, and this

technique could be applied to unveil the structure of other disease-related amyloid fibrils and help inform structure-based drug design (Fitzpatrick et al. 2017).

1.2.2 Pathological tau aggregation

The process by which MT-bound tau is converted to large aggregate structures such as NFTs is suggested to be a multi-step path, which begins with the detachment of tau from the MTs (Ballatore, Lee & Trojanowski 2007). The exact mechanism by which this first step occurs remains unknown, however, it is thought that phosphorylation and dephosphorylation patterns, tau gene mutations and covalent post-translational modifications of tau amongst others trigger the disengagement of tau. Under physiological conditions, tau phosphorylation patterns are under tight regulation by kinases and phosphatases, so that tau is phosphorylated at multiple serine and threonine residues when bound to MTs (Avila et al. 2006). The microtubule binding domains of tau contain a number of lysine residues, whose positive charges drive binding to negatively charged microtubules (Kolarova et al. 2012). Increased phosphorylation on serine and threonine sites on tau disrupts the charge balance and results in reduced tau binding to MTs and/or greater propensity for tau to assemble into fibrils (Del et al. 1996, Wagner et al. 1996, Merrick, Trojanowski & Lee 1997). After dissociation from MTs, higher concentrations of free intracellular tau increase the likelihood of pathogenic conformational changes to occur, ultimately resulting in aggregation and fibrillization of tau. Further fibrillization is facilitated by proteolytic cleavages (Binder et al. 2005, Gamblin et al. 2003, Fasulo et al. 2000), as truncated tau assembles much faster than its native form, probably owing to disruption of the paperclip structure. Small non fibrillar tau deposits (pre-tangles) grow into paired helical filaments (PHF), characterised by β-sheet structure, hyperphosphorylation and cleavage. Finally, PHFs further self-assemble into NFTs (Ballatore, Lee & Trojanowski 2007) (Figure 1.2).

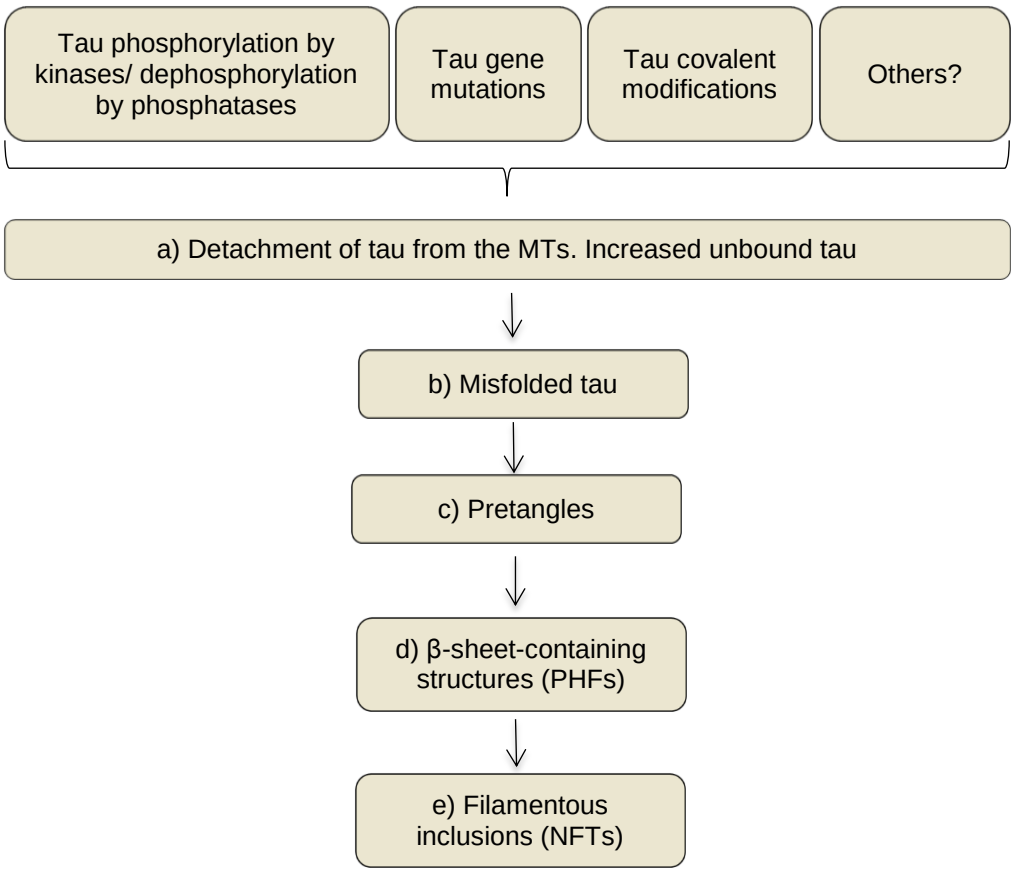

Figure 1.2: Schematic representation of the stages of pathological tau aggregation
Adapted from (Ballatore, Lee & Trojanowski 2007).

a) Tau-mediated neurodegeneration is likely to be initiated by disengagement of tau from the MTs, which results in increase of cytosolic tau. Possible causes of detachment of tau from the MTs include an imbalance of tau kinases and/or phosphatases, mutations of the MAPT gene, covalent modification of tau causing and/or promoting misfolding and other post-translational modifications.
b) Tau misfolding is thought to be a stochastic phenomenon that is more likely to occur at higher cytosolic tau concentrations, once tau is unbound from MTs.
c) Initial deposition of tau forms 'pretangles', which are not stained by β-sheet-specific dyes like Congo red or thioflavin-T (ThioT), indicating that these early deposits have not yet acquired the pleated β-sheet structure typically found in amyloid aggregates.
d) Pretangles transition into more structurally-organized aggregates (PHFs) which then bundle into NFTs (e).

Whatever the pathological conditions that lead to detachment of tau from microtubules, the resulting events are toxic: loss of function, gain of function and mislocalisation have been identified as the main mechanisms of tau-mediated neurodegeneration.

Mutations in either exonic or intronic regions of human *MAPT* might cause a loss of function or a toxic gain of function and thereby lead to neurodegeneration (Figure 1.3). Missense mutations alter the sequence of tau, but may also change the alternative splicing; splicing mutations don't

alter the protein sequence but change the relative ratio of different tau isoforms. Most missense mutations are within or near the microtubule-binding domain (G272V, N279K, ΔK280, P301L, V337M, R406W) and will lead to reduced affinity for microtubules and an increased tendency for aggregation (Hong et al. 1998, Barghorn et al. 2000). Mutations away from the microtubule-binding domain like A152T, R5H may still cause loss of tau function (Magnani et al. 2007, Coppola et al. 2012). The FTD/PSP-associated tau mutation A152T still decreases the binding of tau to microtubules, causing microtubule disassembly (Coppola et al. 2012), and promotes oligomers formation. This mutation is a risk modifier to several neurodegenerative conditions including AD, and does not appear to cause autosomal-dominand disease, unlike the majority of pathogenic mutations in MAPT (Lee et al. 2013). R5H or R5L are located at the N-terminus, but the mechanistic effects of these mutations are poorly understood; it is possible they disrupt the binding of tau to the p150 subunit of the dynactin complex — an essential cofactor for the microtubule motor dynein, thus interfering with general axonal transport (Magnani et al. 2007). Most splicing mutations are within or near intron 10; they usually increase the inclusion of exon 10 (repeat R2) and consequently the ratio of 4R/3R tau. Other mutations (ΔK280, L266V and G272V) inhibit the inclusion of E10 and thus reduce the 4R/3R ratio. The change in the 3R/4R tau ratio triggers tau aggregation as the different isoforms may bind to distinct sites on the microtubules, and have different microtubule-stabilizing capacities (Goode et al. 1997, Goode, Feinstein 1994).

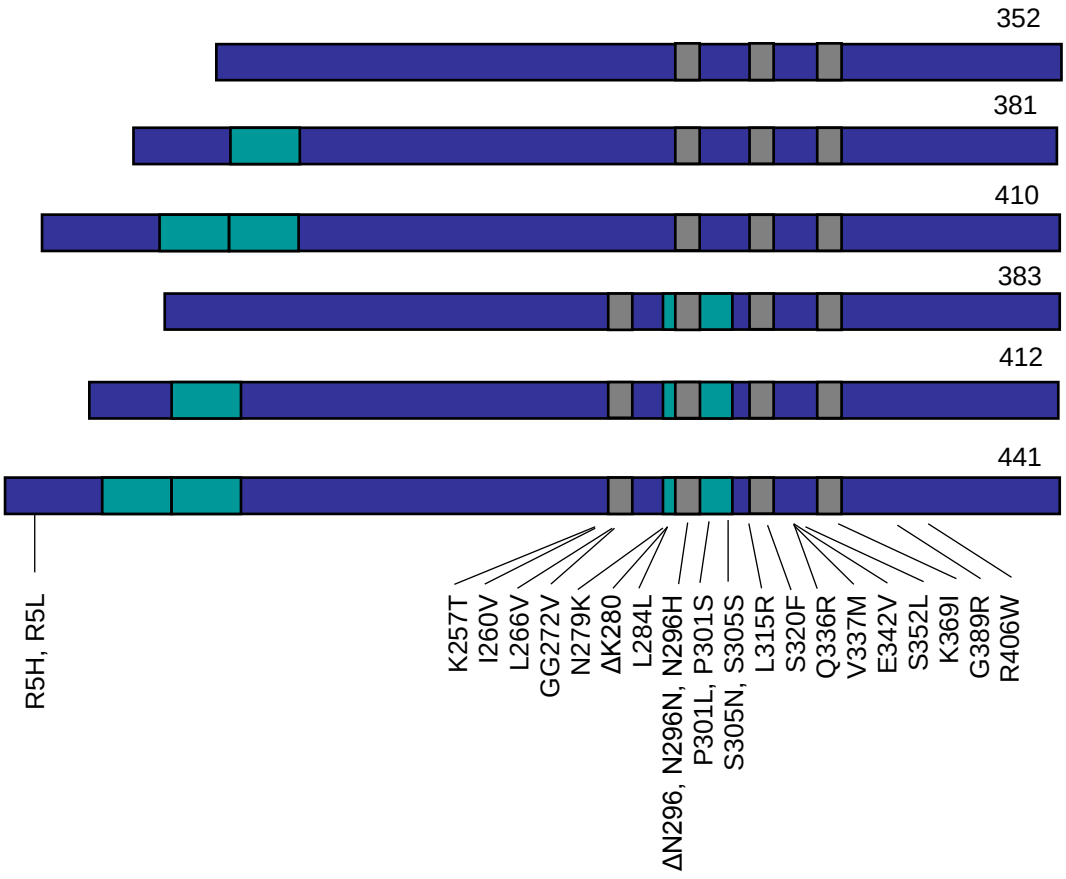

Figure 1.3: Mutations in the tau gene in FTD and FTDP-17. Adapted from (Goedert 2005)**.** Schematic diagram of the 6 tau isoforms (352–441 amino acids) that are expressed in adult human brain, with mutations in the coding region indicated using the numbering of the 441

amino acid isoform. Twenty missense mutations, two deletion mutations, and three silent mutations are shown.

Neurotoxicity from loss of tau function. Loss of normal function of tau induces structural and functional impairments of microtubules in axons, leading to an axonal transport deficit. Animal models suggest that tau function can only be partly compensated by other, redundant microtubule-associated proteins. Aged (~12-month-old) tau KO mice show behavioural impairments and structural abnormalities, suggesting that tau is necessary for normal neuronal and brain function (Lei et al. 2014) and long-term suppression of tau as a therapy for tauopathies might present complications. Loss of tau function is usually attributed to aggregation and post-translational modifications that may affect tau aggregation.

Aggregation decreases levels of soluble unbound tau, which may result in microtubule disassembly. The two short hexapeptide motifs VQIINK (PHF6, residues 306-311) and VQIVYK (PHF6*, residues 275-280) display propensity for forming β-sheet structures and are required for tau aggregation (von Bergen et al. 2000). PHF6 is located at the beginning of the third microtubule binding repeat and therefore is present in all tau isoforms, whereas PHF6* is located at the beginning of the second microtubule binding repeat and therefore is only present in 4R tau isoforms. Abnormal self-assembly of tau will start with dimerization via interactions PHF6- PHF6, PHF6*-PHF6*, or PHF6-PHF6* motif (Peterson et al. 2008); recruitment of tau monomer will produce a nucleation “seed” which will then elongate in a dose- and time-dependent manner into oligomers, and ultimately into tau filaments (Barghorn, Mandelkow 2002). Disruption of these PHF6 and PHF6* motifs (for example, by amino acid substitutions, such as proline residues mutations) render tau incompetent for assembly; by contrast, strengthening the β-structure (for instance, by ΔK280 or P301L mutations) promotes tau aggregation both *in vitro* and *in vivo* (Khlistunova et al. 2006).

Phosphorylation has been assumed to drive tau aggregation because it is observed on aggregated tau in patients with a tauopathy or in transgenic mice, but there is now evidence that tau phosphorylation alone is not sufficient for its aggregation. Some forms of phospho-tau promote aggregation in the brain, and abnormally hyperphosphorylated tau isolated from human AD brains can self-assemble into PHFs *in vitro* (Alonso et al. 2001), but other forms of phospho-tau (for example, in the repeat domain) protects against aggregation (Schneider et al. 1999). Tau aggregation can be induced *in vitro* efficiently by polyanionic cofactors, regardless of phosphorylation (Kampers et al. 1997, Goedert et al. 1996), but it is possible that phosphorylation accelerates aggregation indirectly; for example, hyperphosphorylation of tau at the repeat domain may reduce its ability to bind microtubules, causing microtubule disassembly, leading to axonal transport deficits (Ballatore, Lee & Trojanowski 2007, Wang, Mandelkow 2012). Intact microtubules, functional motor proteins, correct cargo attachment to motors, and sufficient ATP from mitochondria are all necessary for axonal transport; as well as regulating microtubule dynamics, tau affects the activity of motor proteins dynein and kinesin; in particular, tau reduces dynein and kinesin mobility and binding frequency to microtubules, slowing both

anterograde and retrograde axonal transport of cargo (Seitz et al. 2002), ultimately affecting the axonal transport of proteins and organelles, including transport of cargo to synapses, leading to synapse degeneration; moreover, when untransported organelles such as mitochondria accumulate in the neuronal soma, energy deprivation and oxidative stress can occur, contributing to the progression of pathology and neuronal loss in tauopathies (Guo, Noble & Hanger 2017). Also, axonal and cell body accumulations of organelles and other proteins results in axonal swellings and spheroids observed in neurodegenerative diseases (Millecamps, Julien 2013).

Truncation may produce tau fragments containing the repeat domain which has a higher tendency to aggregate, probably owing to misfolding and disruption of the soluble paperclip structure, leading to loss of function. In human AD brains and in the Tg4510 tauopathy mouse model, full-length tau is cleaved by caspase 3 at Asp421 to generate tau1–421, which is prone to aggregation and colocalises with NFTs, indicating that the generation of this tau fragment may be an early event in tangle formation (De Calignon et al. 2010). Tau truncation at Asn368 by asparagine endopeptidase has been observed in human AD brains and in a P301S mouse model of tauopathy; such truncation abolishes the microtubule assembly function of tau and induces its aggregation (Wang et al. 2007, Zhang et al. 2014, Fatouros et al. 2012).

In addition, as tau is involved in multiple novel functions beyond its most well established role of stabilising microtubules, including maintaining structural integrity, axonal transport, signalling within and between neurons, iron transport, neurogenesis, long-term depression (LTD) and neuronal DNA protection (Sultan et al. 2011, Lei et al. 2012, Kimura et al. 2014), its loss of function may also impair these processes and lead to neurodegeneration.

Neurotoxicity from gain of function. Gain of function of tau in the form of aggregation leads to compromised neuronal function, and possible release into the extracellular space and interaction with cell receptors and spreading. As the regional distribution of NFTs in the AD brain correlates with the severity of cognitive deficits, NFTs have long been considered the toxic tau species, leading to neurodegeneration. However, growing evidence has challenged this view, by showing that NFT formation is neither necessary nor sufficient for neurodegeneration (Cowan, Mudher 2013). PHFs or NFTs may actually represent a protective response, through which cells scavenge the toxic monomeric or oligomeric tau species and thus protect neurons from acute assaults (Alonso et al. 2006). In several transgenic mouse models, neuron loss is not correlated with tangle formation, but rather most neurons die without forming NFTs, and tangle-bearing neurons appear to survive without functional impairments (Andorfer et al. 2005, Spires-Jones et al. 2008). In AD brains, tangle-bearing neurons survive for ~20 years (Morsch, Simon & Coleman 1999), and neuron loss in the superior temporal sulcus region exceeds the number of NFTs more than 7-fold, implying that the majority of neurons have died without developing NFTs (Gomez-Isla et al. 1997). Similarly, chimeric mice produced by injecting human neuronal precursor cells into newborn APPPS1 mice showed selective death of human cells over mouse cells, in absence of tau tangles, contributing to the idea that tangles

themselves are not the toxic form of tau. Both mouse and human neurons accumulated hyperphosphorylated tau, but only the human cells contained misfolded, MC1-positive tau, deemed to be one of the earliest alterations of tau in AD (Espuny-Camacho et al. 2017). Instead of being directly toxic, these large tau aggregates may still indirectly cause toxicity by sequestering and depleting other functionally significant proteins and cell components, by affecting the localization of subcellular organelles and cytoplasm organization, and by physically interfering with axonal transport, leading to compromised neuronal function and neurodegeneration. Several studies have suggested soluble tau oligomers, rather than NFTs, to be the toxic species; levels of SDS-stable tau oligomers are increased in AD and PSP brains (Lasagna-Reeves et al. 2012, Maeda et al. 2007). However, the role of tau oligomers in tauopathies is controversial due to their poor characterisation: standardisation of oligomer preparation and assay methods among different groups will be required to pinpoint the toxic tau species; another issue is whether the variety of tau species with differing morphology, solubility, and disease-relevant properties present in vivo can actually be generated in vitro.

Neurotoxicity from mislocalization. In normal neurons, only small amounts of tau localize in the dendritic compartment. In AD and other tauopathies, hyperphosphorylation, mutations and overexpression of tau can cause mislocalization of tau into presynaptic terminals, dendrites and postsynaptic spines, resulting in synaptic dysfunction and destabilisation of microtubules, an effect that can be rescued by microtubule-stabilising drugs (Hoover et al. 2010, Thies, Mandelkow 2007, Tai et al. 2014) as well as abnormal translocation of other proteins and enzymes. In fly and rat neurons, mutated tau reduces synaptic transmission by binding to synaptic vesicles via its N-terminal domain and interfering with presynaptic functions, including synaptic vesicle mobility and release rate (Zhou et al. 2017). Missorted dendritic tau mediates Aβ-induced neurotoxicity through various mechanisms. In cultured neurons, dendritic tau promotes translocation of tubulin tyrosine ligase-like enzyme 6 (TTLL6) into dendrites, where it polyglutamylates the microtubules increasing their susceptibility to severing by spastin, and leading to microtubule depolymerisation (Zempel et al. 2013). In addition, dendritic tau can act as scaffolding protein to deliver the kinase FYN to postsynaptic sites, where FYN phosphorylates subunit 2 of the NMDA receptor (NR2B), resulting in the stabilization of the interaction of this receptor with postsynaptic density protein 95 (PSD95), potentiating glutamatergic signalling and rendering neurons susceptible to excitotoxicity mediated by Aβ (Roberson et al. 2007, Ittner et al. 2010).

Whether disease-associated changes in tau are pathogenic because they induce a loss of its normal function, a novel toxic gain of function, or a combination of both is subject to debate. Neurodegeneration from toxic gain of function may have been the prevailing hypothesis, but as new results unveil yet-unexplored physiological roles of tau, apart from the well-established functions of microtubule stabilization and axonal transport, there is now strong evidence for both gain and loss of function effects; both mechanisms may contribute to neurodegeneration to different extents, and play separate, though complementary, roles in driving the damage which ultimately leads to onset and progression of tauopathies. It will be critical to develop effective

tau therapeutic strategies directed at overcoming tau loss of function and/or minimizing gain-of-function caused by toxic multimeric tau species, depending on which mechanism prevails in each tauopathy. For instance, microtubule-stabilising would be a promising approach in diseases where a tau mutation causes loss of function but not in phenotypes characterised by a novel, microtubule-independent, gain of function, as they don't address the accumulation of toxic tau aggregates. Conversely, tauopathies mainly caused by tau gain of functions could be ameliorated by therapeutic strategies reducing tau (i.e. by increasing its proteolysis and clearance), whereas such strategies could be deleterious in cases of loss-of function mechanisms of tau toxicity, as the sequestration of soluble tau would be exacerbated by the treatment; also, a study in transgenic mice with inducible tau expression showed that after suppression of transgenic tau expression, memory function recovered and neuronal loss ceased, but NFTs continued to accumulate (Santacruz et al. 2005). Therapeutic strategies reducing tau would have to be prolonged enough to thoroughly clear any residual seed-competent tau species from human brains, but this long-term reduction of tau levels may pose safety concerns (Guo et al. 2016).

1.2.3 Spreading of tau pathology

A temporospatial spreading of tau-positive neurofibrillary lesions is observed during the clinical course of AD and AGD, suggesting that once tau pathology is initiated it propagates between neighbouring neuronal cells, possibly spreading along the axonal network. Braak and Braak were the first to propose a 6-tiered system of disease staging based on silver-stained, hyperphosphorylated tau aggregates, currently used to stage tau pathology in AD (Braak, Braak 1991, Braak H et al. 2006, Braak, Del Tredici 2011b) (Figure 1.4). Braak stages I-II correspond to the appearance of NFTs in the transentorhinal and entorhinal cortex and are not associated with clinical dementia. Braak stages III-IV are characterised by more pronounced involvement of these two regions and formation of NFTs in the hippocampus, the fusiform gyrus and temporal cortex; these stages may see the appearance of first clinical symptoms, based on the degree of neuronal damage. Patients at Braak stages V-VI meet the neuropathological criteria for the diagnosis of AD, and present abundant spreading of NFTs to isocortical association areas, accompanied by severe dementia. In human brain, tau inclusions appear at a younger age than beta-amyloid (Aβ) plaques ((Clavaguera et al. 2013, Braak, Braak 1991, Braak, Del Tredici 2011a), and sparse tau pathology has been described in the brains of a substantial proportion of individuals under the age of 30. Braak and Del Tredici reported silver-negative but AT8-positive neuronal tau inclusions (first in proximal axons, and thereafter extending to the entire somatodendritic compartment) in the locus coeruleus of the majority of children and young adults, in the absence of Aβ deposits (Braak, Del Tredici 2011a). Hyperphosphorylated tau accumulated first in the locus coeruleus, from where neurons project to the transentorhinal cortex suggesting anterograde axonal transport of tau aggregates, followed by their neuron-to-neuron transmission to other brain regions. In AD in particular, tau pathology initiates in the enthorinal cortex and locus coeruleous before becoming symptomatic; this silent tau pathology

is present early in life in most healthy people, but does not spread beyond these regions and is not associated with clinical symptoms; pathological, clinical and biomarker data indicate that following accumulation of a high β-amyloid load in isocortical regions, tau pathology is then propagated beyond enthorinal cortex and locus coeruleus with associated symptoms of AD (Vasconcelos et al. 2016). In AGD, a similar classification to the one by Braak and Braak for AD tau pathology has been proposed (Saito et al. 2004). Here, the earliest changes are restricted to the ambient gyrus (stage I), from where the pathological process extends to the anterior and posterior medial temporal lobe (stage II), followed by the septum, insular cortex and anterior cingulate gyrus (stage III). Stage III is typical of patients with a clinical diagnosis of dementia (Saito et al. 2004).

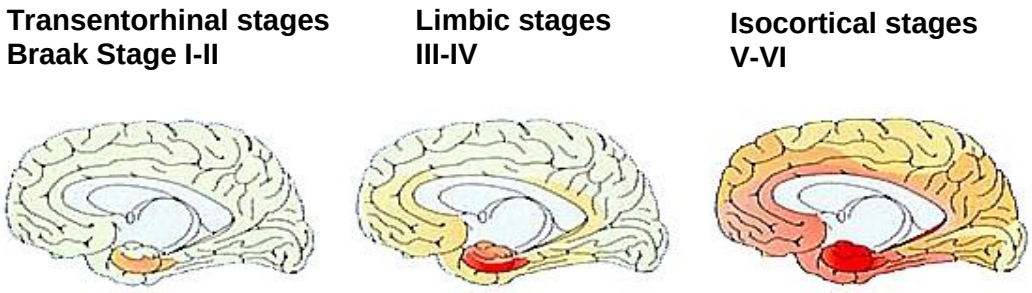

Figure 1.4: Summary diagram of the 6 stages in the development of AD-associated tau pathology. Subcortical pretangle stages are marked in dark red, cortical pretangle stages and NFT/NT stages I–II in medium red, NFT/NT stages III–IV in light red, and NFT/NT stages V–VI in pink. Stages I–II show alterations that are largely confined to the upper layers of the transentorhinal cortex (transentorhinal stages). Stages III–IV are characterized by a severe involvement of the transentorhinal and entorhinal regions, with a less severe involvement of the hippocampus and several subcortical nuclei (limbic stages). Stages V–VI show the massive development of neurofibrillary pathology in neocortical association areas (isocortical stages) and a further increase in pathology in the brain regions affected during stages I–IV. Adapted by permission from Springer Nature Licence, Springer Nature, Acta Neuropathologica, (Braak, Del Tredici 2011b), Copyright 2011. http://www.springer.com/medicine/pathology/journal/401

The molecular mechanisms of tau spreading are the focus of current intense research due to the potential therapeutic implications. This process would involve release of tau from a donor cell, followed or preceded by aggregation of tau, then uptake of tau aggregates by recipient cells and induction of tau aggregation in recipient cells. Some potential mechanisms are illustrated in Figure 1.5.

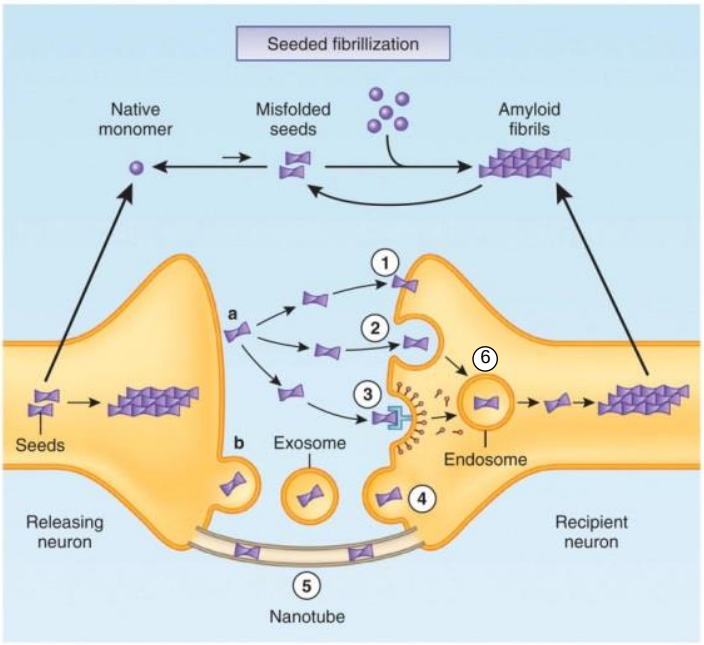

Figure 1.5: Potential mechanisms mediating cell-to-cell transmission of cytosolic protein aggregates. Misfolded protein seeds (for example oligomers and protofibrils) first form in the cytoplasm of the releasing neuron (left) by seeded fibrillization, where soluble native monomers are recruited into large intracellular aggregates (amyloid fibrils) and a positive feedback loop can be initiated by generation of more seeds through fragmentation or secondary nucleation. A small amount of protein aggregates can be released into the extracellular space in the 'naked' form (a) or via membrane-bound vesicles such as exosomes (b). Free-floating seeds may directly penetrate the plasma membrane of the recipient neuron (1) or enter by fluid-phase endocytosis (2) or receptor-mediated endocytosis (3), whereas exosomes containing seeds may fuse with the membrane of the recipient neuron (4). Intercellular transfer of seeds may also occur by nanotubes that directly connect the cytoplasm of two cells (5). Seeds internalized by endocytosis are contained in endosomes (6), from which they exit (by unknown mechanism) to then nucleate the fibrillization of native monomers in the cytoplasm of the recipient neuron (right). Adapted by permission from Springer Nature Licence, Springer Nature, Nature Medicine, (Guo, Lee 2014), Copyright 2014. https://www.nature.com/nm/

The trans-synaptic spreading of tau has been demonstrated in vivo and in culture models (Clavaguera et al. 2014., Ahmed et al. 2014, Calafate et al. 2015) and it is supported by the temporal and spatial pattern of spreading observed in tauopathies, but alternative mechanisms have been proposed other than direct transfer of tau between synaptically connected neurons (Walsh D.M., Selkoe 2016): tau propagation could follow a pattern of selective neuronal vulnerability (due to factors like poor myelination (Braak, Braak 1996), high metabolic rates (Yan, Wang & Zhu 2013), vulnerability to toxins (Nave, Werner 2014); alternatively, tau propagation could follow the progression of neuroinflammation, as microglia has been

implicated in tau propagation through phagocytosis and exosome secretion (Maphis et al. 2015, Asai et al. 2015).

It is clear that the pathophysiological mechanisms of tauopathies are multifactorial. Several hypotheses have been formulated to address them, and in vivo and in vitro models of tauopathies have been designed to test these hypotheses.

1.3 Animal models of tau aggregation and propagation

Cellular and animal models recapitulating features of tauopathies provide a useful tool to investigate the causes and consequences of tau aggregation. Several rodent models have been developed through modulation of endogenous tau or overexpression of human wild-type tau. A nonexhaustive list is given below (Table 2). In addition, rodent models expressing FTDP-17 mutant forms of tau have been developed following the discovery of the first exonic and intronic *MAPT* mutations (Hutton et al. 1998, Spillantini et al. 1998), which proved that neurodegeneration can be caused by genetic defects in tau. A nonexhaustive list is given below (Table 3).

Table 2. Examples of wild type (murine or human) tau transgenic mice. Adapted from (Dujardin, Colin & Buee 2015).

Isoform	Line	Promoter	Tau distribution	Exogenous tau protein	Cell specificity	Huper/abnormal phosphorylation	Altered synaptic function	Cell death	Insoluble tau	Tangles	Motor deficits	Cognitive decline	Reference
h2N4R	Alz17	Mouse Thy1	Spinal cord, hippocampus, striatum	1.5-10X	Neurons	+/nd	nd	nd	+	nd	+	nd	(Probst et al. 2000)
h2N4R	hWT line 23	MoPrP	Cortex, hippocampus, cerebellum, amygdala, brain stem, spinal cord	8-10X	Neurons	Nd/nd	nd	nd	+	-	–	nd	(Zhang et al. 2004)
h2N4R	WTau-tg	CAMKII	Cortex, hippocampus, olfactory bulb, striatum, thalamus	3-5X	Neurons	+/+	+	-	-	-	nd	+	(Kimura et al. 2007)
h1N4R	-	m2'3'-3CNP	CNS, spinal cord	nd	Oligodendrocytes	Nd/nd	nd	-	+	-	nd	nd	(Higuchi et al. 2005)
h1N4R	-	GFAP	Cortex, brainstem, thalamus, spinal cord	0.7-2X	Astrocytes	+/+	nd	-	+	+	+	nd	(Forman et al. 2007)
h1N4R	WT16	MpPrP	Cortex, hippocampus, brain stem, amygdala, spinal cord	5X	Neurons	+/-	nd	nd	nd	-	-	nd	(Yoshiama et al. 2007)
6 isoforms (WT)	8c	hTau	Cortex, hippocampus, striatum	3.7X	Neurons	+/+	nd	nd	-	-	-	nd	(Duff et al. 2000)
6 isoforms (KOMAPT)	hTau	hTau	Cortex, hippocampus	nd	Neurons	+/+	+	+	+	+	+	+	(Andorfer et al. 2003, Polydoro et al. 2009)

Table 3. Examples of mutant rodent transgenic models of tauopathies. Adapted from (Dujardin, Colin & Buee 2015).

Isoform	Line	Promoter	Tau distribution	Exogenous tau protein	Cell specificity	Huper/abnormal phosphorylation	Altered synaptic function	Cell death	Insoluble tau	Tangles	Motor deficits	Cognitive decline	Reference
h0N4RP301L	Tg4510 r	CamKII-tTA	Cortex, hippocampus , striatum, olfactory bulb	13X	Neurons	+/+	nd	+	+	+	+	+	(Santacruz et al. 2005, Ramsden et al. 2005)
h1N4RP301S	PS19	MoPrP	Cortex, hippocampus , brain stem, amygdala, spinal cord	5X	Neurons	+/+	+	+	+	+	+	+	(Yoshiyama et al. 2007, Takeuchi et al. 2011)
h2N4RN279K	T-279	hTau	Cortex, thalamus, olfactory bulb, basal ganglia, cerebellum, spinal cord	0.01X	Neurons/ Astrocytes	+/+	nd	+	-	+	+	+	(Dawson et al. 2007)
ΔK280(4Pχονστ ρυχτ) h2N4RDK280	TauRD	camKIIa-tTA	Cortex, hippocampus , striatum, olfactory bulb	0.7X	Neurons	+/+	+	+	+	+	nd	+	(Sydow et al. 2011, Mocanu et al. 2008)
h2N4RG272VP 301LR406W/ APPK670N-M671L	APPS WtauV LW	mThy1	nd	nd	Neurons	+/nd	nd	+	+	+	nd	+	(Perez et al. 2008, Perez et al. 2005, Ribe et al. 2005)
h0N4RP301L-APPSwe-PS1M146V	3xTg-AD	mThy1.2	Cortex, hippocampus , thalamus, tectum	2-6X	Neurons	+/+	+	nd	nd	+	nd	+	(Oddo et al. 2003, Sterniczuk et al. 2010)
4R-D151-391	SH72/S HR318	mThy1	Cortex, hippocampus , brain stem, spinal cord	3-5X	Neurons	+/nd	nd	-	+	+	+	+	(Filipcik et al. 2012)

Some sporadic tauopathies display a spatiotemporal progression of neurofibrillary degeneration. For example, in AD, neurodegeneration emerges in the trans-entorhinal cortex, spreads to the hippocampal formation, anterior temporal cortex, and polymodal and unimodal association areas, and eventually affects the whole cerebral cortex (Figure 1.4)(Braak, Braak 1991, Duyckaerts et al. 1997, Delacourte et al. 1999). To reproduce this progression, a new class of murine models of tauopathy based on trans-synaptic propagation have been developed, and recent studies provided in vivo evidence of seeded aggregation of tau in mice (Dujardin, Colin & Buee 2015) (Table 4). In the first study, brain extracts from mice transgenic for human mutant P301S tau with abundant silver-positive tau inclusions, when injected into the brains of ALZ17 mice expressing human wild-type tau (lacking tau inclusions), induced the slow assembly of wild-type tau into silver-positive, filamentous and hyperphosphorylated tau species several months post-injection, detectable at the injection site and in closely connected brain regions, suggesting that tau –or a particular species of tau, such as hyperphosphorylated tau, misfolded tau, or a fragment of tau—may have been released at the synapses (Clavaguera et al. 2009). A similar mechanism was also observed after intraperitoneal injection of TgP301S brain lysates (Clavaguera et al. 2014). Similarly, injection of TgP301S tau extracts from the hindbrain of symptomatic mice into the hippocampus and overlying cerebral cortex of non-symptomatic mice transgenic for human P301S tau, induced the formation of tau inclusions in the hippocampus, which spread rapidly (2-4 weeks) to synaptically connected brain regions, showing the transmissibility of tau pathology (Ahmed et al. 2014). These studies led to hypotheses about the 'prion-like' behaviour of tau, specifically that individual strains of misfolded tau proteins could recruit native tau and show intercellular propagation through the brain.

The induction and spreading of tau pathology through synapses has also been demonstrated following the restricted expression of human mutant tau in transgenic mice; two teams independently developed a new transgenic model where the neuropsin promoter drives overexpression of aggregation-prone P301L truncated tau in the entorhinal cortex, the initial site of AD-like tau pathology. From layer II of the entorhinal cortex, the original site of expression, trans-synaptic spreading of tau pathology to the hippocampus was detected (de Calignon et al. 2012, Liu et al. 2012). Another strategy to initiate tau pathology in a defined brain area uses lentiviruses (LVs) for local overexpression without diffusion; L.Buée's team demonstrated that wild-type (WT) tau protein is transferred long distances through a trans-synaptic mechanism in vivo (Dujardin et al. 2014), whereas the neuron-to-neuron spreading of tau pathology was much more limited using mutated P301L tau, possibly due to the mutant protein aggregating more readily, leaving fewer soluble species to migrate through axons. Similar data on the mechanism of cell-to-cell transfer was produced in a lamprey model of tauopathies (Kim, Lee & Hall 2010b), which consists of the microinjection of plasmids in giant anterior bulbar neurons to induce the overexpression of WT or mutated human tau (Lee et al. 2009).

A further study has shown that intracerebral injection of brain homogenates derived from human tauopathies (including AD, PSP, AGD, CBD, PiD and TD) into the brains of mice transgenic for human wild-type tau (ALZ17) induced the formation of specific silver-positive tau inclusions (Clavaguera et al. 2013). Neurofibrillary tangles, argyrophilic grain and Pick bodies, similar to those observed in human brains, were produced upon injection of brain homogenates from AD, AGD and PD, respectively. This work revealed the likely existence of distinct conformers (strains) of assembled tau, specific for each tauopathy, because following injection of the corresponding brain extracts, the light microscopic hallmark lesions of each distinct tauopathy were recapitulated. Work in M. Diamond's group also suggests the existence of different tau strains, as they injected various clones of truncated tau recombinant aggregates from HEK293 cells into hippocampus of young TgP301S mouse brains (Sanders et al. 2014.) and observed that the resulting brain depositions were reminiscent of the injected clone. They were also able to stably propagate tau species through multiple generations of mice in a prion-like fashion, showing that the pathology observed in subsequent generations was not due to residual tau seeds from the original inoculum, and that endogenous tau was being templated with high fidelity; after showing that tau pathologies induced by these clones were stable through serial transmission in TgP301S mice, HEK cells expressing 4 tau repeat domains were seeded with homogenates from these brains, and formed identical inclusions to those present in the original cells. This is in agreement with the prion hypothesis, where misfolded tau protein strains recruit native tau proteins to convert them into pathological species. The same group was able to show that antibodies blocking tau aggregate seeding improve cognition in vivo (Yanamandra et al. 2013b) and that tau strains may explain the diversity of human tauopathies, as they isolated a number of tau clones from HEK293 cells, injected into TgP301S (PS19) mouse brains and observed strain-specific patterns of tau pathology (Kaufman et al. 2016).

Table 4: Examples of non transgenic animal models of tau propagation (based on local delivery). Adapted from (Dujardin, Colin & Buee 2015).

Injected product	Injection site	Genetic background	Cell type specificity	DNF initiation	Hyper/abnormal phosphorylation	SD localization	Altered synaptic function	Neuronal death	Insoluble tau	Tangles	Cognitive decline	Reference
Plamids encoding various tau constructs WT or mutant	Giant anterior bulbar neurones	WT lampreys	neurons	9 days	+/+	+	+	+	+	+	nd	(Hall et al. 2001)

h2N4R Recombinant tau oligomers	Adeno-associated viral vector serotype 2 encoding h0N4RP301L	Adeno-associated viral vector serotype 1/2 encoding h2N4RWT or h2N4RP301L	Brain lysate of TgP301S transgenic mice	Adeno-associated viral vector serotype 2, 8, 9 or 10 encoding h2N4RP301L	Adeno-associated viral vector serotype 2 encoding h2N4RWT or h2N4RP301L	Adeno-associated viral vector serotype 2 encoding h2N4RP301L	Adeno-associated viral vector serotype 2 encoding h2N4RP301L
Hippocampus	Entorhinal cortex	Hippocampus	Hippocampus/ cerebral cortex	Substantia Nigra	Substantia Nigra	Hippocampus	Medial septum
C57BL/6 WT mice	WT Sprague–Dawley rats	WT FVB/N mice	Alz17 mice	WT Sprague–Dawley rats	WT Sprague–Dawley rats	PS1/APP mice	WT Sprague–Dawley rats
nd	neurons	neurons	nd	neurons	neurons	nd	neurons
nd	<3 months post-injection	-	6 months post-injection	nd	3 weeks post-injection	12 months post-injection	3 weeks post-injection
nd	+/+	nd	+/+	nd	nd	nd	+/+
+	+	+	+	nd	+	+	+
+	-	+	nd	nd	nd	nd	nd
+	-	+	nd	+	+	nd	nd
nd	+	nd	+	nd	+	nd	+
nd	+	-	+	nd	+	+	+
+	+	nd	nd	nd	nd	nd	nd
(Lasagna-Reeves et al. 2011)	(Ramirez et al. 2011)	(Jaworski et al. 2009)(Jaworski et al. 2011)	(Clavaguera et al. 2009)	(Klein et al. 2008)	(Klein et al. 2005)	(Klein et al. 2004)	(Klein et al. 2004)

Brain lysate of TgP301S transgenic mice	Human brain derived tau oligomers	Recombinant fibrils of truncated tau	Brain lysate of TgP301S transgenic mice	h2N4RP301L or truncated tau fragment K18 Recombinant	h2N4R Recombinant full-length tau fibrils	Lentiviral vectors encoding h1N4RP301L or h1N4RWT	Human brain lysate from various Tauopathies
Hippocampus/ cerebral cortex	ICV	Hippocampus	Peritoneum	Hippocampus/ Striatum/Cortex	Cortex	Hippocampus (CA1)	Hippocampus/ cerebral cortex
TgP301S transgenic mice	homozygous Htau mice	TgP301S mice	Heterozygous TgP301S	PS19 mice	C57BL6/J WT mice	WT Wistar rats	ALZ 17 mice
neurons	nd	nd	nd	nd	nd	neurons	neurones/ astrocytes
1 month	nd	3 weeks post-injection	6 months post-injection	1 month	nd	2 months post-injection	6 months post-injection
+/+	nd	+/+	nd	+/+	nd	+/+	+/+
+	+	+	+	+	+	+	+
nd	nd	nd	nd	nd	nd	nd	nd
-	nd	nd	nd	-	nd	+	nd
+	+	+	+	+	+	+	+
+	+	+	+	+	nd	+	+
nd	+	nd	nd	nd	nd	nd	nd
(Ahmed et al. 2014)	(Castillo-Carranza et al. 2014)	(Sanders et al. 2014)	(Clavaguera et al. Feb 2014)	(Iba et al. 2013)	(Holmes et al. 2013.)	(Caillierez et al. 2013)(Dujardin et al. 2014)	(Clavaguera et al. 2013)

As regard to which molecular tau species are responsible for seeding tau pathology, different groups have published various hypothesis. Only aggregated tau was able to recruit endogenous tau in a WT mice model injected with recombinant fibrils (Holmes et al. 2013), supporting the initial work by Clavaguera et al. 2009. Synthetic tau fibrils injected into young mice transgenic for human mutant tau were able to convert soluble tau into NFT-like inclusions and induce widespread time- and dose-dependent transmission of AD-like pathology from the injection site to the interconnected brain regions (Iba et al. 2013), whereas another group showed that upon injection of fibrils, oligomers or monomers of tau, only oligomers were able to not only induce strong tau pathology at the injection site, with neurodegeneration and behavioural deficits, but also transmit transynaptically (Lasagna-Reeves et al. 2012, Lasagna-Reeves et al. 2011,

Gerson, Kayed 2013). Also in an vivo model of sporadic tauopathy, soluble/oligomeric forms of tau protein appear to drive spreading, rather than aggregates (Dujardin et al. 2014).

All of these studies opened a new and exciting avenue to unravel the pathophysiology of tauopathies and expedite the development of therapeutics, but many questions remain to be answered about whether protein strains are the cause of different tauopathies in vivo. Cell-based models, nevertheless, remain an invaluable tool to dissect tau aggregation mechanisms in a complex cellular system.

1.4 Cell models of tau aggregation

Since tau is a highly soluble and naturally unfolded protein, it has been notoriously difficult to make it aggregate in cultured cells and produce cell-based models that develop tau aggregates similar to those observed in tauopathies. Strategies employed to produce tau tangles in cells are summarised in Table 5 (Lim et al. 2014). E. Mandelkow's group generated tau-inducible cell lines that overexpressed tau via a doxycycline-inducible system, since tau overexpression was toxic in N2a neuroblastoma cells (Khlistunova et al. 2006). Overexpression of truncated tau, that fibrillizes more readily than full-length tau (Wang et al. 2007, Khlistunova et al. 2006), produced robust tau aggregation in N2a cells, which was detected by a fluorescence dye, Thioflavin-S (ThioS). J. Kuret's group also generated a tetracycline-inducible tau cell line where tau aggregation was promoted by the addition of aromatic dyes such as Congo red, a known small-molecule aggregation inducer, to overcome the kinetic barrier of fibrillization within cells expressing full length tau isoform (Bandyopadhyay et al. 2007). Other groups also used overexpression of aggregation-prone tau mutants (Vogelsberg-Ragaglia et al. 2000) or treatment conditions such as tau kinases that promote pathological tau phosphorylation, which resulted in the formation of short tau fibrils that were detergent-insoluble and Thioflavin-S-reactive (Sato et al. 2002). It has been reported that tau fibril assembly occurs by a nucleation-dependent mechanism, whereby oligomeric intermediates form during an initial lag phase followed by a relatively rapid elongation phase (Friedhoff et al. 1998b). Therefore, Lee's group used a "seeding" reaction with preformed tau fibrils added to QBI-293 cells to accelerate fibrillization of monomeric tau and bypass the rate-limiting nucleation step (Guo, Lee 2011); they demonstrated that the formation of intracellular tau tangles can be accelerated by using mutant tau seeds and expressing mutant tau carrying FTDP-17 associated mutations that were shown previously to increase the fibrillization propensity and/or reduce the MT-binding affinity of tau (Hong et al. 1998, Hasegawa, Smith & Goedert 1998, Nacharaju et al. 1999, von Bergen et al. 2001). P301L, the most aggressive FTDP-17 mutation among the ones tested by Guo and Lee (ΔK280, P301L and R406W), dramatically promoted aggregation in a mammalian cell-based model, particularly when used in both exogenous seeds and cellular tau. In addition, Nonaka's group also introduced the treatment of exogenous tau fibrils to facilitate intracellular tau aggregation. In their study, full-length tau was expressed in SHSY5Y cells and tau aggregation was induced by the treatment of preformed tau fibrils, which act as a seed for intracellular tau aggregation (Nonaka et al. 2010). Other publications that showed induction of intracellular

aggregates by exogenously derived amyloid fibrils from tau and other proteins involved in neurodegenerative disorders include (Ferrari et al. 2003) (addition of pre-aggregated amyloid-β fibrils in SHSY5Y cells) and (Frost, Jacks & Diamond 2009) (addition of pre-aggregated microtubule-binding region of tau (K18) in C17.2 and HEK293 cells). Recently, modelling tau aggregation in human iPSC-derived neurons, whose biology resembles human neurons more closely than mammalian cell lines, has shown promise. One group used iPSC-derived neurons transduced with P301L tau seeded by heparin-aggregated P301L-K18 to detect aggregation measured by AlphaLisa and western blot, which could be reduced by autophagy inducers (Verheyen et al. 2015). Another publication claimed that their 3D human neural cell culture system recapitulated both Aβ and tau pathology, as they showed that 3D-differentiated neuronal cells expressing FAD mutations exhibited high levels of Aβ deposits, as well as detergent-resistant, silver-positive tau filaments; β- or γ-secretase inhibitors not only decreased Aβ pathology, but also attenuated tauopathy, supporting the idea that accumulation of Aβ drives tauopathy (Choi et al. 2014). By introducing the tau repeat domain (RD) carrying the P301L and V337M mutations into human iPSC-derived neurons, Reilly et al. could detect endogenous aggregation without the addition of recombinant tau fibrils, and spreading of tau pathology between neurons via conditioned media (Reilly et al. 2017).

Standard approaches to monitor intracellular tau aggregation require secondary methods such as Thioflavin-S or immuno-stains against phosphorylated tau; to directly measure intracellular tau aggregation, several fluorescence labels (GFP, CFP, and YFP) were introduced and showed tau aggregation in living cells (Nonaka et al. 2010, Lu & Kosik 2001). In addition, fluorescence protein technologies such as fluorescence resonance energy transfer (FRET) or bimolecular fluorescence complementation (BiFC) have been employed to investigate tau–tau interaction in living cells. During FRET, energy is transferred from a donor fluorophore (CFP) to an acceptor fluorophore (YFP), both tagged to the proteins of interest (Rizzo et al. 2004), only when those proteins in are close proximity (typically 2–6 nm), allowing differentiation of aggregated species from non-aggregated species in living cells. G.V. Johnson's group co-expressed full-length tau-CFP and caspase-cleaved tau-YFP in HEK293 cells (Chun W, Johnson GV 2007); when tau aggregation was induced by GSK3β, the two different tau isoforms bound to each other, thereby enabling the quantitation of tau aggregation. M. Diamond's group used a FRET technique to demonstrate trans-cellular propagation of tau aggregates (Kfoury et al. 2012); when they expressed K18(ΔK280)-CFP and K18(ΔK280)-YFP in separate cells populations, they observed a FRET signal derived from trans-cellular movement and co-aggregation of tau aggregates moving between cells, that was abrogated if either one of the constructs contained a double proline mutation to block β-sheet formation. More recently, the group improved the FRET assay to detect seeding activity with ultrahigh sensitivity and specificity; they engineered a monoclonal FRET biosensor HEK293T cell line ("tau biosensor cells") to stably express the tau repeat domain (RD) with the disease-associated P301S mutation fused to either CFP or YFP. After application of exogenous seeds, the nucleated aggregation of the tau FRET reporter proteins is detected by flow cytometry, rather than a FRET plate reader, with a reported sensitivity in the femtomolar range; in a P301S

mouse model of human tauopathy, the detection of proteopathic seeding by tau biosensor cells preceded the detection of standard histopathological markers, suggesting that seeding plays an early role in the pathology of tauopathies (Holmes et al. 2014). Although FRET is clearly an outstanding method to quantify protein–protein interactions in living cells, the use of a bulky fluorescence protein tag adds an artificial manipulation to the system and might interfere with the interaction between the proteins of interest. Also, the FRET-based tau aggregation sensor needs fine-tuning to measure tau aggregation, rendering it not suitable for high-throughput drug screening that needs a robust screening platform. The BiFC technique reduces the size of tagging by using a fluorescence protein split into 2 non-fluorescent fragments, subsequently tagged to the proteins of interest. Only when those proteins of interest are associated together is fluorescence measured (Outeiro et al. 2008, Kerppola 2006, Chen et al. 2006). Johnson's group applied a split green fluorescent protein (GFP) complementation technique to quantify tau aggregation by BiFC in situ (Chun, Waldo & Johnson 2011, Chun, Waldo & Johnson 2007); full-length tau protein was directly fused to a smaller GFP fragment (GFP11), and co-expressed in cells with a larger GFP fragment (GFP1–10). Only tau monomers or low degree aggregates allow the large GFP fragment to access the small fragment fused to tau, leading to the association of the fluorescently active GFP. Tau aggregation prevents the reconstitution of active GFP, leading to reduced GFP fluorescence in cells. An intrinsic shortcoming of this fluorescence “turn-off” approach is the fact that it detects early processes of tau aggregation, such as soluble tau intermediates. On the other hand, in Venus-based “turn-on” BiFC systems, only when tau assembles together is fluorescence produced; Venus fluorescence protein is split into two non-fluorescent N- and C-terminal fragments (VN173 and VC155), used to label tau (Tak et al. 2013); there is little fluorescence background in basal conditions, but Tau–BiFC fluorescence turned on dramatically when tau aggregation was stimulated by treatment with small molecules inducing tau phosphorylation.

Table 5: Induction of tau aggregation in cells. Adapted from (Lim et al. 2014).
K18 = truncated tau containing only the four MT-binding repeats
Tau37 = 1N3R tau
Tau39 = 2N3R tau
Tau40 = 2N4R tau

Tau isoform	Mutants	Host cell	Expression	Aggregation inducer	Detection	Reference
K18	ΔK280 ΔK280/PP (I277P/I308P)	N2a	Stable doxyclicin inducible	-	ThS	(Khlistunova et al. 2006)
Tau40	-	HEK293	Stable tetracyclin inducible	Congo red	Antibody	(Bandyopadhyay et al. 2007)
Tau40	N279K ΔK280	CHO	Stable expression	-	Antibody	(Vogelsberg-Ragaglia et al.

	P301L S305N V337M R406W					2000)
Tau40	-	COS-7	Transient expression	GSK3β, JNK3	ThioS	(Sato et al. 2002)
Tau40	- ΔK280 P301L R406W	QBI-293	Transient expression	Exogenous tau	Antibody	(Guo, Lee 2011)
Tau40 Tau37	-	SHSY5Y	Transient expression	Exogenous tau	Antibody GFP	(Nonaka et al. 2010)
Tau40	- P301L	SHSY5Y	Stable expression	Exogenous Aβ	Antibody	(Ferrari et al. 2003)
Tau40	-	C17.2 HEK293	Transient expression	Exogenous tau	YFP Alexafluor Antibody	(Frost, Jacks & Diamond 2009)
Tau40 Tau39	P301L V337M R406W	NIH 3T3	Stable expression	-	GFP CFP YFP	(Lu M, Kosik KS 2001)
Tau40 Tau (1-421)	-	HEK293	Transient expression	GSK3β	FRET (CFP, YFP)	(Chun W, Johnson GV 2007)
K18	ΔK280 P301L V337M I277P I308P	HEK293	Transient expression	K18	FRET (CFP, YFP)	(Kfoury et al. 2012)
Tau40 K18	ΔK280 I277P I308P	HEK293	Transient expression	GSK3β	BiFC (GFP11, GFP1-10)	(Chun, Waldo & Johnson 2007)
Tau40	-	HEK293	Stable expression	Forskolin okadaic acid	BiFC (VN173, VC155)	(Tak et al. 2013)
K18	P301S	HEK293	Stable expression	-	FRET (CFP, YFP)	(Holmes et al. 2014
3-repeats and 4-repeats tau	-	3D-differentiated neurons expressing FAD mutations	Stable expression	-	Antibody	(Choi et al. 2014)
3-repeats and 4-	P301L	hiPSC-derived neurons	Transient expression	K18	Antibody	(Verheyen et al. 2015)

repeats tau						
K18	P301L V337M	hiPSC-derived neurons	Transient expression	-	ThioT, antibody	(Reilly et al. 2017)

These studies successfully demonstrated that overexpressed tau could be aggregated in cells. These cellular systems enabled the spatial and temporal resolution of tau aggregation and also the investigation of pathological mechanism of tau aggregation. Several models for tau aggregation exist but none are currently available that have all the ideal features for allowing screening of compounds that affect tau aggregation.

1.5 Thesis aims

Cellular and animal models recapitulating features of tauopathies provide a useful tool to study the causes and consequences of tau aggregation. Some key questions in the field include which species of tau are competent to act as pathological seeds, and what are the molecular mechanisms controlling their uptake and release. In order to answer these critical questions, we developed a novel cell model for tau aggregation.

The specific aims of this project are:

1. To develop a robust and reproducible cell model of tau aggregation.
2. To extensively characterise this cell model in term of tau uptake and release: which tau species are transferred between cell to cell, which mechanisms are involved in the transfer, and which tau species constitute a seed.
3. To confirm the findings in a neuronal cell model and determine whether the mammalian cell model is a good surrogate for neurons.

For these purposes, our lab initially developed a seeded transient cell model of HEK293T cells transiently transfected with P301S 1N4R tau, with the aim of understanding mechanisms of tau aggregation and cell-to-cell propagation and also allowing screening of tool molecules. We chose to express P301S mutated tau, among the dominantly inherited tau mutations in FTDP-17, because of the high propensity of induced aggregation (Clavaguera et al. 2009, Allen et al. 2002, Bellucci et al. 2004, Scattoni et al. 2010). Also, the P301S mutation was chosen to match with the sarkosyl-insoluble TgP301S mouse-derived tau extract used for seeding (TgP301S seed), as it has been demonstrated that template-based seeding requires homotypic interactions between seed and substrate, consistent with the existence of seeding barriers (Sanders et al. 2014., Collinge, Clarke 2007). Subsequently, the transient system was migrated to an inducible model which is less labour intensive as no tau transfection is required, more reproducible as tau expression is regulated by tetracyline induction and is not dependent on transfection efficiency, more robust and more amenable to higher throughput assays. An inducible HEK T-REx cell line stably expressing P301S 1N4R tau (Falcon et al. 2015) was therefore used to further investigate the seeding process. The migration from transient to inducible system involved a change of cell line, but did not change the seeding process, which consisted of adding sarkosyl-insoluble TgP301S mouse-derived tau extract (TgP301S seed).

Our cell model differs from the existing ones by being inducible, hence more robust, by using sarkosyl-insoluble tau extracts from transgenic mice instead of recombinant tau as seeding agent, and by expressing full length tau and not the MB domain fragment, thus providing a more biologically relevant mechanism of nucleation and propagation of tau aggregation.

First, to investigate whether endocytosis is the main mechanism of tau uptake in this model, we explored the effect of different endocytosis modulators during seeding. Then, we explored the effect of temperature and transfection reagents on seed uptake. Next, we investigated colocalization between tau seed and endocytic markers (dextran, early endosome antigen 1 (EEA1), CD63) by immunofluorescence. Finally, following the incidental observation of tunnelling nanotubes (TNTs) in our cell model, we characterised them by confocal microscopy and explored the effect of the F-actin-depolymerising compound latrunculin A on tau intercellular propagation.

We then focused on tau release by characterising the tau species in conditioned media from unseeded vs seeded HEK T-REx P301S tau inducible cells, to investigate the presence of post-translational modifications (phosphorylation, truncation,..) aggregation state, size and encapsulation in vesicles of extracellular tau.

Next, to better investigate the molecular mechanisms of tau malfunction, we created a neuronal model recapitulating the main features of seeded tau pathology, using hippocampal neurons from TgP301S mice expressing 0N4R P301S tau, or rat cortical neurons expressing 1N4R P301S tau. Employing a neuronal cell model is of importance not only to confirm the findings obtained in the mammalian inducible model of tau aggregation, but also to be able to observe mechanisms that may be neuron-specific.

Some of the work described below has been included in recent publications. In Falcon et al. 2015 we described the development of a cell model to understand the relationship between tau conformation, phosphorylation state and seeding ability. Using both recombinant and native tau aggregates, we provided evidence that despite being taken up by cells to the same degree, native tau aggregates have a higher seeding potency than recombinant tau aggregates; the latter though can acquire the conformation and seeding potency of the former by templated assembly, demonstrating for the first time that conformation and not phosphorylation determines the seeding potency of tau aggregates (Falcon et al. 2015). In Jackson et al. 2016 we characterized by sucrose gradient and immunodepletion the native tau species responsible for seeding and pathology spreading in TgP301S mice. Tau species that were aggregated, AT8-, and nY29-positive with structure ranging from ring-like to small fibrils of 179–250 nm were able to seed tau aggregation in our inducible cell model and initiate *trans*-synaptic spreading in TgP301S mice in vivo, indicating that short fibrils are the most potent species capable of seeding tau pathology (Jackson et al. 2016).

Not only do our cell-based tauopathy models provide a tool for investigating the pathogenesis of tau aggregation, but also offer an invaluable system for identifying therapeutic strategies against neurodegenerative tauopathies, such as small molecules inhibiting tau fibrillization or antibodies blocking the spontaneous cellular uptake of tau.

2. EXPERIMENTAL PROCEDURES

2.1 Reagents and antibodies

For endocytosis modulation studies, Earle Balanced Salt Solution #14155 was purchased from Invitrogen; sodium azide NaN3 #S8032, Latrunculin A #L5163, 5-(N-ethyl-N-isopropyl)amyloride (EIPA) #A3085 and 2-deoxy-D-glucose #D6134 were obtained from Sigma. Transfection reagent Fugene was purchased from Roche and Lipofectamine 2000 from Invitrogen. For cellular fractionation, N-laurosarkosine #L9150 was obtained from Sigma. TgP301S transgenic mice over-expressing the shortest 4R form (0N4R) of human tau bearing an FTDP-17 mutation (P301S) under the mouse Thy1 promoter (Allen et al. 2002) were licensed from M. Goedert, Cambridge.

Table 6: Antibodies

Antibody	Target	Host	Supplier	Catalogue number	Dilution for WB	Dilution for IF
DA9	Total tau	mouse	P. Davies		2000	1000
TG5	Total tau	mouse	P. Davies		-	-
PG5	pS409-tau	mouse	P. Davies		-	1000
MC6	pS235-tau	mouse	P. Davies		-	-
PHF1	pS396-tau	mouse	P. Davies		-	-
MC1	Conformationally changed tau	mouse	P. Davies		-	8000
CP27	Total human tau	mouse	P. Davies		-	1500
AT8	pS202/pT205-tau	mouse	In-house		35,000	16,000
nY29	nY29-tau	mouse	Covance	sig-339349-500	-	1000
1N	1N tau	mouse	Covance	#MMS-5066		100
GAPDH	GAPDH	mouse	Ambion	#AM4300	6000	
EEA1	EEA1	mouse	BD Biosciences	#610457		500
CD63	CD63	mouse	Iowa DSHB	#H5C6		400

2.2 Sarkosyl-insoluble tau extraction from P301S and WT mice

A68 buffer composed of 10 mM Tris-HCl (SAFC #RES3094T-B102X) pH 7.4, 0.8 M sodium chloride (NaCl, Sigma), 1 mM ethylene glycol-bis(β-aminoethyl ether)-N,N,N',N'-tetraacetic acid (EGTA, Sigma), 5 mM ethylenediaminetetraacetic acid (EDTA, Sigma), 10% sucrose (Sigma), Complete (Roche cat# 11697498001) protease Inhibitor tablet, 1 mM phenylmethylsulphonyl fluoride (PMSF, Sigma, #93482), was used to prepare 0N4R tau sarkosyl-insoluble extract (“seed”) by sarkosyl extraction of TgP301S mice brains as previously described (Falcon et al.

2015). Briefly, homozygous mice transgenic for 0N4R tau with the P301S mutation showing severe paraparesis (~4.5 months) were killed by cervical dislocation. Whole brains were homogenised in Dulbecco's phosphate-buffered saline (DPBS, Invitrogen) by needle extrusion and brain homogenates were pooled; the pool was diluted with A68 buffer to 5 mg/ml of protein, measured by Bradford assay (Thermo Scientific #23236), and centrifuged twice at 13,000g for 20 min. Combined supernatants were made to final concentration of 1% sarkosyl from a 10% sarkosyl stock solution in dH2O and incubated at room temperature for 1 hour under agitation; following sarkosyl extraction, the mixture was centrifuged at 100,000g for 1 hour at 4°C. The resulting pellet, named TgP301S seed, was washed once with A68 buffer, resuspended in 50 mM Tris-HCl pH 7.4, sonicated and frozen as single-use aliquots at −80 °C. WT seed was prepared according to the same protocol from aged C57BL/6S mice.

2.3 Transient cell line culture and seed inoculation

HEK293T cells (ECACC) were transiently transfected with pcDNA3.1 constructs encoding human tau using Lipofectamine-2000. The cells were split the following day and grown overnight. They were then seeded with sarkosyl-insoluble tau (at the concentrations stated in the figure legends) diluted in OptiMEM (Gibco 31985-070). After 3 hours the seed/OptiMEM mix was removed and replaced with fresh complete medium [Dulbecco's Modified Eagle's medium (DMEM, Gibco #11960-044) plus 10% foetal calf serum (FCS)] supplemented with penicillin/streptomycin (Gibco 10378), blasticidin (Calbiochem 203350) and hygromycin (Roche 10843555001). Cells were then incubated for 3 days. Cells were passaged once weekly in T175 flasks, washed with Hank's balanced salt solution (HBSS, Gibco 14170-088), detached with 0.05% trypsin (#L11-003 PAA, GE Healthcare) in HBSS and typically split at a 1:40/1:50 dilutions into new flasks.

2.4 Inducible cell line culture and seed inoculation

To produce a stable inducible cell line, HEK293 T-REx cells (Invitrogen) were transfected with human 1N4R P301S tau/pcDNA 4T/O using FuGene 6. Clones were selected in the growth media containing 5 µg/ml blasticidin (Calbiochem #203350) and 200 µg/ml zeocin (Sigma #R25001). Following clone selection, expression of tau was induced in medium containing 1 µg/ml of tetracycline (T7660, Sigma) for 24/48 hours and expression levels were evaluated by western blotting with DA9 antibody. HEK T-REx inducible cells expressing human 1N4R tau bearing the P301S mutation were grown in full media (DMEM, 10% foetal bovine serum (FBS) supplemented with penicillin/streptomycin, blasticidin and zeocin (Sigma #R25001). Cells were passaged once weekly in T175 flasks, washed with HBSS, detached with 0.05% trypsin in HBSS and typically split at a 1:40/1:50 dilutions into new flasks.

Cells were plated in 6-well tissue culture plates (Corning) (for biochemical analysis) or 96-well poly-d-lysine coated imaging plates (Becton Dickinson #359271) (for imaging analysis) and induced with 1 µg/ml tetracycline. 24 hours later the TgP301S sarkosyl-insoluble tau seed diluted in OptiMEM was added to the cells for 3 hours at tau concentrations of 50-500 ng/ml. Cells were then treated with 0.0125% trypsin for 1 minute at room temperature to digest

extracellular seed (unless otherwise stated), and placed on induction medium (containing 1 µg/ml tetracycline) for 24 hours, after which the induction was stopped by replacing the media. 3 days after seeding, cells were harvested and fractionated for biochemical analysis, or fixed with 4% paraformaldehyde (PFA, Affimetrix, #19943)/1% Triton X-100 (Sigma, #X100) (unless otherwise stated) and prepared for immunofluorescence and imaging analysis.

For the time course profile of the seeding phase, cells were seeded for 10 or 30 or 60 minutes, followed by a 3-day post-seeding phase. For the time course profile of the post-seeding phase, cells were seeded for 3 hours followed by 0, 1, 2 or 3 days growth. For studying the effect of temperature on seed uptake, cells were seeded for 3 hours at 37˚C or 4˚C, followed by a 3-day propagation phase. For studying the effect of ATP depletion on seed uptake, medium was replaced by Earle's Balanced Salt Solution containing 10 mM sodium azide and 10 mM 2-deoxy-D-glucose for 2.5 h before inoculation with TgP301S sarkosyl-insoluble seed for 2 hours. For endocytosis modulation studies, cells were pre-incubated with compounds for 30 minutes prior and during inoculation with seed for 3 hours. Cells were subsequently grown for further 3 days and fixed with PFA 4%/Triton X-100 1% before aggregate uptake was monitored by high content imaging, or were fixed immediately after seeding and imaged by confocal microscopy. For actin depolymerisation experiments, cells were inoculated with seed for 3 hours, then seed was removed and replaced with media containing 300-0.4nM latrunculin A for 1, 2, or 3 days before fixation with PFA 4%/Triton X-100 1% and confocal and high content imaging analysis.

2.5 Sequential extraction and biochemical analysis

Sample fractionation for biochemical analysis was performed as previously described (Falcon et al. 2015) to produce total lysate and soluble and insoluble fractions from cell lysate samples. Briefly, cells were washed once with PBS before being scraped into 1 ml/well of DPBS; cells from 2 duplicate wells of a 6-well plate were combined and pelleted at 1000g for 5 minutes. Cell pellets were resuspended in 500 ul of fractionation buffer composed of 50 mM sodium phosphate (Sigma), pH 7.0, 10 mM sodium pyrophosphate (Sigma), 0.5 mM phenylmethylsulphonyl fluoride (PMSF), 2 mM sodium ortho-vanadate (Sigma), 2 mM EGTA, 2 mM EDTA, 20 mM sodium fluoride (Sigma), 1 mM dithiothreitol (DTT, Sigma #D0632), phosphatase inhibitor cocktail 1 (Sigma cat# P2850), phosphatase inhibitor cocktail 2 (Sigma cat# P5726), Complete protease inhibitor cocktail tablet. Following sonication, lysates were centrifuged at 10,000*g* for 10 min to clear cell debris. Supernatants were protein-matched using the Bradford assay and aliquots were kept as "TL Total lysates". When indicated, the remaining total lysates were incubated with 1% sarkosyl (from a 10% sarkosyl solution in dH2O) at room temperature for 1 hour on a flat rotating shaker. After centrifugation of the total lysates at 100,000*g* for 30 min at 4°C, supernatants were saved as "soluble fraction" whereas pellets ("insoluble fractions") were washed twice in fractionation buffer, resuspended in 50 mM Tris-HCl ph 7.4 and sonicated. Aliquots of all the fractions were stored at -80°C.

For sodium dodecyl sulfate polyacrylamide gel electrophoresis followed by western blot (SDS-PAGE-WB), total lysates, soluble fractions and insoluble fractions were mixed with 4X loading

buffer (Invitrogen, NP0007) containing 5% β-mercaptoethanol (Sigma, M7164), boiled 10 minutes at 95˚C and resolved on 8% SDS-polyacrylamide gels, transferred to nitrocellulose membranes, and blocked in 5% milk in Tris buffer saline (TBS) before probing with DA9 (1:2000, from P. Davies, Manhasset, NY), AT8 (1:1000, Thermo Scientific), GAPDH (1:6000, #AM4300 Ambion). Proteins were detected using Supersignal West Femto or West Dura detection systems (Thermo Scientific).

Alphascreen (AS) assays (Perkin Elmer) were performed according to the manufacturer's guidelines using tau specific antibodies. The Alphascreen technology is a sandwich assay for detection of molecules of interest in biological fluids in a sensitive, quantitative, reproducible manner. Essentially, a biotinylated anti-analyte antibody binds to streptavidin-Donor beads while another anti-analyte antibody is conjugated to Acceptor beads. In the presence of the analyte, the beads come into close proximity. The excitation of the Donor beads provokes the release of singlet oxygen molecules that triggers a cascade of energy transfer in the Acceptor beads, resulting in light emission. Optimised Alphascreen assays were set up using biotinylated tau antibodies paired with acceptor beads-conjugated tau antibodies (DA9, MC1, TG5, PG5, from P. Davies, Manhasset, NY; AT8, from Thermo Scientific). 10 µl/well of antibody mix of acceptor-conjugated and biotinylated antibodies were added to 384 well assay plates (#784075, Greiner) together with 5 µl/well of total lysate, soluble fraction, insoluble fraction sample or standard diluted in assay buffer (0.1% casein (Sigma) in DPBS). After overnight incubation at 4˚C, 5 µl/well of streptavidin-coated donor beads diluted in assay buffer were added to each well and plates incubated in the dark with gentle agitation at room temperature for 4 hours. Plates were read at excitation 680 nm and emission 520-620 nm using an Envision plate reader (Perkin Elmer). Two-tailed paired Student's *t* test or one-way Anova were used for all the comparisons in the study, and differences with *p* values less than 0.05 were considered significant. Alphascreen data was expressed as "Relative Alphascreen units" because the magnitude of the signal is dependent on the aggregation state of tau, therefore an absolute quantitation cannot be made.

2.6 Immunofluorescence

Cells were washed twice with DPBS and fixed with 4% PFA/1% Triton X-100 for 15 min to remove soluble proteins (Guo, Lee 2011). After blocking with 5% fat-free milk in TBS for 1 hour at room temperature, cells were incubated with primary antibodies overnight at 4°C followed by staining with appropriate Alexa Fluor-conjugated secondary antibodies for 1 hour at room temperature. Hoechst 33342 (Invitrogen) diluted 1:1000 in TBS was added for 30 minutes to label cell nuclei. PG5 and CP27 tau antibodies were obtained from P. Davies, Manhasset, NY. EEA1 antibody was from BD Biosciences #610457. CD63 antibody developed by Dr. David R. Soll was obtained from the Developmental Studies Hybridoma Bank developed under the auspices of the NICHD and maintained at The University of Iowa, Department of Biology, Iowa City, IA 52242. Lysosomal-associated membrane protein 1 (LAMP1) antibody was from BD Biosciences #555798. Alexa Fluor-labelled phalloidin for labelling F-actin was obtained from Invitrogen. Epifluorescence images were acquired using BD Bioscience Pathway, TTP Labtech

Acumen bioimaging systems (high content imaging assay, HCI) and an Olympus Fluoview 1000 inverted confocal microscope was used for confocal imaging with a 40X or 60X oil objective. Images were typically 1024 × 1024 pixels. For quantifying the percentage of cells carrying tau aggregates, 9 random-field images were taken per well at 20X magnification, and at least 6 replicate wells were used in each experiment, which was repeated at least twice (n=2). Two-tailed paired Student's *t* test or one-way Anova were used for all the comparisons in the study, and differences with *p* values less than 0.05 were considered significant.

2.7 Expression and purification of recombinant tau

The nucleotide sequences encoding untagged full-length human P301S mutants of 0N4R Tau (NP_058518.1) and 1N4R Tau (NP_001116539.1) were inserted into pET21d (Novagen) vector. Bacterial BL21(DE3) (Novagen) was used as an expression host, and the induction of protein expression was carried out in 2xTY media with 1 mM IPTG at 18^0C overnight. Cells were harvested, and the fresh cell pellets were lysed by stir-boiling in lysis buffer (20 mM MES, pH 7.3, 5 mM DTT, 0.2% Triton X-100, 1 mM PMSF) for 30 min followed by cooling on ice with stirring for 30 min. All subsequent purification steps were conducted at 4^0C. Cell lysates were clarified by centrifugation in a Beckman JA-18 rotor at 40,000g for 20 min. The supernatant was incubated with SP Sepharose Fast Flow (GE Healthcare) for 2 h. Proteins were eluted with 0-1 M NaCl gradient in buffer A (25 mM MES, pH 7.3, 2 mM DTT, 0.5 mM PMSF). Tau-containing fractions were pooled, concentrated and loaded onto a HiLoad 26/600 Superdex 200 column (GE Healthcare) and eluted in either buffer A (PBS, pH 7.4, 1 mM DTT, 5% glycerol) for 0N4R Tau or buffer B (10 mM HEPES, pH 7.4, 100 mM NaCl, 0.1 mM PMSF) for 1N4R. Fractions containing tau were pooled and protein concentration determined by UV280. The purified protein was aliquoted and stored at -80^0C. To obtain monomeric tau, purified recombinant tau was centrifuged at 100,000g at 4°C for 1 h and the supernatant used.

2.8 In *vitro* seeded assembly of recombinant tau

Recombinant 0N4R P301S tau was diluted to 135 µg/mL in PBS/1 mM DTT and incubated at 37 °C in an 800µL reaction volume with or without 5% (v/v) TgP301S tau sarkosyl-insoluble brain extract. An aliquot of the samples was added to 15 µM Thioflavin T (ThioT, Sigma, #T3516) in a 384-well plate (Corning #4514) and ThT fluorescence monitored over time with excitation and emission filters set to 444 and 485 nm, respectively, in an Envision (Perkin Elmer) plate reader. Fluorescence readings were taken every 20 min, with agitation in between each reading. The aggregation reaction was stopped, by snap-freezing the samples, when the ThioT signal reached a plateau. Samples were sarkosyl-extracted, as described below, and the pellets washed and resuspended in 50 mM Tris-HCl, pH 7.4. Samples were run on SDS-PAGE and probed with total tau antibody DA9. Equal amounts of tau protein were then added to HEK T-REx P301S 1N4R tau inducible cells following the seeding paradigm described above.

2.9 Conditioned media and cells collection

HEK-T-REx-293 P301S inducible cells were plated in triple layered flasks (Thermo Scientific Nunc #132913, Nunclon Delta surface), induced with 1 ug/ml tetracycline and 24 hours later

seeded with P301S mice derived brain extract diluted in OptiMEM for 3 hours as described above, in presence or absence of Lipofectamine. Cells were treated with 0.0125% trypsin for 1 min at RT to remove residual seed and placed again on induction medium containing 1ug/ml tetracycline. Phenol-red free DMEM (Gibco #21063-029) was used in the medium in order to diminish the interference with Alphascreen assay. Conditioned medium from these cells was collected at different time points post-seeding (0-1-2-3 days post seeding), spun 5 minutes at 200g and concentrated using Amicon Ultra-15 Centrifugal filter units with Ultracel 10K membrane or Centricon Plus-70 device, 10K, #UFC701008. Protein concentration in media samples was measured by Bradford assay and samples were normalised to the lowest protein concentration with DPBS. Tau concentration was measured by Alphascreen assay to normalise tau levels, then media samples were then used to seed naïve HEK-T-REx-293 P301S inducible cells, according to the seeding paradigm previously described (3 hours exposure to seed followed by 3 days of growth). Cells were also washed and collected at different time points post-seeding (0-1-2-3 days post seeding). After pelleting, the cells were lysed by sonication in tau fractionation buffer (50 mM sodium phosphate pH 7.4, 10 mM sodium pyrophosphate, 2 mM EGTA, 2 mM EDTA, 20 mM sodium fluoride, 1 mM dithiothreitol, supplemented with phosphatase inhibitor cocktail 2, phosphatase inhibitor cocktail 3, 0.5 mM PMSF, 2 mM sodium orthovanadate ($NaVO_3$) and Complete protease inhibitor cocktail tablets. The cell lysate was then spun at 13,000g for 5 minutes to pellet cell debris and the protein concentration was determined in the supernatant by Bradford assay, normalising all the samples to the lowest protein concentration in tau fractionation buffer. This supernatant was the cell total lysate (TL).

2.10 Cytotoxicity assays

The presence of cell death was measured by Trypan blue cell count and LDH assay (Roche) in the media. HEK T-REx P301S tau inducible cells, uninduced, unseeded and treated 4 hours with 1% Triton X-100 were used as “high control” (100% cytotoxicity); HEK T-REx P301S tau inducible cells, uninduced, unseeded were used as “low control”; sample from unconditioned media was used as “background control”. The samples’ cytotoxicity was calculated as follow: Cytotoxicity (%) = (Exp value - Low Control)/(High Control - Low Control) x 100.

2.11 Sarkosyl extraction of conditioned media and total lysate samples

Conditioned media and total lysate samples were incubated with 1% sarkosyl (from a 10% solution of sodium lauryl sarcosinate in water) for 1 hour, shaking, at room temperature. At the end of the incubation, the samples were spun for 1 hour at 235,400g at 4°C.

The resulting supernatants were collected and frozen as “sarkosyl-soluble fractions”, while the pellet was washed by adding A68 buffer (10 mM Tris-HCl pH 7.4, 0.8 M NaCl, 1 mM EGTA, 5 mM EDTA, 10% sucrose, protease inhibitor tablet, 1 mM PMSF) and centrifuged 10 minutes at 235,400g at 4°C. All the remaining supernatant was discarded, pellets were dried and then sonicated 5 x 1 s pulses in $1/10^{th}$ of the volume spun of 50 mM Tris-HCl pH 7.4, supplemented with Complete protease inhibitor tablet and 1 mM PMSF and frozen as “sarksosyl-insoluble fractions”.

2.12 Immunodepletion

Activated sepharose 4 Fast Flow (GE Healthcare) was conjugated to the antibody of choice at 5 mg/ml, as per manufacturer's instructions, and stored in PBS containing 0.01% sodium azide. Following washing, 250 ul beads were incubated with 5 mg TgP301S tau brain lysate and rotated overnight at 4°C. Sepharose was removed through centrifugation at 1000*g* and depleted lysates stored at -80°C until further analysis.

2.13 TgP301S primary neuronal cultures

Primary neuronal cultures were prepared from E17 embryos from time-mated TgP301S and C57BL/6S female mice (Charles River, UK). Dissociated hippocampal/cortical neurons were plated onto poly-D-lysine coated 96-well plates. Media was made with Neurobasal medium (Invitrogen 21103-049) supplemented with MACS Neurobrew-21 (Miltenyl Biotec 130-093-566) and L-glutamine (Life Technologies 25030-024). Seeding was performed at day-in-vitro 7 (DIV7), when sarkosyl-insoluble TgP301S 0N4R tau seed was diluted in medium before being added to neurons. Neurons were fixed for immunocytochemistry at DIV14 in 4% PFA containing 2% sucrose and 1% Triton X-100 for 15 min to remove soluble proteins, as previously described (Guo, Lee 2013). After blocking with 0.5% BSA/0.1% Triton X-100/TBS for 1 h at RT, neurons were incubated with specific primary antibodies overnight at 4ºC followed by staining with appropriate AlexaFluor-conjugated secondary antibodies (Invitrogen) and Hoechst for 1 h at RT. Epifluorescence images were acquired using BD Bioscience Pathway, TTP Labtech Acumen bioimaging systems (high content imaging assay, HCI) and an Olympus Fluoview 1000 inverted confocal microscope was used for confocal imaging with a 40X or 60X oil objective.

2.14 Rat primary neuronal cultures

Primary neuronal cultures (rat cortical neurons, RCNs) were prepared from E12 embryos from time-mated CR rats. Dissociated cortical neurons were plated onto poly-D-lysine coated 96-well or 6-well plates. Media was made with Neurobasal medium supplemented with MACS Neurobrew-21 and L-glutamine. Cultures were transduced at DIV0 with P301S 1N4R tau vectors (Vector Biolabs). Plasmids were subcloned into AAV vector with synapsin promoter and WPRE transcrptional enhancer, and packaged into AAV virus particles. The vector used was the P2A fusion eGFP-P2A-MAPT(P301S), which is subjected to cleavage by endogenous proteases. The P2A peptide sequence is GSGATNFSLLKQAGDVEENPGP. After cleavage, the red sequence remains with eGFP, and green sequence remains with tau, resulting in GFP-labelled cells but unlabelled tau protein.

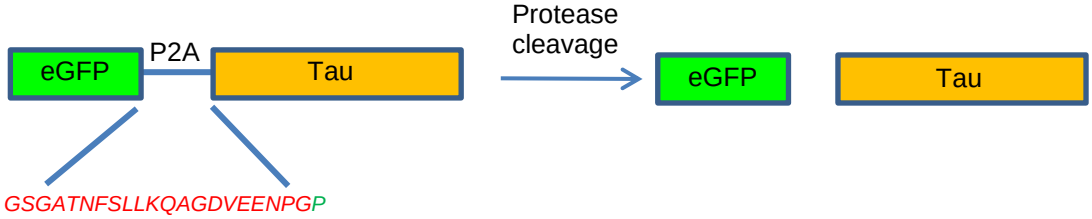

Seeding was performed at DIV8, when sarkosyl-insoluble TgP301S 0N4R tau seed was diluted in medium before being added to neurons. Neurons were collected for analysis at DIV15. For immunocytochemistry, neurons were fixed in 4% PFA containing 2% sucrose and 1% Triton X-100 for 15 min to remove soluble proteins, as previously described (Guo, Lee 2013). After blocking with 0.5% BSA/0.1% Triton X-100/TBS for 1 h at RT, neurons were incubated with specific primary antibodies overnight at 4C followed by staining with appropriate AlexaFluor-conjugated secondary antibodies (Invitrogen) and Hoechst for 1 h at RT. Epifluorescence images were acquired using BD Bioscience Pathway, TTP Labtech Acumen bioimaging systems (high content imaging assay, HCI) and an Olympus Fluoview 1000 inverted confocal microscope was used for confocal imaging with a 40X or 60X oil objective. For biochemical analysis, cells were collected as above for HEK T-REx P301S inducible cells.

2.15 Statistical analysis

Statistical analysis was carried out using Prism statistical analysis software (GraphPad Software Inc.). Differences between two groups were compared using a two-tailed paired Student's t test. Differences between multiple groups were compared using one-way ANOVA and then groups compared using a post-hoc Dunnet test.

RESULTS

3. DEVELOPMENT OF TRANSIENT AND INDUCIBLE CELL MODELS OF SEEDED TAU AGGREGATION

Our lab initially developed a seeded transient cell model of HEK293T cells transiently transfected with P301S 1N4R tau, with the aim of understanding mechanisms of tau aggregation and cell-to-cell propagation and also allowing screening of tool molecules. We chose to express P301S mutated tau, among the dominantly inherited tau mutations in FTDP-17, because of the high propensity of induced aggregation (Clavaguera et al. 2009, Allen et al. 2002, Bellucci et al. 2004, Scattoni et al. 2010). Also, the P301S mutation was chosen to match with the sarkosyl-insoluble TgP301S mouse-derived tau extract used for seeding (TgP301S seed), as it has been demonstrated that template-based seeding requires homotypic interactions between seed and substrate, consistent with the existence of seeding barriers (Sanders et al. 2014., Collinge, Clarke 2007). The first aim of this thesis was to migrate this transient system to an inducible model which is less labour intensive as no tau transfection is required, more reproducible as tau expression is regulated by tetracyline induction and is not dependent on transfection efficiency, more robust and more amenable to higher throughput assays. This chapter will present the characterisation of the transient model, followed by the development and characterisation of seeded tau aggregation assays in the inducible cell model.

3.1 Spontaneous uptake of seed without transfection reagent induces endogenous tau aggregation in HEK293T cells

To explore the capability of TgP301S sarkosyl-insoluble tau seed to nucleate intracellular fibrillization of soluble tau, HEK293T cells transiently transfected with the 1N4R human tau isoform bearing the P301S mutation were treated for 3 hours with sarkosyl-insoluble 0N4R tau extract generated from TgP301S transgenic mice, in absence of transfection reagent, and cultured for a further 3 days. Sequential extraction (fractionation) of cell lysates performed in presence of 1% sarkosyl produced a pellet named “sarkosyl-insoluble fraction” and a supernatant named “sarkosyl-soluble fraction”. Total lysates recovered in fractionation buffer, sarkosyl-soluble and sarkosyl-insoluble fractions were resolved by SDS-PAGE. Immunoblotting with AT8 (pS202/pT205-tau) and DA9 (total tau) antibodies revealed accumulation of abundant sarkosyl-insoluble tau in seed-treated cells (Figure 3.1). Since the endogenous tau isoform being used was 1N4R and exogenous seeding tau 0N4R, the two isoforms could be distinguished by size in WB, as well as by isoform-specific antibodies (see Figure 3.6). Therefore AT8 immunoreactivity in seed-treated cells can be entirely attributed to the transiently expressed 1N4R P301S tau, and not to exogenously supplied tau seed. The insoluble 1N4R tau separated at a higher molecular weight than the input 0N4R tau, suggesting that the 0N4R tau inocula entered cells and recruited 1N4R tau into sarkosyl-insoluble hyperphosphorylated tau species. In the absence of tau expression, seeding with sarkosyl-insoluble native tau did not result in any insoluble, aggregated tau. In addition, cells that were not treated with TgP301S sarkosyl-insoluble native tau, but expressed tau, did not form sarkosyl insoluble tau.

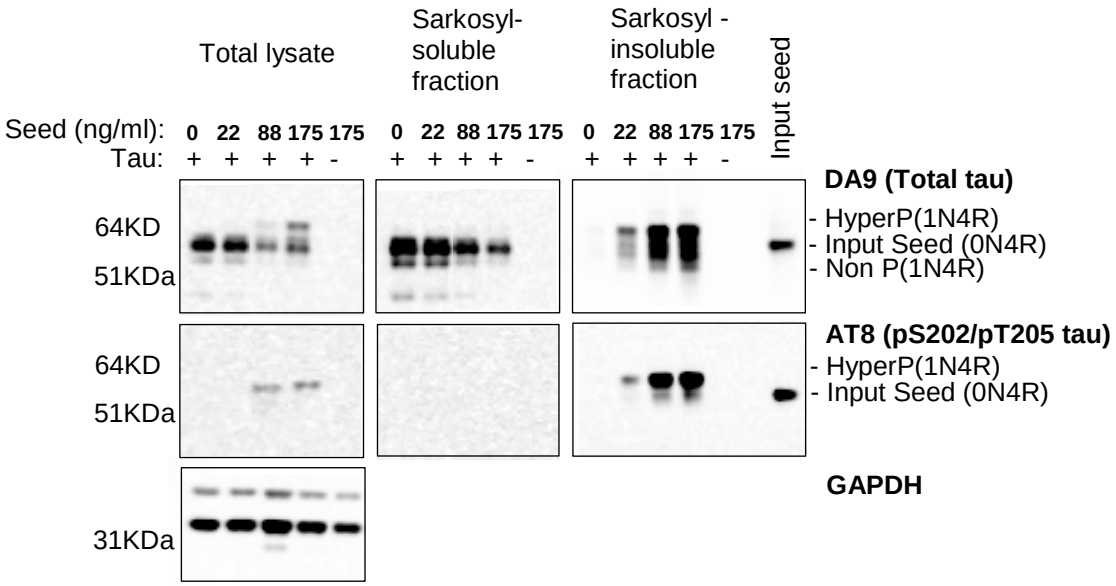

Figure 3.1: Accumulation of sarkosyl-insoluble tau in seed-treated cells. Western blot with anti-tau antibodies DA9 (phosphorylation-independent) and AT8 (pS202/pT205) of the total lysate, sarkosyl-soluble and sarkosyl-insoluble fractions from HEK293T cells transiently transfected with or without P301S 1N4R tau DNA. Cells were exposed for 3 h to increasing amounts of sarkosyl-insoluble material from TgP301S 0N4R tau mice brains, followed by 3 days of incubation. A total lysate loading control for GAPDH is also shown. Data shown is representative of 2 independent experiments.

An Alphascreen was used to measure the levels of different tau species (Figure 3.2). In the absence of seed, sarkosyl-soluble tau was phosphorylated at the MC6 (pS235) epitope. Following treatment with TgP301S tau seed, there was a dose-dependent reduction in sarkosyl-soluble total tau (Figure 3.2 i) and sarkosyl-soluble tau phosphorylated at the MC6 epitope (Figure 3.2 iii) and a parallel increase in sarkosyl-insoluble total (Figure 3.2 v) and sarkosyl-insoluble MC6-positive tau (Figure 3.2 vii), suggesting that soluble tau was being converted into insoluble tau aggregates. In the sarkosyl-soluble fraction, a small amount of tau was MC1 (conformationally changed)-positive, and it increased dose-dependently following seed treatment for 3 h and growth for 3 days (Figure 3.2 ii). Sarkosyl-soluble tau was also AT8-positive, but only following seed treatment (Figure 3.2 iv). We cannot completely exclude the possibility of an incomplete separation between sarkosyl-soluble and sarkosyl–insoluble material, although no differences in the amounts of MC1- and AT8-positive tau in the sarkosyl-soluble fractions were observed following 100,000g centrifugations at 30 min, 1 h and 24 h (data not shown). Following incubation with TgP301S tau seed, a dose-dependent increase in the levels of MC1- and AT8-positive sarkosyl-insoluble tau was observed (Figure 3.2 vi and viii) (Falcon et al. 2015).

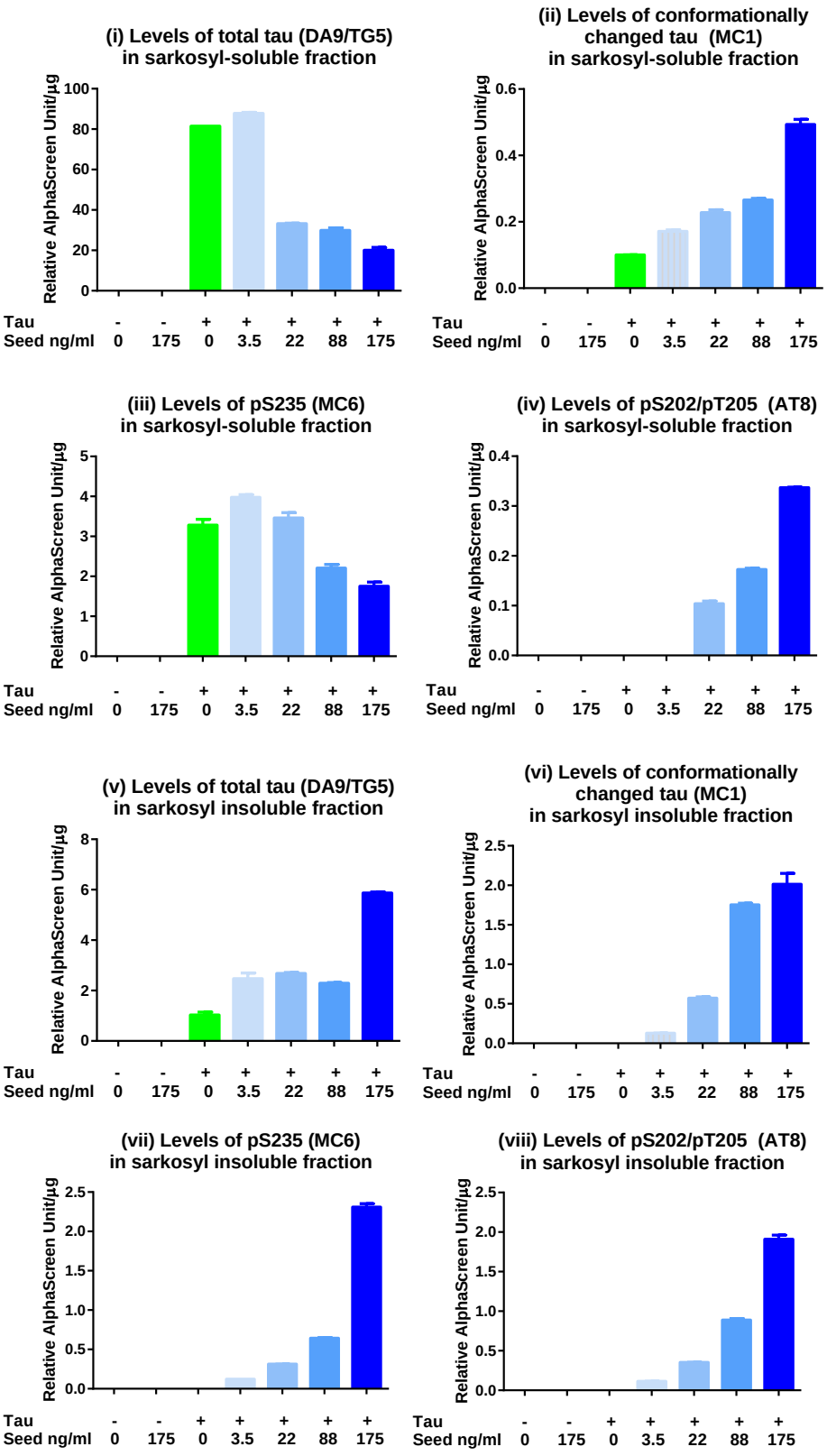

Figure 3.2: Accumulation of sarkosyl-insoluble tau in seed-treated cells. Alphascreen showing levels of total tau (DA9) (i and v), conformationally changed tau (MC1) (ii and vi), tau phosphorylated at S235 (MC6) (iii and vii) or S202/T205 (AT8) (iv and viii) in HEK 293T cells transiently transfected with or without human P301S 1N4R tau, exposed for 3 h to increasing amounts of sarkosyl-insoluble material from the brains of P301S 0N4R tau mice, followed by 3 days of incubation. The results are the means ± SEM (n=3). Absolute quantification of the

levels of sarkosyl-soluble (upper panel) and sarkosyl-insoluble (lower panel) tau cannot be made, because the magnitude of the signal is dependent on the aggregation state of tau.

3.2 Trypsin digestion of inocula

In agreement with what had been shown by other groups for tau (Frost, Jacks & Diamond 2009) and SOD1 (Munch, O'Brien & Bertolotti 2011) we found that TgP301S sarkosyl-insoluble tau seed was completely digested when treated with 0.0125% trypsin for 1 min at room temperature (Figure 3.3). This is 4-fold lower than the level of trypsin routinely used to re-plate cells in tissue culture (0.05% for 3 min at 37C); this relative sensitivity of the extracellular aggregates to proteolysis allowed us to incorporate a trypsin treatment following seeding in our model, without the need to re-plate the cells.

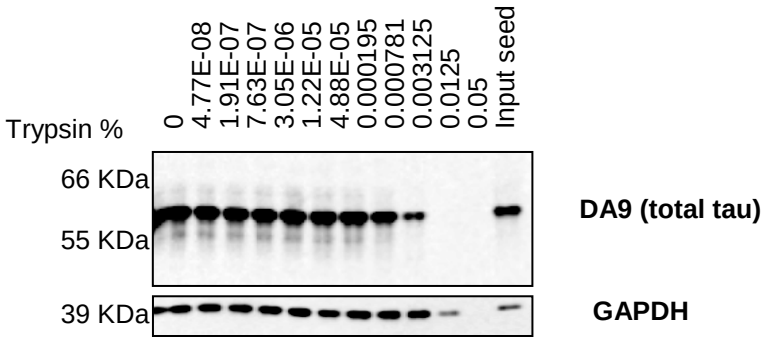

Figure 3.3: Aggregated tau is sensitive to trypsin digestion. TgP301S mouse sarkosyl-insoluble extract treated with up to 0.05% trypsin in HBSS for 1 minute at room temperature and resolved by SDS-PAGE, followed by immunoblotting with DA9 (total tau) antibody and GAPDH (loading control). 0.0125% trypsin is sufficient to completely digest the seed.

3.3 Development and characterisation of a seeded tau aggregation: biochemical assay in HEK T-REx P301S tau inducible cells

An inducible HEK T-REx cell line stably expressing P301S 1N4R tau was produced by S. Glover, Eli Lilly, Windlesham, and used in all subsequent experiments to further investigate tau seeded assembly and seed uptake.

HEK T-REx inducible cells that had been expressing the 1N4R human tau isoform bearing the P301S mutation for 24 hours, were treated for 3 hours with sarkosyl-insoluble 0N4R tau extract generated from TgP301S transgenic mice, in absence of transfection reagent, and cultured for a further 3 days.

*S*equential extraction (fractionation) of cell lysates performed in presence of 1% sarkosyl produced a pellet named “sarkosyl-insoluble fraction” and a supernatant named “sarkosyl-soluble fraction”; *s*equential extraction performed without 1% sarkosyl produced a pellet named “insoluble fraction” and a supernatant named “soluble fraction”. Samples were resolved by SDS-PAGE. When sarkosyl-extraction was performed, similarly to what we observed in the transient

cell model, immunoblotting with AT8 antibody revealed accumulation of abundant insoluble tau in seed-treated cells (Figure 3.4 A). The sarkosyl-insoluble 1N4R tau separated at a higher molecular weight than the input seed (0N4R tau) suggesting that the 0N4R tau inocula entered cells and recruited the endogenous 1N4R tau into sarkosyl-insoluble hyperphosphorylated tau species. When the total lysate extraction was performed in absence of 1% sarkosyl, again a dose dependent increase in levels of insoluble AT8-positive tau was observed upon seed treatment; however, cells treated with Optimem alone as controls showed low levels of insoluble tau recognised by DA9 antibody, which was not AT8-immunoreactive (Figure 3.4 B). Unseeded cells extracted in presence of 1% sarkosyl did not retain any tau species recognised by AT8 or DA9 antibody by WB, whereas the same cells extracted in absence of sarkosyl showed basal level of tau recognised by DA9 but not AT8 antibody; this means that AT8-positive sarkosyl-insoluble tau species are only formed upon seed addition.

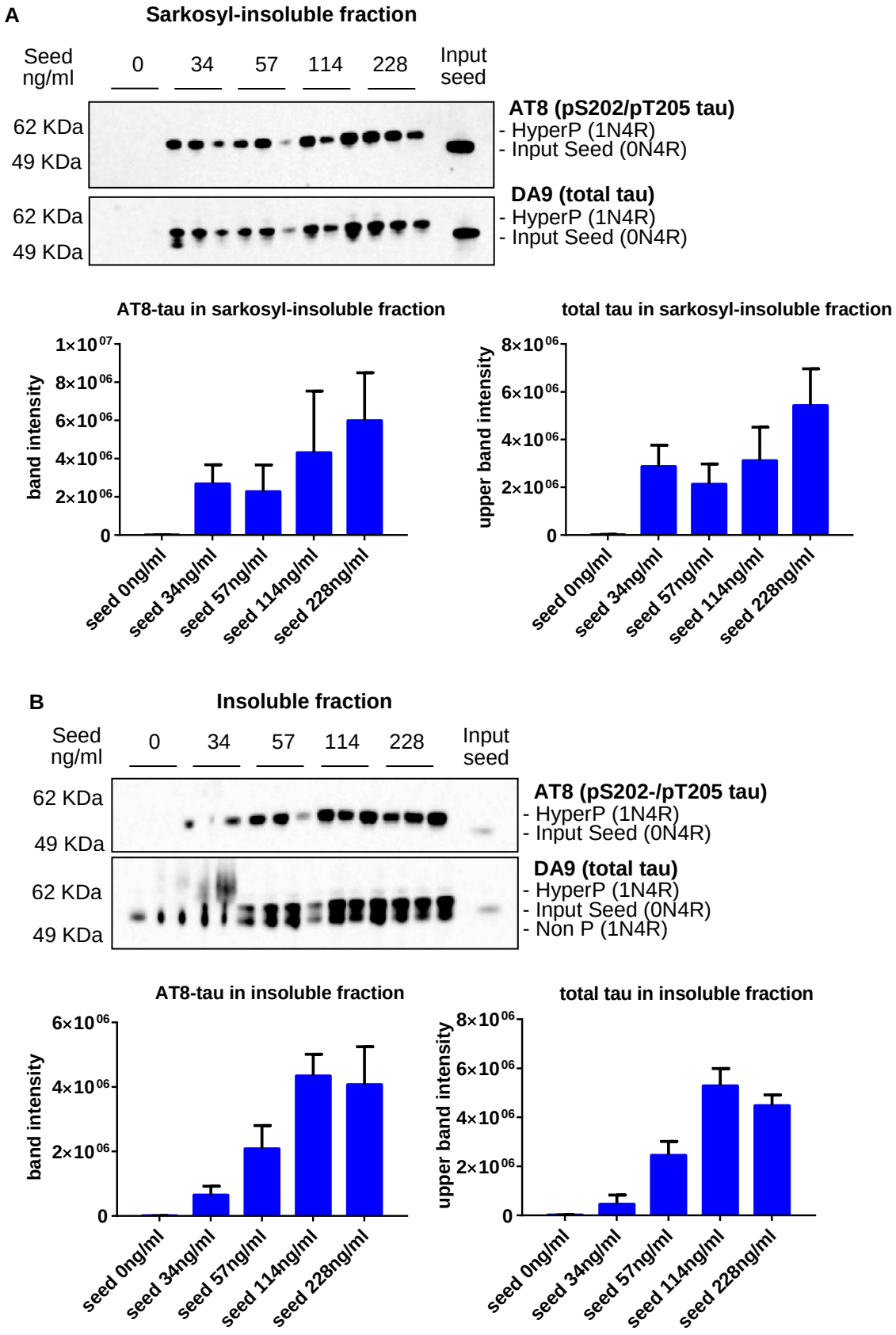

Figure 3.4: Dose-dependent accumulation of aggregated tau 3 days post-seeding.

Western blot with total tau antibody (DA9) and pS202/pT205 tau antibody (AT8) of fractions extracted of HEK T-REx P301S 1N4R tau inducible cells fractionated in presence (A) and

absence (B) of 1% sarkosyl. Quantifications of the blots are shown in the graphs. Cells were treated with increasing concentration of TgP301S mouse sarkosyl-insoluble extract for 3 hours, followed by 3 days of growth. Data shown are mean ± SEM (n=2).

Similarly, Alphascreen assays showed a dose-dependent accumulation of hyperphosphorylated tau aggregates, upon treatment with TgP301S seed, in the insoluble fraction, detected by antibody AT8 (Figure 3.5).

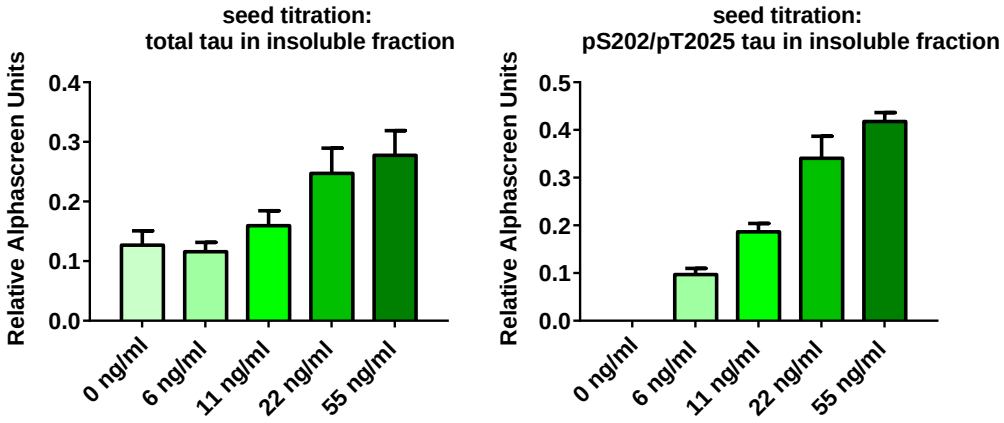

Figure 3.5: Dose-dependent accumulation of aggregated tau 3 days post-seeding. Alphascreen assays showing levels of total tau (DA9-TG5 antibodies) or hyperphosphorylated tau (AT8-DA9 antibodies) in the insoluble fractions following 3 hour inoculation with increasing concentrations of TgP301S mouse sarkosyl-insoluble extract and 3 days growth. Data shown are mean ± SEM (n=2).

An anti-1N tau antibody was also employed to confirm the endogenous nature of tau aggregates by WB (Figure 3.6).

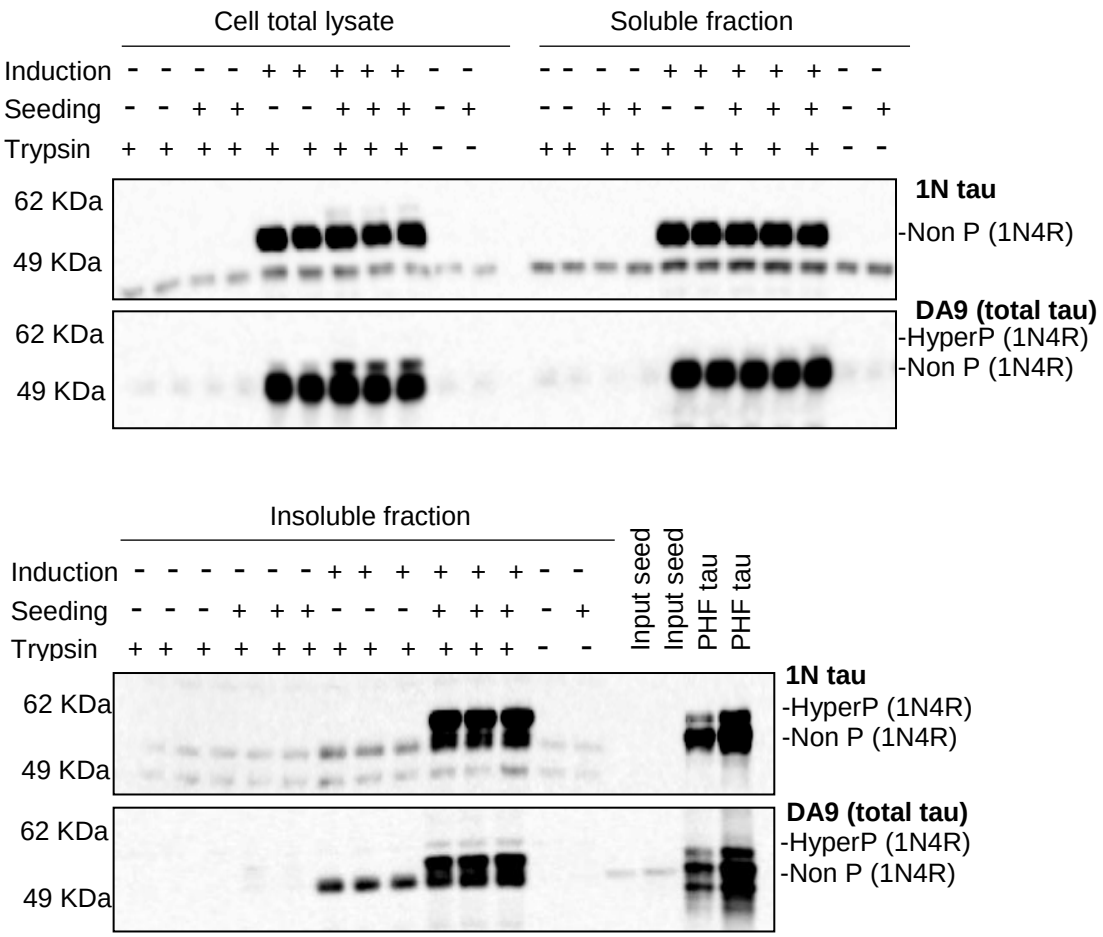

Figure 3.6: Accumulation of endogenous aggregated tau 3 days post-seeding. Western blot with 1N tau antibody and total tau antibody (DA9) in different fractions of HEK T-REx P301S 1N4R tau inducible cells treated with TgP301S mouse sarkosyl-insoluble extract, followed by trypsinisation, reveals accumulation of abundant insoluble endogenous 1N4R tau in seeded cells. Sequential extraction (fractionation) was performed; total lysates (cellular fraction recovered in fractionation buffer), soluble and insoluble fractions were loaded on SDS-PAGE. Input seed (expected to contain 0N4R P301S tau, and no 1N-tau) was loaded as negative control for the 1N-tau antibody. PHF from AD brain (expected to contain 0N-, 1N-, 2N-tau) was loaded as positive control for the 1N-tau antibody. Data shown is representative of 2 independent experiments.

3.4 Development and characterisation of seeded tau aggregation: imaging assays in HEK T-REx P301S 1N4R tau inducible cells

Abundant Triton X-100-insoluble phospho-tau aggregates were detected by immunofluorescence using anti-phosphoS409-tau antibody PG5 after 1% Triton X-100 extraction during fixation to remove soluble proteins (Figure 3.7 A). Quantification of the % of aggregate-bearing cells induced by TgP301S seed inoculation was performed by BD pathway high-content imaging: treatment of 1N4R P301S tau-expressing cells with 0N4R seed for 3 hours followed by 3 days of growth yielded aggregates in up to ~12% of cells, in a dose-dependent fashion (Figure 3.7 B).

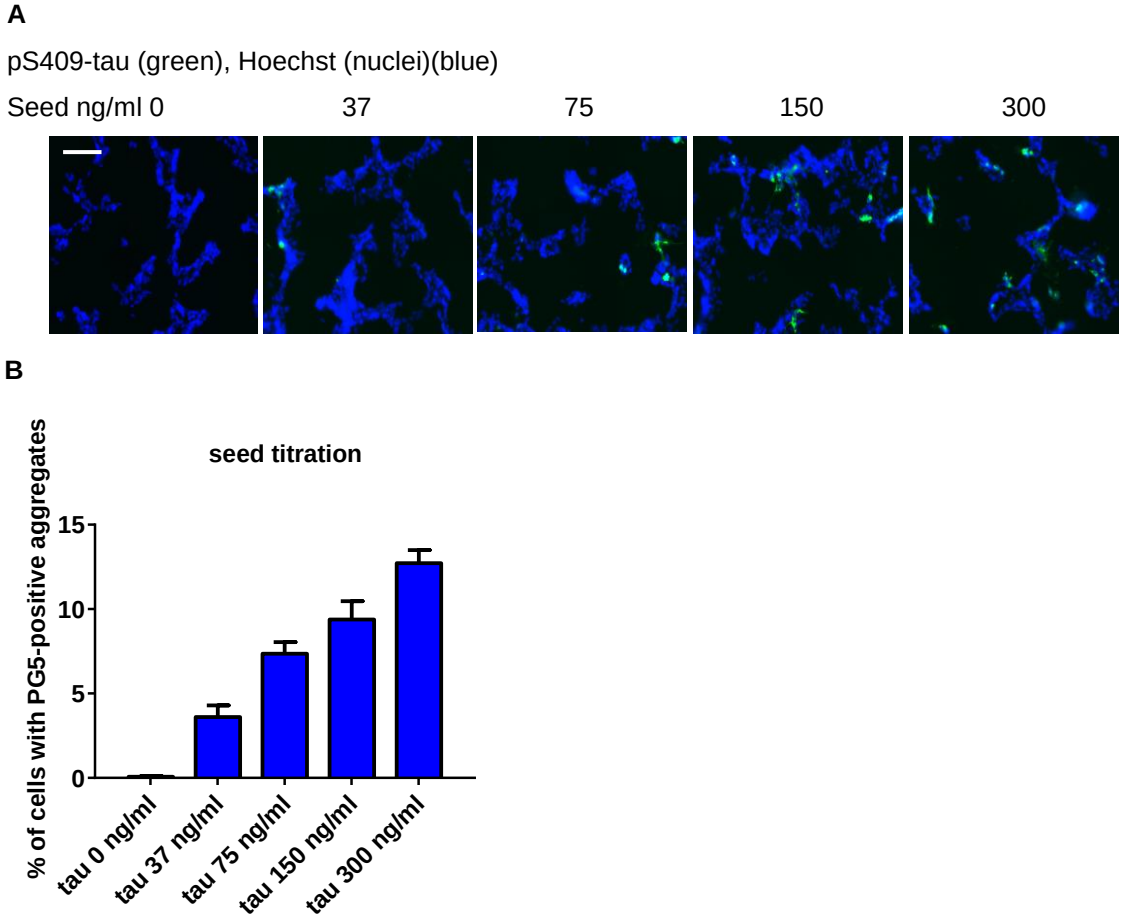

Figure 3.7: High-content imaging (HCI) assay shows dose-dependent accumulation of aggregated tau 3 days post-seeding. (A) After incubation of HEK T-REx P301S 1N4R tau cells with tau seed for 3 hours, followed by 3 days of growth, accumulation of Triton X-100-insoluble endogenous tau recognised by PG5 antibody (green) was detected by HCI in up to 12% of total cells. Soluble proteins were extracted by 1% Triton X-100 during fixation of the cells. Cell nuclei were stained by DAPI (blue). Scale bar 50 µm. (B) Quantification of (A). Data shown are mean ± SEM (n=2).

Confocal microscopy showed that treatment with TgP301S (0N4R) sarkosyl-insoluble seed resulted in punctate, intracellular PG5-positive tau inclusions in cells. These inclusions were absent in unseeded cells, in which the phosphorylated tau recognized by antibody PG5 (tau pS409) was extracted by 1% Triton X-100 during fixation; similar images were obtained with anti

pS202/pT205-tau antibody AT8 (Figure 3.8 A) and anti-nitrated Y29-tau antibody nY29 (Figure 3.8 B). These epitopes are associated with filamentous tau as they are present in PHFs.

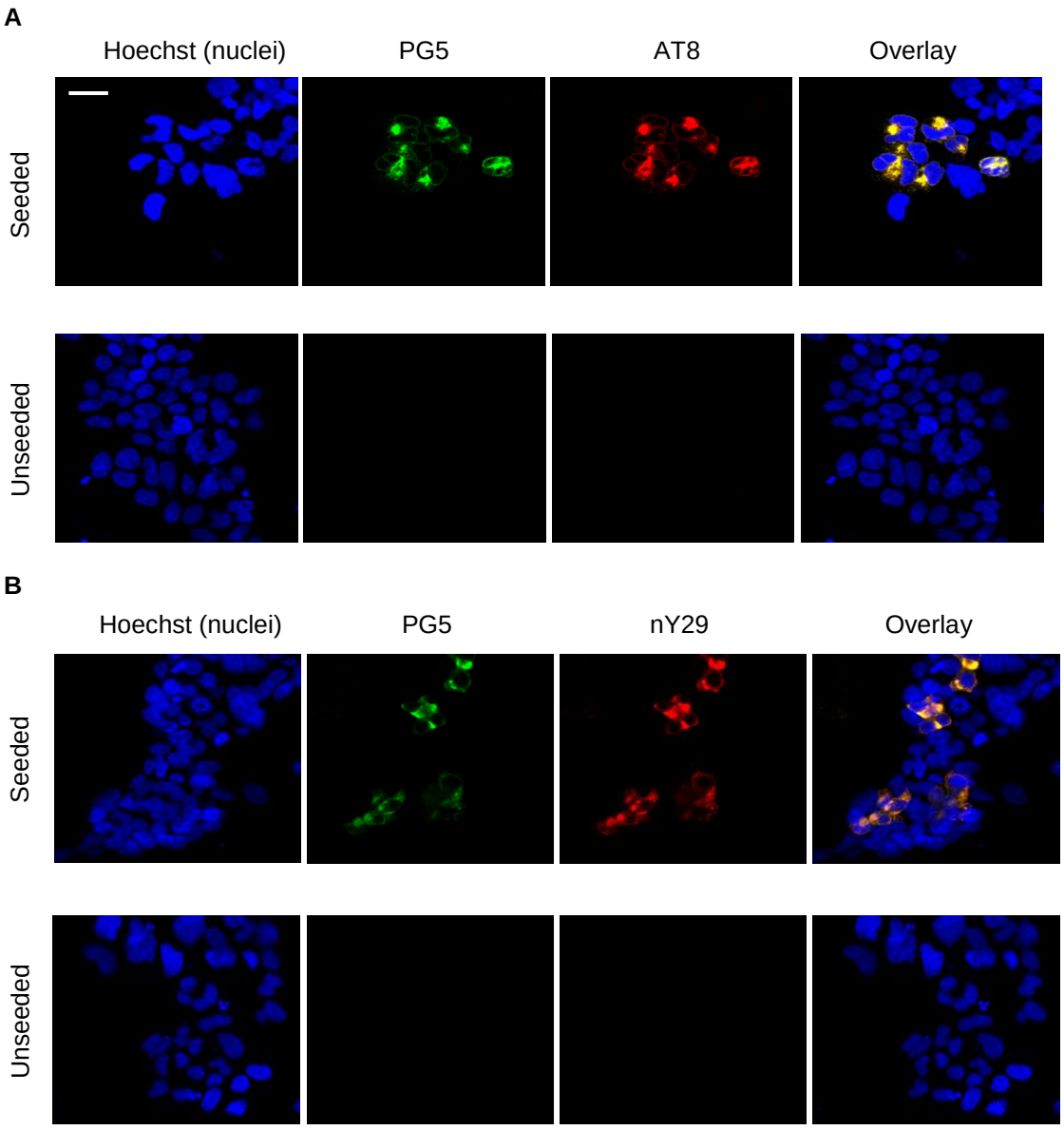

Figure 3.8: **Confocal imaging assay shows modifications at epitopes associated with PHFs.** pS409 (PG5) - positive tau inclusions (green) in inducible HEK T-REx cells expressing human 1N4R P301S tau, following exposure to TgP301S mouse-derived sarkosyl-insoluble material for 3 h followed by 3 days of growth. (A) Colocalization with anti pS202/pT205 tau antibody AT8 (red) is shown. (B) Colocalization with anti nY29 tau antibody (red) is shown. Scale bar 40 µm.

Confocal microscopy experiments comparing the effect of 1 minute treatment with 0.0125% trypsin at room temperature following TgP301S seed treatment revealed that the inoculated TgP301S seed was truly internalized (Figure 3.9).

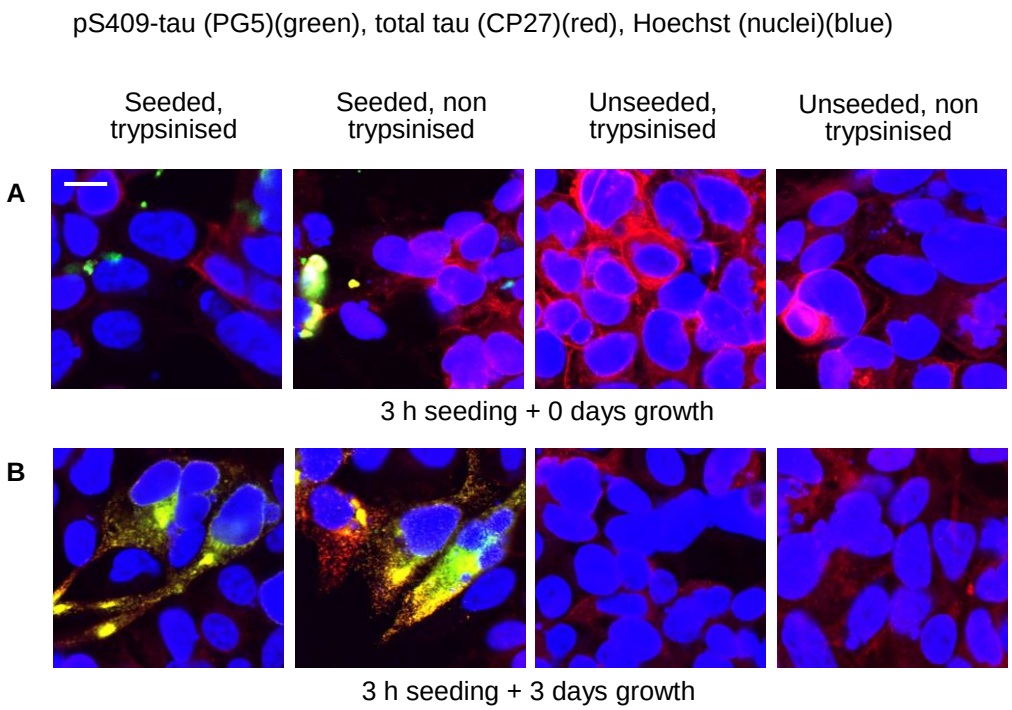

Figure 3.9: Confocal imaging in absence vs presence of trypsin shows that the inoculated TgP301S seed is truly internalized. Confocal imaging showing PG5-positive tau inclusions (tau pS409, green) in HEK T-REx inducible cells expressing P301S 0N4R tau following inoculation with sarkosyl-insoluble TgP301S tau mouse seed for 3 hours, followed by 0 days of grows (A) or 3 days of growth (B). Total tau was visualised with CP27 antibody (red) and the nucleus was visualised with Hoechst (blue). Cells were treated with or without 0.0125% trypsin after seeding. Scale bar 20 µm.

An anti-1N tau antibody was also employed to confirm the endogenous nature of tau aggregates by confocal microscopy (Figure 3.10).

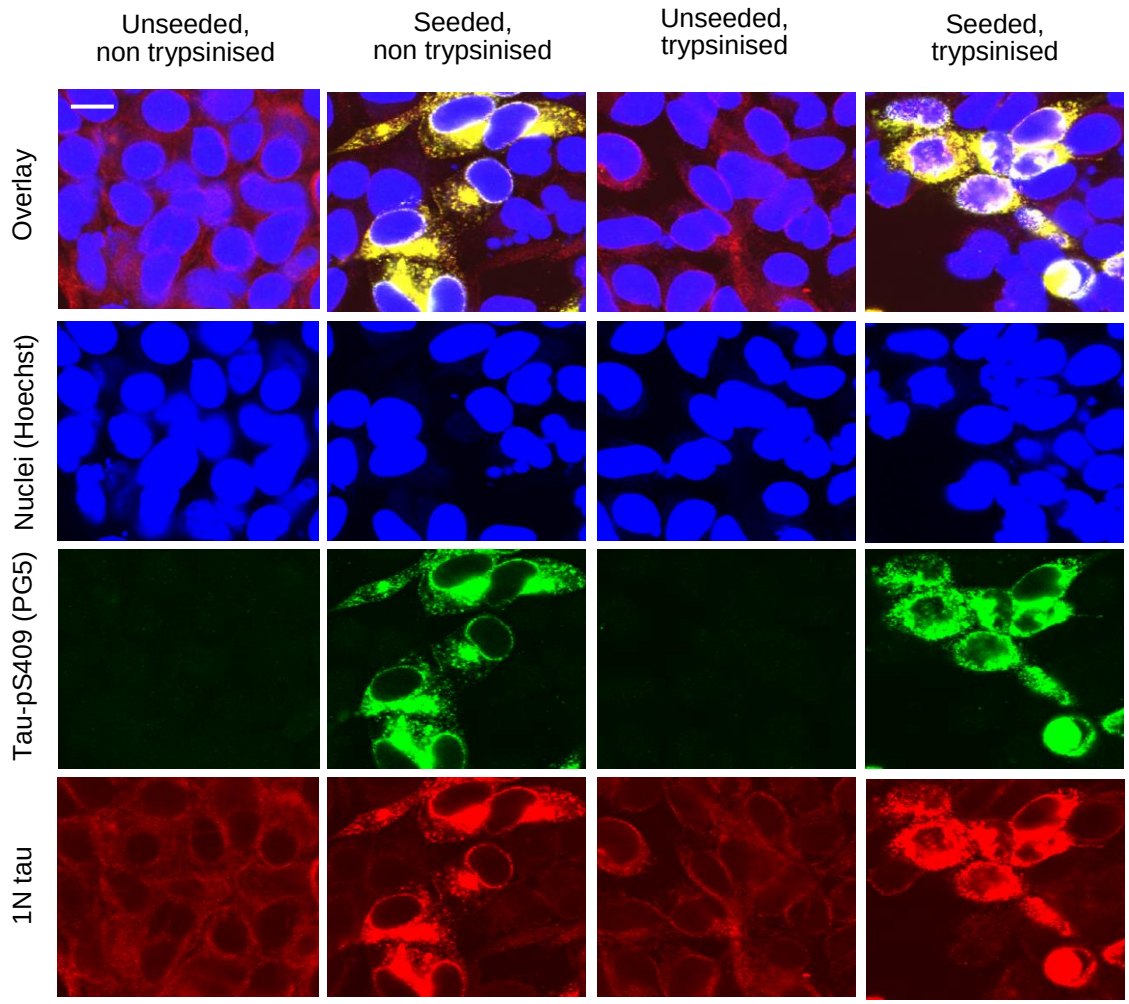

Figure 3.10: Accumulation of endogenous aggregated tau 3 days post-seeding. pS409-positive tau inclusions (PG5, green) in inducible HEK T-REx cells expressing human 1N4R P301S tau, following exposure to TgP301S mouse-derived sarkosyl-insoluble material for 3 h followed by 3 days of growth. Total tau was visualised with an antibody specific for 1N tau (red). Scale bar 20 µm.

In summary, after incubation of HEK T-REx P301S 1N4R tau inducible cells with TgP301S tau seed for 3 hours, followed by 3 days of growth, accumulation of Triton X-100-insoluble endogenous tau was detected by HCI in about 12% of total cells, accompanied by appreciable accumulation of insoluble tau detected by western blot and Alphascreen.

Taken together, these different readouts showed that the sarkosyl-insoluble, native TgP301S tau preparation entered HEK T-REx P301S 1N4R tau-expressing inducible cells and recruited endogenous tau to form intracellular tau fibrils. Upon seed treatment, a dose dependent increase in levels of insoluble AT8-positive tau was observed.

3.5 Discussion on HEK T-REx P301S tau inducible cell-based assay

Aggregation has been well studied in vitro using diverse disease-associated recombinant proteins and proceeds by nucleated growth polymerization, a process that can be accelerated by addition of preformed aggregates or seeds. Recent studies have indicated that aggregation of Aβ42, polyQ peptides, tau and α-synuclein can be induced experimentally by exogenous seeds (Clavaguera et al. 2009, Meyer-Luehmann et al. 2006b, Yang et al. 2002, Yang et al. 2002, Ren et al. 2009, Li et al. 2008, Desplats et al. 2009). Several publications have now demonstrated high efficiency recruitment of soluble tau into authentic NFT-like aggregates in cultured cells, providing unequivocal evidence for the seeding phenomenon in cell models of tauopathies (Guo, Lee 2011, Frost, Jacks & Diamond 2009). In this work, the induction and formation of intracellular aggregates in cell culture presents important differences from these previous studies:

1) We converted a transient cell system into an inducible one, expressing human mutated tau upon addition of tetracycline to the cell media, which increased the robustness of the assay by reducing variability in tau expression, compared to a transient system which relies on transfection reagents.

2) Recombinant aggregated tau (full length or microtubule binding region, MTBR) has been shown to enter cells and recruit endogenous soluble tau into fibrillar tau (Guo, Lee 2011, Frost, Jacks & Diamond 2009, Kfoury et al. 2012, Falcon et al. 2015, Wu et al. 2013). Here we used native tau seed as opposed to recombinant pre-formed fibrils; the sarkosyl-insoluble TgP301S tau extract we introduced into cells contains a heterogeneous mixture of fibrillar species with varying dimensions. We have previously characterized the biophysical properties of these seeding species, showing that sarkosyl-insoluble tau from the brains of TgP301S transgenic mice exhibits increased seeding potency than sarkosyl-insoluble aggregates of recombinant P301S tau (Falcon et al. 2015). Other groups have used native seeds in non-neuronal cells. When Wu et al incubated HeLa cells with sarkosyl extracted, *in vivo*-derived tau filaments from aged rTg4510 mice for 12 h, these were not taken up by cells, likely due to their excessive size; only recombinant oligomers and short fibrils were taken up by their cell system (Wu et al. 2013). Santa-Maria et al showed for the first time that HEK-293T and SHSY5Y cells overexpressing GFP-tagged tau, treated with isolated fractions of human AD-derived PHFs for 24 h developed intracellular GFP-tau aggregates resembling aggresomes, but the signal window of their assay was poor, as PHF-treated cells displayed a 3-fold increase in the content of sarkosyl-insoluble GFP-Tau as compared with non-treated cells (Santa-Maria et al. 2012). Sanders et al. 2014 produced human brain homogenates from distinct tauopathies (AD, CBD, AGD), and transduced IP'ed or crude homogenate into the monoclonal Tet Off-tau RD-YFP HEK293 cell line, used for its relatively high tau RD expression and greater seeding efficacy, and observed a unique inclusion morphology produced by each tauopathy; caveats here were the expression of RD as opposed to full-length tau, and the use of Lipofectamine to deliver seeds into the cells as opposed to spontaneous uptake (Sanders et al. 2014.).

3) The use of protein delivery reagents to enhance introduction of seed into cells has been shown to provide better efficiency of tau seed entry (Guo, Lee 2011), but we opted for a reagent-free inoculation of seed to avoid confounds in characterising the uptake mechanism

and produce a more physiological experimental setting. Indeed, the authors found that protein delivery reagent improved the efficiency of tau pre-formed fibrils entry (from 10% aggregate-bearing cells in absence of reagent to 35% aggregate-bearing cells when seeding in presence of reagent) but they concluded that tau pre-formed fibrils alone are sufficient to recruit endogenous tau into fibrils, and they chose to conduct mechanistic studies on spontaneous uptake of ppfs, in absence of protein delivery reagent.
4) Rather than expressing endogenous tau tagged with a fluorescent protein, which may impair the conformational change required for efficient tau fibril assembly, our system employs untagged tau so that recruitment of endogenous tau is presumably facilitated; despite widespread use of tagged tau constructs in the literature, i.e. FRET biosensor HEK293T cell line ("tau biosensor cells") stably expressing tau repeat domain (RD) fused to either CFP or YFP (Holmes et al. 2014), internal work at Eli Lilly showed greater seeding efficiency in rat cortical neurons expressing endogenously cleavable tau-GFP constructs, as opposed to stable ones. Additionally, our seeding tau is a distinct isoform from our endogenous tau, in order to demonstrate that the intracellular inclusions in our system are composed of recruited, phosphorylated endogenous tau, rather than simply the original tau seed.
5) It has been shown that the MT-binding repeats of tau are both necessary and sufficient for tau aggregation into straight and paired-helical filaments (von Bergen et al. 2000, Gamblin, Berry & Binder 2003), and the repeat domain alone has a higher fibrillogenic tendency than full-length tau (Wille et al. 1992); our model exclusively employs full-length tau, both endogenously and as exogenous seed, providing a more biologically relevant system; recent data also highlighted the fact that a rapid propensity to aggregation in vitro, as observed for the K18 fragment, does not correlate with ability to seed aggregation in cells, as the latter seems to depend on the secondary structure produced by the aggregates (Stohr et al. 2017); since full-length tau aggregates may display greater structural heterogeneity and complexity than short fragments, they may offer more opportunities for interactions with tau protein in cells.

An obvious limitation of cell models of tauopathies, including ours, is their clear temporal discrepancy with neurodegenerative processes in humans, which typically occur only after much longer incubation times. A couple of factors are worth considering: first, the rate-limiting step of protein aggregation is the formation of small assemblies of misfolded proteins, or seeds (nucleation phase)(Friedhoff et al. 1998a, Wood et al. 1999); this nucleation phase is accelerated in our cell model by addition of exogenous seeds, and similarly in animal models where misfolded proteins are directly delivered into the brain, and aggregation is observed within weeks or months; but in aged brains, where misfolded proteins are no longer efficiently cleared by the proteolytic machinery, a slow accumulation of tau seeds in neurons over decades only eventually reaches a critical concentration to initiate a cascade of recruitment and aggregation of soluble tau, initiating a self-perpetuating process of tangle formation; secondly, seeded fibrillization is a concentration-dependent process, and our HEK Trex P301S tau inducible cells overexpress tau, carrying a disease-causing mutation that further promote aggregation, similarly to animal models of mutant tau overexpression, whereas the incubation time is much longer in human tauopathies and other neurodegenerative diseases, where the

disease-associated proteins are not usually upregulated. It will be important to demonstrate robust propagation of templated pathology in non-overexpressing and non-transgenic in vitro and in vivo models which may mimic better the slow progression of tauopathies, however for practical reasons such models will always be an accelerated version of the human diseases.

Another limitation of our cell model is the absence of detectable cell death (see chapter 6); however, cell death was observed when concentrations of tetracycline higher than 1 µg/ml were used to induce tau expression. Other groups similarly reported no obvious cellular toxicity after induction of tau aggregates in cultured cells or tau transgenic mice (Guo, Lee 2014, Clavaguera et al. 2014., Iba et al. 2013, Guo, Lee 2011, Guo, Lee 2013), but there are examples of reported cytotoxicity in cell models. In one publication, HEK-293 cells stably or inducibly overexpressing the longest human tau isoform (htau40) were incubated with varying concentrations of Congo red for 7 days to drive aggregation; viability was detected by ToPro-3 uptake, a fluorescent DNA-intercalating dye taken up by dead but not live cells (Vogelsberg-Ragaglia et al. 2000); tetracycline-inducible cells were treated with or without 10 µM Congo red for up to 4 days (to avoid underestimation of dead cells because of media change); tau overexpression and aggregation induced by Congo red caused a 5.9-fold increase in ToPro-3 fluorescence intensity, compared with non-tau expressing cells grown in the absence of Congo red; in this system, tau aggregation did not cause acute toxicity, but decreased cell viability in a time dependent manner, reaching statistical significance by 4 days in culture (Bandyopadhyay et al. 2007). Another publication used N2a inducible Tet-on cells with overexpressed mutant tau 4-repeat domain, harboring the FTDP-17 mutation K280 ("pro-aggregant" TauRDΔK280) (Wang et al. 2007, Khlistunova et al. 2006), where TauRDΔK280 forms aggregates and causes toxicity. Inhibition of autophagy increased the number of aggregates and exacerbated cytotoxicity (Wang et al. 2009). Activation of autophagy by trehalose reduced endogenous tau, suppressed tau aggregation and reduced cytotoxicity measured by LDH assay in medium; upon trehalose treatment the cytotoxicity induced by Tau_{RD}ΔK expression (~24%) dropped back to baseline (~10%) (Kruger et al. 2012). Elevated levels of tau cause aggregation and toxicity in neurons (Morris et al. 2011), but HEK-293 cells have been shown to tolerate high-level tau overexpression without serious toxicity (Li, Yin & Kuret 2004). Cell toxicity may also be dependent on the tau conformers used to confer seeding or produced from seeding: Sanders et al. generated a monoclonal HEK293 cell line that stably expresses the tau repeat domain fused to YFP (RD-YFP); after induction of aggregation with recombinant fibrils, they selected clonal lines that indefinitely propagate reproducible and unique aggregate structures from one generation to the next. The clones showed a variety of inclusion morphology and size, sedimentation profile, seeding capacity, protease digestion patterns, subcellular localization, as well as cell toxicity; in particular, different clones showed different degrees of cell death as measured by DAPI stain and LDH release, with some clones eliciting cytotoxicity unly upon RD expression (Sanders et al. 2014.). Overall, the occurrence of cell death in a particular cell model seems to depend on tau expression levels and tau strains present in that particular model. The lack of cytotoxicity in our and other models could also be explained by the very nature of seeded fibrillization, whereby addition of exogenous seeds bypasses the slow nucleation phase,

characterised by oligomers/pre-fibrils, which are believed to be more toxic than mature fibrils (Cowan, Mudher 2013, Alonso et al. 2006, Lasagna-Reeves et al. 2012, Maeda et al. 2007).

Our cell based assay also merits further characterisation to corroborate its relevance as a model for tauopathy; for instance, in our publication (Falcon et al. 2015) we have shown by electron microscopy that endogenous tau aggregates formed following seeding are fibrillar, but we have not fully characterised their morphology in term of twist periodicity, flexibility and width of the filaments, to assess their fidelity to the ones observed in human tauopathies; furthermore, we have not estimated tau intracellular concentrations in our cell model, and compared them to physiological tau concentrations in human brains.

In summary, we have established a novel, simple and yet highly reproducible and robust cellular system of tau aggregation. Within the limitation of using non-neuronal cells, our model still provides a system to dissect the mechanisms underlying the propagation of tau protein misfolding. In particular, we used this system to investigate some of the unresolved questions in the field, in particular what mechanisms allow tau uptake and release, and what factors influence seeding efficiency.

4. CHARACTERISATION OF SEED UPTAKE

Here, we wanted to dissect the mechanisms of TgP301S seed uptake in our inducible cell model; we explored the effect of temperature and transfection reagents on seed uptake. To investigate whether endocytosis is the main mechanism of tau uptake in this model, we explored the effect of different endocytosis modulators during seeding. Next, we investigated colocalization between tau seed and endocytic markers (EEA1, CD63) by immunofluorescence. Finally, following the incidental observation of tunnelling nanotubes (TNTs) in our cell model, we characterised them by confocal microscopy and explored the effect of the F-actin-depolymerising compound latrunculin A on tau intercellular propagation.

4.1 Tau seed uptake is enhanced by transfection reagents

Protein delivery/transfection reagents were not used during endocytosis studies as not only could they have affected the analysis, but they were also not required as we have shown that sarkosyl-insoluble TgP301S tau seed can be taken up spontaneously in the absence of protein delivery reagents. Consistent with published literature on the uptake of pre-formed tau fibrils in cell-based models (Guo, Lee 2011), we found that transfection reagents like Lipofectamine 2000 increased the amount of Triton X-100-insoluble tau in TgP301S seed-treated cells in a dose-dependent manner, without inducing accumulation of insoluble tau in unseeded cells (from ~10% cells containing PG5-positive aggregates in absence of Lipofectamine up to ~40% in presence of Lipofectamine) (Figure 4.1).

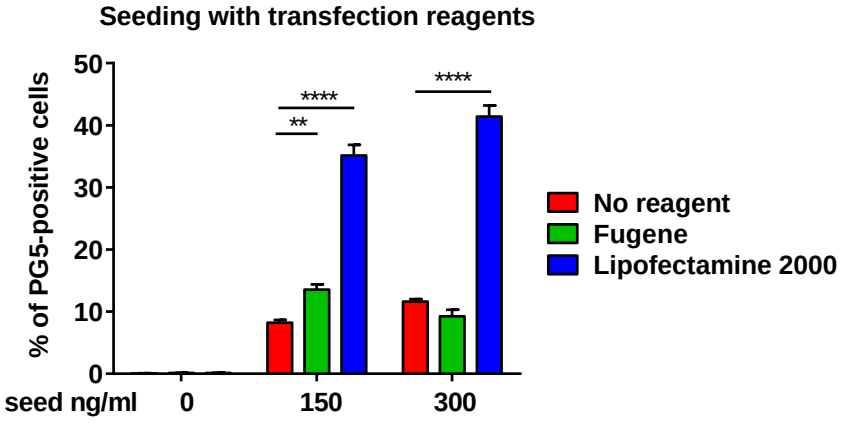

Figure 4.1: Lipofectamine 2000 increases the amount of Triton X-100-insoluble tau in TgP301S seed-treated cells. High content imaging assay showing the % of cells containing PG5-positive tau inclusions in HEK T-REx P301S 1N4R tau inducible cells expressing P301S 0N4R tau following 3 hour inoculation with sarkosyl-insoluble TgP301S tau mouse seed in presence of transfection reagents. Seeding was followed by 3 days growth. Data shown are mean ± SEM (n=2). Statistical analysis: one-way ANOVA with Dunnett's *post hoc* test. *p<0.05, ****p<0.0001, compared with "no reagent" control.

In the case of Lipofectamine, a transfection reagent for DNA transfections, the positive surface charge of the liposomes mediates the interaction of the nucleic acid and the cell membrane, allowing for fusion of the liposome/nucleic acid ("transfection complex") with the negatively

charged cell membrane. The transfection complex is thought to enter the cell through endocytosis, whereby a localized region of the cellular membrane uptakes the DNA/liposome complex by forming a membrane bound/intracellular vesicle. Once inside the cell, the complex must escape the endosomal pathway, diffuse through the cytoplasm, and enter the nucleus for gene expression. It is plausible that the same process also applies to protein delivery. Therefore, increased intracellular tau aggregate formation by transfection aid reagents is likely due to enhanced internalization of TgP301S seed. Taken together, these results show that spontaneous TgP301S seed entry seems to occur at least in part through endocytosis, which can be potentiated by Lipofectamine 2000. For all the remaining experiments we opted for a transfection reagent-free inoculation of seed to avoid confounds in characterising the uptake mechanism and produce a more physiological experimental setting.

4.2 Time course of seeding and post-seeding phase

To examine the progression of TgP301S seed-induced endogenous tau aggregation, we dissected the experimental protocol into a “seeding” phase followed by a “post-seeding growth” phase, and performed a time course of both phases, monitoring the extent of tau aggregation by imaging and biochemical assays. We measured seed-induced 1N4R P301S tau aggregation in HEK T-REx P301S 1N4R tau inducible cells after different lengths of seed incubation at 37°C (10, 30, 60 or 180 minutes), followed by 3 days growth, and after 3 hours of seed incubation at 37°C, followed by different lengths of growth (0, 1, 2 or 3 days). The TgP301S seed was taken up in a time-dependent manner. Both WB (Figure 4.2) and AS (Figure 4.3) showed a difference in the extent of aggregation induced by 10 minutes vs 30 minutes vs 3 h incubation with seed, indicating a time-dependent internalization of TgP301S seed (from 0.2 up to 1 Alphascreen units). The seed-induced aggregation did not increase between the “30 minute seeding” and “60 minute seeding” timepoints, but it did increase further in the “180 minutes seeding” timepoint, suggesting a slow but continuous uptake of TgP301S seed. Similarly to the seeding phase, extending the growth phase up to 3 days led to increasing accumulation of intracellular aggregates (from 0 up to 1 Alphascreen units). 3 hour incubation with TgP301S tau seed at 37°C followed by 3 days growth resulted in the highest incidence of aggregates. Accumulation of AT8-positive insoluble tau aggregates failed to occur when sarkosyl-insoluble tau generated from wt C57Bl6 mice was inoculated into cells (WT seed).

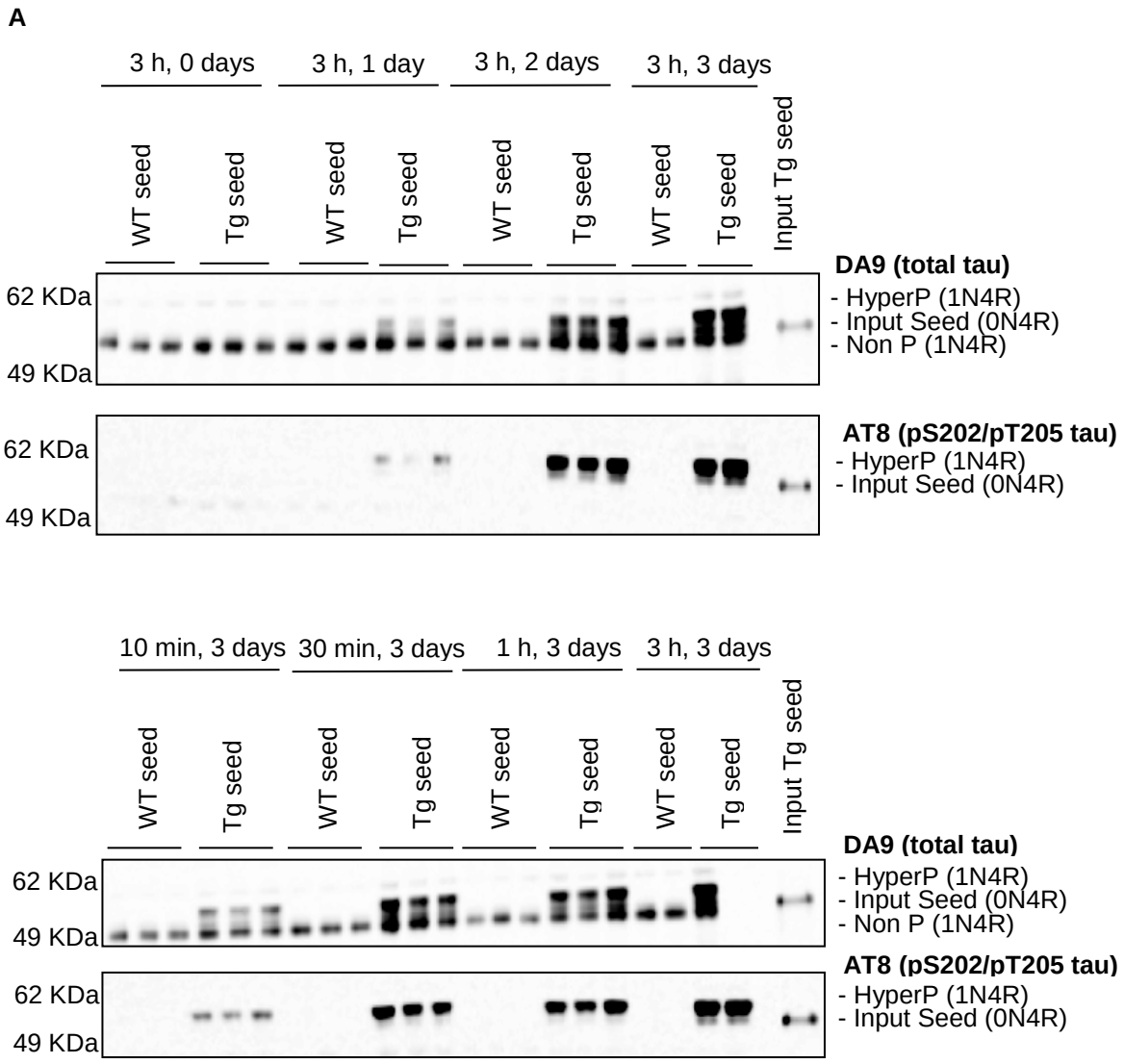

Figure 4.2: Time dependent internalisation and accumulation of aggregated tau in seeded HEK T-REx P301S tau inducible cells. Legend on the next page.

B

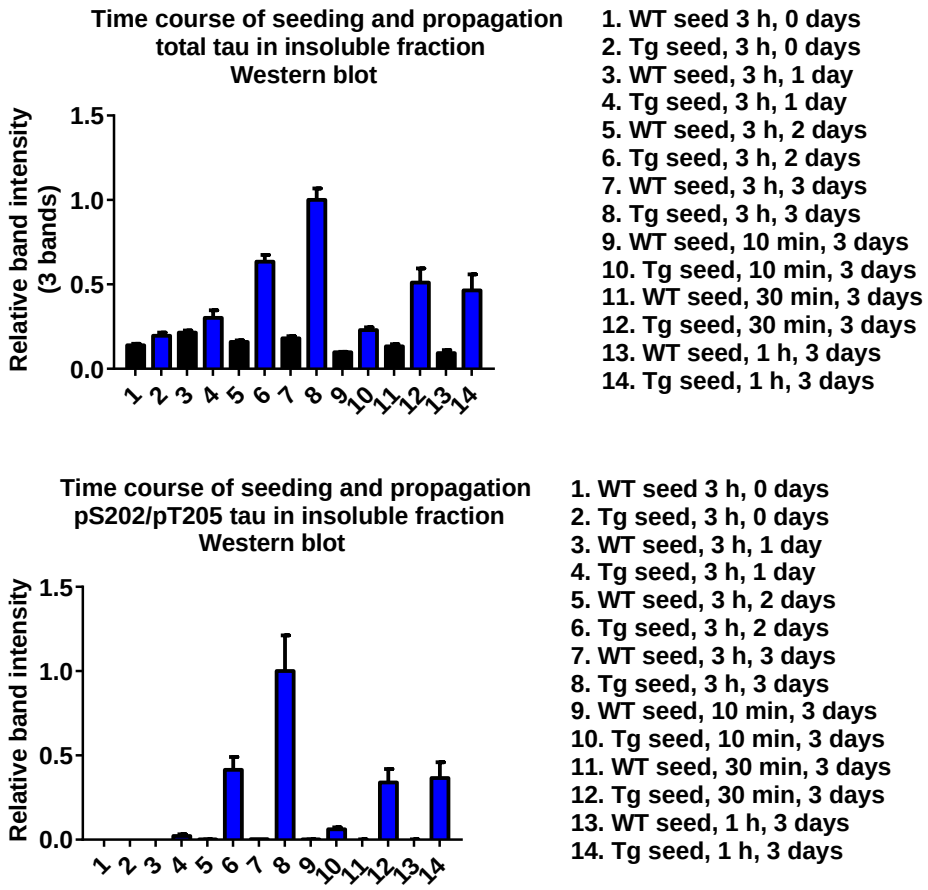

Figure 4.2: Time dependent internalisation and accumulation of aggregated tau in seeded HEK T-REx P301S tau inducible cells. (A) Western blot with total tau antibody DA9 and tau pS202/pT205 antibody (AT8) of the insoluble fraction from HEK T-REx inducible cells expressing P301S 1N4R tau, inoculated with TgP301S mouse sarkosyl-insoluble extract of WT mouse sarkosyl-insoluble extract. For a time course of the seeding phase, cells were seeded for 10, 30, 60 or 180 minutes, followed by 3 days growth. For a time course of the post-seeding phase, cells were seeded for 3 hours followed by 0, 1, 2 or 3 days growth. Residual seed was removed by 0.0125% trypsin for 1 minute at room temperature after seeding. (B) Corresponding densitometry analysis. Data shown are mean ± SEM (n=3).

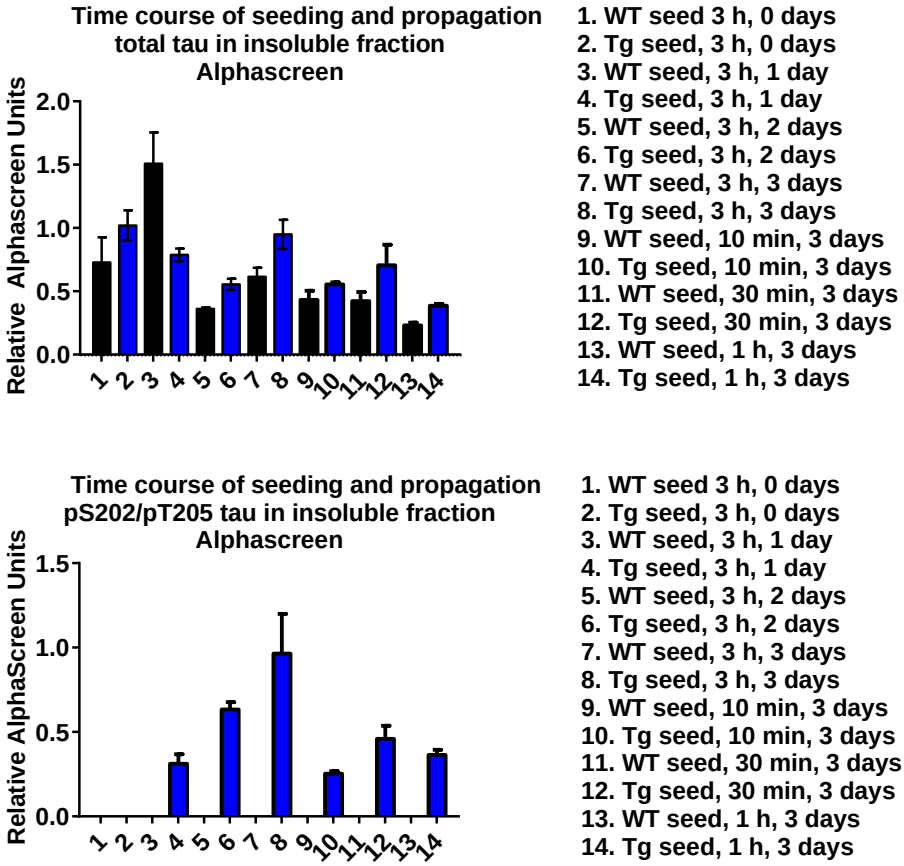

Figure 4.3: Time dependent internalisation and accumulation of aggregated tau in seeded HEK T-REx P301S tau inducible cells. Alphascreen assays showing levels of total tau (capture with DA9, detect with TG5 antibodies) and pS202/pT205 tau (capture with AT8, detect with DA9 antibodies) in the same samples shown in figure 4.2. Data shown are mean ± SEM (n=3).

Alphascreen data for total tau did not mirror the corresponding WB data; this discrepancy may be due intrinsic differences between the two assays, i.e. samples are boiled in presence of 7-13% LDS (lithium dodecyl sulphate) for WB, whereas for Alphascreen they are not denatured; samples are probed with a single antibody (DA9) for WB, whereas for Alphascreen they are recognised by an antibody pair (DA9-TG5).

High-content image analysis showed a difference in the extent of aggregation induced by 3 hours vs 1 hour vs 30 minutes vs 10 minutes of incubation with TgP301S seed (from ~1.5% up to ~12% aggregate-bearing cells) indicating a time-dependent internalization (Figure 4.4). 1 day after seed inoculation, focal inclusions were not frequent, and Triton X-100-insoluble tau was found in about 6% of total cells; 2 days after seeding, about 8% of the cells showed PG5 immunoreactivity, and 3 days after seed treatment, about 12% of total cells were presenting PG5-positive Triton X-100-insoluble tau inclusions. As a control, cells were treated with either Optimem alone or with sarkosyl-insoluble tau extract generated from wt C57Bl6 mice; under

these conditions, phosphorylated tau recognized by antibody PG5 (tau pS409) was completely soluble and extracted by 1% Triton X-100 during fixation.

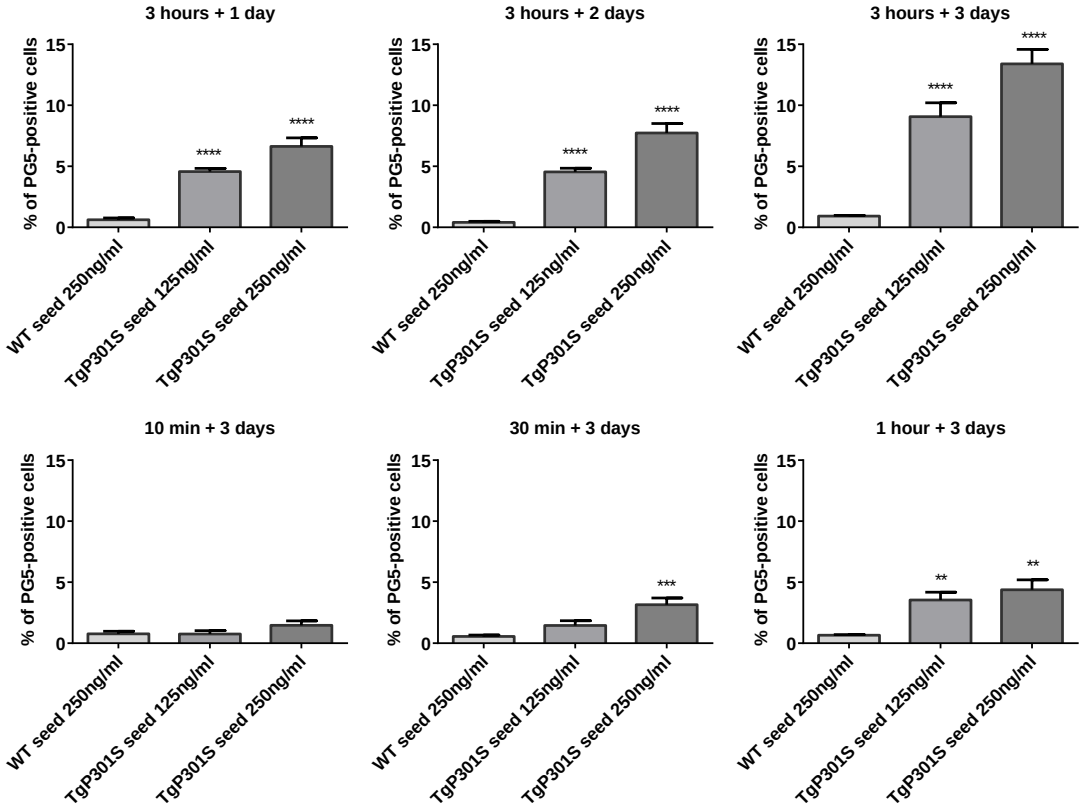

Figure 4.4: Time dependent internalisation and accumulation of aggregated tau in seeded HEK T-REx P301S tau inducible cells. High content imaging assay showing the % of cells containing PG5-positive tau inclusions in HEK T-REx P301S 1N4R tau inducible cells expressing P301S 1N4R tau following inoculation with TgP301S mouse sarkosyl-insoluble extract or WT mouse sarkosyl-insoluble extract for 10, 30, 60 or 180 minutes, followed by 3 days growth, or inoculation for 3 hours followed by 1, 2 or 3 days growth. Residual seed was removed by 0.0125% trypsin for 1 minute at room temperature after seeding. Data shown are mean ± SEM (n=2). Statistical analysis: one-way ANOVA with Dunnett's *post hoc* test. *p<0.05, ****p<0.0001, compared with WT seed control.

Observation by confocal microscopy of cells inoculated with mutant TgP301S tau aggregates for 3 hours and grown for increasing lengths of time showed that internalized aggregates increased in size over time (Figure 4.5). The time course post-seeding showed that 1 day after the incubation with TgP301S seed, a small percentage of cells started showing accumulations of Triton X-100-insoluble tau (PG5); 2 days post-seeding, more cells developed aggregates, and 3 days post-seeding, PG5-positive aggregates were more frequently seen. Quantification was not preformed on confocal images as the % of cells with PG5-positive aggregates was measured by high-content imaging assay.

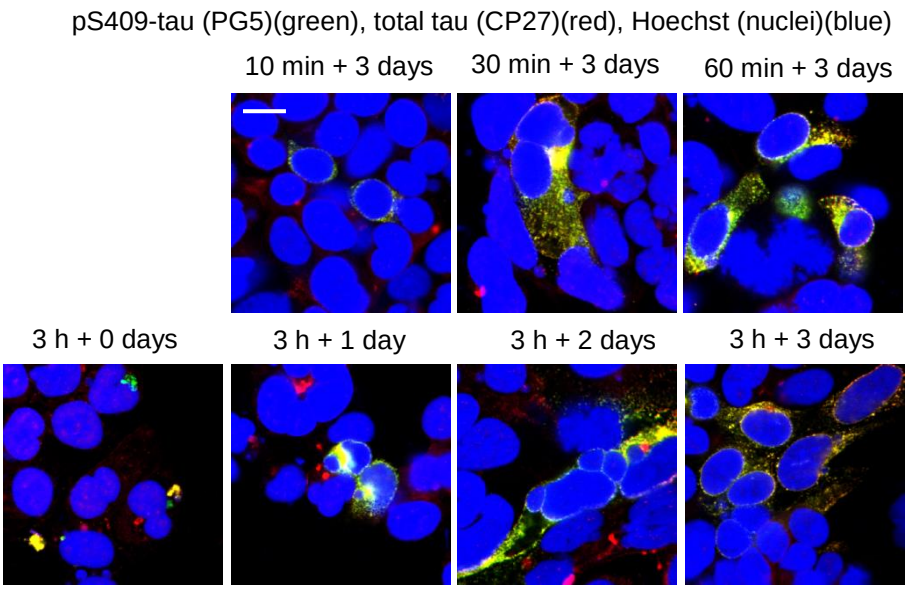

Figure 4.5: Confocal imaging shows time-dependent development of Triton X-100-insoluble tau aggregates. PG5-positive tau inclusions (tau pS409, green) in HEK T-REx inducible cells expressing P301S 1N4R tau following inoculation with TgP301S sarkosyl-insoluble extract for 10, 30, 60, 180 minutes, followed by 3 days growth, or inoculation for 3 hours followed by 0, 1, 2, 3 days growth. Total tau was visualised with CP27 antibody (red) and the nucleus was visualised with Hoechst (blue). Soluble proteins were extracted by 1% Triton X-100 during fixing. Scale bar 20 µm.

Both biochemical and imaging readouts suggest that seed internalisation and formation of endogenous aggregates after seeding are time-dependent processes.

4.3 Spontaneous seed uptake occurs by endocytosis as it is sensitive to temperature

To further investigate whether seed uptake is mediated by endocytosis, we incubated HEK T-REx P301S 1N4R tau inducible cells with sarkosyl-insoluble TgP301S tau seed for 3 hours at either 37°C or 4°C to block endocytosis, a temperature-dependent mechanism (Guo, Lee 2011). As an indirect readout of seed entry, we quantified insoluble endogenous tau aggregates produced by the cells 3 days after seeding.

By high-content imaging, TgP301S sarkosyl-insoluble tau seed incubation at 37°C for 3 hours followed by an additional 3-day incubation resulted in ~8% of total cells containing PG5-positive Triton X-100-insoluble tau, whereas 3 hours of seed incubation at 4 °C followed by exactly the same treatment resulted in a significant reduction of cells containing tau aggregates (~3%), suggesting that tau seed uptake is a temperature-dependent process (Figure 4.6 A). A 3 hour treatment with tau seed at 37°C but not at 4°C, followed by 3 days growth, resulted in detectable Triton X-100-insoluble aggregates. Minimal aggregation was observed with 3 hours of seed treatment at 4°C, followed by 3 days growth. Quantification from Alphascreen and western blot experiments reproduced a significant reduction (~50%) in aggregate-bearing cells when 3-hour seeding was performed at 4°C instead of 37°C (Figure 4.6 B, C).

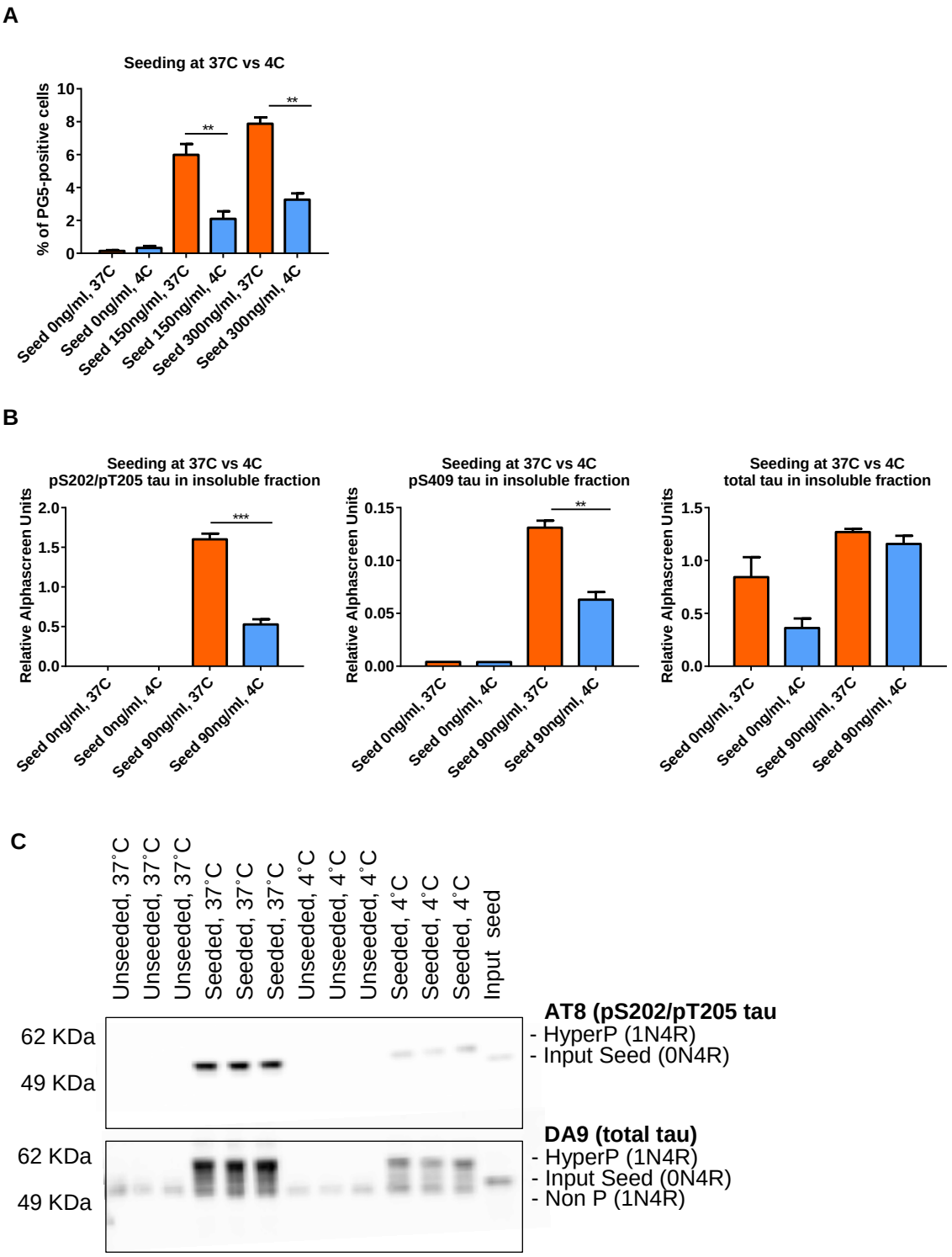

Figure 4.6: Seed uptake is a temperature-dependent process. (A) High-content imaging assay showing the % of cells containing PG5-positive tau inclusions in HEK T-REx inducible cells expressing P301S 1N4R tau following 3 hour inoculation with TgP301S mouse sarkosyl-insoluble extract at 37˚C vs 4˚C, and 3 days growth. Data shown are mean ± SEM (n=2). Statistical analysis: t test comparing 37˚C vs 4˚C. (B) Alphascreen assays showing levels of total tau (DA9-TG5 antibodies) or hyperphosphorylated tau (pS202/pT205-tau, AT8-DA9 antibodies; pS409-tau, PG5-DA9 antibodies) in the insoluble fraction of HEK T-REx inducible cells expressing P301S 1N4R tau following 3 hour inoculation with TgP301S mouse sarkosyl-

insoluble extract at 37˚C vs 4˚C, and 3 days growth. Statistical analysis: t test comparing 37˚C vs 4˚C. (C) Western blot with total tau antibody (DA9) and tau pS202/pT205 antibody (AT8) on the same samples. Data shown are mean ± SEM (n=2).

4.4 Endocytosis inhibitors reduce seed-induced tau aggregation by impairing spontaneous seed uptake

Having shown that sarkosyl-insoluble TgP301S tau extract efficiently penetrates inside cells, we explored this phenomenon further by systematically examining which of the various endocytic pathways contributed to the uptake of mutant tau aggregates. HEK T-REx P301S 1N4R tau inducible cells were incubated with TgP301S seed, without transfection reagent, and in the presence of concentration of compounds known to inhibit specific endocytic pathways (Munch, O'Brien & Bertolotti 2011); cells were further grown for 3 days, fixed and examined by high-content imaging assay to measure the % of aggregate-bearing cells (Figure 4.7).

To determine whether tau seed penetrates inside the cells via an active process, cells were exposed to sodium azide and 2-deoxyglucose (Munch, O'Brien & Bertolotti 2011) to deplete cellular ATP prior to the exposure to aggregates. ATP-depletion reduced the % of cells with aggregation by 30% at 10 μM (Figure 4.7 A). To determine whether tau seed penetrates inside the cells via a dynamin-dependent mechanism, cells were exposed to dynasore (Munch, O'Brien & Bertolotti 2011) prior to and during the exposure to aggregates. This treatment did not affect seed uptake, apart from a 30% reduction at 1 mM (Figure 4.7 B). To determine whether tau seed penetrates inside the cells via a clathrin-dependent mechanism, cells were exposed to chlorpromazine (Munch, O'Brien & Bertolotti 2011) prior to and during the exposure to aggregates. The highest concentrations 30 μM, 10 μM reduced tau uptake by 30% (Figure 4.7 C). To determine whether tau seed penetrates inside the cells via macropinocytosis, cells were exposed to 5-(N-Ethyl-N-isopropyl)amiloride (EIPA) (Munch, O'Brien & Bertolotti 2011) to inhibit Na+/H+ transport prior to and during the exposure to aggregates. This treatment attenuated the internalization of seed by 50% at the highest concentrations 100 μM, 33 μM (Figure 4.7 D).

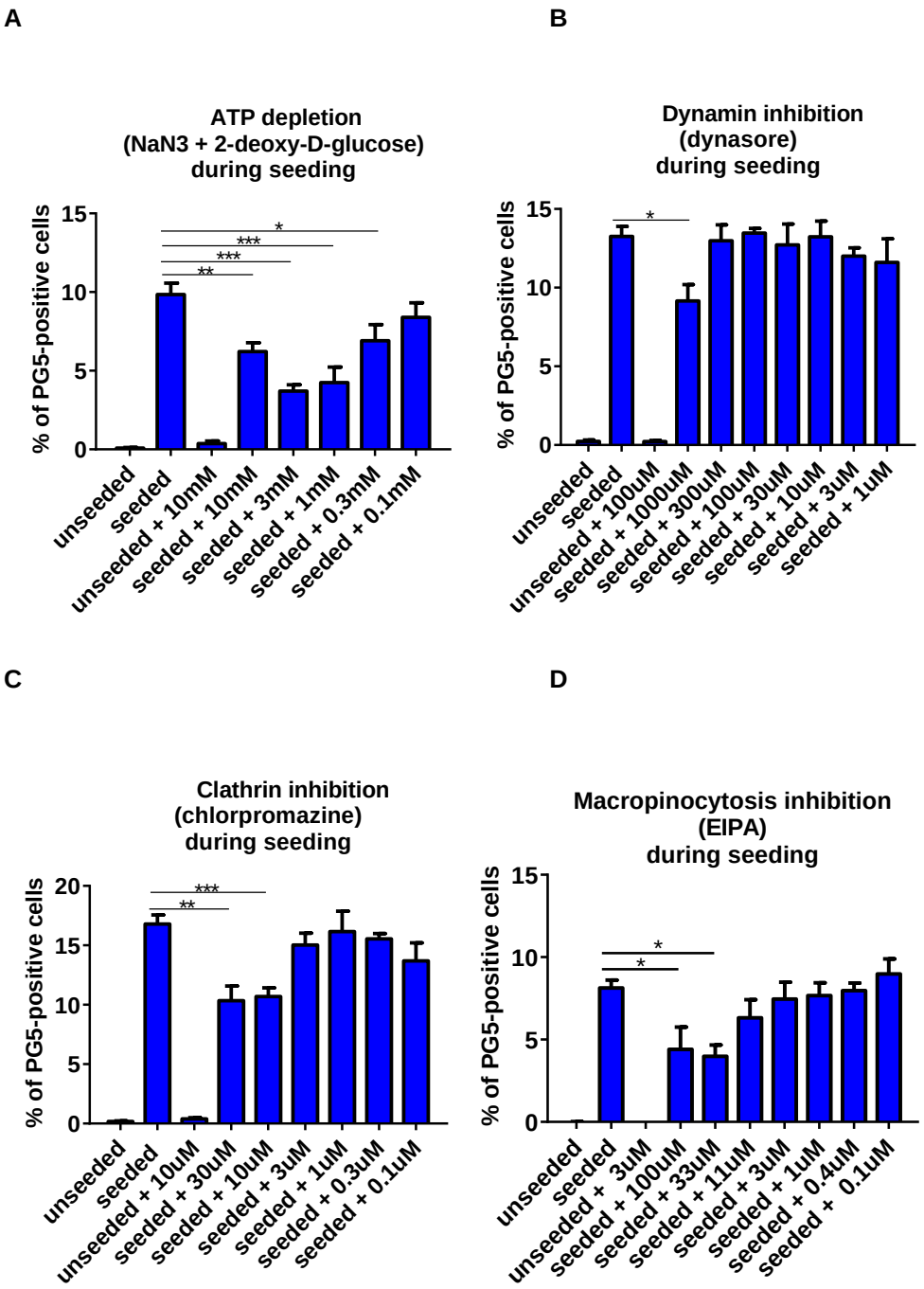

Figure 4.7: Endocytosis inhibitors reduce tau aggregates uptake. High content imaging assay showing the % of cells containing PG5-positive tau inclusions in HEK T-REx inducible cells expressing P301S 1N4R tau, inoculated with TgP301S mouse seed sarkosyl-insoluble extract for 2-3 hours in conditions of (A) ATP-depletion (sodium azide and 2-deoxyglucose were added 2.5 h prior to and during exposure to aggregates); (B) dynamin inhibition (dynasore was added 30 minutes prior to and during exposure to aggregates); (C) clathrin inhibition (chlorpromazin was added 30 minutes prior to and during exposure to aggregates); (D) macropinosomes inhibition (EIPA was added 30 minutes prior to and during exposure to aggregates). Seeding was followed by 3 days growth. Data shown are mean ± SEM (n=2). Statistical analysis: one-way ANOVA with Dunnett's *post hoc* test. *p<0.05, ****p<0.0001, compared with untreated control.

To further dissect the uptake mechanism and allow a more direct measure of seed uptake, we repeated the treatment with EIPA during seeding, but fixing the cells straight after seeding, as opposed to allowing further 3 days of growth. Again, in this experimental system, EIPA treatment markedly attenuated the internalization of seed by 50% at the highest concentrations 100 µM, 33 µM (Figure 4.8).

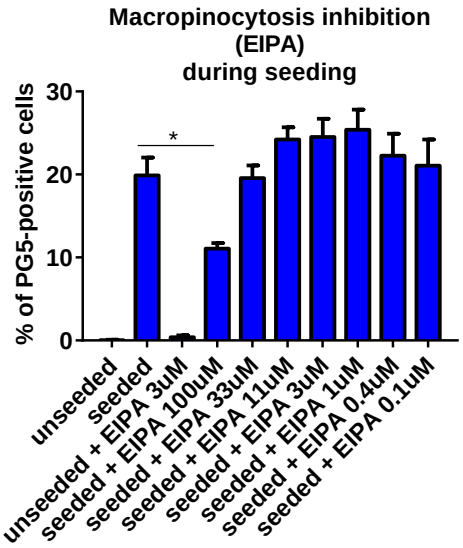

Figure 4.8: Tau aggregates enter cells by macropinocytosis. High content imaging assay showing the % of cells containing PG5-positive tau inclusions in HEK T-REx inducible cells expressing P301S 1N4R tau, inoculated with TgP301S mouse sarkosyl-insoluble extract for 3 hours in conditions of macropinocytosis inhibition (EIPA was added 30 minutes prior to and during exposure to aggregates). Cells were fixed straight after seeding. Data shown are mean ± SEM (n=2). Statistical analysis: one-way ANOVA with Dunnett's *post hoc* test. *p<0.05, ****p<0.0001, compared with untreated control.

4.5 Tau aggregates are transferred along the endosome/lysosome pathway

Dysfunction of the endosomal-lysosomal pathway causes the earliest known neuronal pathology in AD and is promoted by genetic factors that cause early-onset AD or increase risk of late-onset AD. The earliest disease-specific pathologic change in sporadic AD – appearing before beta-amyloid is deposited in the neocortex, and before the appearance of NFTs – is the enlargement of Rab5- and Rab7-positive neuronal endosomes, which reflects a pathological acceleration of endocytosis (Nixon, Yang 2011).

To determine whether aggregates were processed via the endocytic pathway, cells were inoculated with mutant tau aggregates for various periods of time (from 10 minutes to 24 hours), then fixed with 4% PFA/0.1% Triton X-100 and stained for tau (PG5 antibody), EEA1 (early endosome marker, (Filimonenko et al. 2007) (Figure 4.9 A) and CD63 (late endosome marker, (Kobayashi et al. 2000) (Figure 4.9 B).

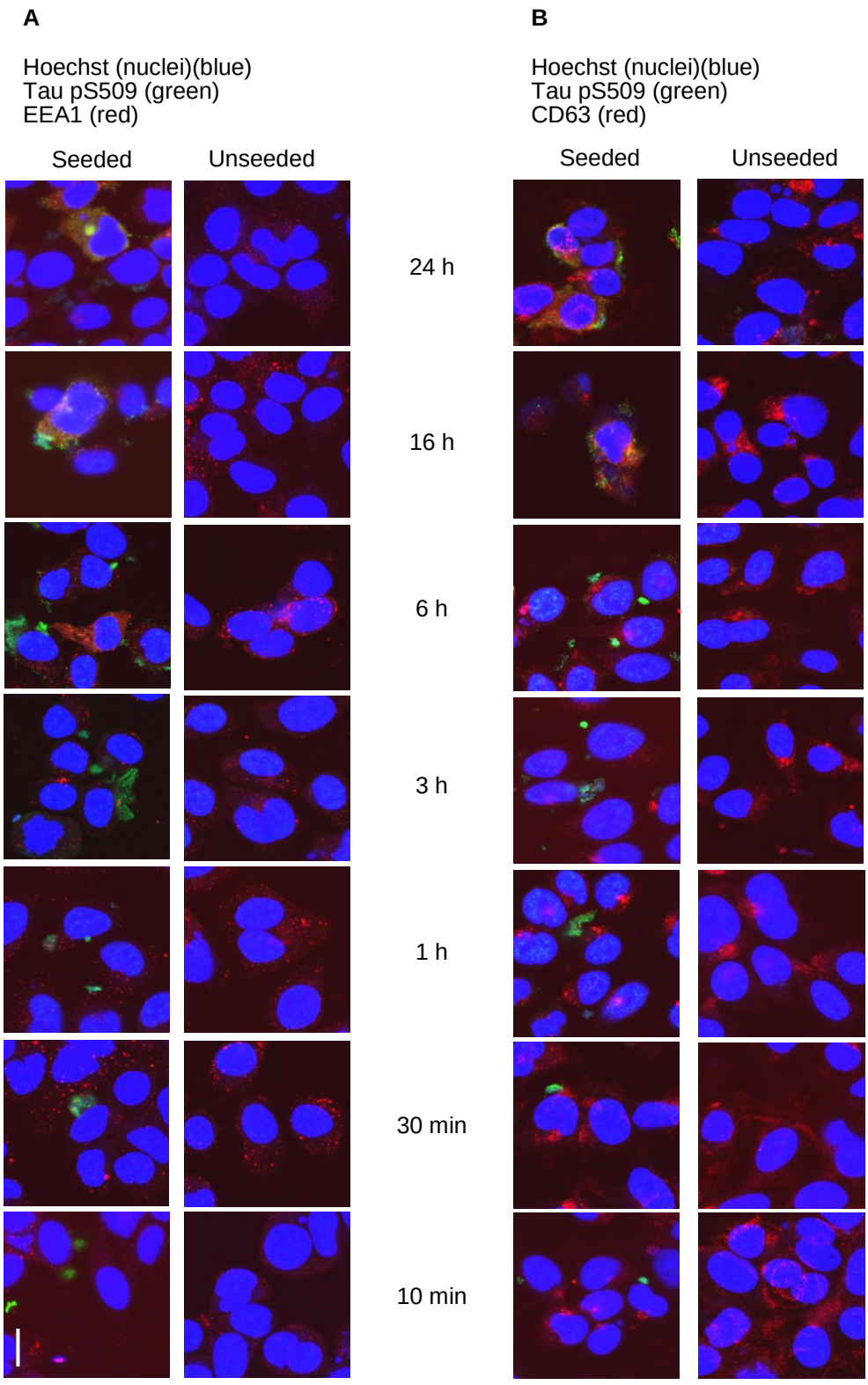

Figure 4.9: Tau aggregates colocalize with markers of the endocytic pathway. Confocal micrographs of cells after inoculation with TgP301S tau aggregates in a time-course fashion before trypsinization to remove residual seed, fixation with 4% PFA and permeabilization with 0.1% Triton X-100. Nuclei were stained with Hoechst (blue). Tau aggregates were immunostained with PG5 antibody (green). (A) Early endosomes were immunostained with a

specific antibody (EEA1, red). (B) Late endosomes were immunostained with a specific antibody (CD63, red). Scale bar 20 μm.

The colocalization of TgP301S seed with early endosomal marker EEA1 and late endosomal marker CD63 was evident at 16 and 24 hours after inoculation, indicating that tau seeds can be internalized into endocytic vesicles, and possibly escape the endocytic compartment to seed aggregation of the endogenous protein.

4.6 Discussion on seed uptake in HEK T-REx P301S tau inducible cells

This study reveals that aggregates of the FTDP17-causing P301S tau mutant penetrate inside P301S tau-expressing cells and trigger aggregation of the endogenous mutant protein. By high-content imaging assay, as little as 10 minute incubation with TgP301S seed led to detectable accumulation of Triton X-100-insoluble PG5-positive tau; the presence of tau inclusions after such a short incubation with seed is suggestive that internalization of minute quantities of seed is sufficient to induce recruitment of endogenous tau into inclusions, even in the absence of any transfection reagent. Substantial aggregation of soluble tau can be induced by spontaneous uptake of TgP301S seed, which seems to occur via endocytic pathways that are temperature-, time- and ATP-dependent, can be potentiated by transfection reagents and impaired by pharmacological agents. No complete abolition of seed uptake was observed when blocking endocytosis by seeding at 4˚C; this suggests that seed entry may not occur exclusively by endocytosis; another possible explanation for the small number of cells with tau aggregates still detected after 4 °C incubation with seed could be due to the ongoing internalization of residual membrane-associated fibrils during the post-seeding phase.

Fluid-phase endocytosis is a low efficiency, non-specific process that involves the bulk uptake of solutes in exact proportion to their concentration in the extracellular fluid. Alternative processes are absorptive endocytosis, where molecules are bound to the cell surface and concentrated before internalization, and receptor-mediated endocytosis, where molecules bind to cell surface receptors and become concentrated before internalization. Depending on the composition of the coat, the size of the membrane-bound, intracellular vesicles, and the fate of the internalized cargo, endocytosis can occur by macropinocytosis, caveolar endocytosis, clathrin-mediated endocytosis, and clathrin/caveole-independent endocytosis (Khalil et al. 2006).

We used the dynamin inhibitor dynasore and the clathrin inhibitor chlorpromazine to probe the clathrin-mediated pathways, since dynamin proteins are GTPases that are essential for budding of clathrin vesicles from the plasma membrane (Urrutia et al. 1997). Dynasore reduced tau uptake only at 1 mM; other groups did not observe tau uptake inhibition by dynasore, but their experimental settings were different: Holmes et al used dynasore at lower concentration (80 μM) in a different cell line (Holmes et al. 2013.); Munch et al used dynasore at lower concentration (100 μM) in a different cell line, to inhibit SOD1 uptake and not tau (Munch, O'Brien & Bertolotti 2011)); Wu et al pre-treated cells with 80 μM dynasore to probe for

dynamin-specific endocytosis and 30 µM Pitstop 2B to probe for clathrin-specific endocytosis, but their data suggested a dynamin-dependent, clathrin-independent mechanism (Wu et al. 2013); Calafate et al. treated their mammalian-neuronal mixed culture cell system with 0.3, 1, 3 µM of both dynasore and the more specific dynamin inhibitor JNJ (Gordon et al. 2013) and reported a reduction, but not complete abrogation of tau pathology propagation at 1, 3 µM, suggesting that other routes are contributing to this process (Calafate et al. 2016). Chlorpromazine reduced tau uptake at 30 µM, and again other groups that did not see effect of chlorpromazine used it at lower concentrations (5 µM) in a different cell line, to inhibit SOD1 uptake and not tau (Munch, O'Brien & Bertolotti 2011). In summary, we only saw inhibitory effects of dynasore and chlorpromazine at high concentrations, which could elicit non-specific effects, but we cannot exclude that the clathrin-dependent pathway plays a role in tau aggregates uptake.

Wu et al. reported that exogenously added recombinant (heparin-induced) tau low-MW aggregates (dimers/trimers) and small fibrils (40-250 nm), but not monomeric tau or long fibrils, are internalized via bulk endocytosis in neurons at the somatodendritic compartment or the axon terminals, and transported anterogradely and retrogradely; the internalized aggregates are transported in endosomal vesicles and later trafficked through the endosomal pathway to the lysosomes: 6 hours post-addition, internalised tau aggregates co-localised with dextran, marker of bulk endocytosis, and later (12 hours) they co-localised with endolysosomal markers (Rab5, a GTPase that is enriched in early endosomes; lysosomal-associated membrane protein 1 (LAMP1); substrate DQ-BSQ) in neurons and HeLa cells (Wu et al. 2013). We used specific antibodies for EEA1, marker for early endosomes, and CD63, marker of lysosomes, to further interrogate the endocytic pathway, and we observed colocalisation with tau seeds from 16 h onwards; moreover, in our recent publication, we observed co-localization of TgP301S tau aggregates and recombinant P301S tau aggregates with dextran after 1 hour as shown by immunofluorescence with HT7 antibody (Falcon et al. 2015); for a thorough investigation, other markers should also be investigated (Rab5 for early endosomes, Lamp1, DB-BSQ for lysosomes) (Wu et al. 2013); using higher doses of tau seeds, as well as quantitatively measuring the dyes colocalisation, could potentially allow us to determine whether colocalisation with endocytosis markers occurs at earlier timepoints.

Macropinocytosis is the actin-driven invagination of the cell membrane to form large endocytic vesicles of irregular shape and size, which then travel into the cytosol and fuse with endosomes and lysosomes. Macropinosomes are large vesicles characterised by a diameter of up to 2.5 µm (Khalil et al. 2006). The dose-dependent effect on seed uptake we observed with EIPA in our system is not conclusive, but it is suggestive that macropinocytosis is the prevalent mechanism of tau uptake. The following are further experiments we could carry out to confirm this: 1) Estimate the size of the endocytic vesicles containing tau aggregates by confocal microscopy to confirm whether they had a diameter consistent with macropinosomes (> 1 µm), and larger than other endocytic vesicles (Holmes et al. 2013.); 2) Macropinocytosis is an actin-dependent process which requires actin rearrangement to create lamellipodia-like membrane protrusions; cells could be stained with fluorescently-tagged phalloidin to label filamentous actin to show its

engulfment of tau inclusions (Holmes et al. 2013.); 3) HIV-derived transactivator of transcription (TAT) peptide is a known substrate of macropinocytosis; cells could be co-treated with fluorescently-labelled TAT and tau seeds to show their co-localisation (Holmes et al. 2013.). In our recent publication (Falcon et al. 2015) we also showed that native TgP301S tau aggregates enter cells through the same mechanism as recombinant P301S tau aggregates, consistent with macropinocytosis, as it inhibited by 100 μM EIPA. Therefore, like SOD1 aggregates (Munch, O'Brien & Bertolotti 2011), PrP^{sc} (Magalhaes et al. 2005) several viruses (Mercer, Helenius 2009), recombinant tau (Holmes et al. 2013., Frost, Jacks & Diamond 2009, Falcon et al. 2015) and perhaps other prion-like aggregates, we have observed that native TgP301S tau aggregates can hijack macropinocytosis to penetrate into the cytosol of host cells.

There is now in vitro and in vivo evidence that pathological tau can transfer inter-cellularly and transmit a misfolded state to cytosolic soluble tau (Hasegawa, Nonaka & Masuda-Suzukake 2017). Here, we established a cell model that allowed us to study the mechanisms of tau uptake and will allow us to assess therapeutic strategies with a potential to affect disease progression. Further studies will be required to fully describe the tau species involved in cellular uptake and determine the best molecular targets to prevent internalisation of tau misfolded seeds.

4.7 Nanotubes in cell culture: a potential mechanism of tau transmission?

Tunneling nanotubes (TNTs), a cell-to-cell communication between animal cells based on the formation of thin membrane channels, were first reported in cultures of rat pheochromocytoma (PC12) cells (Rustom et al. 2004); similar TNT-like connections were subsequently identified for several permanent cell lines and primary cultures (Gerdes, Bukoreshtliev & Barroso 2007). Typical TNTs connecting PC12 cells have a 50–200 nm diameter, can stretch to lengths up to several cell diameters, interconnecting cells at their nearest distance (Rustom et al. 2004, Hodneland et al. 2006) and appear to be floating in the medium without contact to the substratum, unlike other cellular protrusions. Structurally, F-actin is the prominent cytoskeleton component of TNTs between PC12 cells, but no microtubules are present. At the ultra-structural level, the TNTs surface membrane is shown to connect seamlessly with the plasma membranes of the connected cells. TNTs structural integrity is sensitive to mechanical and chemical stress, as well as prolonged light exposure (Gurke, Barroso & Gerdes 2008).

Thin tau-positive channels interconnecting cells were visualised by confocal microscopy in both TgP301S-seeded and unseeded cells in our inducible cell model; to ascertain that such structures were bona fide TNTs, their architecture was explored further: by immunofluorescence they appeared to be tau- and F-actin-positive (Figure 4.10), and a z-stack showed that they were stretched between interconnected cells attached at their nearest distance and did not contact the culture surface (Figure 4.11).

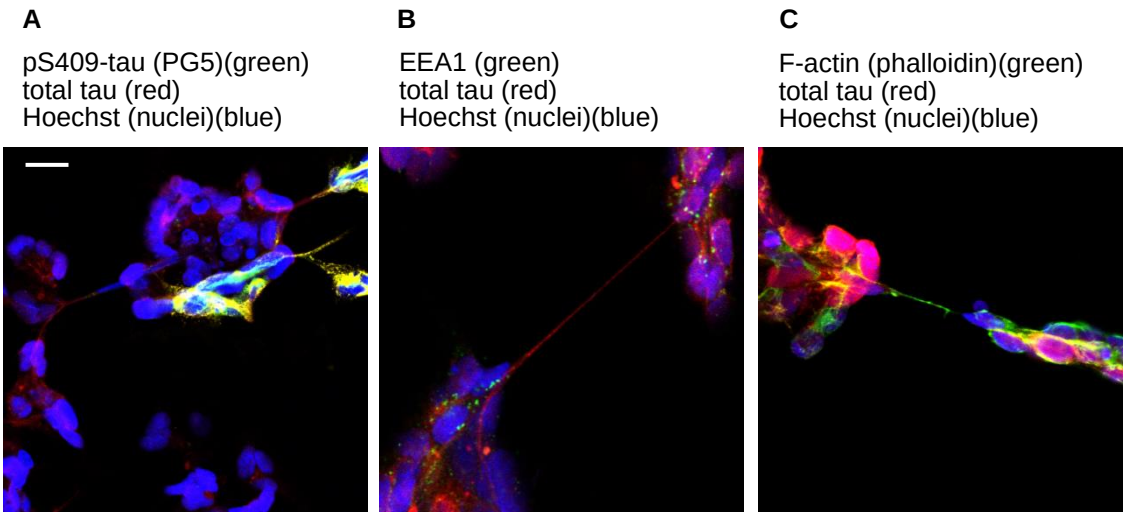

Figure 4.10: Confocal imaging shows tau-positive TNTs in cell culture. Confocal imaging showing TNTs in HEK T-REx P301S 0N4R tau inducible cells following inoculation with sarkosyl-insoluble P301S tau mouse seed for 3 hours, followed by 3 days growth. (A) Total tau was visualised with CP27 antibody (red), pS409-tau with PG5 antibody (green) and the nucleus with Hoechst (blue). (B) Total tau was visualised with CP27 antibody (red), early endosomes with EEA1 antibody (green) and the nucleus with Hoechst (blue. (C) Total tau was visualised with CP27 antibody (red), F-actin with phalloidin-AlexaFluor488 (green) and the nucleus with Hoechst (blue). TNTs positively stained for pS409-tau (PG5), total tau (CP27), and F-actin (phalloidin-AF488). Scale bar 40 μm.

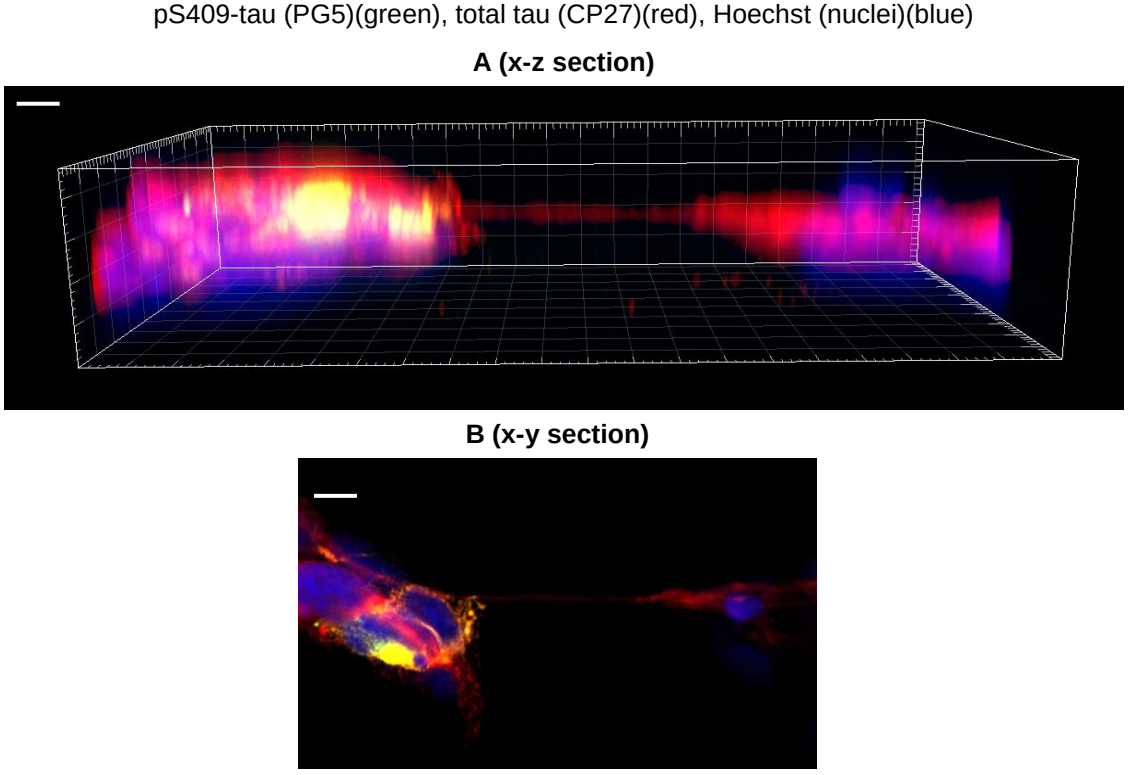

Figure 4.11: Confocal imaging shows tau-positive TNTs in cell culture. Confocal imaging showing an x-z section (A) and an x-y section (B) of a TNT in HEK T-REx P301S 1N4R tau

inducible cells following inoculation with sarkosyl-insoluble P301S tau mouse seed for 3 hours, followed by 3 days growth. Total tau was visualised with CP27 antibody (red), pS409-tau with PG5 antibody (green) and the nucleus with Hoechst (blue). Z-stack taken with a 40X objective, 0.5 µm slices, 1024x1024 pixels. Scale bar (A) 5 µm (B) 40 µm.

TNTs were shown to mediate membrane continuity between connected cells and facilitate the intercellular transport of cargo: organelles, cytoplasmic molecules, membrane components (Gerdes, Bukoreshtliev & Barroso 2007), mitochondria (Koyanagi et al. 2005) and pathogens like viruses and bacteria have been shown to exploit cellular protrusions to transfer from cell to cell (Cudmore et al. 1996, Favoreel et al. 2006, Onfelt et al. 2004, Onfelt et al. 2006). TNTs can also form between neuronal cells and prions have been reported to traffic through these structures between infected and non-infected cells (Gousset, Zurzolo 2009). Once delivered to the target cells, the transferred endocytic vesicles fuse with their counterparts (Rustom et al. 2004); this may provide a way to integrate signalling information and coordinate cell behaviour by dissemination from a single cell to a larger community (Gurke, Barroso & Gerdes 2008).

Actin polymerization is a key event for TNT formation (Gerdes, Bukoreshtliev & Barroso 2007) and actin-depolymerizing drugs have been shown to abolish TNTs formation (Rustom et al. 2004); therefore, to determine whether tau aggregates could be trafficked across cells via TNTs, HEK T-REx P301S 1N4R tau inducible cells were exposed to latrunculin A (Gousset, Zurzolo 2009) for up to 3 days to cause actin depolymerisation following exposure to sarkosyl-insoluble 0N4R P301S tau aggregates. Increasing doses of latrunculin A did not result in less frequent phospho-tau (PG5-positive) aggregates in the cell culture as detected by HCI assay (Figure 4.12).

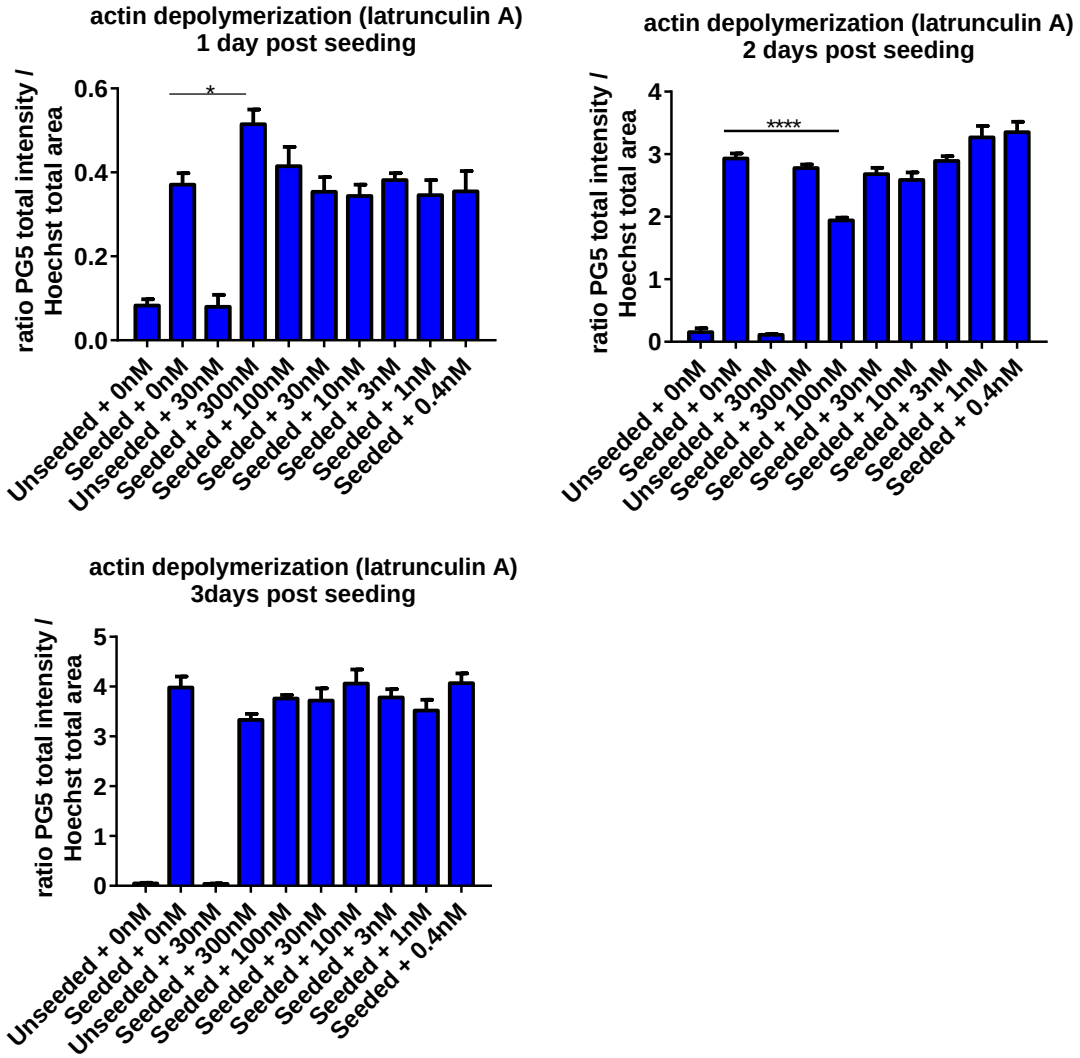

Figure 4.12: Actin depolymerization agent latrunculin A post-seeding does not affect tau aggregation. HCI assay measuring PG5-positive tau inclusions in HEK T-REx P301S 1N4R tau inducible cells inoculated with sarkosyl-insoluble P301S 0N4R tau seed for 3 hours, followed by incubation with actin depolymerization agent latrunculin A (added straight after seeding for 1-2-3 days). Data shown are mean ± SEM (n=2). Statistical analysis: one-way ANOVA with Dunnett's *post hoc* test. *p<0.05, ****p<0.0001, compared with untreated control.

With a view of studying the mechanisms of tau transfer, our lab also generated and optimized a co-culture HEK cell system that robustly develops intracellular tau aggregates following addition of exogenous mutant tau. Briefly, sarkosyl-insoluble tau extracted from tgP301S mice was used to trigger aggregation in HEK T-rex P301S tau inducible cells, which were then co-cultured with HEK cells stably expressing GFP and transiently transfected with P301S tau. Immunofluorescence readout showed that exogenous seeds efficiently enter cells and trigger aggregation of endogenous protein, resulting in the time-dependent accumulation of insoluble tau fibrils, which are transferred from donor to acceptor cells (Cavallini et al. 2014.). We then employed latrunculin A to examine the transfer mechanisms of mutant tau aggregates in our co-culture system. TgP301S seed was used to trigger aggregation in HEK T-REx P301S tau inducible cells, which were then co-cultured with HEK GFP-expressing P301S tau-transfected

cells for 3 days, in presence of latrunculin A, before being fixed and analysed by immunofluorescence. Latrunculin A inhibited transfer of aggregates from donor to acceptor cells in a dose-dependent manner (from 12% donor cells containing PG5-positive aggregates in absence of treatment, to 4% at the highest concentration of Latrunculin A) (Figure 4.13).

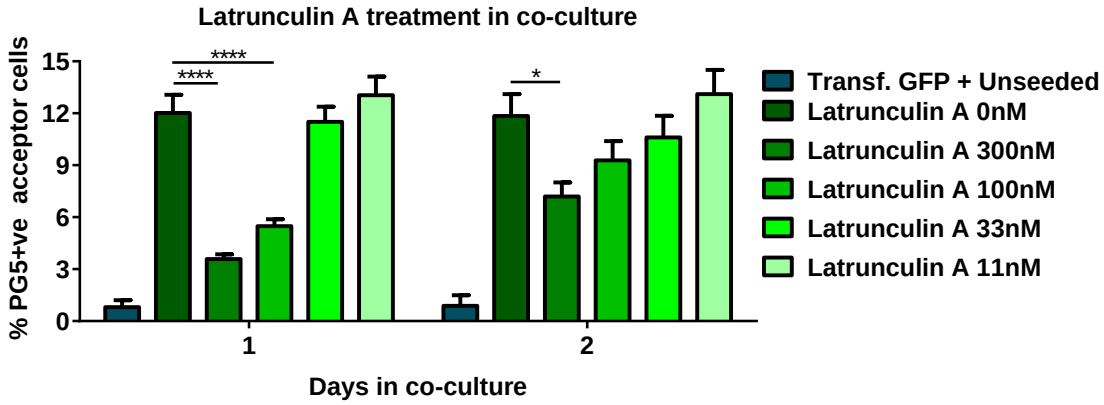

Figure 4.13: Actin depolymerization agent latrunculin A affects transfer of aggregates in a co-culture setting. HCI assay measuring PG5-positive tau inclusions in GFP-positive acceptor cells co-cultured with TgP301S-seeded donor cells for 3 days, in presence of actin depolymerization agent latrunculin A. Data shown are mean ± SEM (n=2). Statistical analysis: one-way ANOVA with Dunnett's *post hoc* test. **p*<0.05, *****p*<0.0001, compared with untreated control.

4.8 Discussion on nanotubes in HEK T-REx P301S tau inducible cells

We incidentally observed tunnelling nanotubes (TNTs) in our cell model, and described their main features by confocal microscopy. Since it has been shown that tunnelling nanotubes can form between neuronal cells and prions appear to traffic through these structures between infected and non-infected cells (Gousset, Zurzolo 2009), we asked whether nanotubes could allow cell-to-cell propagation of tau aggregates. Since all the TNTs we observed were tau-positive, it is possible that tau, together with F-actin, is a specific constitutive marker of TNTs. We therefore explored the effect of the F-actin-depolymerising compound latrunculin A (Rustom et al. 2004) post-seeding in a bid to disrupt intercellular propagation of tau aggregate via TNTs. One of the reasons why latrunculin A did not seem to affect tau transfer between HEK T-REx P301S tau inducible cells might lie in the dynamic nature of TNT-like structures, leading to only transient bridges with variable lifetimes, ranging from a few minutes up to several hours; or TNTs could be playing a minor role among multiple mechanisms of tau transmission, and their relative contribution may be difficult to measure; another possibility is that the aggregates intercellular transfer is not efficiently modelled by our mammalian cell inducible system, and may mainly occur from mother to daughter cells during cell division. Nevertheless, in a co-culture setting, latrunculin A induced dose-dependent inhibition of aggregate transfer from donor to acceptor cells at 1-2 days in co-culture. The extent of the effect we observed suggests that disrupting the actin cytoskeleton with latrunculin A may have an impact not necessarily only on nanotubes, but possibly on other actin-dependent mechanisms of tau release and uptake,

therefore further experiments should focus on dissecting these mechanisms and study the effect of latrunculin A on tau extracellular concentration in co-culture media.

In summary, our cell model allowed us to characterise TNTs and formulate the hypothesis that they may be a mean of tau propagation between cells. Since the pharmacological modulation of these structures suggested that actin-dependent processes are involved in tau intercellular transfer in our cell model, further experiments should employ pharmacological and genetic modulators to further dissect these mechanisms; ultimately, whether TNTs facilitate the intercellular spread of pathological tau will also have to be confirmed in vivo in tauopathy brains.

5. CHARACTERISATION OF NATIVE VS RECOMBINANT SEED

In this section we focus on investigating the tau species that constitute seeds; some of the work presented below has been included in recent publications. In Falcon et al. 2015 we described the development of a cell model to understand the relationship between tau conformation /phosphorylation state and seeding ability. Using both recombinant and native tau aggregates, we provided evidence that despite being taken up by cells to the same degree, native tau aggregates have a higher seeding potency than recombinant tau aggregate; the latter though can acquire the conformation and seeding potency of the former by templated assembly, demonstrating for the first time that conformation and not phosphorylation determines the seeding potency of tau aggregates (Falcon et al. 2015). In Jackson et al. 2016 we characterized by sucrose gradient and immunodepletion the native tau species responsible for seeding and pathology spreading in TgP301S mice. Tau species that were aggregated, AT8-, and nY29-positive with structure ranging from ring-like to small fibrils of 179–250 nm were able to seed tau aggregation in our inducible cell model and initiate *trans*-synaptic spreading in TgP301S mice in vivo, indicating that short fibrils are the most potent species capable of seeding tau pathology (Jackson et al. 2016).

5.1 Sarkosyl extraction enriches for seed-competent tau

Having characterised the mechanisms of TgP301S seed uptake in our cell model, we then wanted to compare this transgenic-derived seed to a recombinant, heparin-aggregated seed. The sarkosyl-insoluble (SI) fraction and the total lysate (TL) from the brains of TgP301S tau mice were compared (Falcon et al. 2015). Tau levels were normalized and the levels of MC1 (conformationally changed) and AT8 (pS202/pT205) -positive tau determined by Alphascreen assays. Sarkosyl treatment enriched for MC1- and AT8-positive tau relative to the total brain lysate (~130- and ~100-fold, respectively, taking into account that the sarkosyl-insoluble pellet was resuspended in 1:10 of the volume of the total lysate) (Figure 5.1 A). We next compared the seeding abilities of these preparations in our inducible cell model. While sarkosyl-insoluble TgP301S tau at 45 ng/ml led to the accumulation of sarkosyl-insoluble AT8-positive tau, the total brain lysate failed to seed at this concentration (Figure 5.1 B).

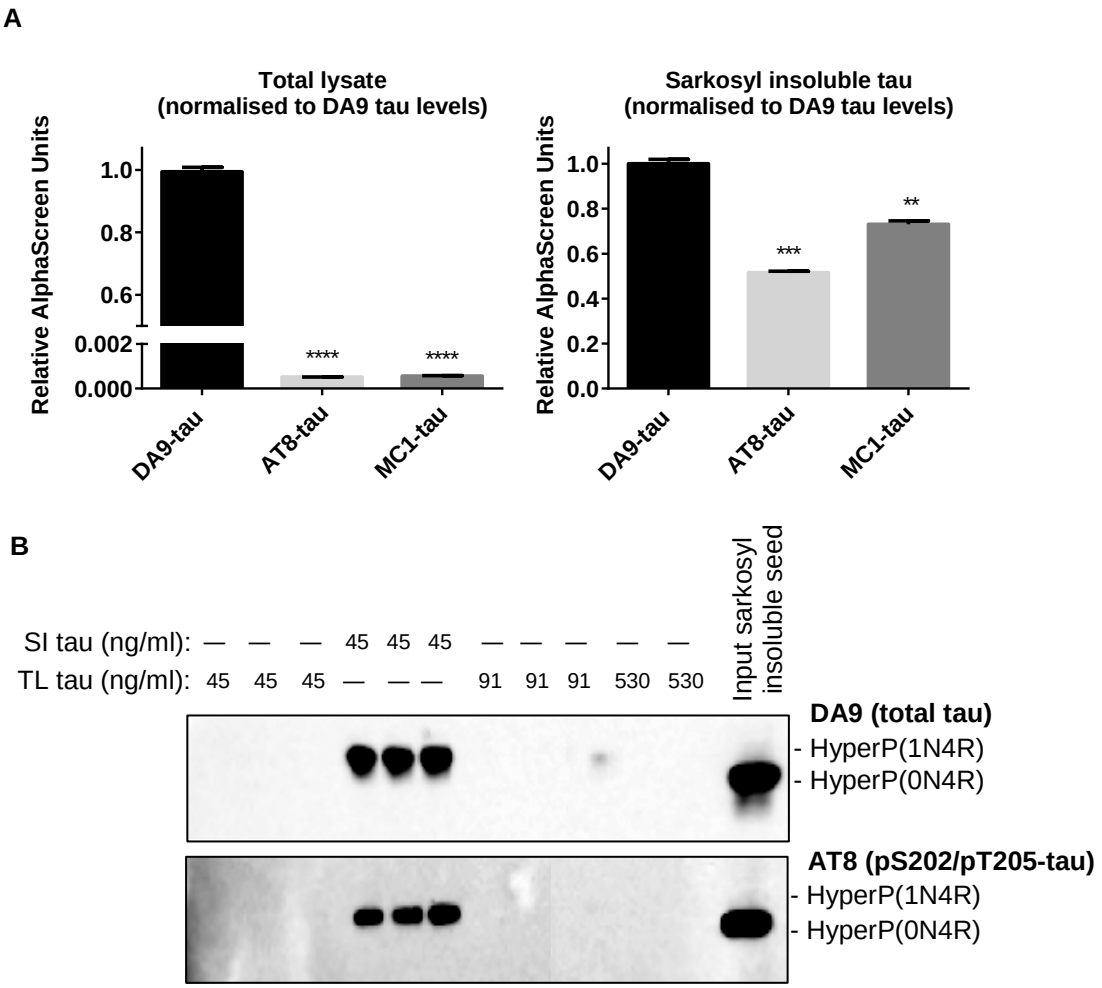

Figure 5.1: Sarkosyl insoluble fraction is enriched for seed-competent tau. (A) Alphascreen assays showing the levels of DA9 (phosphorylation-independent)-, MC1 (conformationally changed) - and AT8 (pS202/pT205) -positive tau in the total lysate and the sarkosyl-insoluble fraction from TgP301S tau mice brains. The results are the means ± SEM (n=3). The levels of AT8- and MC1-positive tau are expressed relative to total tau levels. Statistical analysis: one-way ANOVA with Dunnett's *post hoc* test. **p*<0.05, *****p*<0.0001, compared with total tau. (B) Western blot showing DA9- and AT8-positive tau in the sarkosyl-insoluble fraction of HEK 293T cells expressing P301S 1N4R tau, following the addition of either total lysate (TL) or sarkosyl-insoluble (SI) material [normalized for DA9-positive tau] for 3 h, followed by 3 days of incubation.

5.2 Reduced seeding following tau immunodepletion

We next used several biochemical techniques to dissect the molecular characteristics of native tau protein conformers from TgP301S tau mice brain lysates. As part of the characterisation of seed-competent tau in the TgP301S transgenic model, we assessed the seeding abilities of brain lysates from symptomatic TgP301S tau mice following immunodepletion with a number of anti-tau antibodies (both phosphorylation-independent and phosphorylation-dependent). Immunodepletion of TgP301S total lysates was performed using DA9, AT8, PG5, PHF1, and total IgG as isotype control. WB was carried out to quantify the extent of depletion of DA9- and

AT8-positive species (Figure 5.2). Immunodepletion with AT8, PG5, or PHF1 only significantly reduced 64k Da aggregate-derived AT8-positive tau (AT8 (-96%) > PHF1 (-75%)> DA9 (-72%) > PG5 (-70%) relative to control IgG) without reducing total tau (DA9) levels, whereas immunodepletion with DA9 removed DA9 reactivity and reduced the amount of 64 kDa AT8-positive tau. Since DA9 reduced the amount of 64 kDa AT8-positive tau without completely removing it, it is likely that this pan-tau antibody preferentially recognises soluble tau and it is not able to remove all tau species. Depletion with IgG isotype control did not significantly reduce DA9 or AT8 levels.

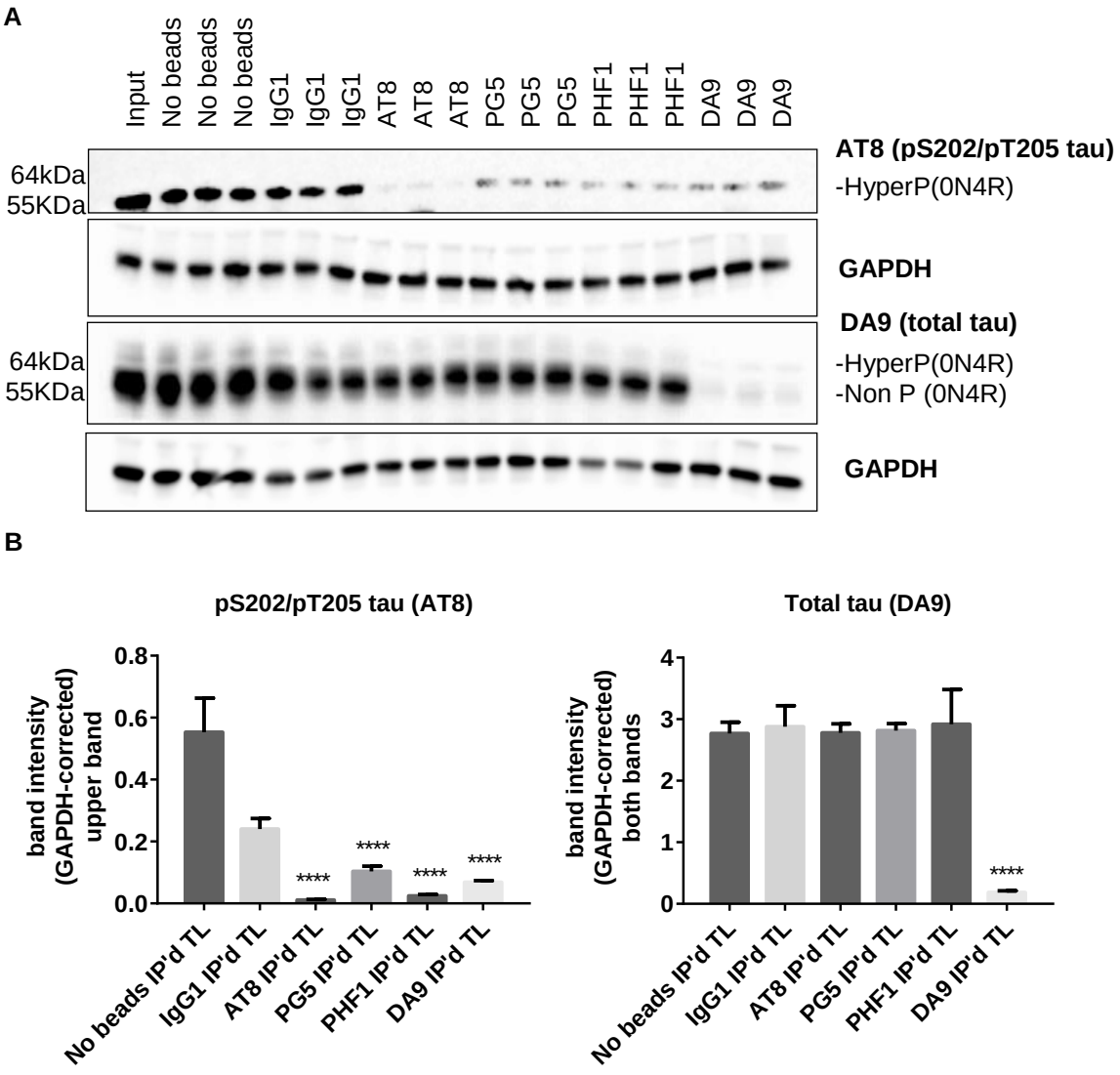

Figure 5.2: Immunodepletion with tau antibodies significantly reduces 64kDa aggregate-derived AT8-positive tau in TgP301S mice brain lysates. (A) WB with AT8 or DA9 antibodies of brain lysates from symptomatic TgP301S tau mice following immunodepletion with phosphorylation-independent anti-tau antibody DA9 or phosphorylation-dependent antibodies AT8, PG5, and PHF1 or IgG1 isotype control. A representative blot from 3 separate experiments is shown, each with 3 replicates per condition. GAPDH was used as the loading control. Immunodepletion reduced levels of the 64 kDa AT8-positive band by all antibodies to varying degrees (AT8 > PHF1 > DA9 > PG5); only DA9 significantly reduced the 55 kDa tau

species. (B) Quantification of (A). The quantification results are the mean ± SEM (n=3); 64 kDa band quantified for AT8 blot; sum of 64 and 55 kDa bands quantified for DA9 blot. Statistical analysis: one-way ANOVA with Dunnett's *post hoc* test. *p<0.05, ****p<0.0001, compared with IgG1 isotype control.

We then tested the seeding ability of the immunodepleted samples in HEK T-REx P301S 1N4R tau inducible cells. Immunodepletion with anti-tau antibodies, but not control IgG, reduced the seeding ability of TgP301S tau brain lysates in a manner proportional to the reduction of the 64 kDa aggregate-derived AT8-positive tau observed in the samples (AT8 (-75%) > PHF1 (-30%) > DA9 (-32%) > PG5 (-50%), relative to control IgG) (Figure 5.3).

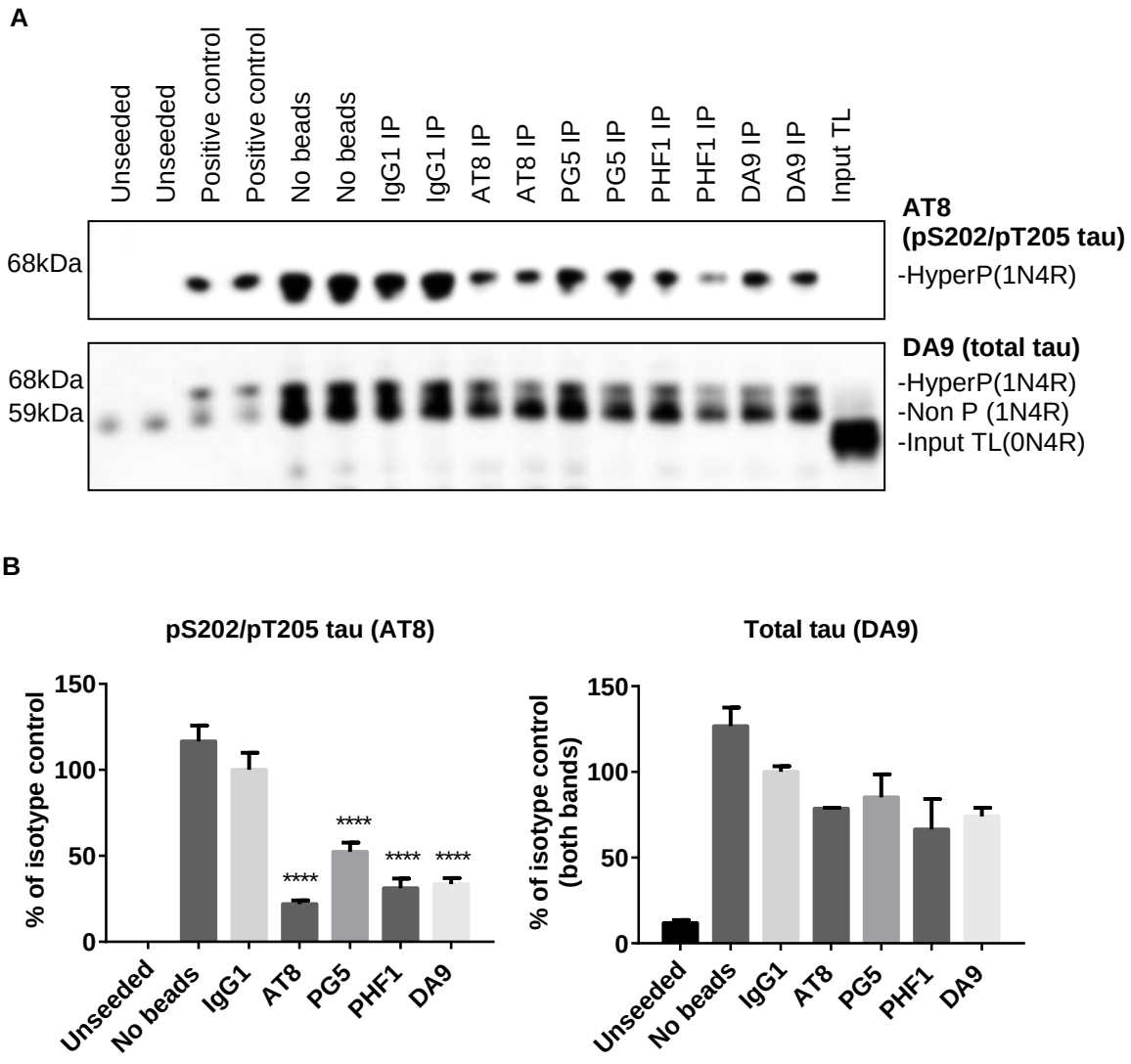

Figure 5.3: Immunodepletion with tau antibodies reduces the seeding ability of TgP301S mice brain lysates. (A) WB with anti-tau antibodies DA9 and AT8 of the insoluble fraction extracted from HEK T-REx P301S tau inducible cells following seeding with immunodepleted TgP301S total lysate samples. Positive control was sarkosyl-extracted tau from symptomatic TgP301S mice ("TgP301S seed"). A representative blot from 3 separate experiments is shown. (B) Quantification of (A). Results are the means ± SEM (n=3); 68 kDa band quantified for AT8

blot; sum of 68 and 59 kDa bands quantified for DA9. Statistical analysis: one-way ANOVA with Dunnett's *post hoc* test. *p<0.05, ****p<0.0001, compared with IgG1 isotype control.

There was also a strong positive correlation (R^2 = 0.85, p <0.0001) between the levels of 64 kDa AT8-positive tau present in the TgP301S brain lysates after immunodepletion (AT8 input) and the levels of seeded aggregation observed in cells following incubation with each immunodepleted brain lysate, as measured by AT8-positive insoluble tau (AT8 output). No correlation was observed between the levels of total, DA9-positive tau (comprising soluble and insoluble tau) in brain lysates (DA9 input) and the levels of seeded aggregation (AT8 output) (Figure 5.4).

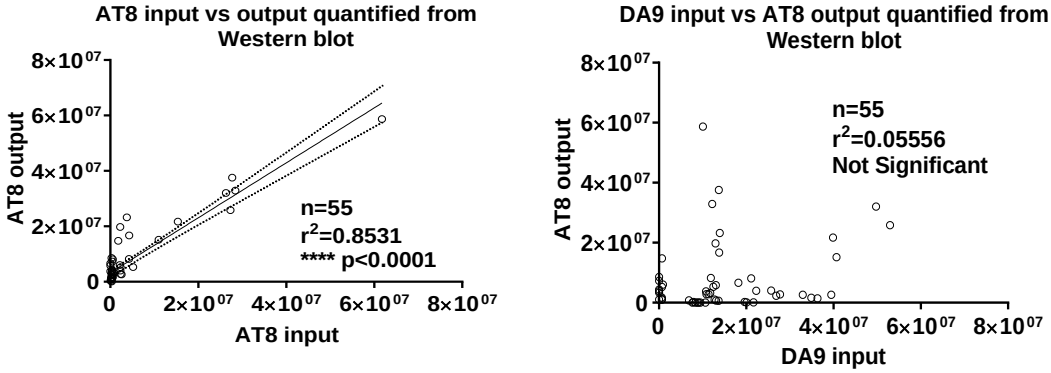

Figure 5.4: Seeding efficiency correlates with level of 64 kDa hyperphosphorylated tau. The levels of 64 kDa, AT8-positive tau in the TgP301S brain lysate (AT8 input) correlated with its seeding ability in cells (AT8 output) measured by WB. No correlation was observed with DA9-positive tau as the input. Linear regression was performed to determine the relationships between input and output tau.

To determine overlap of species being identified by different antibodies, we performed immunodepletion of TgP301S brain lysates with a combination of phospho-tau antibodies AT8 and PHF1, and compared it with immunodepletion with either AT8 alone or PHF1 alone; unconjugated Sepharose beads (no antibody) were used as control. WB showed that the pairing of AT8 and PHF1 did not result in any additional species being depleted (Figure 5.5).

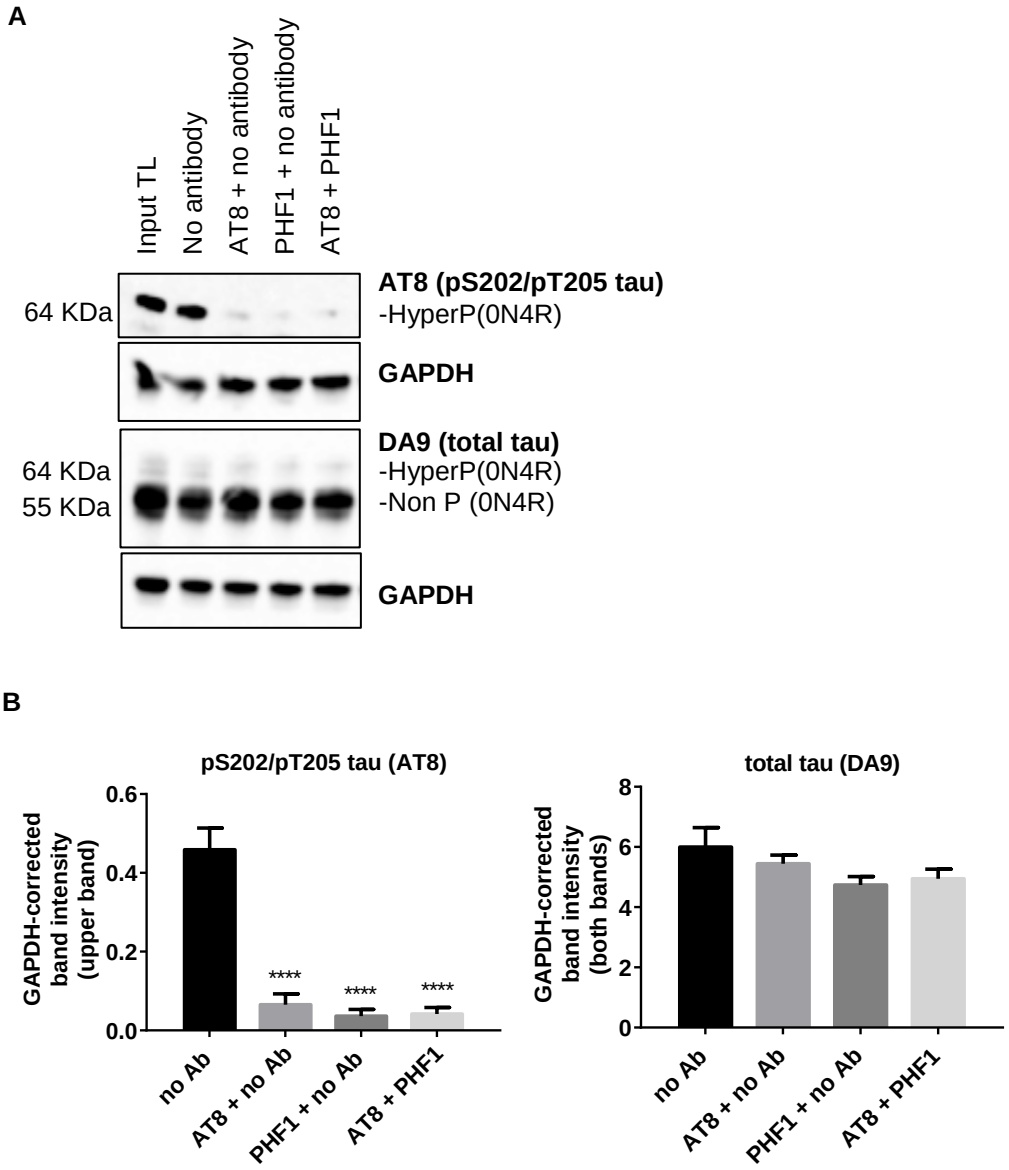

Figure 5.5: Double immunodepletion with phospo-tau antibodies does not remove additional species. (A) WB of AT8-tau and total tau remaining following immunodepletion of TgP301S mouse brain lysate with AT8 alone (AT8 + no Ab), PHF1 alone (PHF1 + no Ab) or AT8 and PHF1 together (AT8+PHF1). No-antibody Sepharose beads (no Ab) were used as control. When the antibodies were used alone, an equal volume of unconjugated beads was added, so that the beads volume would be the same in each condition. A representative blot from 2 separate experiments is shown. (B) Quantification of (A). Results are the means ± SEM (n=2). Statistical analysis: one-way ANOVA with Dunnett's *post hoc* test. **p*<0.05, *****p*<0.0001, compared with no-antibody control.

Similarly, when the immunodepleted lysates were tested for seeding in HEK T-REx P301S 1N4R tau inducible cells, the seeding ability of the doubly immunodepleted lysate was comparable to lysate immunodepleted by single antibody AT8 or PHF1 (Figure 5.6).

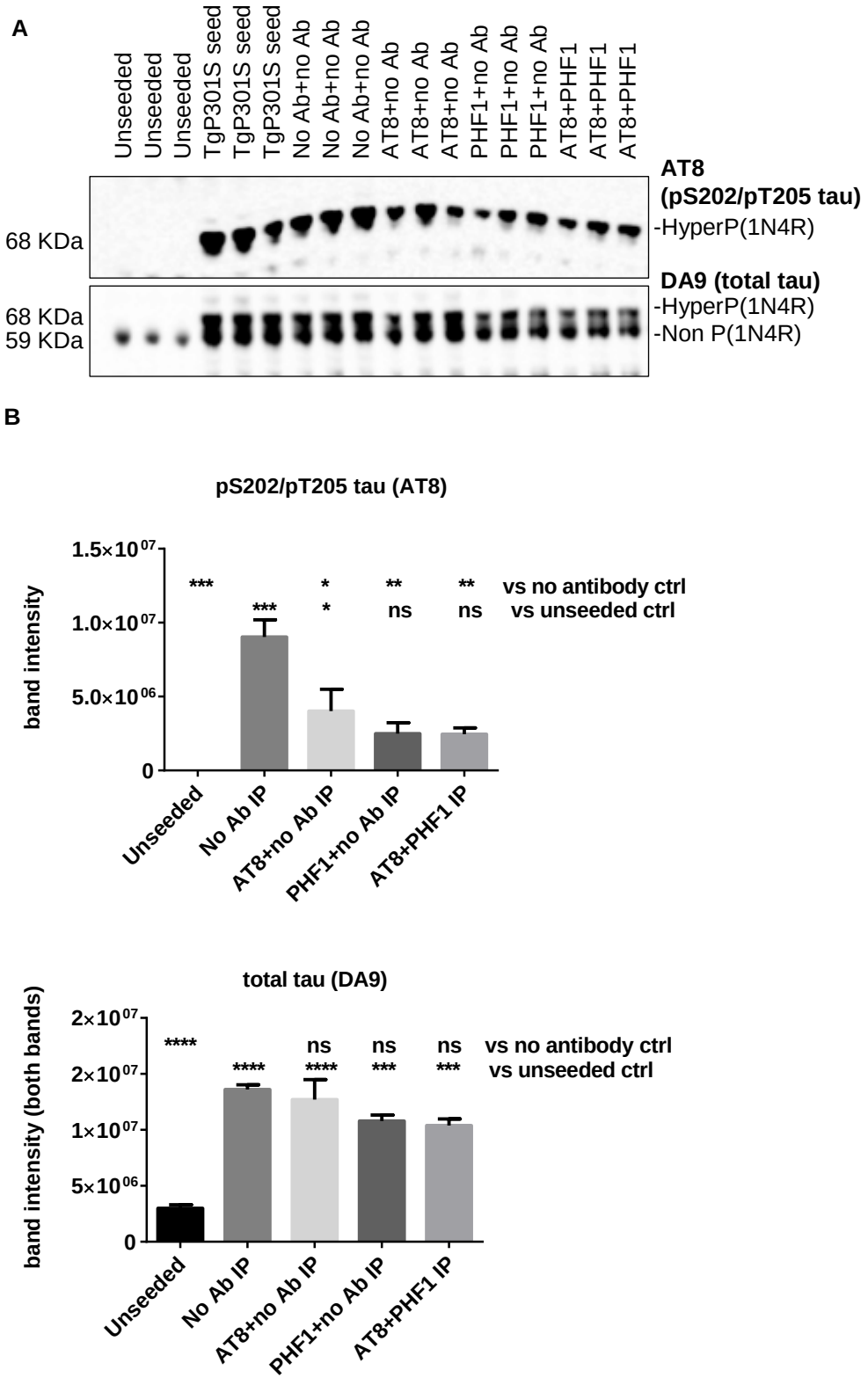

Figure 5.6: Double immunodepletion with phospo-tau antibodies does not remove additional species. (A) WB with anti-tau antibodies DA9 and AT8 of the insoluble fraction extracted from HEK T-REx P301S tau inducible cells following seeding with TgP301S total lysate samples immunodepleted with a combination of AT8 and PHF1 antibodies. Positive control was sarkosyl-extracted tau from symptomatic TgP301S mice ("TgP301S seed"). A representative blot from 2 separate experiments is shown. (B) Quantification of (A). Results are

the means ± SEM (n=2); 68 kDa band quantified for AT8 blot; sum of 68 and 59 kDa bands quantified for DA9. Statistical analysis: one-way ANOVA with Dunnett's *post hoc* test. *p<0.05, ****p<0.0001, compared to "no antibody control" or "no seeding control".

5.3 Discussion on characterisation of seed-competent tau

We compared the total lysate from the brains of TgP301S tau mice with the sarkosly-insoluble fraction extracted from the lysate itself, and showed that the sarkosyl-insoluble fraction was enriched for MC1- (conformationally changed) and AT8- (pS202/pT205) positive tau and had a seeding activity superior to the total lysate, when the two preparations were normalised for total tau; this indicates that sarkosyl treatment enriches for seed-competent tau. Conversely, we showed in immunodepletion experiments that a reduction of AT8-positive tau reduces the amount of seed-competent tau in total lysate from the brains of TgP301S mice. We performed the immunodepletions of all the antibodies at the same concentration, as we wanted to rank the antibodies that would preferentially remove or reduce the 64 kDa seeding-competent species. Total tau antibody DA9 removed and reduced the 64 kDa AT8-positive tau as well as total tau immunoreactivity in the TgP301S lysate, whereas antibodies that recognise pathological/phosphorylated tau (AT8, PG5, and PHF1) did not reduce total tau levels but significantly reduced the 64 kDa AT8-positive tau in the TgP301S lysate. Despite being a pan-tau antibody, DA9 was not the most effective antibody at reducing seed-competent tau, suggesting that it may not be able to recognise all forms of tau and it may preferentially recognise soluble tau species. This is corroborated by further data that we published (Jackson et al. 2016): in a native-PAGE of sucrose gradient fractions derived from TgP301S brain lysate and blotted with DA9 (total tau), AT8 (pS202/pT205-tau), nY29 (nitrated Y29-tau) and PHF1 (pS396-tau), we showed that DA9 recognises small tau species in the low-density sucrose fractions that are not labelled by AT8, nY29 or PHF1 antibodies; conversely, DA9 did not recognise small oligomeric species (~400 kDa) that were AT8- and nY29-positive. Also, preliminary experiments showed that the immunodepletion was dose-dependent, but even higher concentrations of DA9 did not completely suppress the 64 kDa species. Taken together, the results suggest that pan-tau antibody DA9 does not recognise all forms of tau equally and therefore does not remove all tau species from the TgP301S lysate.

We observed a strong positive correlation between the reduction of the 64 kDa AT8-positive tau in the TgP301S lysate and the reduction of the seeding potency of the lysate; no correlation was observed between the reduction of total tau immunoreactivity in the TgP301S lysate and the reduction of the seeding potency; this confirms that seeding is conferred by AT8-positive tau species and is not just the result of the mere addition of tau protein to the cells. The reduction of AT8-positive tau in the TgP301S lysates by the different antibodies tended to be more conspicuous than their corresponding reduction of the seeding ability of the TgP301S lysate (compare AT8 (-96%) > PHF1 (-75%)> DA9 (-72%) > PG5 (-70%) immunodepletion relative to control IgG, vs AT8 (-75%) > PHF1 (-30%) > DA9 (-32%) > PG5 (-50%) seeding reduction relative to control IgG); for instance, although AT8 nearly completely abolished the AT8

immunoreactivity of the TgP301S lysate (-96%), it only partially suppressed the seeding ability of the immunodepleted lysate (-75%); this may indicate that AT8-positive tau species may be the main species responsible for seeding but possibly not the only ones. Further studies should elucidate the characteristics of seed-competent tau in more details, i.e. immunodepletion experiments with a wider range of antibodies, targeting different epitopes and including conformational and C- and N-terminus antibodies should help identify the most efficient therapeutic antibody. We and others (Guo & Lee, 2011) have shown that small amounts of tau seeds are sufficient to induce robust endogenous tau fibrillization in cell models; furthermore, Guo et al. investigated the turnover of tau aggregates in cells and highlighted the need to fully remove seed-competent species: they generated a monoclonal QBI-293 cell line with doxycycline-regulated inducible expression of GFP-tagged 2N4R human tau carrying the P301L mutation; after transduction with recombinant Myc-K18/P301L pre-formed fibrils, followed by single cell cloning, they generated monoclonal cell lines with persistent tau inclusions that were faithfully transmitted through mitosis; they selected a clone where 95% cells maintained tau aggregates even after more than 100 days of passaging in culture; in this system, tau aggregates can be gradually removed from cells when soluble tau expression is turned off for 7 days, however, the presence of even minuscule amounts of residual aggregates remaining after clearance is sufficient to rapidly reinstate tau aggregation once tau expression is restored (Guo et al. 2016). This suggests that a tau immunotherapy approach would require a total suppression of seed-competent tau species, to prevent small residual seeds from perpetuating the recruitment and aggregation of monomer. This may be further challenged by the existence of different pathological tau strains, as an antibody may not be able to form high-affinity complexes with all the strains present in a given diseased brain; rather than targeting highly-specific epitopes, antibodies targeting shared conformation of multiple strains may have better chances of therapeutic success.

Our results with a combination of AT8 and PHF1 antibodies did not show enhanced immunodepletion compared to using single antibodies, suggesting that a combination of these antibodies would not offer a therapeutic advantage over single administration, possibly due to the fact that AT8 and PHF1 antibodies target similar tau species. However, in principle, a multi-epitope strategy could be beneficial to reach complete clearance of seed-competent tau; this could be a combination of different monoclonal antibodies targeting different species, or a polyclonal antibody. A polyclonal antibody strategy has been tried for targeting beta-amyloid in AD, however high regulatory hurdles for approval of studies with polyclonal antibodies have so far limited their numbers. Intravenous immunoglobulin (IVIG) products are prepared from plasma immunoglobulins from large numbers of healthy donors. Before being trialled for AD, they had been used to treat a range of autoimmune, infectious, and idiopathic disorders (Scheinfeld 2017). Commercially available IVIGs from healthy and diseased donors contain naturally occurring autoantibodies against beta-amyloid (Dodel et al. 2002), however their concentration is reduced in patients with AD (Du et al. 2001, Weksler et al. 2002, Britschgi et al. 2009, Pul, Dodel & Stangel 2011). This provided the rationale for the use of IVIGs in AD trials, until negative results were reported in phase III IVIG studies in 2013 and since then, efforts

towards IVIGs as a treatment for AD have been reduced (Loeffler 2013). A downside of polyclonal immunotherapy with IVIGs is that these preparations differ in their concentrations of antibodies to beta-amyloid (Safavi et al. 2016, Balakrishnan et al. 2010) and tau protein (Smith et al. 2013) therefore their efficacy as AD therapy would be difficult to standardise. Most approaches currently in pre-clinical or clinical phases use single monoclonal tau antibodies.

Open questions in the tau propagation field are what species of tau constitute a seed, and what are the minimal requirements for tau to be seed-competent. In a recent publication (Jackson et al. 2016) we used several biochemical techniques to dissect the molecular characteristics of native tau protein conformers from TgP301S tau mice and showed that seed-competent tau species comprise small fibrils capable of seeding tau pathology in cell and animal models. In particular we found that sucrose gradient fractions from TgP301S brain lysates seeded cellular tau aggregation only when large (>10 mer) aggregated, hyperphosphorylated (AT8- and AT100-positive), misfolded (MC1-positive) and nitrated (nY29-positive) tau was present. Sucrose fractions containing small, oligomeric (<6 mer) tau were unable to seed. Immunodepletion of the large aggregated AT8-positive tau strongly reduced seeding, and the seeding ability of TgP301S brain lysates correlated with the levels of AT8-positive tau; moreover, fractions containing these species initiated the formation and spreading of filamentous tau pathology *in vivo*, whereas fractions containing tau monomers and small oligomeric assemblies did not. By electron microscopy, seed-competent sucrose gradient fractions contained aggregated tau species ranging from ring-like structures to small filaments.

In summary, our cell model allowed us to characterise by sucrose gradient and immunodepletion the native tau species responsible for seeding and pathology spreading in TgP301S mice (Jackson et al. 2016), providing us with a powerful tool to investigate the tau species that constitute seeds in a tauopathy model. Results obtained in cells were replicated in our in vivo model of tau propagation (Ahmed et al. 2014), showing the potential of our cell system as a good surrogate for in vivo studies. Future experiments should aim at further elucidating the properties of seed-competent tau species to better tailor therapeutic strategies.

5.4 Recombinant tau seeded with native tau aggregates acquires the same seeding potency as native tau aggregates

We previously showed (Falcon et al. 2015) that when comparing sarkosyl-insoluble 0N4R tau aggregates from the TgP301S tau mice brains to sarkosyl-insoluble, heparin-assembled full-length recombinant P301S 0N4R tau, native tau aggregates have a higher seeding potency than recombinant tau aggregates in our inducible cell model. After measuring ThioT binding, equating filament length by sonication and normalizing tau concentration by immunoblotting, we assessed the seeding potencies of the two preparations in the cell-based assay. Approximately 50 times more synthetic P301S tau seed than TgP301S tau seed was needed to produce equivalent amounts of sarkosyl-insoluble tau from expressed protein in cells.

To examine the effect of aggregate conformation on seeding potency and to control for the presence of heterologous components in the TgP301S aggregates, we seeded recombinant P301S tau in the absence of heparin with 5% (v/v) sarkosyl-insoluble fraction from P301S mice brains. We monitored aggregation of recombinant P301S tau by ThioT binding over time (Figure 5.7).

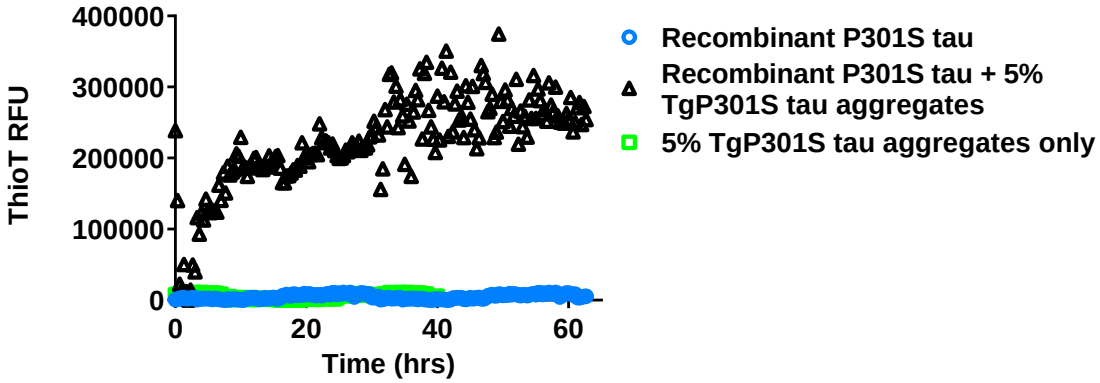

Figure 5.7: Aggregation of seeded recombinant tau. Aggregation of soluble recombinant P301S tau in the presence of 5% (v/v) sarkosyl-insoluble fraction from P301S mice brains, and in absence of heparin, as measured by Thioflavin T binding over time. RFU: Relative Fluorescence Units.

When normalised for total tau levels and filament length, the recombinant tau aggregates seeded by aggregated TgP301S tau in the absence of heparin were equally potent to aggregated TgP301S tau in our seeding assay (Figure 5.8).

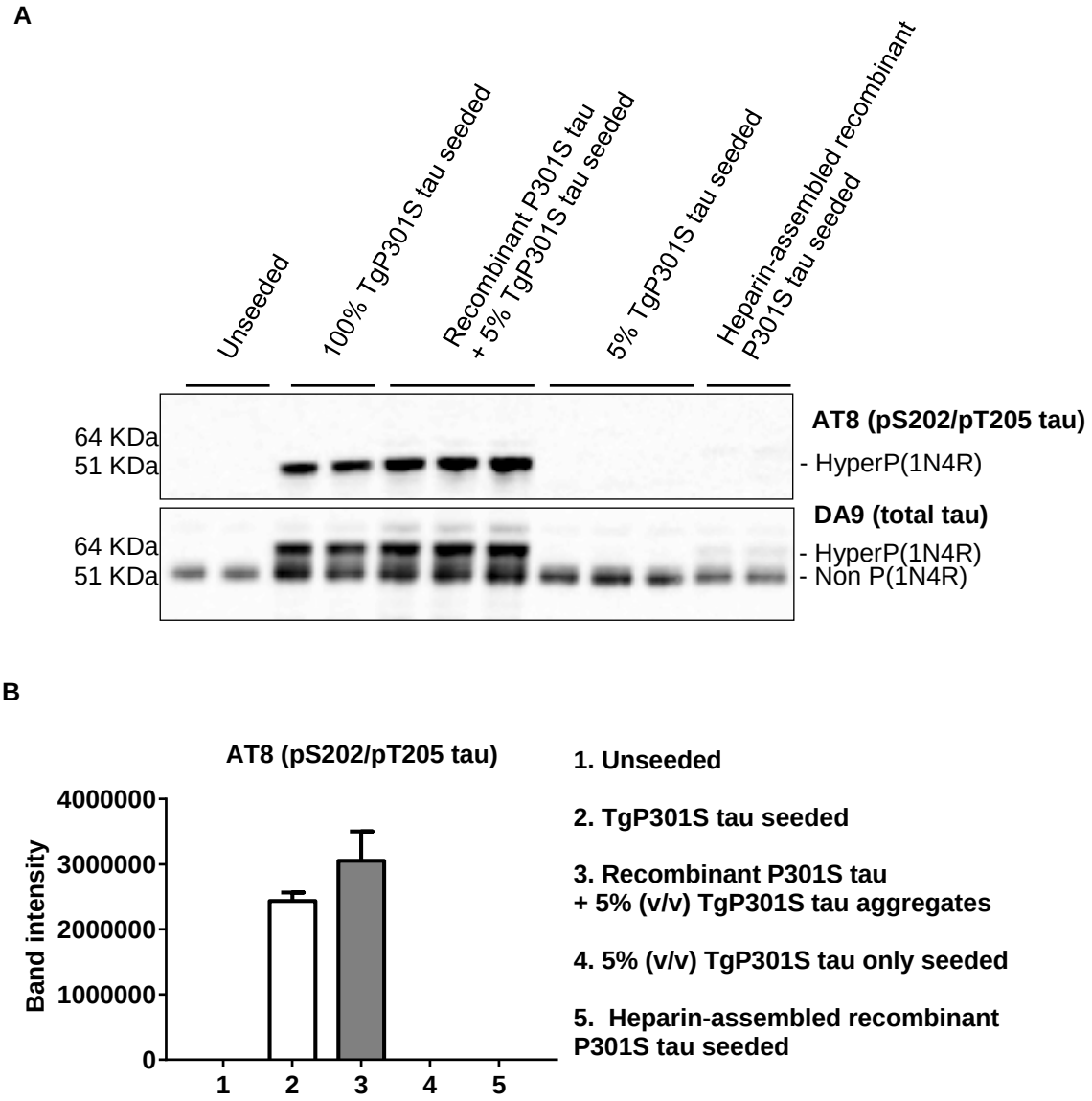

Figure 5.8: Recombinant tau seeded with native tau aggregates acquires the same seeding potency as native tau aggregates. (A) Western blots with anti-tau antibodies DA9 (phosphorylation-independent) and AT8 (pS202/pT205) of the insoluble fraction from inducible HEK293T cells expressing P301S 1N4R tau seeded for 3 h with either TgP301S tau aggregates, or equivalent concentration of recombinant P301S tau seeded with 5% (v/v) TgP301S tau aggregates, or equivalent concentration of heparin-assembled recombinant P301S tau aggregates, or the 5% (v/v) TgP301S tau aggregate component alone, followed by 3 days incubation. (B) Quantification of (A). Seeding with TgP301S tau aggregates and recombinant P301S tau seeded with (5%v/v) TgP301S tau aggregates were not significantly different. Statistical analysis: t test. The values are the means ± SEM (n=3).

5.5 Discussion on seeding potency of native and recombinant seeds

Some of the work described above has been included in a recent publication (Falcon et al. 2015) where we described the development of a cell model to understand the relationship between tau conformation /phosphorylation state and seeding ability.

Using our cell-based assay, we first compared the seeding activity of the sarkosyl-insoluble fraction from TgP301S tau mice brain with that of total brain lysate. The sarkosyl-insoluble fraction, which was enriched in aggregated and AT8-positive tau, had a greater seeding activity than the lysate, when normalized for total tau. This indicates that the tau species required for seeding are likely to be sarkosyl-insoluble. We then used our cell-based assay to compare the seeding activity of the sarkosyl-insoluble fraction from TgP301S tau mouse brain with that of sarkosyl-insoluble P301S recombinant tau. We used sonication and electron microscopy to ensure equal filament length between the two preparations and we observed that, similarly to synthetic prions (Kim et al. 2010, Tanaka et al. 2006, Legname et al. 2006, Legname et al. 2005), α-synuclein aggregates (Luk et al. 2012) and Aβ assemblies (Meyer-Luehmann et al. 2006a, Stöhr et al. 2012), synthetic tau aggregates had a greatly reduced seeding activity compared to sarkosyl-insoluble tau from P301S tau mouse brain; both preparations entered cells through a mechanism consistent with macropinocytosis, demonstrating that the difference in their seeding activity is unlikely to be the result of different uptake mechanisms.

We showed that synthetic tau aggregates were more resistant to disaggregation by guanidine hydrochloride and digestion by proteinase K than tau aggregates from TgP301S tau mouse brain, consistent with the hypothesis that more stable aggregates possess lower seeding activity. Also, low concentrations of guanidine hydrochloride enhanced exposure of the HT7 antibody epitope on tau aggregates from P301S mice brain but not on synthetic tau aggregates, suggesting a different molecular organization of the two types of preparations. Our findings are in agreement with a study showing that tau filaments produced by incubating recombinant human tau with heparin were more stable than paired helical filaments from AD brain (Morozova et al. 2013). Structural differences among the two preparations could be further confirmed by an array of techniques like trypsin digestion, electron microscopy, Congo red stain, thermostability, native gel, circular dichroism.

Since we used heparin to form synthetic aggregates, which has been shown to compact the repeats and induce dimerisation of tau, with filaments growing through monomer addition (Ramachandran, Udgaonkar 2011, Elbaum-Garfinkle, Rhoades 2012), we postulated that heparin-induced synthetic tau aggregates have distinct conformations to that of brain-derived native tau aggregates. To demonstrate this hypothesis, we produced synthetic tau filaments seeded with TgP301S tau aggregates, and showed that they have a resistance to disaggregation by guanidine hydrochloride similar to P301S tau seeds. Importantly, in our inducible cell assay, synthetic tau aggregates seeded by aggregated TgP301S tau in the

absence of heparin acquired the seeding potency of brain-derived P301S tau seeds, in agreement with the prion hypothesis (Prusiner 2013).

Cumulative data from this thesis and from our publications (Falcon et al. 2015, Jackson et al. 2016) show that the seeding activity of tau from TgP301S mouse brain correlates with AT8 phosphorylation. AT8 recognises tau phosphorylated at both Ser202 and Thr205 and is one of the most common antibodies presently used for AD diagnostics, as it recognises AD-derived tau; AT8 stains hyperphosphorylated tau in late-stage human AD brain as well as in cell and animal models (Biernat et al. 1992, Goedert et al. 1995, Braak et al. 2006). However, in Falcon et al. 2015, we compared the seeding potency of TgP301S brain-derived tau seeds and recombinant P301S tau seeds, and noted that a major difference is that the former are hyperphosphorylated, whereas the latter are unphosphorylated. We tested whether phosphorylation could account for the superior seeding potency of TgP301S tau seeds, by producing hyperphosphorylated recombinant P301S tau aggregates *in vitro*. Sequential phosphorylation of recombinant P301S tau with PKA and SAPK4, in the presence of heparin produced 64 kDa tau hyperphosphorylated at epitopes characteristic of pathological tau (S422, the AT8 epitope (pS202/pT205) and the AT100 epitope (pS212/pT214/pT217)) (Goedert et al. 1997). Hyperphosphorylation was retained following purification of sarkosyl-insoluble tau (Yoshida et al. 2006). When we tested the seeding ability of the preparations, TgP301S tau aggregates were still more potent seeds than phosphorylated recombinant P301S tau aggregates, which retained the same potency as unphosphorylated recombinant P301S aggregates; in conclusion, hyperphosphorylation did not increase the seeding potency of recombinant tau aggregates. Moreover, hyperphosphorylated and unphosphorylated heparin-assembled recombinant P301S tau aggregates had similar stability to guanidine hydrochloride and proteinase K digestion, hinting that they had a similar conformation. Taken together, our data support the conclusion that phosphorylation at the AT8 epitope is a marker for pathological tau, but is not the main driver of the seeding potency of tau aggregates; conformation determines the seeding potency of tau seeds (Falcon et al. 2015). Although our findings apply to tau carrying the P301S mutation, similar observations were made by Guo et al. for WT tau (Guo et al. 2016). Abnormal phosphorylation has been believed to be the trigger of tau deposition, but a more recent hypothesis is that phosphorylation may occur after its aggregation (Hasegawa et al. 2017). Further work should explore the effect of other post-translational modifications on tau seeding ability, as they may have a more crucial role than phosphorylation.

In summary, using both recombinant and native tau aggregates, our cell model allowed us to demonstrate for the first time that, despite being taken up by cells to the same degree, native tau aggregates have a higher seeding potency than recombinant tau aggregate; the latter though can acquire the conformation and seeding potency of the former by seeded assembly, demonstrating that conformation and not phosphorylation determines the seeding potency of tau aggregates. Our work supports the hypothesis that conformationally distinct tau strains exist, and might be associated with individual tauopathies (Clavaguera et al. 2013, Frost,

Diamond 2010). In the future, it will be important to characterise tau conformations in human brains diagnosed with tauopathies, and determine whether the different diseases can be defined by aggregate structures, as this could aid drug design and creation of PET ligands specific to human tauopathies; further research should also examine whether there are genetic or environmental factors that promote particular tau conformations, and whether these could constitute therapeutic targets for tauopathies.

6. CHARACTERISATION OF TAU SPECIES IN CONDITIONED MEDIA

Here we focused on tau release by characterising the tau species in conditioned media from unseeded vs seeded HEK T-REx P301S 1N4R tau inducible cells, to investigate the presence of post-translational modifications (phosphorylation, truncation,..) aggregation state, size and encapsulation in vesicles of extracellular tau; we also collected and concentrated the conditioned media to test its ability to seed endogenous tau aggregation in naïve induced cells.

6.1 Seed-competent species are present in conditioned media from cell culture (biochemical assay in presence and absence of Lipofectamine)

Conditioned media experiments were carried out in our cell model to investigate the tau species involved in intercellular transfer. HEK-T-REx-293 P301S inducible cells were seeded with TgP301S mice derived brain extract, in presence or absence of Lipofectamine, and the seed was removed after 3 h. Cells were treated with 0.0125% trypsin for 1 min at RT to remove residual seed. Conditioned medium was collected at different timepoints after seeding (0-1-2-3 days post seeding) and assayed by Alphascreen to normalise the samples for total tau levels, before being added to a new population of HEK-T-REx-293 P301S inducible cells, in absence of transfection reagents. The transfer of conditioned medium from seeded cells was sufficient to induce tau aggregation in the second population of cells, as detected by western blot of insoluble fraction derived from total lysates (Figure 6.1). Media from unseeded cells failed to cause accumulation of insoluble tau in the second population of cells, whereas media from cells seeded in absence of Lipofectamine could induce accumulation of insoluble tau in recipient cells, albeit to a much lower extent than media from cells seeded in presence of the delivery reagent. Lipofectamine produced a greater accumulation of insoluble tau in the second population of cells, but this was accompanied by increased cytotoxicity (up to 15%), as measured by LDH assay (Figure 6.2). Therefore, the increase in the levels of seed-competent tau in the media caused by Lipofectamine is potentially being caused by release of tau from dead cells or leakage of tau from the cell membrane.

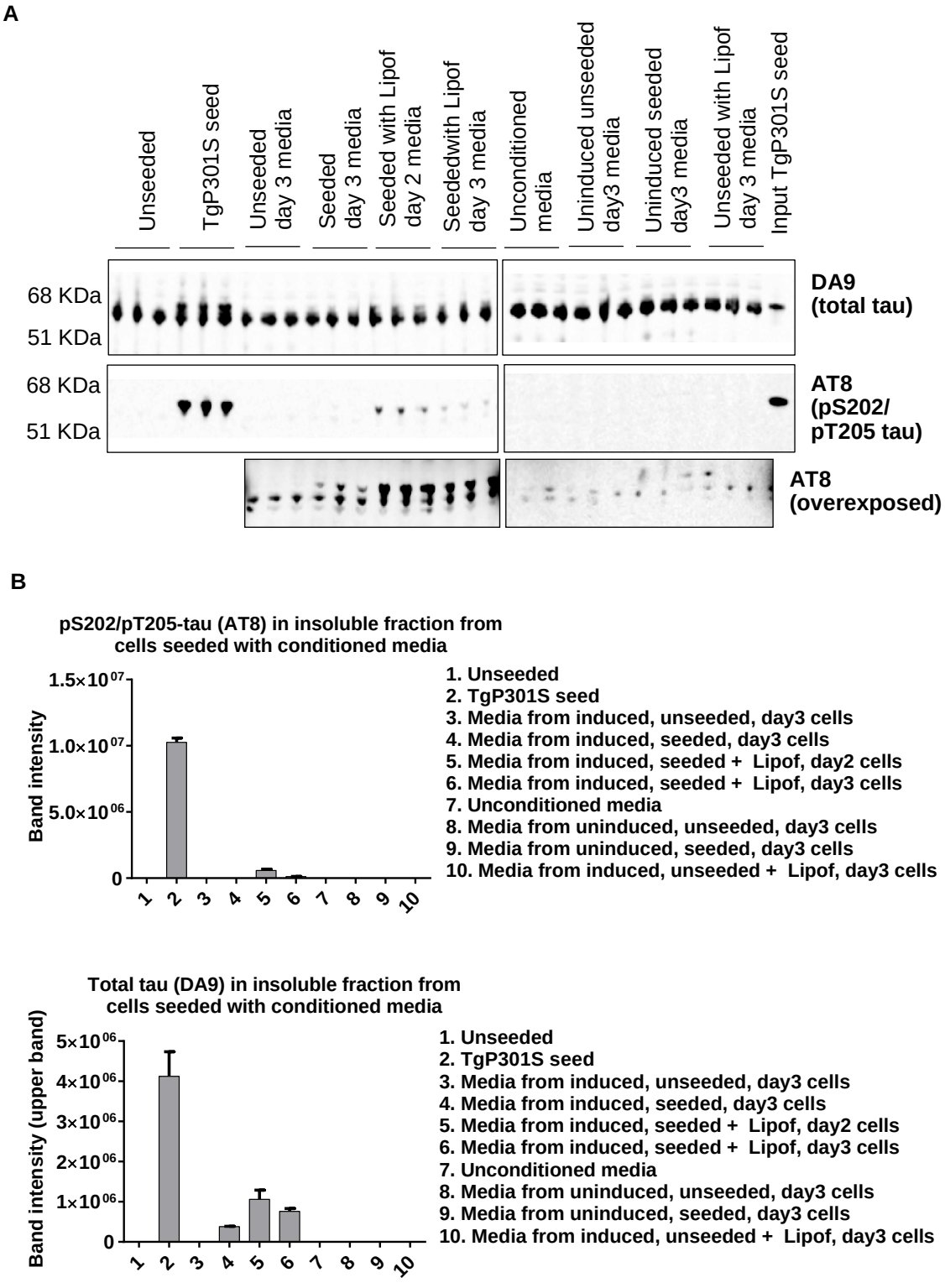

Figure 6.1: Conditioned media from seeded TgP301S tau inducible cells contains seed-competent tau species. (A) Western blot with total tau antibody (DA9) and pS202/pT205 antibody (AT8) in insoluble fraction of HEK T-REx P301S tau inducible cells treated with conditioned media from cells seeded with P301S mouse brain-derived tau extract shows accumulation of insoluble tau. Sequential extraction (fractionation) was performed. (B) Quantification of blots. The values are the means ± SEM (n=2).

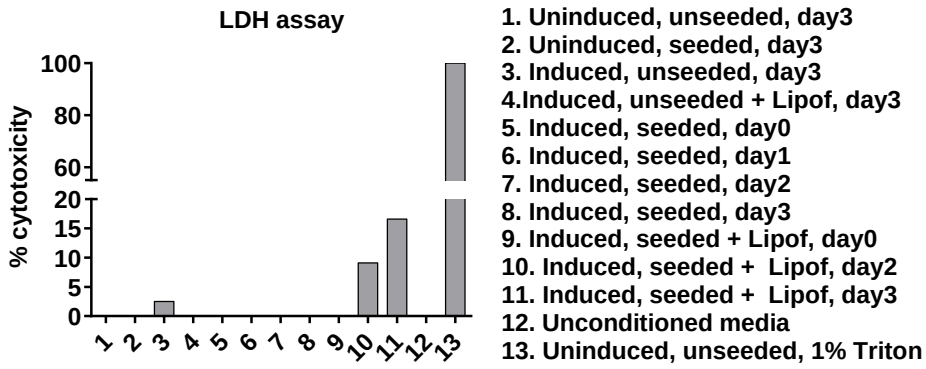

Figure 6.2: Lipofectamine induces tau release from cell death as shown by LDH assay. LDH assay in conditioned media samples from cells seeded with P301S mouse brain-derived tau extract and collected 0-1-2-3 days post seeding shows negligible levels of cell death measured in the media, apart from samples from cells seeded in presence of Lipofectamine 2000. The values are the means ± SEM (n=2).

6.2 Seed-competent species are present in conditioned media from cell culture (imaging assay in absence of Lipofectamine)

To investigate the tau species involved in intercellular transfer and minimise the spill of intracellular tau into the media due to Lipofectamine-induced cell death, conditioned media was collected after seeding HEK-T-REx-293 P301S inducible cells with P301S mice derived brain extract, in absence of transfection reagents, at different timepoints (0-1-2-3 days post seeding). Cells were treated with 0.0125% trypsin for 1 min at RT to remove residual seed. The media was concentrated and assayed by Alphascreen for total tau (DA9-TG5, to normalise the samples for total tau levels), pS202/pT205-tau, conformational changed tau (MC1-DA9) and pT181-tau (AT270-TG5) (Figure 6.3). Total tau, MC1-positive tau and pT181-tau were present in a time dependent manner in media from both unseeded and seeded. Total tau increased up to 30 units in media collected 3 days post-seeding; MC1-tau increased up to 0.3 units in media collected 3 days post-seeding; pT181-tau increased up to 1 unit in media collected 3 days post-seeding. On the other hand, AT8-positive tau was present in a time dependent manner only in media from seeded cells. Media from cells that were induced, seeded and grown for the longest period (3 days) contained the highest amount of AT8-tau (0.1 unit), followed by the Induced-Seeded-Grown 2 days (0.06 units) and the Induced-Seeded-Grown 1 day (0.02 units) samples. Samples which were either not seeded or not induced showed no presence of AT8-tau.

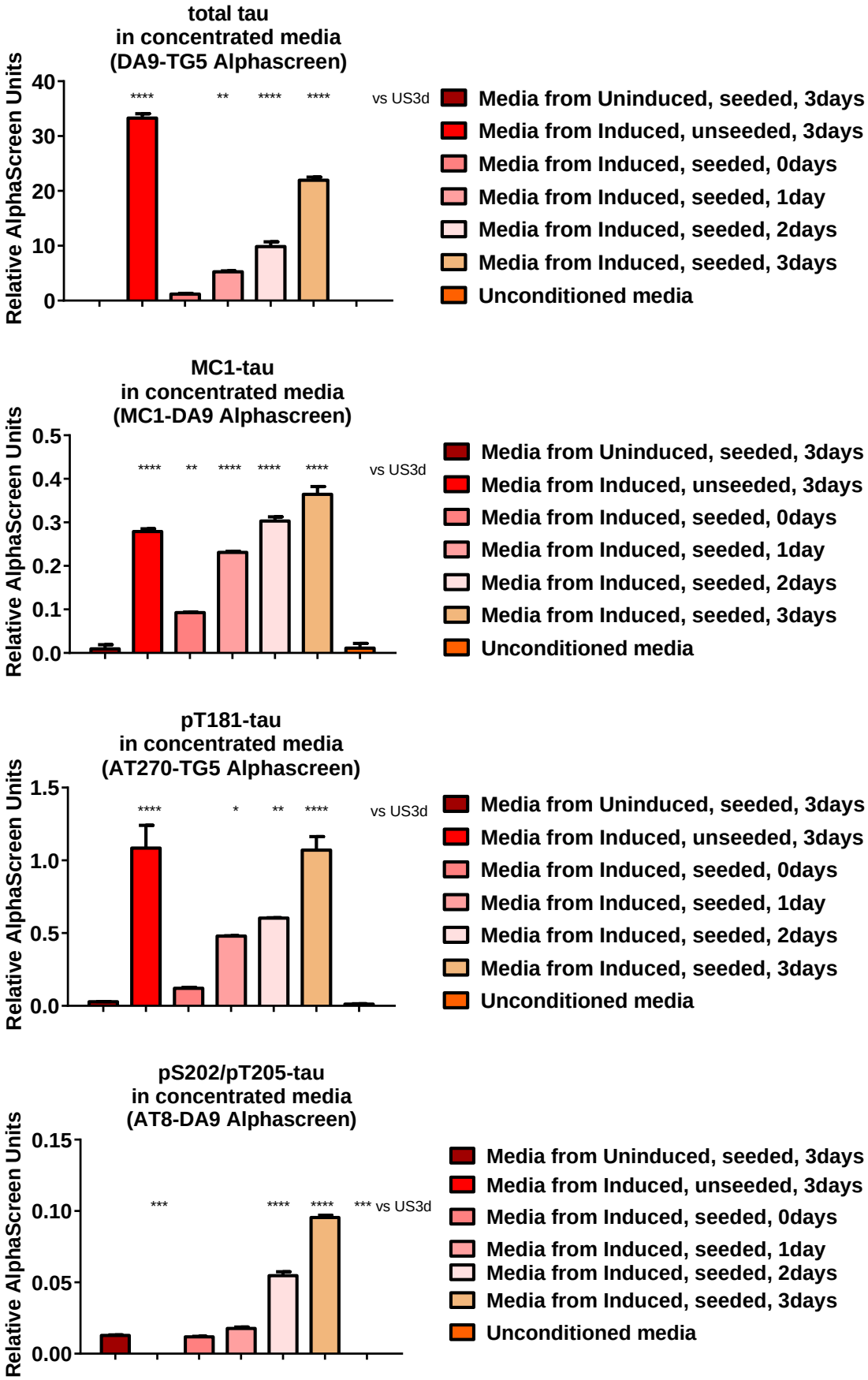

Figure 6.3: AT8-positive tau is present in media from seeded TgP301S tau inducible cells. Alphascreen assay in conditioned media samples from cells seeded with TgP301S mouse brain-derived tau extract and collected 0-1-2-3 days post seeding. Statistical analysis: one-way

ANOVA with Dunnett's *post hoc* test. *p<0.05, ****p<0.0001 compared with controls (Uninduced, seeded, 3 days). The values are the means ± SEM (n=2).

Conditioned media samples, matched for total tau levels using Alphascreen, were added to a new population of HEK-T-REx-293 P301S inducible cells, in absence of transfection reagents. The transfer of conditioned medium from seeded cells was sufficient to induce tau aggregation in the second population of cells, where insoluble tau was extracted by 1% Triton X-100; cells were analysed by high-content imaging assay (measuring tau aggregation as ratio "PG5 total intensity / Hoechst total area" or "MC1 total intensity / Hoechst total area") (Figure 6.4) and confocal imaging (Figure 6.5). Seeding in the imaging assay 96-well format required lower volumes of media sample than the ones required for the 6-well biochemical assay, allowing us to perform a minimal dilution of the media samples, and therefore see a bigger seeding effect than the one seen by biochemical assay. We found that media from seeded cells could induce accumulation of PG5-and MC1-positive, insoluble tau in recipient cells, proportional to the amount of AT8-tau measured by Alphascreen in the media. Media from unseeded cells failed to cause accumulation of insoluble tau in the second population of cells.

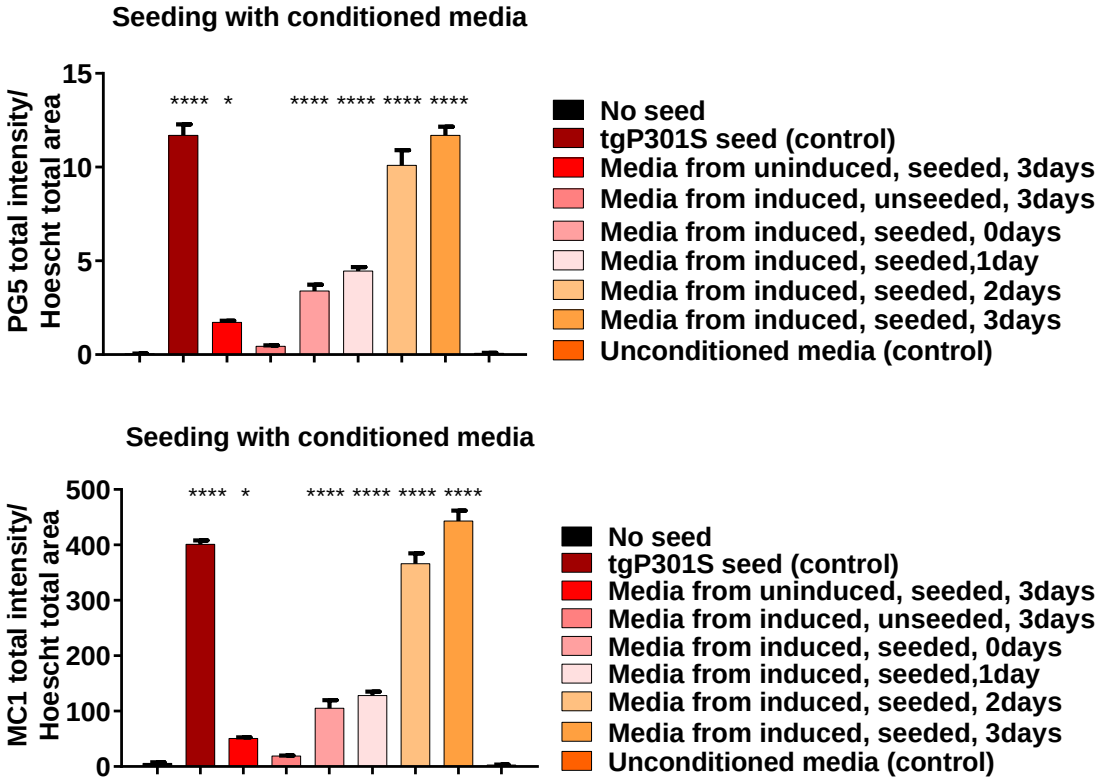

Figure 6.4: Conditioned media from seeded TgP301S tau inducible cells induces seeding in a new population of cells. HCI assay using PG5 antibody (pS409-tau) (upper panel) and MC1 antibody (lower panel) in HEK T-REx P301S tau inducible cells treated with conditioned media from cells seeded with TgP301S mouse brain-derived tau extract shows accumulation of abundant Triton X-100-insoluble tau. Statistical analysis: one-way ANOVA with Dunnett's *post hoc* test. *p<0.05, ****p<0.0001, compared with unseeded controls. The values are the means ± SEM (n=2).

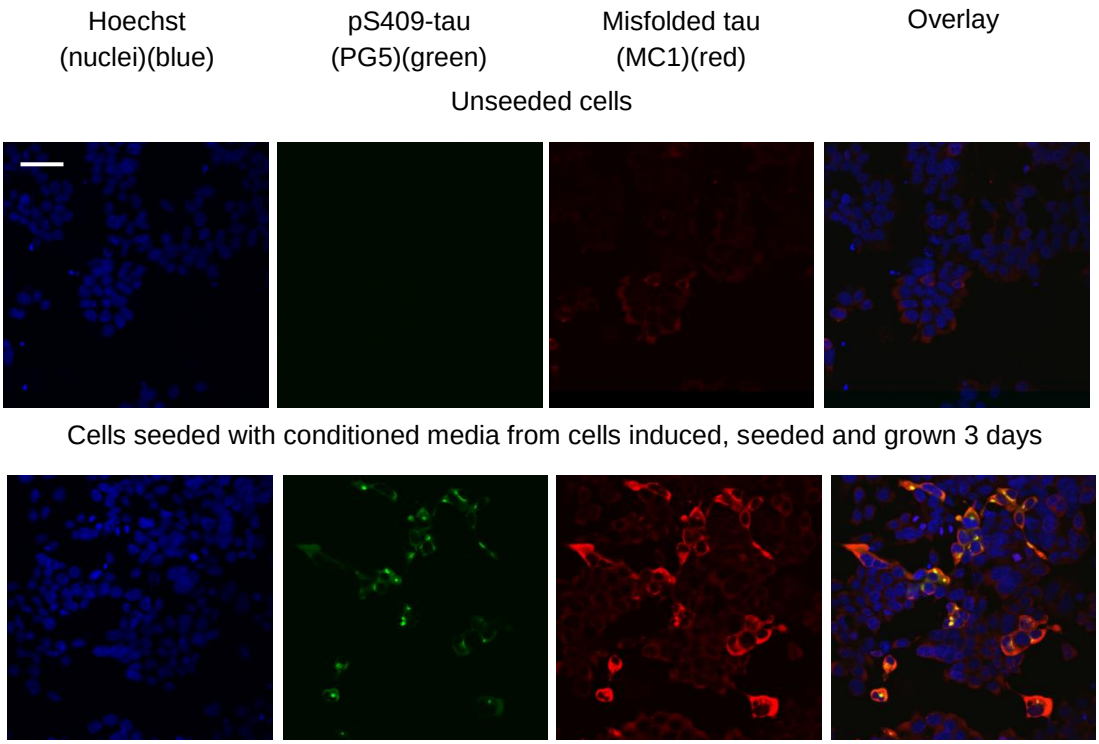

Figure 6.5: Conditioned media from seeded TgP301S tau inducible cells induces seeding in a new population of cells. Confocal imaging assay using PG5 antibody (pS409-tau) and MC1 antibody (conformationally-changed tau) in HEK T-REx P301S tau inducible cells treated with conditioned media from cells seeded with TgP301S mouse brain-derived tau extract shows accumulation of abundant Triton X-100-insoluble tau. Scale bar 50 µm.

A strong positive correlation (R^2 =0.9156) was observed between the levels of AT8-positive tau present in conditioned media samples (input) and the levels of seeded aggregation observed in the cells, as measured by the levels of PG5-positive Triton X-100-insoluble tau following seeding with each conditioned media sample (output). No correlation (R^2 = 0.02624) was present between the levels of total tau in conditioned media samples measured by Alphascreen (input) and the levels of seeded aggregation in cells (output) (Figure 6.6).

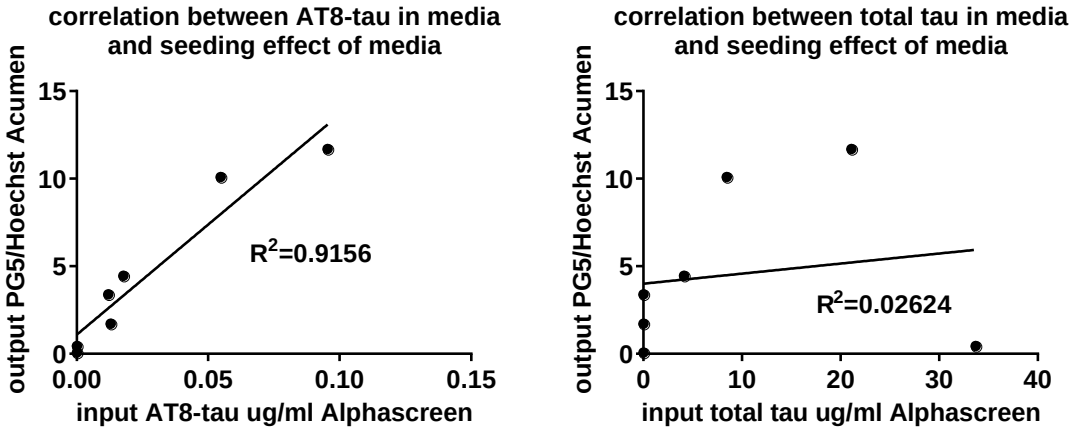

Figure 6.6: Positive correlation between levels of AT8-positive tau in conditioned media (input) and levels of aggregation in seeded cells (output). Correlation and linear regression were performed to determine relationships between input and output tau in the cell-based seeding assay. The levels of AT8-positive tau in conditioned media measured by Alphascreen assay correlated with the seeding ability measured by HCI assay (r^2 = 0.9156). No correlation was observed with total tau as the input (r^2 = 0.02624).

The presence of tau in the extracellular medium may result from either active secretion or neuronal cell death. Therefore we tried to minimize cell death during the course of the experiment to investigate whether tau can be released from intact cells. In addition, we controlled for cell damage induced by tau expression and/or seeding in our culture conditions. All the conditioned media samples subject to analysis were assessed for LDH activity, a normally cytoplasmic enzyme, while the corresponding cells were assessed by Trypan blue cell count. We observed that while tau was progressively secreted in the extracellular medium, LDH activity or Trypan blue stain did not change according to the same pattern as tau; the LDH assay showed no significant difference in cytotoxicity across media samples, as did the cell death count by Trypan blue assay, both measuring up to 10% cytotoxicity across samples (Figure 6.7).

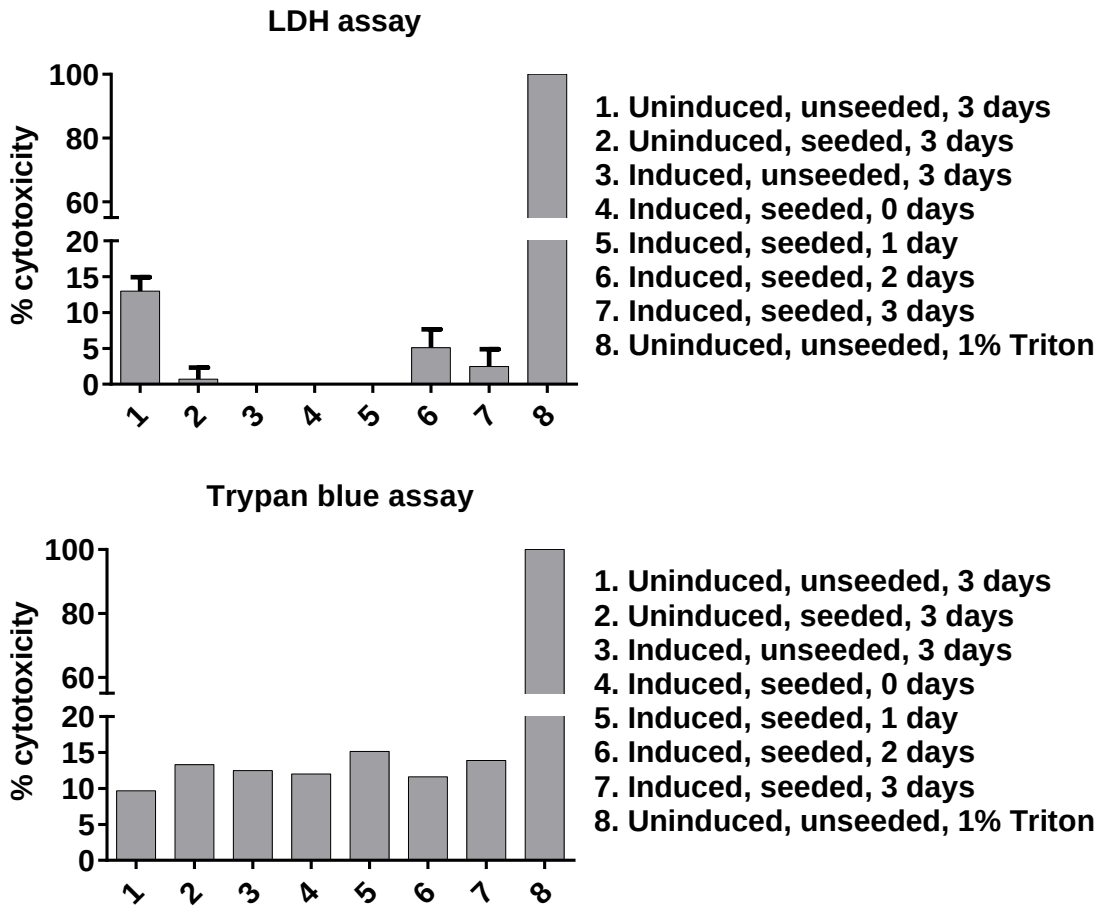

Figure 6.7: Seed-competent tau species in conditioned media do not derive from cell death. (Upper panel) LDH assay in conditioned media samples from cells seeded with TgP301S mouse brain-derived tau extract and collected 0-1-2-3 days post seeding shows negligible levels of cell death measured in the media. (Lower panel) Trypan blue cell death assay in cells seeded with TgP301S mouse brain-derived tau extract and collected 0-1-2-3 days post seeding shows that levels of cell death are consistent across samples. Media from 1% Triton X-100-treated cells was used as high control. The values are the means ± SEM (n=2).

In summary, we showed that conditioned media collected from seeded cells is able to induce seeding in naïve cells, confirming the presence of extracellular seed-competent tau species. Similarly to what we observed for TgP301S lysate, the seeding ability of the conditioned media correlated to its levels of AT8-positive tau.

6.3 Discussion on extracellular tau in HEK T-REx P301S tau inducible cells

Several prior studies investigated tau release in various cell culture systems, such as overexpression models (Kim, Lee & Hall 2010a, Kim et al. 2010, Chai, Dage & Citron 2012, Plouffe et al. 2012, Simon et al. 2012), untransfected cells (Chai, Dage & Citron 2012, Karch, Jeng & Goate 2012, Bright et al. 2015) or primary cortical rodent neurons (Karch, Jeng & Goate 2012, Pooler et al. 2013, Kanmert et al. 2015) and found that tau detected in cell medium is released by an unconventional secretion mechanism, but none of them used a seeded cell model of tau aggregation. Here, we investigated the presence of extracellular tau in conditioned

media from our well established cell-based model of seeded tau aggregation (Falcon et al. 2015). HEK T-REx P301S 1N4R tau inducible cells were initially seeded with sarkosyl-insoluble TgP301S tau via reagent-free inoculation (to avoid any confound in characterising tau species present in media) in order to collect and concentrate the derived conditioned media, and ultimately test its ability to seed endogenous tau aggregation in naïve induced cells. We found that only conditioned media from seeded cells, containing AT8+ve tau, induced seeding in a new population of cells. Controlling for cell death is critical for the interpretation of the very low level of tau release that we are investigating; we measured accumulation of tau in the absence of increased LDH activity in the medium, ruling out unspecific release based on cell death. We did not apply any detergent treatment of the conditioned media, yet tau was readily detectable, suggesting the presence of released free-floating tau species. Our findings are in agreement with other groups, which have reported endogenous tau to be released free in a dephosphorylated full-length form (Pooler et al. 2013) or as N-terminally truncated fragments (Bright et al. 2015, Kanmert et al. 2015). Total tau levels measured by Alphascreen in media from induced, unseeded cells were higher (32 units) than in media from induced, seeded cells (22 units) at the same time point; the reason for this is unknown and was not observed for other tau epitopes measured by Alphascreen (MC1-tau, pT181-tau) and it is not attributable to tau release from cytotoxicity, as shown by LDH and Trypan blue assays (Figure 6.7). Since seeding seems to have a specific effect of reducing total tau release, but increasing AT8-positive tau release, further studies should be carried out to establish the specific effect of seed-competent species on tau release.

Our data suggests that tau transfers via the extracellular medium, however we have not yet confirmed this by showing modulation of tau release; for instance, we have not investigated whether beta-amyloid or small molecules can influence the levels and forms of tau released from cells. Also, we collected the media at different timepoints after seeding cells with a single concentration of TgP301S seed; in future experiments, we could collect media at a fixed timepoint after seeding with a range of concentrations of TgP301S seed. An alternative experiment to prove that the cell-to-cell transfer depends on release of aggregates in the extracellular space, rather than on cell-to-cell contacts, would be to show its dependency from culture media volume; for instance, efficiency of SOD1 aggregates transfer between co-cultured cells dramatically decreased when increasing the volume of the cell culture media, thereby diluting the transferring species (Munch, O'Brien & Bertolotti 2011). In future studies, we would also need to develop orthogonal methods to identify more rigorously the tau species detected in media; for this, we would need high-sensitive assays, i.e. Simoa (Single Molecule Array), differentiating between full-length tau, mid-region-bearing fragments, and C- and N-terminal fragments; future experiments should also aim at collecting conditioned media from seeded cells and subject it to immunodepletion or immunoprecipitation with different antibodies, to define the molecular identity of extracellular tau.

In summary, our cell model allowed us to measure extracellular tau species and characterise their ability to seed naïve cells. Importantly, the transcellular spread of tau by extracellular

release provides a molecular basis for tau immunotherapies targeting extracellular species. Further studies are needed to investigate whether secretion of misfolded tau into the extracellular space is a factor contributing to disease progression, whether it can be blocked by antibodies or small molecules, and whether tau conformation plays a role in the propagation of the tau lesions. Given that tau has been shown to exist in different conformational states (strains) with varying degrees of neurotoxicity and seeding properties, it is plausible that effective immunotherapy strategies will have to be conformation-specific, and possibly targeting multiple amyloidogenic proteins, at various levels of the disease progression.

7. DEVELOPMENT OF NEURONAL MODELS OF TAU AGGREGATION

After developing a useful non-neuronal model for studying the pathogenesis of tauopathies, we wanted to replicate our findings in neurons, the cell type most relevant for neurodegenerative tauopathies. We also wanted to employ a neuronal model to be able to investigate the mechanisms of neuron-to-neuron propagation, and the role of synaptic transmission on tau propagation, which are still unanswered questions. We created a neuronal model recapitulating the main features of seeded tau pathology, using hippocampal neurons from TgP301S mice expressing 0N4R P301S tau, or rat cortical neurons expressing 1N4R P301S tau.

7.1 Development of a tau aggregation model in TgP301S mouse hippocampal neurons

Having found that TgP301S and recombinant P301S seeds can spontaneously enter non-neuronal cells and recruit normal tau into pathological accumulations, we wanted to replicate this phenomenon in a cell type more relevant for tauopathies. Primary hippocampal neurons dissociated from P301S and C57Bl6 mouse embryos were seeded at DIV7 with sarkosyl-insoluble tau extracted from TgP301S mice ("TgP301S seed") or C57Bl6 mice ("WT seed"), containing equivalent amounts of total tau, according to 3 different seeding paradigms: seeds added for 3 hours, then replaced with fresh media; seeds added for 6 hours, then replaced with fresh media; seeds added and not removed (but cultures were half-fed at DIV11, 4 days post seeding). Neurons were cultured until DIV14, then fixed, stained and imaged by high-content imaging assay measuring tau aggregation as ratio "AT8 total intensity / Hoechst total area". Addition of TgP301S seed to neurons at DIV7, without any transduction reagent, led to robust accumulation of AT8-phosphorylated tau that resisted Triton X-100 extraction at 7 days post-seeding (AT8/Hoechst ratio ~10), whereas addition of WT seed did not cause significant increase in AT8-positive tau compared to unseeded cells (AT8/Hoechst ratio ~4) (Figure 7.1 A). The amount of AT8-positive tau inclusions induced in WT neurons by both TgP301S and WT seeds was highly limited compared to that observed in TgP301S neurons, most likely due to lack of overexpression of mutated tau; only when the TgP301S seed was left on and not removed, WT neurons showed phosphorylated tau recognized by AT8 that remained Triton X-100-insoluble, suggesting the detection of residual seed rather than bona fide intracellular endogenous tau aggregates (AT8/Hoechst ratio ~2) (Figure 7.1 B).

A

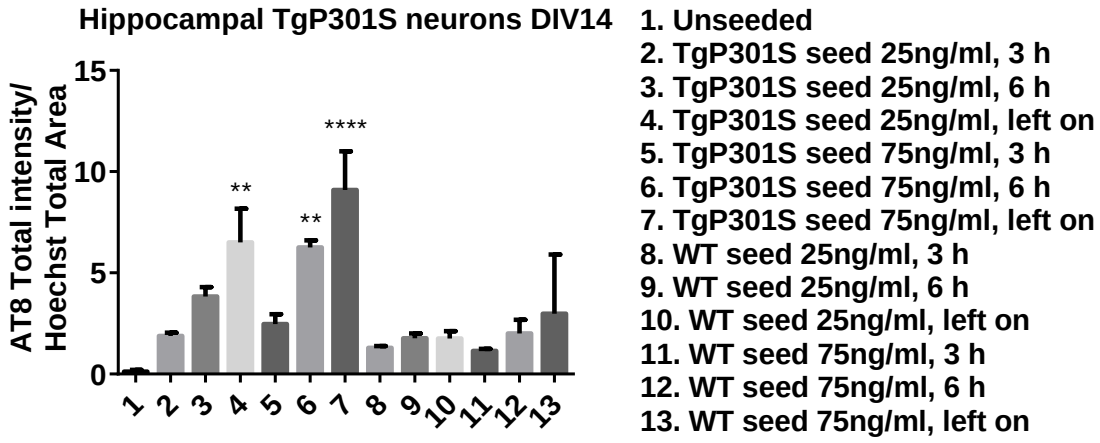

B

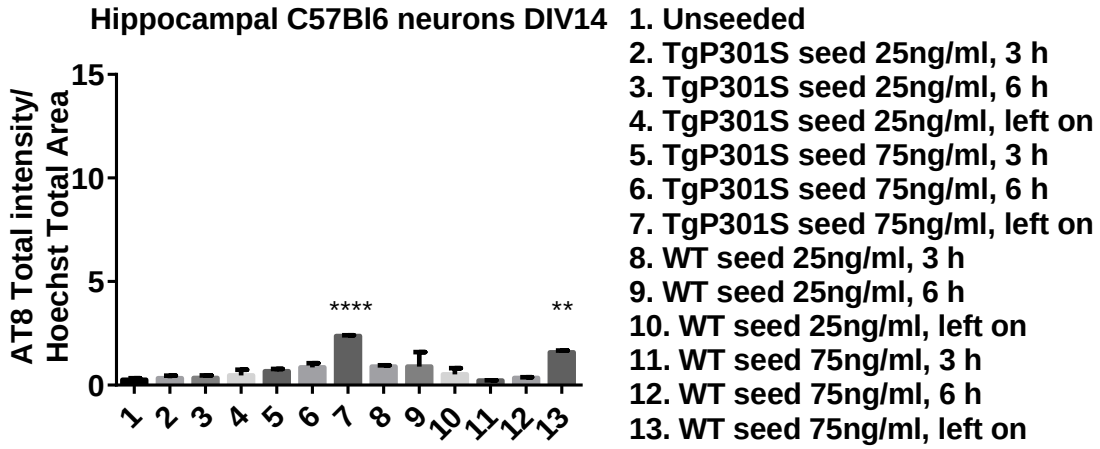

Figure 7.1: Triton X-100-insoluble tau accumulation in TgP301S primary hippocampal neurons after incubation with TgP301S seed, but not WT seed. Neurons were immunostained with phospho-tau mAb AT8 with 1% Triton X-100 extraction during fixing. Statistical analysis: one-way ANOVA with Dunnett's *post hoc* test. *p<0.05, ****p<0.0001, compared to unseeded controls. (A) Hippocampal TgP301S neurons treated with TgP301S seed and WT seed. (B) Hippocampal WT neurons treated with TgP301S seed and WT seed. The values are the means ± SEM (n=2).

Since our readout signal (AT8 Total intensity/Hoechst total area) will not discriminate between exogenously added TgP301S seed and genuine intracellular aggregates of overexpressed P301S tau resulting from seeding, Figure 7.2 shows the seeding assay in TgP301S neurons corrected for the presence of residual TgP301S seed, (by subtracting the values of AT8 Total intensity/Hoechst total area measured in WT neurons from the ones measured in TgP301S neurons in the corresponding conditions); a time-dependent and dose-dependent seeding pattern is clearly observed.

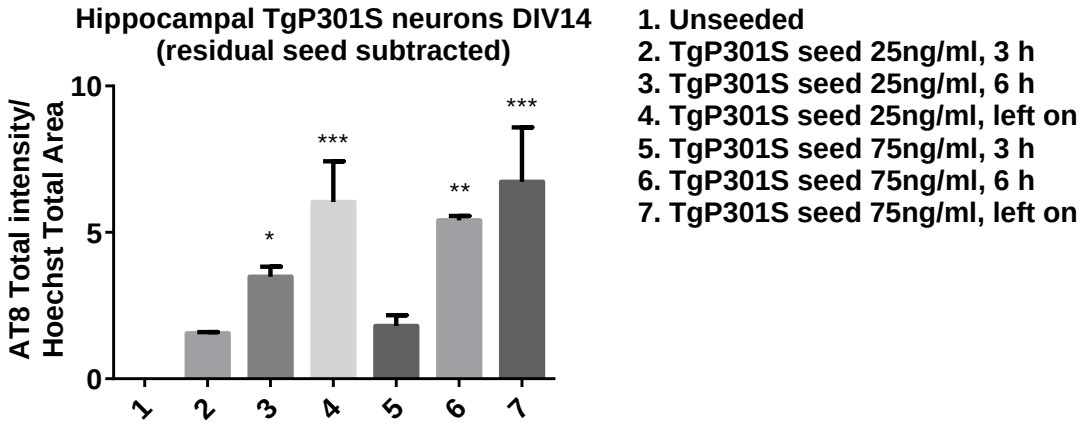

Figure 7.2: Triton X-100-insoluble tau accumulation in TgP301S primary hippocampal neurons after incubation with TgP301S seed is dose-and time-dependent. Hippocampal TgP301S neurons treated with TgP301S seed (signal corrected for the presence of residual seed). Statistical analysis: one-way ANOVA with Dunnett's *post hoc* test. *p<0.05, ****p<0.0001, compared to unseeded controls. The values are the means ± SEM (n=2).

In the same experiment, aggregates in TgP301S neurons treated with TgP301S seed, but not WT seed, were intensely labelled by disease-specific conformational antibody MC1, indicating that the aggregates acquired a pathological conformation (Figure 7.3).

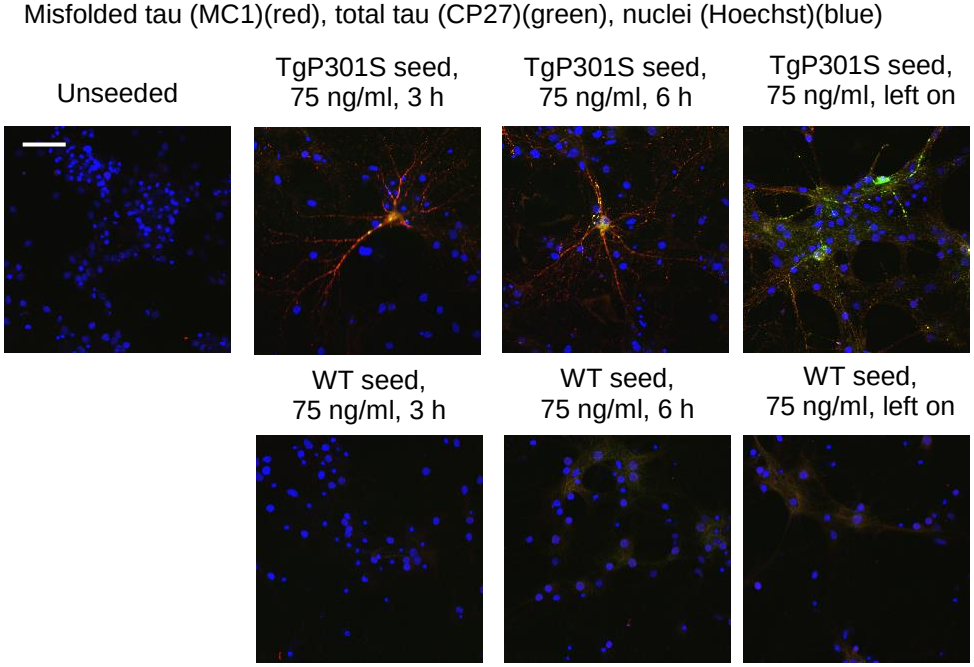

Figure 7.3: Triton X-100-insoluble tau accumulation in TgP301S primary hippocampal neurons after incubation with TgP301S seed, but not WT seed. Confocal imaging showing punctate accumulations of Triton X-100-insoluble tau in the neurites of TgP301S neurons after 3 h, 6 h or prolonged incubation (seed left on, half media change 4 days post-seeding) with TgP301S seed, but not WT seed. Neurons were immunostained with MC1 antibody (conformational changed tau, red) and CP27 antibody (total human tau, green) with 1% Triton

X-100 extraction during fixing. Scale bar 100 µm. Data shown is representative of 2 independent experiments.

Both TgP301S and WT seeds were also tested in non-Tg primary neurons for their ability to seed endogenous tau fibrillization without overexpressed human mutant tau; confocal imaging showed no tau aggregate formation upon TgP301S or WT seed treatment in non-transgenic neurons after 3h, 6h or prolonged incubation with seeds; both seeds demonstrated no seeding efficiency in this system, where only residual TgP301S seed was detected in the “seed left on” paradigm. Since CP27 antibody recognizes human tau only, endogenous mouse tau in C57Bl6 neurons displayed no immunoreactivity with this antibody (Figure 7.4).

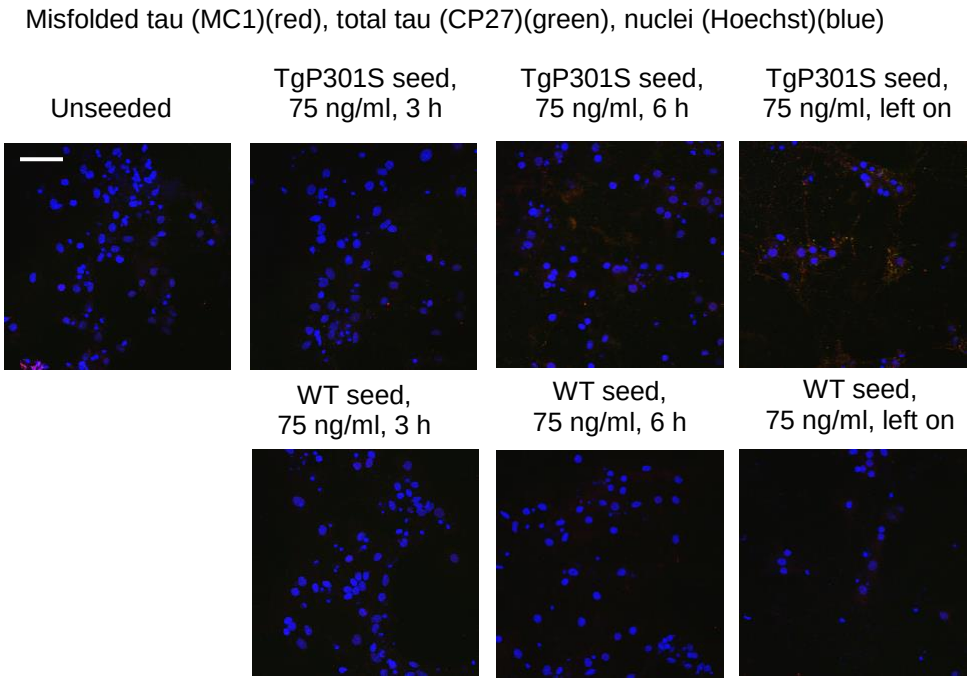

Figure 7.4: Confocal imaging shows no tau aggregates formation upon TgP301S or WT seed treatment in non-transgenic neurons. Neurons were immunostained with MC1 antibody (conformational changed tau, red) and CP27 antibody (total human tau, green) with 1% Triton X-100 extraction during fixing. Scale bar 100 µm. Data shown is representative of 2 independent experiments.

In summary, this neuronal system relies on spontaneous uptake of native forms of tau aggregates and potentially provides a tool for understanding the mechanisms of tau dysfunction. However, due to poor viability of the cultures, we decided to create a more reliable neuronal model using rat neurons, generally deemed more robust than mice neurons.

7.2 Development of a tau aggregation model in rat cortical neurons

Primary rat cortical neurons (RCNs) overexpressing TgP301S 1N4R tau by lentiviral infection were treated for 24 h with TgP301S 0N4R tau seed at DIV8, and cultured until DIV15 (Figure 7.5).

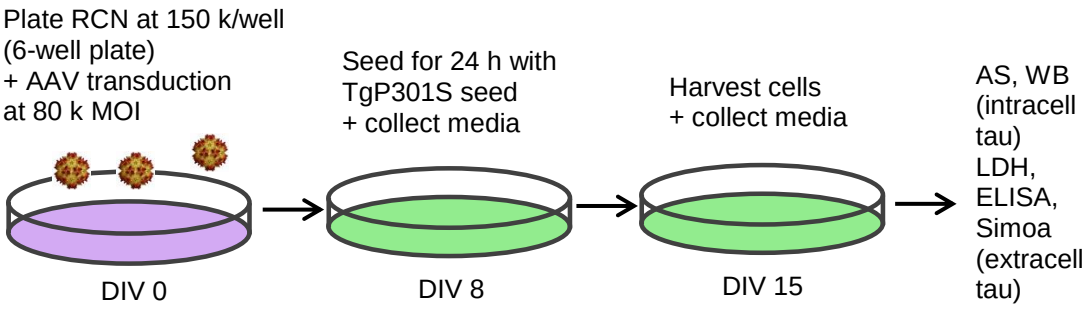

Figure 7.5: Schematic representation of the cell-based seeded tau aggregation assay in rat cortical neurons. Untransfected neurons were used as a control for absence of tau expression. Neurons treated with buffer were used as control for absence of seeding.

Biochemical analysis (western blot and Alphascreen) of sarkosyl extracts from cell lysates after 15 days revealed that the internalized tau seed initiated accumulation of sarkosyl-insoluble, AT8-positive aggregates, only in neurons overexpressing human P301S 1N4R tau, and not in uninfected neurons (Figure 7.6); AT8-tau was measured by AT8-DA9 Alphascreen to be 0.2 units when the highest seed concentration was used; aggregated tau was measured by MC1-MC1 Alphascreen to be 1.5 units when the highest seed concentration was used; total human tau was measured by DA9-CP27 Alphascreen to be 0.1 units when the highest seed concentration was used.

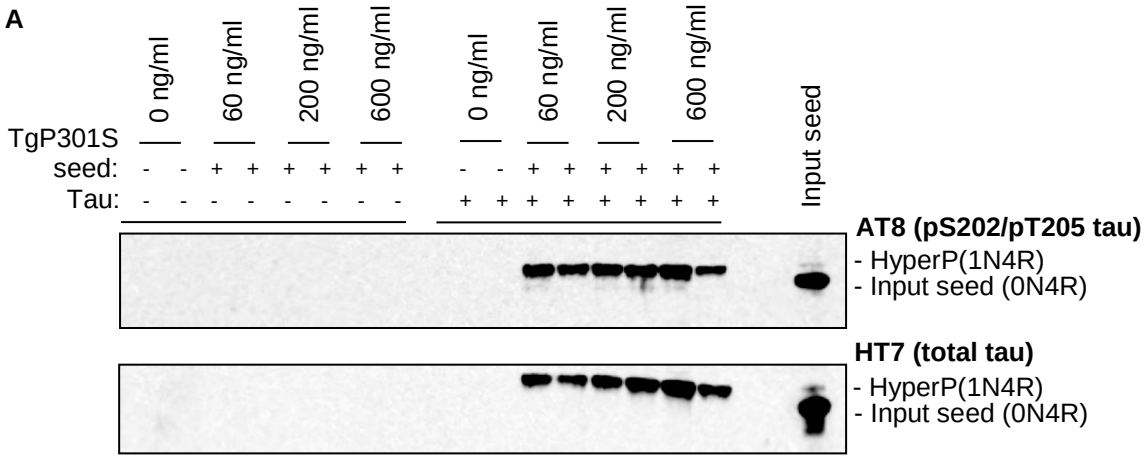

Figure 7.6: Dose-dependent accumulation of tau aggregates in seeded RCNs expressing P301S tau. Legend on the next page.

B

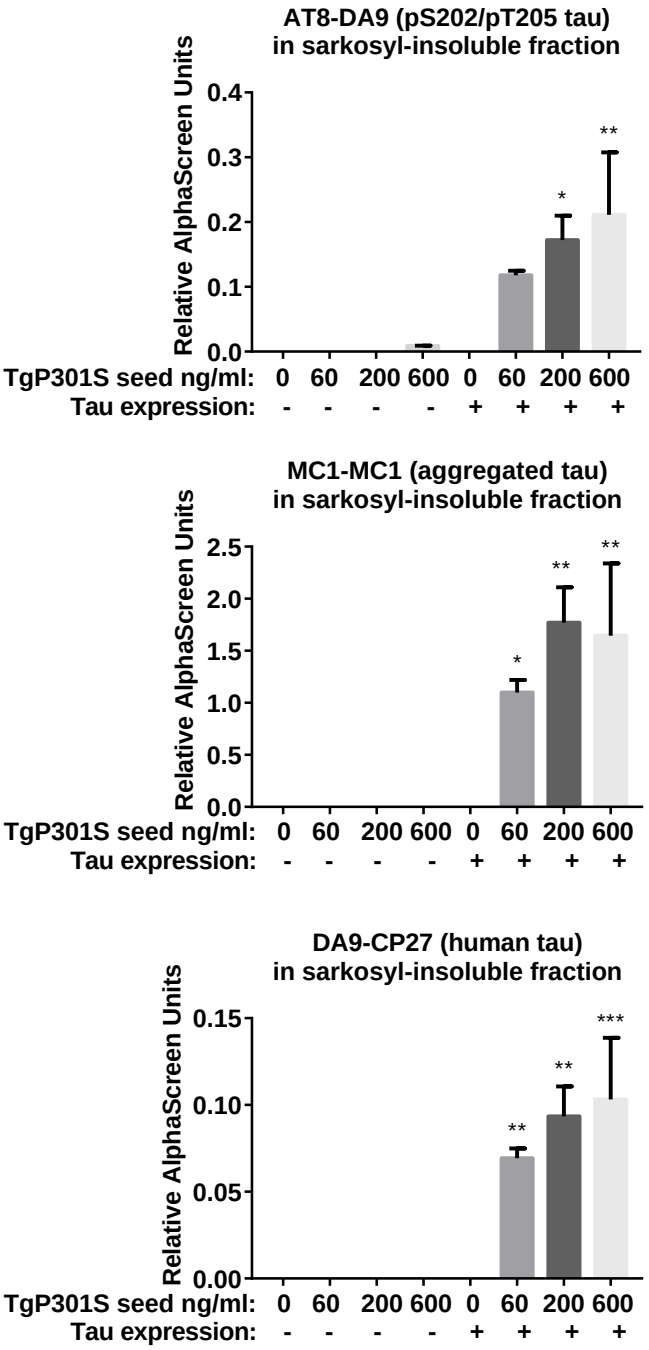

Figure 7.6: Dose-dependent accumulation of tau aggregates in seeded RCNs expressing P301S tau. WB (A) and Alphascreen (B) of sarkosyl-insoluble human tau accumulation in rat cortical neurons virally transduced with human P301S 1N4R tau, after 24 h incubation with TgP301S 0N4R tau seed. Blots were probed with AT8 antibody, and human tau-specific antibody HT7. Statistical analysis: one-way ANOVA with Dunnett's *post hoc* test. *p<0.05, ****p<0.0001, compared to uninfected, unseeded controls. The values are the means ± SEM (n=2).

Extended seeding time was also tested; primary rat cortical neurons (RCNs) overexpressing TgP301S 1N4R tau by lentiviral infection were treated with TgP301S 0N4R tau seed at DIV8, and cultured until DIV15. Seed was not deliberately removed, but media was half-changed at DIV11, 3 days after seeding. Imaging analysis after 15 days revealed that the internalized tau seed initiated accumulation of MC1- and PG5-positive aggregates, only in neurons overexpressing human P301S 1N4R tau, and not in uninfected neurons or neurons expressing WT 1N4R tau (Figure 7.7).

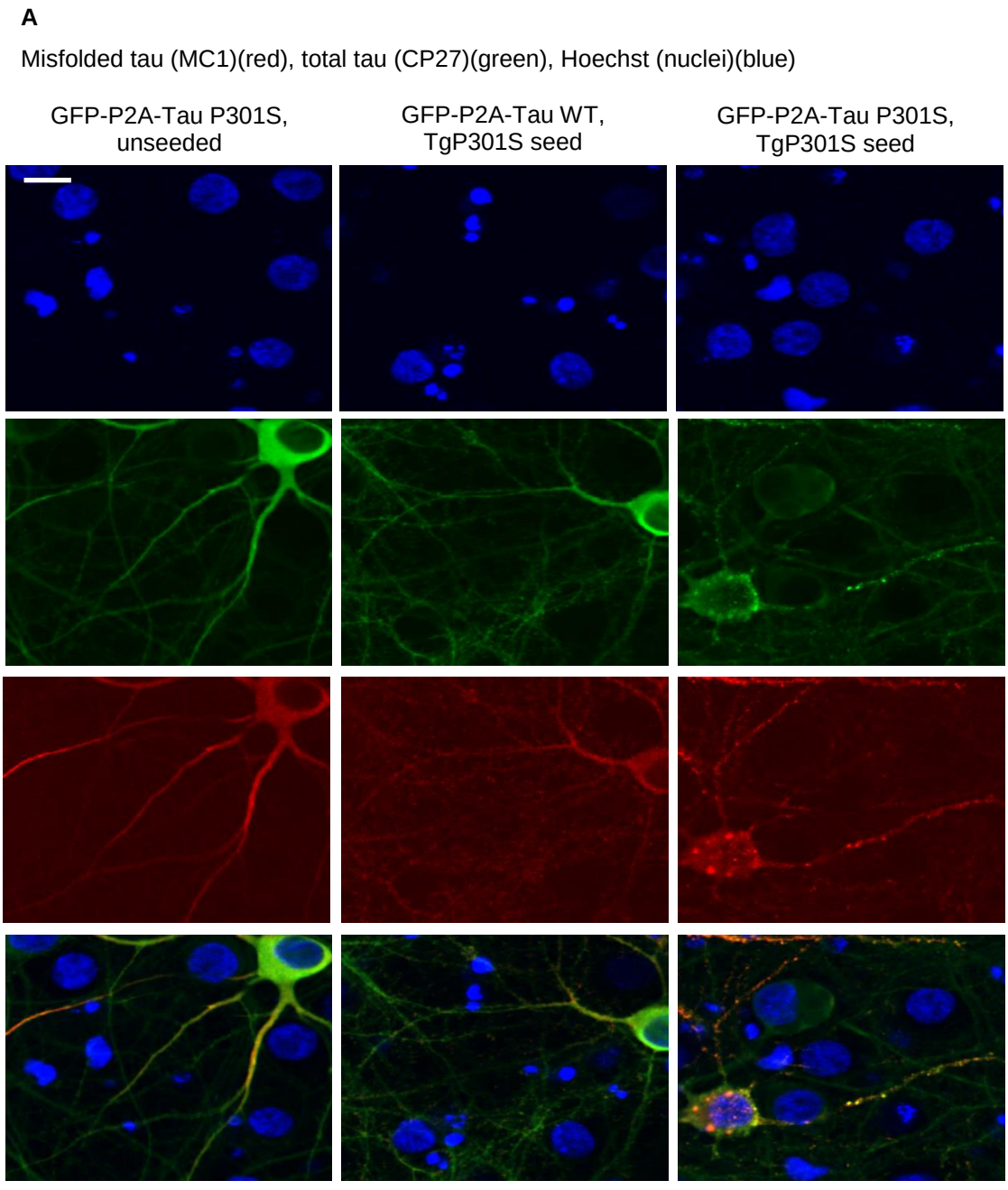

Figure 7.7: Accumulation of tau aggregates in seeded RCNs expressing P301S tau.
Legend on the next page.

B

pS409-tau (PG5)(red), total tau (CP27)(green), Hoechst (nuclei)(blue)

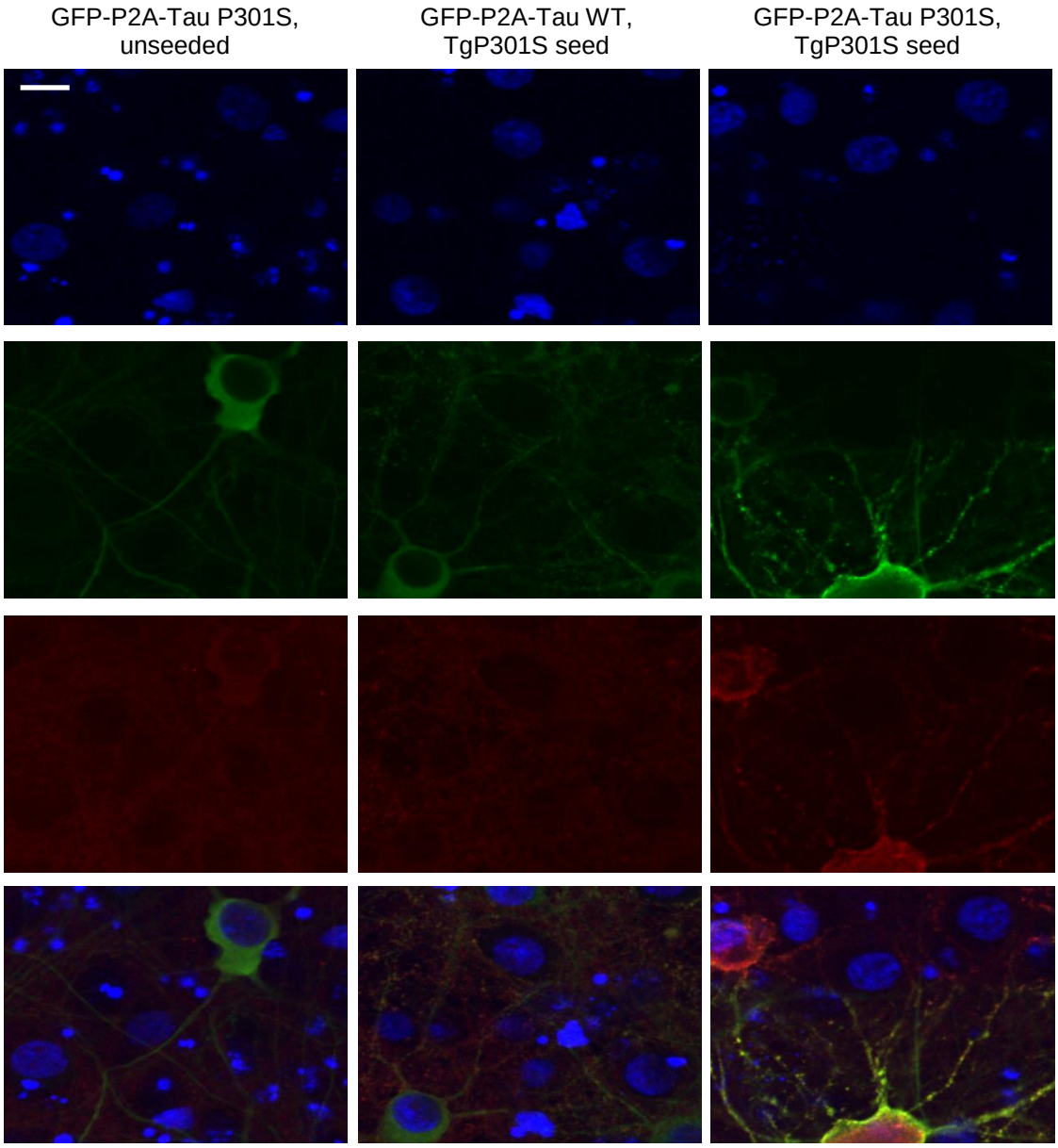

Figure 7.7: Accumulation of tau aggregates in seeded RCNs expressing P301S tau. Confocal imaging showing tau aggregates formed upon TgP301S seed treatment in rat cortical neurons expressing P301S 1N4R human tau, but not WT 1N4R tau, after prolonged incubation with tgP01S 0N4R tau seed (seed not removed). Neurons were immunostained with (A) MC1 antibody (conformational changed tau, red) or (B) PG5 antibody (pS409-tau, red) and CP27 antibody (total human tau, green) with 0.1% Triton X-100 extraction during fixing. Scale bar 20 µm. Data shown is representative of 2 independent experiments.

In summary, this overexpression neuronal system relies on spontaneous uptake of native forms of tau aggregates; behaving similarly to the HEK T-REx P301S tau inducible cell model, it provides a valuable tool for understanding the mechanisms of tau dysfunction and for screening therapeutics for the treatment of tauopathies.

7.3 Discussion on neuronal cell-based assay

After developing a useful non-neuronal model for studying the pathogenesis of tauopathies, we wanted to replicate our findings in neurons, the cell type most relevant for neurodegenerative tauopathies. We also wanted to employ a neuronal model to be able to investigate the mechanisms of neuron-to-neuron propagation, and the role of synaptic transmission on tau propagation, which are still unanswered questions. Guo and Lee (Guo, Lee 2013) demonstrated that synthetic tau fibrils triggered robust aggregation of otherwise soluble endogenous tau into NFT-like inclusions in primary neurons dissociated from embryonic hippocampus of PS19 transgenic mice, which express human 1N4R P301S tau. We used a similar system of primary hippocampal neurons overexpressing human mutant tau and showed that transgenic mice-derived exogenous aggregates time-dependently recruit endogenous tau into aggregates. Importantly, seed-induced tau aggregation did not occur in non-tg neurons in the absence of overexpression. Consistent with Guo and Lee (Guo, Lee 2013), who found that mutant tau pre-formed fibrils resulted in dramatically more abundant pathology than wt tau pre-formed fibrils in PS19 neurons overexpressing mutant tau, we also found that tau aggregates only formed upon TgP301S seed treatment in TgP301S hippocampal neurons, and not in the other conditions, in the timeframe of our assay (up to 1 week post-seeding). Similarly, rat cortical neurons overexpressing P310S tau, but not WT tau, also showed tau aggregation upon seeding with TgP301S seed.

Non-neuronal cell lines have the advantage of low cost and unlimited proliferation, allowing screening of large numbers of compounds, but their response to genetic modifications or drug treatments may be different from neurons, so the translatability from mammalian cells to neuronal cells is not always guaranteed. High cost and relatively long cultivation periods of iPSC-derived neurons preclude them from use for primary screening of tau therapeutics. On the other hand, our RCN neuronal model is amenable to high-throughput screening (high content imaging assay in 96-well format) and could serve as a more relevant biological tool to confirm hits from a primary aggregation inhibition assay.

However, neuronal cultures also have their limitations, as other in vitro techniques can be a more reliable representation of the in vivo environment. For instance, organotypic hippocampal slices are explants of hippocampal tissue that can be maintained in culture for months, and present a more naturalistic synaptic organization than routine culture dissociated neurons methods. Basic advantages of slices over cultured cells is the preservation of the 3-dimension tissue architecture, presence of multiple cell types, glial-neuronal interaction, synapses network connectivity and long term viability, while the in vitro nature of the slices enables direct control of the environment, direct access for various imaging, biochemical and electrophysiology assays, easy gene manipulation and precise pharmacological intervention; overall, slice cultures are an ex vivo model that bridges cell culture and in vivo models, and could offer a more accurate representation of the in vivo environment than cell cultures.

Another limitation of our neuronal cell model is that it is characterised by tau overexpression, coupled to a mutation that further enhance tau fibrillization propensity (P301S). However,

upregulation of tau is not a cause of AD or the majority of neurodegenerative diseases in humans, where the disease-associated proteins are not usually up-regulated; moreover, tauopathies are mostly sporadic, and mutations on the tau gene (MAPT) are only present in rare cases of frontotemporal dementia dementia with parkinsonism associated with chromosome 17 (FTDP-17) (Hutton et al. 1998, Rizzu et al. 1999, Goedert, Jakes 2005, Spillantini, Bird & Ghetti 1998); recent data has shown that the heterogeneity of tauopathies can be attributed to different tau strains (Clavaguera et al. 2013), therefore our neuronal system is strictly applicable to modelling a specific form of tauopathy. In an effort to better recapitulate AD pathology, we are currently developing a seeded neuronal model that expresses WT tau, using non-transgenic tau seed derived from human AD brain.

In summary, we created a neuronal model recapitulating the main features of seeded tau pathology, using a rat cortical overexpression system that relies on spontaneous uptake of native forms of tau aggregates; behaving similarly to the HEK T-REx P301S tau inducible cell model, our neuronal cell-based assay provides a valuable tool for understanding the mechanisms of tau dysfunction and a platform for screening therapeutics for the treatment of tauopathies. Further work should aim at improving existing models or establishing new cellular models that are physiologically and pathologically relevant, good surrogate for in vivo studies and also highly suitable for screening of drug candidates, to expedite the development of therapeutics.

8. DISCUSSION

We have established a HEK T-REx cell culture model where the inducible expression of mutant tau, accompanied by the introduction of aggregated mutant tau extracted from transgenic mouse brain, leads to endogenous tau aggregation and filament assembly, suggesting a seeding process as a likely mechanism underlying NFT formation. We found that substantial aggregation of soluble tau into Triton X-100-insoluble tau can be induced by spontaneous uptake of mutant tau aggregates, which are internalised through an endocytic mechanism that is temperature-, time- and ATP-dependent, can be potentiated by transfection reagents and impaired by pharmacological agents inhibiting macropinocytosis, suggesting a potential mechanism for the propagation of tau pathology in tauopathy brains (Figure 8.1). We also found that seed-competent tau species are sarkosly-insoluble, tagged by AT8 and MC1 antibodies, and are present in conditioned media from seeded cells. Finally, we established a more physiologically relevant model of seeded tau aggregation in rat cortical neurons.

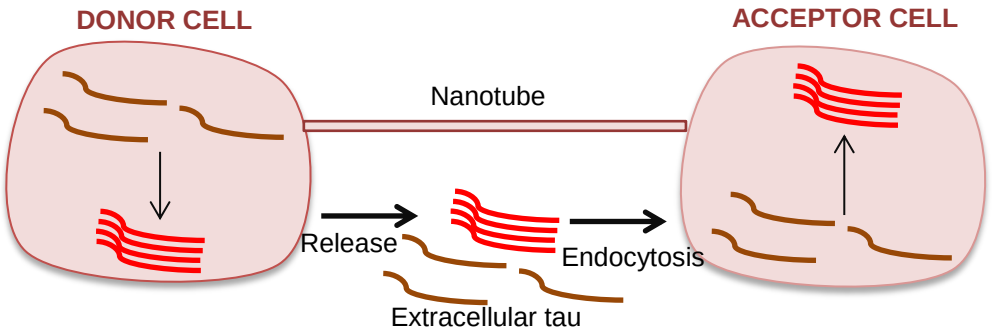

Figure 8.1: Potential mechanisms mediating cell-to-cell transmission of tau aggregates. Exocytosis from a donor cell followed by endocytosis by a recipient cell is one possible route for tau transfer between cells. Tau aggregates can be released into the extracellular space as free-floating seeds or via membrane-bound vesicles. Tunneling nanotubes, which have been shown to transport both organelles and proteins such as prions between cells, remains an unexplored possible mechanism for cell-to-cell transfer of tau seeds. Internalized seeds then nucleate the fibrillization of native monomers in the cytoplasm of the recipient cell.

8.1 Discussion on seed uptake

Macropinocytosis is the actin-driven invagination of the cell membrane to form large endocytic vesicles of irregular shape and size, which then travel into the cytosol and fuse with endosomes and lysosomes. Macropinosomes are large vesicles characterised by a diameter of up to 2.5 µm (Khalil et al. 2006). In our HEK Trex P301S tau inducible cells, seed uptake occurs via macropinocytosis, the prevalent mechanisms reported for tau uptake. In our recent publication (Falcon et al. 2015) we also showed that native TgP301S tau aggregates enter cells through the same mechanism as recombinant P301S tau aggregates, consistent with macropinocytosis. Therefore, like SOD1 aggregates (Munch, O'Brien & Bertolotti 2011), PrP^{sc} (Magalhaes et al. 2005) several viruses (Mercer, Helenius 2009), recombinant tau (Holmes et al. 2013., Frost, Jacks & Diamond 2009, Falcon et al. 2015) and perhaps other prion-like aggregates, we have observed that native TgP301S tau aggregates can hijack macropinocytosis to penetrate into the

cytosol of host cells. This implies that tau aggregates released from neurons or from “ghost tangles” are possibly using this mechanism to access neighbouring healthy neurons and trigger fibrillization of soluble tau in tauopathy brains. Internalised seeds may escape from macropinosomes by disrupting the vesicle membrane, and seed aggregation in the cytosol; this is plausible, since tau oligomers have been shown to cause destabilisation of the lipid bilayer of membranes (Flach et al. 2012); moreover, macropinosomes have been reported to be relatively “leaky” and lacking physical structure compared to other endosomes (Holmes et al. 2013., Flach et al. 2012, Conner, Schmid 2003) and a number of bacteria and viruses have been reported to exit macropinosomes and reach the cytosol (Conner, Schmid 2003), as well as SOD1 aggregates (Zeineddine et al. 2015). Aggresomes, stress-induced perinuclear inclusion bodies that form in response to the presence of a high load of abnormal cytosolic protein (Johnston, Ward & Kopito 1998), have also been proposed to be the site of seeded aggregation in the cytosol. Santa-Maria *et al.* demonstrated that mammalian cells internalize AD patient-derived paired helical filaments (PHFs) by an endocytic mechanism, and the induced tau aggregates co-localized with the aggresome markers γ-tubulin and vimentin, supporting the idea that endocytosed tau fibrils can exit the vesicular lumen to access the cytosol and seed aggregation of cytosolic tau monomer (Santa-Maria et al. 2012). One way to show the release of internalised seeds from macropinosomes would be to test whether the internalized aggregates are ubiquitinated; looking at different time points after inoculation, labelling the internalised seeds with a polyubiquitin antibody would suggest a cytosolic location.

In our analysis in HEK Trex P301S tau inducible cells, both monomeric and aggregated tau enter cells by a mechanism consistent with macropinocytosis with equal efficiency, however monomeric tau lacks seeding ability (Falcon et al. 2015). However, this finding may be cell-specific, since it has been reported that, unlike oligomers and short fibrils, soluble monomeric tau was not internalised in HeLa cells and mouse primary neurons (Wu et al. 2013).
Neurons express cell surface receptor complexes that have been shown to facilitate binding of viruses and activation of macropinocytosis: heparan sulfate proteoglycans (HSPGs), RAGE, CD36, integrins and receptor tyrosine kinases such as EphA2 and EphA4 (Yerbury 2016); heparan sulphate proteoglycans allow heparin-induced recombinant tau fibrils in neural cell lines and primary neurons alike (Holmes et al. 2013.). If macropinocytosis is to become a therapeutic target, it will be important to further characterise the neuron-specific machinery of cell surface proteins that are responsible for the binding and uptake of tau seeds, and avoid general blocking of all macropinocytosis in the brain, including microglial and astrocytic macropinocytosis. Calafate et al. developed a cell-to-neuron co-culture model where tau pathology propagates from clonal HEK293 donor cells to hippocampal neuron acceptor cells. To create this system, a polyclonal HEK293 cell line inducibly expressing GFP-tagged human mutant 2N4R P301L tau (‘‘clone 1’’) was treated with recombinant preformed synthetic HA-K18P301L fibrils (Guo, Lee 2011); sub-clones were isolated and assessed for the ability to stably produce tau aggregates throughout cellular generations, without addition of exogenous pre-formed fibrils; ‘‘clone 2’’ was chosen for its robustness in constitutively showing AT8-positive tau aggregates; finally, “clone 2” cells were co-cultured with hippocampal neurons (DIV7)

expressing human mutant P301L 2N4R Tau, not GFP-tagged. In this model, they showed that non-synaptic mechanisms were mediating baseline propagation, in absence of synaptic contacts; when synaptic contacts between donor and acceptor cells were induced by expression of synaptogenic adhesion proteins, propagation was enhanced above the baseline conditions, showing that both synaptic and non-synaptic mechanisms may contribute to tau pathology spreading. Their cell-to-neuron model presents the advantage of not requiring addition of exogenous tau seeds and allows screening for pre- and post-synaptic agents that may be involved in tau propagation, such as adhesion molecules, membrane receptors, and other synaptic machinery proteins. Synapses seem to be actively participating in cell-to-cell tau transmission, but tau has also been identified as causal factor in synaptic loss in AD, where synaptic degeneration correlated with cognitive decline (Selkoe 2002, Spires-Jones, Hyman 2014, Lu et al. 2013, Serrano-Pozo et al. 2011); more studies are needed to shed light on the link between these two processes, and determine whether synaptic rescue therapies will ultimately be beneficial or detrimental (Calafate et al. 2015). Blocking tau uptake via immunotherapy has been proved promising in animal models, but still to be determined is whether any receptors contribute to tau transmission, whether any cofactors facilitate tau uptake, and whether different uptake mechanisms apply to different neuron populations. Recently, McEwan et al. (McEwan et al. 2017) published a study that unveils a possible mechanism of action of tau therapeutic antibodies, involving Tripartite motif protein 21 (TRIM21), a cytoplasmic receptor that recognizes the Fc region of antibodies, binds to antibody-coated pathogens internalised by cells, and promotes their degradation by the proteasome and the unfoldase valosin-containing protein (VCP). They found that after cultured neurons took up tau aggregates complexed with anti-tau antibodies, the complexes bound to TRIM21, which acts as a tag for the proteasome degradation pathway. Of course this may be just one of multiple mechanisms of protein clearance by tau immunotherapies, i.e. blocking tau uptake, and the mechanism of action may be antibody-dependent; also, TRIM21 expression is higher in microglia and astrocytes, therefore the TRIM21 clearance pathway may be exploited by glial cells more than neurons; further research should investigate the role of TRIM21 in vivo, and whether the TRIM21-dependent immune response may work towards clearance of other protein aggregates like huntingtin and α-synuclein.

8.2 Discussion on nanotubes

It has been shown that tunnelling nanotubes can form between neuronal cells and prions appear to traffic through these structures between infected and non-infected cells (Gousset, Zurzolo 2009); in our HEK cell co-culture model, we used latrunculin A to verify whether nanotubes could allow cell-to-cell propagation of tau aggregates. The extent of the effect we observed suggests that disrupting the actin cytoskeleton with latrunculin A may have an impact not necessarily only on nanotubes, but possibly on other actin-dependent mechanisms of tau release and uptake, therefore further experiments should focus on dissecting these mechanisms and study the effect of latrunculin A on tau extracellular concentration, in co-culture media. Other compounds with an opposite effect to latrunculin A could be used to observe modulation of the actin cytoskeleton: several actin polymerising agents (phalloidin,

jasplakinolide, cytochalasin) are available and have been used in cell models to study the actin-dependent exocytosis of lytic granues by cytotoxic T lymphocytes (Lyubchenko, Georjeana & Zweifacht 2003). A recent paper similarly showed that TNTs may be involved in the prion-like propagation of tau assemblies, and tau facilitates their formation (Tardivel et al. 2016). In two different cellular models (CAD neuronal cells and rat primary embryonic cortical neurons), exogenous recombinant tau species (both monomers and fibrils) induced formation of TNTs, which subsequently facilitated the intercellular spread of pathological tau fibrils. Their data also suggests that tau might be transported into TNTs via actin, as tau progressively induced formation of long and thick F-actin structures, which were absent in absence of tau. Several in vitro models have implicated TNTs in the transport of many pathological proteins and pathogens (Rustom et al. 2004), however to date there have been no reports of TNTs in tauopathy brains, and only two reports of TNTs in vivo: in an animal model (for myeloid cells in corneas of wild type and transgenic mice) (Chinnery, Pearlman & McMenamin 2008), and in humans (for human mesothelioma cells) (Lou et al. 2012), therefore the relevance of this tau transmission mechanism in vivo remains to be confirmed.

8.3 Discussion on seeding properties

In our recent publication (Falcon et al. 2015) we used our cell-based assay to compare the seeding activity of sarkosyl-insoluble TgP301S tau with P301S recombinant tau. We observed that, similarly to synthetic prions (Kim et al. 2010, Tanaka et al. 2006, Legname et al. 2006, Legname et al. 2005), α-synuclein aggregates (Luk et al. 2012) and Aβ assemblies (Meyer-Luehmann et al. 2006a, Stöhr et al. 2012), synthetic tau aggregates had a greatly reduced seeding activity compared to sarkosyl-insoluble tau from TgP301S tau mouse brain; importantly, in our inducible cell assay, synthetic tau aggregates seeded by aggregated TgP301S tau in the absence of heparin acquired the seeding potency of brain-derived TgP301S tau seeds. In agreement with our findings, Guo et al. (Guo et al. 2016) established a mouse model of sporadic tauopathies and found that intracerebral inoculation of tau fibrils purified from AD brains, but not synthetic tau fibrils, resulted in the formation of abundant tau inclusions in anatomically connected brain regions in nontransgenic mice. Parallel with our findings, they found that human brain–derived tau fibrils are superior to synthetic tau fibrils in seeding physiological levels of WT tau in vivo (Guo et al. 2016). Recombinant human tau seeded by AD-tau produced unique conformational features, distinct from synthetic tau fibrils, which could underlie the differential potency in seeding physiological levels of tau to aggregate. Other disease-associated proteins, including prion, Aβ, and α-syn, similarly show different potency between synthetic- and brain-derived protein aggregates (Guo et al. 2016). The reasons for this phenomen could be:

a) The effect of post-translational modifications that are found in vivo but are absent in recombinant tau. Although we and others (Guo et al. 2016) showed that phosphorylation of tau does not contribute to its seeding efficiency, the effect of other post-translational modifications such acetylation, glycosylation, ubiquitination, glycation, prolyl-isomerization, polyamination, oxidation, nitration, and sumoylation should be explored in future studies.

b) The pathogenic tau strains produced in vivo in human brain may be the result of selection processes that cannot be recreated in vitro; tau conformers that are kinetically favoured, more resistant to degradation, and more readily transmitted than other conformers are more likely to be created in diseased brain, and not during in vitro fibrillization. Similarly, the complexity of the cellular environment and the presence of particular cofactors may generate particular pathogenic tau strains in the diseased brain that cannot be created in vitro (Guo et al. 2016).
c) Heparin is widely used as inducer of tau fibrillization in vitro, but was also shown to interfere with propagation of the AD-tau conformation (Morozova et al. 2013).
d) Synthetic aggregates are usually produced from a single isoform of tau, whereas brain-derived aggregates will typically contain a mixture of isoforms, whose interaction may result in conformations not observed in vitro.

In summary, using both recombinant and native tau aggregates, we provided evidence that despite being taken up by cells to the same degree, native tau aggregates have a higher seeding potency than recombinant tau aggregates; the latter though can acquire the conformation and seeding potency of the former by seeded assembly, demonstrating that conformation and not phosphorylation determines the seeding potency of tau aggregates. Our work supports the idea that distinct conformers of assembled tau exist, reminiscent of prion strains; their heterogeneity may explain the variety of human tauopathies, including genetic tauopathies like FTDP-17T, where different MAPT mutations produce different filament morphologies (Crowther, Goedert 2000) and the selective neuronal vulnerability of different tauopathies, with different aberrant conformers initiating disease processes in different brain cells, from where they spread to connected regions (Goedert 2015).

In future experiments, the comparison between native and recombinant seeds could be expanded to include brain extracts from different human tauopathies to characterise their seeding properties, possibly using antibodies and structural biology techniques to determine structures and conformational epitopes specific to individual diseases, and confirm the hypothesis that conformationally distinct tau strains might be associated with individual tauopathies (Clavaguera et al. 2013, Frost, Diamond 2010). Indeed a study found that inoculation of transgenic human tau mice with brain homogenates from patients with different tauopathies recapitulates certain pathological features of the diseases (Clavaguera et al. 2013); similarly, another group isolated a number of tau clones from HEK293 cells, injected into TgP301S (PS19) mouse brains and observed strain-specific patterns of tau pathology (Kaufman et al. 2016); this understanding could help facilitate therapeutic strategies tailored towards the underlying protein pathology. Similarly, at ADPD 2017 conference, J. Steen from Harvard Medical School, Boston, USA presented data from a mass spectroscopy-based technique called FLEXITau; while previously the authors applied this technique to map tau post-translational modifications (PTMs) in AD brain (Mair et al. 2016), more recently FLEXITau enabled the comprehensive, unbiased, robust and highly sensitive identification and quantification of tau PTMs in 4 different tauopathies; analyzing 129 postmortem brain samples from AD, PSP, CBD, PiD, and aged-matched controls, they discovered and quantified 74 PTMs,

over 60% of which have not previously been described in human tau; they found that each disease had its own distinctive pattern of tau PTMs (phosphorylation, acetylation, ubiquitination, and fragmentation); combining the FLEXITau signatures with computational analysis, they developed a classifier for tauopathies that correctly identified disease type with an accuracy of 94% for AD, 96% for CBD, 92% for PiD and 82% for PSP samples. The technique holds promise for a number of applications, including patient stratification, identification of therapeutic epitopes that should be targeted in each disease (the authors are currently generating disease-specific antibodies in collaboration with P. Davies, Manhasset, NY), screening of small compounds, and in vivo diagnostic biomarker for tau derived from peripheral fluids.

In additional experiments, recombinant P301S tau seeded with TgP301S tau could subsequently be used to seed a new generation of P301S recombinant tau, and the process could carry on along a number of generations, to see whether the conformation acquired by recombinant tau is stable and is maintained along several seeding generations. Tau post-translational modifications like cleavage, acetylation and O-GlcNac-ilation could be explored as potential factors that affect tau seeding potency. It will also be important to thoroughly characterise the seed-competent tau conformation using stability assays, conformational antibodies and small molecules, with a view to developing diagnostic tests and therapies. A similar potency comparison between transgenic and recombinant seeds could also be carried out for other known amylodogenic proteins, i.e. a-synuclein.

8.4 Discussion on seed competent species

Our findings indicate that a range of filamentous tau aggregates are the major species that underlie the spreading of tau pathology in the P301S transgenic model (Jackson et al. 2016). A recent paper reported that a tau trimer was the minimal particle size that could seed intracellular tau aggregation (Mirbaha et al. 2015), whereas our data shows that such small (low-*n*) oligomeric tau assemblies in brain extracts from TgP301S mice are not seed competent; it is important to note that Mirbaha et al. used different techniques and different brain material: they separated tau protein from one AD and one age-matched control brain using size-exclusion chromatography; their seeding assay in biosensor cells measures dimerization of tau repeats (K18) with the P301S mutation, rather than aggregation of full-length tau (Holmes et al. 2014); they did not confirm tau seeding and propagation in an *in vivo* model; consistent with our findings, they observed more efficient seeding of intracellular tau with assemblies larger than trimers, suggesting that although trimers can propagate, only larger tau species may have the structural complexity to produce bona fide tau strains, and it is possible that trimers have to convert to larger assemblies before being able to seed aggregation in cells. Another publication (Wu et al. 2013) showed that low molecular weight tau assemblies (~10–40 nm, consistent with dimers and trimers) and short tau filaments (~40–250 nm) were taken up by primary neurons from the extracellular space and transported through axonal terminals; however the authors only examined the internalisation of these tau assemblies and not their seeding ability. It is clear that many factors such as tau mutations, tau isoforms, seed preparation (i.e. sonication of

seeds), source of seeds, can influence the ability of tau to conformationally template; a lack of standardization of techniques and materials is a possible explanation for differences in seeding efficiency observed between different studies.

Our immunodepletion experiments support the idea that antibody-mediated removal of pathological forms of tau may block propagation. Various tau antibodies directed against distinct epitopes have been tested in vitro and in vivo, including N-terminal antibodies (Yanamandra et al. 2013a, Umeda et al. 2015), phospho-specific antibodies, (Collin et al. 2014, Chai et al. 2011, D'Abramo, Acker & Davies 2011, Sankaranarayanan et al. 2015, Boutajangout et al. 2011, Castillo et al. 2012) and conformation-dependent antibodies. (Chai et al. 2011, Castillo et al. 2012). Despite some promising results in tau-transgenic mice that showed improvement of cognitive impairments and tau neuropathology, determining which antibody / epitope can most efficiently and selectively remove tau species involved in AD pathogenesis is still in progress. Recently, Nobuhara et al. tested the effects of a panel of tau antibodies on neuronal uptake and aggregation in vitro, to identify the best target epitopes (Nobuhara et al. 2017). Immunodepletion was performed on brain extract from aged Tg4510 mice and postmortem AD brain which were added to a cell-based FRET assay (Holmes et al. 2014). Similar to our results, they found that antibodies reduced tau uptake to different extents: a C-terminal tau antibody had little effect, whereas N-terminal and mid-domain antibodies successfully prevented uptake of tau species, with the most efficient also blocking neuron-to-neuron spreading of tau in a three-chamber microfluidic device, even after uptake had begun. They found that phosphorylation-dependent antibodies 40E8 (pS202/pT205-tau) and p396 (pS396-tau)) also reduced tau uptake despite removing less total tau by immunodepletion, suggesting that most of the tau taken up by neurons is phosphorylated at these three sites. Despite low immunoprecipitation efficiency, 40E8 and p396 reduced neuronal uptake of Tg4510 extract by 40% and 80% respectively, and neuronal uptake of AD extract by 65% and 53% respectively, suggesting that the blocking efficiency is relative to the extract used. Even though we used antibodies against the same epitopes (AT8 for pS202/pT205-tau and PHF1 for pS396-tau), substantial differences in the materials and assays used preclude a direct comparison with our data. Taken together, our and their results imply that the efficacy of antibodies in blocking uptake and seeding of tau derived from tau-transgenic mouse and the human AD brain is epitope-dependent. Moreover, the blocking efficiency of certain antibodies may be dependent on the distinct pool of pathological forms of tau present in each individual diseased brain, which renders tau immunotherapy approaches particularly challenging.

8.5 Discussion on extracellular tau

The transynaptic pathway has been implicated in the spreading of tau pathology from neuron to neuron (de Calignon et al. 2012, Liu et al. 2012, Gomez-Ramos et al. 2008), but (Maphis et al. 2015) showed that reactive microglia drives tau pathology in a cell-autonomous manner in tau transgenic mice, suggesting that glial cells could also have a role in tau spreading; the authors created a mouse model of tauopathy (hTauCx3cr1-/-mice) where deficiency of the microglial

fractalkine receptor (CX3CR1) caused elevated microglia activation, acceleration of tau pathology and memory impairment (Bhaskar et al. 2010); in an age-based study in 2-, 6-, 12- and 24-month old hTauCx3cr1-/- mice, they observed a spatio-temporal correlation between CD45+ microglial activation and spread of tau pathology in anatomically connected regions of the hippocampus; purified microglia from hTauCx3cr1-/- mice brain induced tau hyperphosphorylation and a pre-tangle phenotype when inoculated in the brains of non-transgenic mice; all together, the data suggests that reactive microglia drives tau pathology and correlate with its spread in a transgenic mouse model. Tau has also been shown to be internalized by glial cells in vitro and in vivo and to colocalise with microglia in postmortem AD brains (Bolos et al. 2015); also, depletion of microglia dramatically suppresses tau propagation from the entorhinal cortex to the dentate gyrus in a mouse model (Asai et al. 2015); in particular, inhibition of exosome synthesis reduces tau propagation, highlighting secretion of exosomes as a mechanism by which microglia spread tau, and suggesting microglia as a potential therapeutic target to enhance clearance of extracellular tau in neurodegenerative diseases.

The presence of tau and α-synuclein in human cerebrospinal fluid has been reported (Tapiola et al. 2009, Mollenhauer et al. 2013, van Dijk et al. 2014), and thanks to microdialysis techniques, measurable levels of tau and α-synuclein were found in the interstitial fluid of healthy mice, suggesting a constitutive efflux from healthy neurons (Emmanouilidou et al. 2011); the release of tau monomer in particular is increased by neuronal activity (Pooler et al. 2013, Yamada et al. 2014). A recent publication (Wu et al. 2016) used optogenetic and chemogenetic approaches to show that increased neuronal activity stimulates the release of tau *in vitro* and enhances tau pathology *in vivo*; in particular, human iPSC neurons, primary mouse neurons expressing endogenous tau and neurons overexpressing mutant hTau (rTg4510 line) were stimulated with picrotoxin, a noncompetitive channel blocker for the GABA receptor chloride channels, which increased tau in the media by 150–210%, without causing cell death; since amyloid β is known to cause neuron excitability, this data could explain how amyloid pathology catalyzes tau propagation. Also (Croft et al. 2017) investigated tau release from organotypic brain slice cultures prepared from wild-type and 3xTg-AD mice (Oddo et al. 2003a, Oddo et al. 2003b): stimulation of neuronal activity with KCl increased tau release from wild-type slices, whereas tau release from 3xTg-AD slices could not be further stimulated with KCl, possibly due to saturation of synaptic activity caused by overexpression and changes in the subcellular distribution of tau in this model; future experiments should aim at determining whether tau released from 3xTg-AD slices is aberrantly phosphorylated, cleaved, vescicle-associated or free-floating, compared to tau from wild-type slices, and to be relevant for AD and the majority of human tauopathies these findings should be replicated in a mouse model that expresses wild-type human tau rather than P301L FTDP-tau.

Exosomes have been implicated in the propagation of PrPSc (Vella et al. 2007), and non-fibrillar (monomeric or oligomeric) α-synuclein and tau have also been shown to be secreted into the cell culture medium by exosomes (Simon et al. 2012, Emmanouilidou et al. 2010, Danzer et al. 2012, Saman et al. 2012, Wang et al. 2017) but others found no evidence for tau in exosomes

(Karch, Jeng & Goate 2012), with one study showing that an antibody against tau repeat domain (RD) affected tau intercellular propagation in HEK293 cells transfected with tau RD(ΔK280), with no effect on intracellular aggregation of tau, suggesting that tau aggregates are not encapsulated into a membrane when released into the extracellular space (Kfoury et al. 2012) and can be trapped outside the cells by an antibody. Ectosomes, plasma membrane-derived vesicles, have been shown to account for a small proportion of endogenous tau released under basal conditions (Dujardin et al. 2014), but in cell models where tau was exogenously expressed or in a highly phosphorylated misfolded state, a small proportion of released tau was associated with MVB-derived vesicles, the exosomes (Plouffe et al. 2012, Simon et al. 2012, Saman et al. 2012). Discrepancies in findings from different groups raise several questions about a universal mechanism of tau release; within a complex biological system, the release of tau protein may be a combination of each of the possible release mechanisms, which makes tau release a difficult therapeutic target; most likely physiological species of soluble tau are released from healthy neurons via a distinct mechanism from pathological tau, since studies in models of tau overexpression tend to claim vesicular release of tau, whereas at physiological tau expression levels, non-vesicular release is mostly observed; therefore, the effect of tau overexpression in in vitro systems should be taken into account, as it will affect the localisation and post-translational modifications of tau, and consequently its release. Also, the impact of disease-relevant tau mutations on tau release needs investigating, as conflicting findings have been reported: *in vitro*, expression of P301S tau in human neuroblastoma cells decreases tau release (Karch, Jeng & Goate 2012), whereas *in vivo*, mice expressing human P301S tau show 5-fold higher tau levels in the brain and in interstitial fluid compared with wild-type littermates (Yamada et al. 2011). Overall, findings from different groups suggest that different mechanisms may govern the release of functionally distinct pools of tau: in the healthy brain, physiological tau may contribute to neuronal signalling, whereas pathological tau may drive spread of pathology and disease progression within diseased brain. Blocking tau release as therapeutic target poses the challenge of selectively targeting abnormal tau release, and since it may be beneficial for the cell to reduce the intracellular tau burden, its blockade could even be detrimental.

While the intracellular role of tau in microtubule stabilization and axonal transport is well established, the role of extracellular tau is still being elucidated. Since tau pathology in AD and other tauopathies propagates following a stereotypically defined pattern, it could be mediated by the spreading of tau seeds from cell to cell. Studies in cell culture models have shown intercellular transfer of tau (Guo, Lee 2014, Holmes et al. 2013., Guo, Lee 2011, Frost, Jacks & Diamond 2009, Kfoury et al. 2012, Wu et al. 2013, Santa-Maria et al. 2012), and numerous groups replicated these findings for α-synuclein (Desplats et al. 2009, Hansen C et al. 2011, Freundt et al. 2012, Lee et al. 2010, Luk et al. 2009, Volpicelli-Daley et al. 2011), SOD1 (Munch, O'Brien & Bertolotti 2011), huntingtin (Ren et al. 2009) and TDP-43 (Furukawa Y et al. 2011). Further studies are needed to investigate whether secretion of misfolded tau into the extracellular space is a factor contributing to disease progression, and whether tau conformation plays a role in the propagation of the tau lesions. We are currently looking at the

effect of the ionophore ionomycin on tau levels in media from RCN overexpressing TgP301S 0N4R tau. We are planning to collect conditioned media from seeded HEK P301S tau inducible cells or RCNs and test its ability to produce aggregation in a new population of RCNs. Exosomal fractions could be extracted according to published protocols (Saman et al. 2012) from our cell models of tau aggregation and probed for tau. Another open question in the field is whether synaptic activity plays a role in transcellular propagation of tau; using microfluidic chambers, (Calafate et al. 2015) demonstrated that blocking either synaptic connectivity or synaptic activity blocked tau aggregation in the downstream chamber, supporting a trans-synaptic pathway for conveying tau between cells. We will use our RCNs neuronal model in microfluidic chambers to create two fluidically isolated microenvironments and allow delivery of exogenous seeds to one cell population, without them crossing over to the other cell population, hence avoiding the confound of detecting residual seeds in the conditioned media. Moreover, with a view of studying the mechanisms of tau transfer, our lab has generated and optimized a co-culture HEK cell system that robustly develops intracellular tau aggregates following addition of exogenous mutant tau and provides mechanistic insights into NFT pathogenesis and propagation (Cavallini et al. 2014.).

8.6 Discussion on neuronal model of tau aggregation

Consistent with Guo and Lee (Guo, Lee 2013), who found that mutant tau pre-formed fibrils resulted in dramatically more abundant pathology than wt tau pre-formed fibrils in PS19 neurons overexpressing mutant tau, we also found that tau aggregates only formed upon TgP301S seed treatment in TgP301S hippocampal neurons, and not in the other conditions, in the timeframe of our assay (up to 1 week post-seeding). Similarly, rat cortical neurons overexpressing P310S tau, but not WT tau, also showed tau aggregation upon seeding with TgP301S seed. The causes of the asymmetrical seeding observed, which has also been reported in non-neuronal models (Clavaguera et al. 2014.), are likely to be due to conformational and isoform disparities between WT and mutant tau. Similarly, P301L tau seeds promoted fibrillization of P301L tau but not WT tau, whereas R406W tau seeds supported fibrillization of both R406W and WT tau, as did WT tau seeds, as measured by electron microscopy in an *in vitro* aggregation system of recombinant tau in the presence of heparin (Aoyagi, Hasegawa & Tamaoka 2007). The substructures of these seeds were shown to be different by proteolytic analysis; these results correlate with the patterns of tau depositions in FTDP-17 brains with these mutations: only P301L mutant tau is deposited in FTDP-17 with P301L mutation, whereas both WT and R406W tau are deposited in FTDP-17 with R406W mutation. A seeding barrier between 3R- and 4R-tau has been reported (Dinkel et al. 2011): in developing non-transgenic neurons the predominantly expressed isoform is 3R-tau, which has lower propensity to aggregate than 4R-tau (Dotti, Banker & Binder 1987, Ferreira et al. 1997, Zhong et al. 2012), and it is not efficiently recruited by the seed-derived 4R-tau. Similarly, a seeding barrier has been previously reported for prion disorders, for which incubation times and infectivity depend on the correspondence between the amino acid sequence, and consequently the conformation, of the infectious prion and that of the host prion protein (Scott et al. 1993). More studies are needed to determine the effect of tau

isoforms and tau mutations on seeding efficiency, and whether these seed barriers observed could explain the diversity of human tauopathies.

We know in AD misfolded, hyperphosphorylated tau first accumulates in the locus coeruleus, from where it appears to spread to entorhinal cortex, hippocampus and neocortex. This differential distribution underlies the Braak stages of tau pathology (Braak, Braak 1991, Braak, Del Tredici 2011b). Stereotypical temporospatial spreading of tau pathology has also been described in argyrophilic grain disease (AGD) (Saito et al. 2004). Transmission and spreading of tau pathology can be shown experimentally (Goedert, Clavaguera & Tolnay 2010). Thus, brain extracts from mice transgenic for human mutant P301S tau with abundant silver-positive tau inclusions, when injected into the brains of ALZ17 mice expressing human wild-type tau (lacking tau inclusions), induced the slow assembly of wild-type tau into silver-positive inclusions. Moreover this tau pathology was observed to spread to neighbouring brain regions (Clavaguera et al. 2009). Aggregated recombinant tau was also sufficient to convert soluble tau into aggregates (Clavaguera et al. 2013, Iba et al. 2013). As previously stated, infusion of TgP301S tau extracts from the hindbrain of symptomatic mice into the hippocampus and overlying cerebral cortex of non-symptomatic mice transgenic for human P301S tau, induced the formation of tau inclusions in the hippocampus, which spread rapidly (2-4 weeks) to synaptically connected brain regions (Ahmed et al. 2014), which suggests that tau—or a particular species of tau, such as hyperphosphorylated tau, misfolded tau, or a fragment of tau—may have been released at the synapses. The induction and spreading of tau pathology through synapses has also been demonstrated following the restricted expression of human mutant tau in transgenic mice (de Calignon et al. 2012, Liu et al. 2012) and in cultured hippocampal neurons expressing human mutant tau (Calafate et al. 2015). If human tau protein propagates to synaptically connected brain regions, an in vitro neuronal model would allow us to investigate whether a neuronal tau receptor or a surface protein allows tau release and internalisation, and whether this processes can be modulated. Pharmacological, enzymatic, and genetic manipulations have already been used to implicate heparan sulphate proteoglycans (HSPGs) as key receptors for recombinant full-length and repeat domain tau fibrils in neural cell lines and primary neurons alike (Holmes et al. 2013.).

As well as confirming the above findings in our own neuronal model, we could also explore the colocalization of tau and synaptic markers by immunofluorescence (synapsin1, marker of synaptic vesicles (de Calignon et al. 2012), postsynaptic density protein 95 (PSD95), postsynaptic marker (de Calignon et al. 2012) and see whether modulation of synaptic transmission affects tau propagation in a neuronal model (Calafate et al. 2015). Tau presence at the synapses could be due to tau missorting from the axonal (physiological) to the somatodendritic compartment, where it correlates with loss of microtubules and reduced spine number (Zempel et al. 2013); a microtubule polymerisation assay developed in our laboratory could then be employed to monitor microtubule stability.

A neuronal model is also the best experimental setting to pinpoint the tau species responsible for seeding, i.e. by seeding with transgenic mouse or human brain homogenates subjected to immunodepletion with tau antibodies or sucrose gradient fractionation. A recent paper (Varghese et al. 2016) compared the effect of extracellular PHFs on tau aggregation in mitotic cell cultures and post-mitotic neurons, observing aggresome-type tau depositions and impaired proteasome degradation in mitotic cells, but not in neuronal cells. It is possible that independent mechanisms of propagation of tau pathology also act in our mammalian and neuronal models, so we could investigate the role of the ubiquitin-proteasome system and autophagy in both models. Their findings also highlight the fact that propagation of tau pathology may follow independent mechanisms in mitotic cells such as astrocytes vs post-mitotic cells such as neurons.

8.7 Future development of aggregation assays for screening

Both our mammalian and neuronal cell-based assays could also be part of a drug discovery flowscheme. In a target-based approach, they could be used as secondary assays to confirm actives from a primary screen. For instance, an in vitro tau fibrillization assay, typically monitored by thioflavine T fluorescence, could be used first to interrogate a compound library by high throughput screening (HTS). Active compounds meeting the criteria set for selection in the HTS could be confirmed in our HEK Trex P301S tau inducible cell-based assay using TgP301S seed, deemed more potent than recombinant P301S seed. Alternatively, the HEK Trex P301S tau inducible cell-based assay could be used as primary assay for a phenotypic screen to identify compounds that affect relevant mechanisms such as tau uptake or tau degradation. In both target-based and phenotypic screening strategies, selected potent compounds could then be further evaluated in our RCN overexpression cell-based assay, ultimately leading to hit declaration. Both the HEK Trex and RCN cell-based assays would require prior optimisation and validation; a number of variables should be optimized with regards to SD window, z-factor, %CV and effect of tool molecules, until the validation requirements are met:

- Optimal tau expression (tetracycline dose-response)
- Optimal seed concentration (seed dose-response)
- Optimal cell density
- Optimal detection antibodies (i.e. PG5 vs AT8)
- Optimal nuclear dyes (i.e. Hoechst vs propidium iodide)
- Optimal assay volume (i.e. 50 µl/well vs 100 µl/well)
- Optimal equipment for automation and detection
- Optimal cell fixatives (i.e. formaldehyde vs Prefer)
- Time course
- Effect of trypsinisation

The validation will assess plate uniformity and result reliability (test-retest) and profile a number of tool molecules. Both assays would likely be run in a 96-well plate format with an imaging readout for the highest throughput, but selected compounds could also be investigated by biochemical assay, to demonstrate the reduction of sarkosyl-insoluble tau.

9. CONCLUSIONS

We sought to establish cellular systems with a significant number of NFT-like aggregates to allow investigation of the pathological mechanisms of tau tangle formation as well as tau intercellular transmission. In particular, we used our systems to investigate some of the unresolved questions in the field, in particular what mechanisms allow tau uptake and release, and what factors influence seeding efficiency.

In summary, we have developed new models of tau aggregation and propagation which not only are important tools to gain mechanistic insights into the pathogenesis of tau aggregation, but also offer a robust system for identifying therapeutic strategies to prevent propagation and spreading of tau pathology.

10. ACKNOWLEDGEMENTS

I wish to thank my supervisors Suchira Bose (Eli Lilly and Co, Erl Wood, UK), Adrian Isaacs and Selina Wray (UCL) for their guidance; Michel O'Neill (Head of Molecular Pathology, Eli Lilly and Co, Erl Wood, UK) and Michael Hutton (CSO of Neurodegeneration, Eli Lilly, Erl Wood, UK) for giving me this great opportunity to gain a PhD; all members of the Molecular Pathology group at Eli Lilly, Erl Wood, UK, for their help and support; Peter Davies, Litwin-Zucker Research Center, NY, US, for kindly providing tau antibodies, and Michel Goedert, MRC Laboratory of molecular biology, Cambridge, UK for helpful discussions. This work was supported in whole by Eli Lilly and Co. Ltd.

11. BIBLIOGRAPHY

Ahmed, Z., Cooper, J., Murray, T.K., Garn, K., McNaughton, E., Clarke, H., Parhizkar, S., Ward, M.A., Cavallini, A., Jackson, S., Bose, S., Clavaguera, F., Tolnay, M., Lavenir, I., Goedert, M., Hutton, M.L. & O'Neill, M.J. 2014, "A novel in vivo model of tau propagation with rapid and progressive neurofibrillary tangle pathology: The pattern of spread is determined by connectivity, not proximity.", *Acta Neuropathologica*, vol. 127, no. 5, pp. 667-683.

Allen, B., Ingram, E., Takao, M., Smith, M.J., Jakes, R., Virdee, K., Yoshida, H., Holzer, M., Craxton, M., Emson, P.C., Atzori, C., Migheli, A., Anthony Crowther, R., Ghetti, B., Spillantini, M.G. & Goedert, M. 2002, "Abundant tau filaments and nonapoptotic neurodegeneration in transgenic mice expressing human P301S tau protein.", *Journal of Neuroscience,* vol. 22, no. 21, pp. 9340-9351.

Alonso, A.C., Li, B., Grundke-Iqbal, I. & Iqbal, K. 2006, "Polymerization of hyperphosphorylated tau into filaments eliminates its inhibitory activity", *Proceedings of the National Academy of Science of the United States of America,* vol. 103, pp. 8864-8869.

Alonso, A.D.C., Zaidi, T., Novak, M., Grundke-Iqbal, I. & Iqbal, K. 2001, "Hyperphosphorylation induces self-assembly of into tangles of paired helical filaments/straight filaments.", *Proceedings of the National Academy of Sciences of the United States of America,* vol. 98, no. 12, pp. 6923-6928.

Andorfer, C., Kress, Y., Espinoza, M., de Silva, R., Tucker, K.L., Barde, Y.A., Duff, K. & Davies, P. 2003, “Hyperphosphorylation and aggregation of tau in mice expressing normal human tau isoforms”, *Journal of Neurochemistry,* vol. 86, no. 3, pp. 582–90.

Andorfer, C., Acker, C.M., Kress, Y., Hof, P.R., Duff, K. & Davies, P. 2005, "Cell-cycle reentry and cell death in transgenic mice expressing nonmutant human tau isoforms.", *Journal of Neuroscience,* vol. 25, no. 22, pp. 5446-5454.

Aoyagi, H., Hasegawa, M. & Tamaoka, A. 2007, "Fibrillogenic nuclei composed of P301L mutant tau induce elongation of P301S tau but not wild-type tau", *Journal of Biological Chemistry,* vol. 282, no. 28, pp. 20309.

Arai, T., Ikeda, K., Akiyama, H., Nonaka, T., Hasegawa, M., Ishiguro, K., Iritani, S., Tsuchiya, K., Iseki, E., Yagishita, S., Oda, T. & Mochizuki, A. 2004, "Identification of amino-terminally cleaved tau fragments that distinguish progressive supranuclear palsy from corticobasal degeneration.", *Annals of Neurology,* vol. 55, no. 1, pp. 72-79.

Arriagada, P.V., Marzloff, K. & Hyman, B.T. 1992, "Distribution of Alzheimer-type pathologic changes in non-demented elderly individuals matches the pattern in Alzheimer's disease", *Neurology,* vol. 42, no. 9, pp. 1681-1688.

Asai, H., Ikezu, S., Tsunoda, S., Medalla, M., Luebke, J., Haydar, T., Wolozin, B., Butovsky, O., Kugler, S. & Ikezu, T. 2015, "Depletion of microglia and inhibition of exosome synthesis halt tau propagation", *Nature neuroscience,* vol. 18, no. 11, pp. 1584-1593.

Avila, J., Santa-Maria, I., Perez, M., Hernandez, F. & Moreno, F. 2006, "Tau phosphorylation, aggregation, and cell toxicity.", *Journal of Biomedicine and Biotechnology,* vol. 2006, article ID 74539, pp. 1–5.

Balakrishnan, K., Andrei-Selmer, L.C., Selmer, T., Bacher, M. & Dodel, R. 2010, "Comparison of intravenous immunoglobulins for naturally occurring autoantibodies against amyloid-beta", *Journal of Alzheimer's Disease,* vol. 20, pp. 135.

Ballatore, C., Lee, V.M. & Trojanowski, J.Q. 2007, "Tau-mediated neurodegeneration in Alzheimer's disease and related disorders.", *Nature Reviews Neuroscience,* vol. 8, no. 9, pp. 663-672.

Bandyopadhyay, B., Li, G., Yin, H. & Kuret, J. 2007, "Tau aggregation and toxicity in a cell culture model of tauopathy.", *Journal of Biological Chemistry,* vol. 282, no. 22, pp. 16454-16464.

Barghorn, S. & Mandelkow, E. 2002, "Toward a unified scheme for the aggregation of tau into Alzheimer paired helical filaments.", *Biochemistry,* vol. 41, no. 50, pp. 14885-14896.

Barghorn, S., Zheng-Fischhofer, Q., Ackmann, M., Biernat, J., von Bergen, M., Mandelkow, E.M. & Mandelkow, E. 2000, "Structure, microtubule interactions, and paired helical filament aggregation by tau mutants of frontotemporal dementias", *Biochemistry,* vol. 39, no. 38, pp. 11714-11721.

Bellucci, A., Westwood, A.J., Ingram, E., Casamenti, F., Goedert, M. & Spillantini, M.G. 2004, "Induction of inflammatory mediators and microglial activation in mice transgenic for mutant human P301S tau protein.", *American Journal of Pathology,* vol. 165, no. 5, pp. 1643-1652.

Berriman, J., Serpell, L.C., Oberg, K.A., Fink, A.L., Goedert, M. & Crowther, R.A. 2003, "Tau filaments from human brain and from in vitro assembly of recombinant protein show cross-beta structure.", *Proceedings of the National Academy of Sciences of the United States of America,* vol. 100, no. 15, pp. 9034-9038.

Bhaskar, K., Konerth, M., Kokiko-Cochran, O.N., Cardona, A., Ransohoff, R.M. & Lamb, B.T. 2010, "Regulation of tau pathology by the microglial fractalkine receptor.", *Neuron,* vol. 68, no. 1, pp. 19-31.

Biernat, J., Mandelkow, E.M., Schröter, C., Lichtenberg-Kraag, B., Steiner, B., Berling, B., Meyer, H., Mercken, M., Vandermeeren, A. & Goedert, M. 1992, "The switch of tau protein to an Alzheimer-like state includes the phosphorylation of two serine-proline motifs upstream of the microtubule binding region", *The EMBO journal*, vol. 11, no. 4, pp.1593–1597.

Biernat, J., Gustke, N., Drewes, G., Mandelkow, E.M. & Mandelkow, E. 1993, "Phosphorylation of Ser262 strongly reduces binding of tau to microtubules: Distinction between PHF-like immunoreactivity and microtubule binding.", *Neuron,* vol. 11, no. 1, pp. 153-163.

Binder, L.I., Guillozet-Bongaarts, A.L., Garcia-Sierra, F. & Berry, R.W. 2005, "Tau, tangles, and Alzheimer's disease.", *Biochimica et Biophysica Acta - Molecular Basis of Disease,* vol. 1739, no. 2, pp. 216-223.

Bolos, M., Llorens-Martin, M., Jurado-Arjona, J., Hernandez, F., Rabano, A. & Avila, J. 2015, "Direct Evidence of Internalization of Tau by Microglia In Vitro and In Vivo", *Journal of Alzheimer's disease,* vol. 50, no. 1, pp. 77-87.

Botez, G., Probst, A., Ipsen, S. & Tolnay, M. 1999, "Astrocytes expressing hyperphosphorylated tau protein without glial fibrillary tangles in argyrophilic grain disease.", *Acta Neuropathologica,* vol. 98, no. 3, pp. 251-256.

Boutajangout, A., Ingadottir, J., Davies, P. & Sigurdsson, E.M. 2011, "Passive immunization targeting pathological phospho-tau protein in a mouse model reduces functional decline and clears tau aggregates from the brain.", *Journal of neurochemistry,* vol. 118, no. 4, pp. 658-667.

Braak, H., Alafuzoff, I., Arzberger, T., Kretzschmar, H. & Del Tredici, K. 2006, "Staging of Alzheimer disease-associated neurofibrillary pathology using paraffin sections and immunocytochemistry.", *Acta Neuropathologica,* vol. 112, no. 4, pp. 389-404.

Braak, H. & Braak, E. 1996, "Development of Alzheimer-related neurofibrillary changes in the neocortex inversely recapitulates cortical myelogenesis", *Acta Neuropathologica,* vol. 92, no. 2, pp. 197-201.

Braak, H. & Braak, E. 1991, "Neuropathological stageing of Alzheimer-related changes.", *Acta Neuropathologica,* vol. 82, no. 4, pp. 239-259.

Braak, H., Alafuzoff, I., Arzberger, T., Kretzschmar, H. & Del Tredici, K. 2006 “Staging of Alzheimer disease-associated neurofibrillary pathology using paraffin sections and immunocytochemistry”, *Acta Neuropathologica,* vol. 112, no.4, pp. 389–404.

Braak, H. & Del Tredici, K. 2011a, "The pathological process underlying Alzheimer's disease in individuals under thirty", *Acta Neuropathologica,* vol. 121, no. 2, pp. 171-181.

Braak, H. & Del Tredici, K. 2011b, "Alzheimer's pathogenesis: is there neuron-to-neuron propagation?", *Acta Neuropathologica,* vol. 121, no. 5, pp. 589-595.

Bramblett, G.T., Goedert, M., Jakes, R., Merrick, S.E., Trojanowski, J.Q. & Lee, -.V.M.Y. 1993, "Abnormal tau phosphorylation at Ser396 in Alzheimer's disease recapitulates development and contributes to reduced microtubule binding.", *Neuron,* vol. 10, no. 6, pp. 1089-1099.

Bright, J., Hussain, S., Dang, V., Wright, S., Cooper, B., Byun, T., Ramos, C., Singh, A., Parry, G., Stagliano, N. & Griswold-Prenner, I. 2015, "Human secreted tau increases amyloid-beta production", *Neurobiology of aging,* vol. 36, no. 2, pp. 693-709.

Britschgi, M., Olin, C.E., Johns, H.T., Takeda-Uchimura, Y., LeMieux, M.C., Rufibach, K., Rajadas, J., Zhang, H., Tomooka, B., Robinson, W.H., Clark, C.M., Fagan, A.M., Galasko, D.R., Holtzman, D.M., Jutel, M., Kaye, J.A., Lemere, C.A., Leszek, J., Li, G., Peskind, E.R., Quinn, J.F., Yesavage, J.A., Ghiso, J.A. & Wyss-Coray, T. 2009, "Neuroprotective natural antibodies to assemblies of amyloidogenic peptides decrease with normal aging and advancing Alzheimer's disease", *Proceedings of the National Academy of Sciences of the United States of America,* vol. 106, no. 29, pp. 12145-12150.

Caillierez, R., Begard, S., Lecolle, K., Deramecourt, V., Zommer, N., Dujardin, S., Loyens, A., Dufour, N., Auregan, G., Winderickx, J., Hantraye, P., Deglon, N., Buee, L. & Colin, M. 2013, "Lentiviral delivery of the human wild-type tau protein mediates a slow and progressive neurodegenerative tau pathology in the rat brain.", *Molecular Therapy,* vol. 21, no. 7, pp. 1358-1368.

Calafate, S., Buist, A., Miskiewicz, K., Vijayan, V., Daneels, G., de Strooper, B., de Wit, J., Verstreken, P. & Moechars, D. 2015, "Synaptic Contacts Enhance Cell-to-Cell Tau Pathology Propagation", *Cell reports,* vol. 11, no. 8, pp. 1176-1183.

Calafate, S., Flavin, W., Verstreken, P. & Moechars, D. 2016, "Loss of Bin1 Promotes the Propagation of Tau Pathology", *Cell reports,* vol. 17, no. 4, pp. 931-940.

Castillo, D.L., Lasagna-Reeves, C.A., Guerrero-Munoz, M.J., Sengupta, U., Estes, D.M., Barrett, A.D.T., Dineley, K.T., Jackson, G.R. & Kayed, R. 2014, "Passive immunization with tau oligomer monoclonal antibody reverses tauopathy phenotypes without affecting hyperphosphorylated neurofibrillary tangles" *Journal of Neuroscience,* vol. 34, no. 12, pp. 4260-4272.

Castillo-Carranza, D.L., Sengupta, U., Guerrero-Munoz, M.J., Lasagna-Reeves, C.A., Gerson, J.E., Singh, G., Mark Estes, D., Barrett, A.D.T., Dineley, K.T., Jackson, G.R. & Kayed, R. 2014, "Passive immunization with tau oligomer monoclonal antibody reverses tauopathy phenotypes without affecting hyperphosphorylated neurofibrillary tangles.", *Journal of Neuroscience,* vol. 34, no. 12, pp. 4260-4272.

Cavallini, A., Jackson, S., Sanchez, J.M., Murray, T., Falcon, B., Isaacs, A., Goedert, M., O'Neill, M., Hutton, M. & Bose, S. 2014., "Characterisation of a co-culture cell-based model of Tau aggregation and propagation.", *Alzheimer's and Dementia,* vol. 10, pp. P646.

Chai, X., Dage, J. & Citron, M. 2012, "Constitutive Secretion of Tau Protein by an Unconventional Mechanism", *Neurobiology of Disease,* vol. 48, no. 3, pp. 356-366.

Chai, X., Wu, S., Murray, T.K., Kinley, R., Cella, C.V., Sims, H., Buckner, N., Hanmer, J., Davies, P., O'Neill, M.J., Hutton, M.L. & Citron, M. 2011, "Passive immunization with anti-tau antibodies in two transgenic models: Reduction of tau pathology and delay of disease progression.", *Journal of Biological Chemistry,* vol. 286, no. 39, pp. 34457-34467.

Chen, C., Oh, S., Hinman, J.D. & Abraham, C.R. 2006, "Visualization of APP dimerization and APP-Notch2 heterodimerization in living cells using bimolecular fluorescence complementation.", *Journal of neurochemistry,* vol. 97, no. 1, pp. 30-43.

Chinnery, H.R., Pearlman, E. & McMenamin, P.G. 2008, "Cutting edge: Membrane nanotubes in vivo: a feature of MHC class II+ cells in the mouse cornea", *Journal of immunology,* vol. 180, no. 9, pp. 5779-5783.

Choi, S.H., Kim, Y.H., Hebisch, M., Sliwinski, C., Lee, S., D'Avanzo, C., Chen, H., Hooli, B., Asselin, C., Muffat, J., Klee, J.B., Zhang, C., Wainger, B.J., Peitz, M., Kovacs, D.M., Woolf, C.J., Wagner, S.L., Tanzi, R.E. & Kim, D.Y. 2014, "A three-dimensional human neural cell culture model of Alzheimer's disease", *Nature,* vol. 515, no. 7526, pp. 274-278.

Chun, W. & Johnson, G.V. 2007, "Activation of glycogen synthase kinase 3beta promotes the intermolecular association of tau. The use of fluorescence resonance energy transfer microscopy", *Journal of Biological Chemistry,* vol. 282, no. 32, pp. 23410-23417.

Chun, W., Waldo, G.S. & Johnson, G.V. 2011, "Split GFP complementation assay for quantitative measurement of tau aggregation in situ.", *Methods in molecular biology,* vol. 670, pp. 109-123.

Chun, W., Waldo, G.S. & Johnson, G.V.W. 2007, "Split GFP complementation assay: A novel approach to quantitatively measure aggregation of tau in situ: Effects of GSK3beta activation and caspase 3 cleavage.", *Journal of neurochemistry,* vol. 103, no. 6, pp. 2529-2539.

Clavaguera, F., Hench, J., Lavenir, I., Schweighauser, G., Frank, S., Goedert, M. & Tolnay, M. 2014, "Peripheral administration of tau aggregates triggers intracerebral tauopathy in transgenic mice.", *Acta Neuropathologica,* vol. 127, no. 2, pp. 299-301.

Clavaguera, F., Akatsu, H., Fraser, G., Crowther, R.A., Frank, S., Hench, J., Probst, A., Winkler, D.T., Reichwald, J., Staufenbiel, M., Ghetti, B., Goedert, M. & Tolnay, M. 2013, "Brain homogenates from human tauopathies induce tau inclusions in mouse brain.", *Proceedings of the National Academy of Sciences of the United States of America,* vol. 110, no. 23, pp. 9535-9540.

Clavaguera, F., Bolmont, T., Crowther, R.A., Abramowski, D., Frank, S., Probst, A., Fraser, G., Stalder, A.K., Beibel, M., Staufenbiel, M., Jucker, M., Goedert, M. & Tolnay, M. 2009, "Transmission and spreading of tauopathy in transgenic mouse brain.", *Nature cell biology,* vol. 11, no. 7, pp. 909-913.

Clavaguera, F., Ghetti, B., Schweighauser, G., Akatsu, H., Hench, J., Tolnay, M. & Goedert, M. 2014., "Transmission and spreading of tauopathies in transgenic mouse brain.", *Alzheimer's and Dementia,* vol. 10, no. 4, pp. P162.

Clavaguera, F., Lavenir, I., Falcon, B., Frank, S., Goedert, M. & Tolnay, M. 2013, ""Prion-Like" templated misfolding in tauopathies.", *Brain Pathology,* vol. 23, no. 3, pp. 342-349.

Collin, L., Bohrmann, B., Gopfert, U., Oroszlan-Szovik, K., Ozmen, L. & Gruninger, F. 2014, "Neuronal uptake of tau/pS422 antibody and reduced progression of tau pathology in a mouse model of Alzheimer's disease", *Brain : a journal of neurology,* vol. 137, no. 10, pp. 2834-2846.

Collinge, J. & Clarke, A.R. 2007, "A general model of prion strains and their pathogenicity", *Science,* vol. 318, no. 5852, pp. 930-936.

Conner, S.D. & Schmid, S.L. 2003, "Regulated portals of entry into the cell", *Nature,* vol. 422, no. 6927, pp. 37-44.

Coppola, G., Chinnathambi, S., Lee, J.J., Dombroski, B.A., Baker, M.C., Soto-Ortolaza, A.I., Lee, S.E., Klein, E., Huang, A.Y., Sears, R., Lane, J.R., Karydas, A.M., Kenet, R.O., Biernat, J., Wang, L.S., Cotman, C.W., Decarli, C.S., Levey, A.I., Ringman, J.M., Mendez, M.F., Chui, H.C., Le Ber, I., Brice, A., Lupton, M.K., Preza, E., Lovestone, S., Powell, J., Graff-Radford, N., Petersen, R.C., Boeve, B.F., Lippa, C.F., Bigio, E.H., Mackenzie, I., Finger, E., Kertesz, A., Caselli, R.J., Gearing, M., Juncos, J.L., Ghetti, B., Spina, S., Bordelon, Y.M., Tourtellotte, W.W., Frosch, M.P., Vonsattel, J.P., Zarow, C., Beach, T.G., Albin, R.L., Lieberman, A.P., Lee, V.M., Trojanowski, J.Q., Van Deerlin, V.M., Bird, T.D., Galasko, D.R., Masliah, E., White, C.L., Troncoso, J.C., Hannequin, D., Boxer, A.L., Geschwind, M.D., Kumar, S., Mandelkow, E.M., Wszolek, Z.K., Uitti, R.J., Dickson, D.W., Haines, J.L., Mayeux, R., Pericak-Vance, M.A., Farrer, L.A., Alzheimer's Disease Genetics Consortium, Ross, O.A., Rademakers, R., Schellenberg, G.D., Miller, B.L., Mandelkow, E. & Geschwind, D.H. 2012, "Evidence for a role of the rare p.A152T variant in MAPT in increasing the risk for FTD-spectrum and Alzheimer's diseases", *Human molecular genetics,* vol. 21, no. 15, pp. 3500-3512.

Couchie, D., Mavilia, C., Georgieff, I.S., Liem, R.K., Shelanski, M.L. & Nunez, J. 1992, "Primary structure of high molecular weight tau present in the peripheral nervous system", *Proceedings of the National Academy of Sciences of the United States of America,* vol. 89, no. 10, pp. 4378-4381.

Cowan, C.M. & Mudher, A. 2013, "Are tau aggregates toxic or protective in tauopathies?.", *Frontiers in neurology,* vol. 4, pp. 114.

Croft, C.L., Wade, M.A., Kurbatskaya, K., Mastrandreas, P., Hughes, M.M., Phillips, E.C., Pooler, A.M., Perkinton, M.S., Hanger, D.P. & Noble, W. 2017, "Membrane association and release of wild-type and pathological tau from organotypic brain slice cultures", *Cell death & disease,* vol. 8, no. 3, pp. e2671.

Crowther, R.A. & Goedert, M. 2000, "Abnormal tau-containing filaments in neurodegenerative diseases", *Journal of structural biology,* vol. 130, no. 2-3, pp. 271-279.

Cudmore, S., Reckmann, I., Griffiths, G. & Way, M. 1996, "Vaccinia virus: a model system for actin-membrane interactions", *Journal of cell science,* vol. 109, no. 7, pp. 1739-1747.

D'Abramo, C., Acker, C. & Davies, P. 2011, "Passive immunization of p301l mice with two different tau monoclonal antibodies.", *Alzheimer's and Dementia,* vol. 7, no. 4 SUPPL. 1, pp. S481.

Danzer, K.M., Kranich, L.R., Ruf, W.P., Cagsal-Getkin, O., Winslow, A.R., Zhu, L., Vanderburg, C.R. & McLean, P.J. 2012, "Exosomal cell-to-cell transmission of alpha synuclein oligomers.", *Molecular Neurodegeneration,* vol. 7, no. 42, pp. 42.

Dawson, H.N., Cantillana, V., Chen, L. & Vitek, M.P. 2007, “The tau N279K exon 10 splicing mutation recapitulates frontotemporal dementia and parkinsonism linked to chromosome 17 tauopathy in a mouse model.”, *Journal of Neuroscience*, vol. 27, no. 34, pp. 9155–9168.

De Calignon, A., Fox, L.M., Pitstick, R., Carlson, G.A., Bacskai, B.J., Spires-Jones, T.L. & Hyman, B.T. 2010, "Caspase activation precedes and leads to tangles.", *Nature,* vol. 464, no. 7292, pp. 1201-1204.

De Calignon, A., Polydoro, M., Suarez-Calvet, M., William, C., Adamowicz, D.H., Kopeikina, K.J., Pitstick, R., Sahara, N., Ashe, K.H., Carlson, G.A., Spires-Jones, T.L. & Hyman, B.T. 2012, "Propagation of tau pathology in a model of early Alzheimer's disease", *Neuron,* vol. 73, no. 4, pp. 685-697.

Del, C., Alonso, A., Grundke-Iqbal, I. & Iqbal, K. 1996, "Alzheimer's disease hyperphosphorylated tau sequesters normal tau into tangles of filaments and disassembles microtubules.", *Nature medicine,* vol. 2, no. 7, pp. 783-787.

Delacourte, A., David, J.P., Sergeant, N., Buee, L., Wattez, A., Vermersch, P., Ghozali, F., Fallet-Bianco, C., Pasquier, F., Lebert, F., Petit, H. & Di Menza, C. 1999, "The biochemical pathway of neurofibrillary degeneration in aging and Alzheimer's disease", *Neurology,* vol. 52, no. 6, pp. 1158-1165.

Delacourte, A., Robitaille, Y., Sergeant, N., Buee, L., Hof, P.R., Wattez, A., Laroche-Cholette, A., Mathieu, J., Chagnon, P. & Gauvreau, D. 1996, "Specific pathological Tau protein variants characterize Pick's disease.", *Journal of neuropathology and experimental neurology,* vol. 55, no. 2, pp. 159-168.

Desplats, P., Lee, H., Bae, E., Patrick, C., Rockenstein, E., Crews, L., Spencer, B., Masliah, E. & Lee, S. 2009, "Inclusion formation and neuronal cell death through neuron-to-neuron transmission of alpha-synuclein", *Proceedings of the National Academy of Sciences of the United States of America,* vol. 106, no. 41, pp. 17606.

Dinkel, P.D., Siddiqua, A., Huynh, H., Shah, M. & Margittai, M. 2011, "Variations in filament conformation dictate seeding barrier between three- and four-repeat tau", *Biochemistry,* vol. 50, no. 20, pp. 4330-4336.

Dodel, R., Hampel, H., Depboylu, C., Lin, S., Gao, F., Schock, S., Jackel, S., Wei, X., Buerger, K., Hoft, C., Hemmer, B., Moller, H.J., Farlow, M., Oertel, W.H., Sommer, N. & Du, Y. 2002, "Human antibodies against amyloid beta peptide: a potential treatment for Alzheimer's disease", *Annals of Neurology,* vol. 52, no. 2, pp. 253-256.

Dotti, C.G., Banker, G.A. & Binder, L.I. 1987, "The expression and distribution of the microtubule-associated proteins tau and microtubule-associated protein 2 in hippocampal neurons in the rat in situ and in cell culture", *Neuroscience,* vol. 23, no. 1, pp. 121-130.

Drechsel, D.N., Hyman, A.A., Cobb, M.H. & Kirschner, M.W. 1992, "Modulation of the dynamic instability of tubulin assembly by the microtubule-associated protein tau", *Molecular biology of the cell,* vol. 3, no. 10, pp. 1141-1154.

Du, Y., Dodel, R., Hampel, H., Buerger, K., Lin, S., Eastwood, B., Bales, K., Gao, F., Moeller, H.J., Oertel, W., Farlow, M. & Paul, S. 2001, "Reduced levels of amyloid beta-peptide antibody in Alzheimer disease", *Neurology,* vol. 57, no. 5, pp. 801-805.

Duff, K., Knight, H., Refolo, L.M., Sanders, S., Yu, X., Picciano, M., Malester, B., Hutton, M., Adamson, J., Goedert, M., Burki, K. & Davies, P. 2000, “Characterization of pathology in transgenic mice over-expressing human genomic and cDNA tau transgenes”, *Neurobiology of Disease*, vol. 7, no. 2, pp. 87–98.

Dujardin, S., Begard, S., Caillierez, R., Lachaud, C., Delattre, L., Carrier, S., Loyens, A., Galas, M.C., Bousset, L., Melki, R., Auregan, G., Hantraye, P., Brouillet, E., Buee, L. & Colin, M. 2014, "Ectosomes: a new mechanism for non-exosomal secretion of tau protein.", *PLoS ONE,* vol. 9, no. 6, pp. e100760.

Dujardin, S., Colin, M. & Buee, L. 2015, "Invited review: Animal models of tauopathies and their implications for research/translation into the clinic", *Neuropathology and applied neurobiology,* vol. 41, no. 1, pp. 59-80.

Dujardin, S., Lecolle, K., Caillierez, R., Begard, S., Zommer, N., Lachaud, C., Carrier, S., Dufour, N., Auregan, G., Winderickx, J., Hantraye, P., Deglon, N., Colin, M. & Buee, L. 2014, "Neuron-to-neuron wild-type Tau protein transfer through a trans-synaptic mechanism: relevance to sporadic tauopathies.", *Acta Neuropathologica Communications,* vol. 2, pp. 14.

Duyckaerts, C., Bennecib, M., Grignon, Y., Uchihara, T., He, Y., Piette, F. & Hauw, J.J. 1997, "Modeling the relation between neurofibrillary tangles and intellectual status", *Neurobiology of aging,* vol. 18, no. 3, pp. 267-273.

Elbaum-Garfinkle, S. & Rhoades, E. 2012, "Identification of an Aggregation-Prone Structure of Tau", *Journal of the American Chemical Society,* vol. 134, no. 40, pp. 16607-16613.

Emmanouilidou, E., Elenis, D., Papasilekas, T., Stranjalis, G., Gerozissis, K., Ioannou, P.C. & Vekrellis, K. 2011, "Assessment of alpha-Synuclein Secretion in Mouse and Human Brain Parenchyma", *PLoS One,* vol. 6, no. 7, pp. e22225.

Emmanouilidou, E., Melachroinou, K., Roumeliotis, T., Garbis, S.D., Ntzouni, M., Margaritis, L.H., Stefanis, L. & Vekrellis, K. 2010, "Cell-Produced alpha-Synuclein Is Secreted in a Calcium-Dependent Manner by Exosomes and Impacts Neuronal Survival", *Journal of Neuroscience,* vol. 30, no. 20, pp. 6838-6851.

Espuny-Camacho, I., Arranz, A.M., Fiers, M., Snellinx, A., Ando, K., Munck, S., Bonnefont, J., Lambot, L., Corthout, N., Omodho, L., Vanden Eynden, E., Radaelli, E., Tesseur, I., Wray, S., Ebneth, A., Hardy, J., Leroy, K., Brion, J.P., Vanderhaeghen, P. & De Strooper, B. 2017, "Hallmarks of Alzheimer's Disease in Stem-Cell-Derived Human Neurons Transplanted into Mouse Brain", *Neuron,* vol. 93, no. 5, pp. 1066-1081.

Falcon, B., Cavallini, A., Angers, R., Glover, S., Murray, T.K., Barnham, L., Jackson, S., O'Neill, M.J., Isaacs, A.M., Hutton, M.L., Szekeres, P.G., Goedert, M. & Bose, S. 2015, "Conformation determines the seeding potencies of native and recombinant tau aggregates.", *Journal of Biological Chemistry,* vol. 290, no. 2, pp. 1049-1065.

Fasulo, L., Ugolini, G., Visintin, M., Bradbury, A., Brancolini, C., Verzillo, V., Novak, M. & Cattaneo, A. 2000, "The neuronal microtubule-associated protein tau is a substrate for caspase-3 and an effector of apoptosis.", *Journal of neurochemistry,* vol. 75, no. 2, pp. 624-633.

Fatouros, C., Pir, G.J., Biernat, J., Koushika, S.P., Mandelkow, E., Schmidt, E. & Baumeister, R. 2012, "Inhibition of Tau aggregation in a novel caenorhabditis elegans model of tauopathy mitigates proteotoxicity.", *Human molecular genetics,* vol. 21, no. 16, pp. 3587-3603.

Favoreel, H.W., Van Minnebruggen, G., Van de Walle, G.R., Ficinska, J. & Nauwynck, H.J. 2006, "Herpesvirus interference with virus-specific antibodies: Bridging antibodies, internalizing antibodies, and hiding from antibodies ", *Veterinary microbiology,* vol. 113, no. 3-4, pp. 257-263.

Feany, M.B., Ksiezak-Reding, H., Liu, W., Vincent, I., Yen, S.C. & Dickson, D.W. 1995, "Epitope expression and hyperphosphorylation of tau protein in corticobasal degeneration: Differentiation from progressive supranuclear palsy.", *Acta Neuropathologica,* vol. 90, no. 1, pp. 37-43.

Ferrari, A., Hoerndli, F., Baechi, T., Nitsch, R.M. & Gotz, J. 2003, "beta-Amyloid induces paired helical filament-like tau filaments in tissue culture.", *Journal of Biological Chemistry,* vol. 278, no. 41, pp. 40162-40168.

Ferreira, A., Lu, Q., Orecchio, L. & Kosik, K.S. 1997, "Selective phosphorylation of adult tau isoforms in mature hippocampal neurons exposed to fibrillar A beta", *Molecular and cellular neurosciences,* vol. 9, no. 3, pp. 220-234.

Filimonenko, M., Stuffers, S., Raiborg, C., Yamamoto, A., Malerod, L., Fisher, E.M.C., Isaacs, A., Brech, A., Stenmark, H. & Simonsen, A. 2007, "Functional multivesicular bodies are required for autophagic clearance of protein aggregates associated with neurodegenerative disease", *Journal of Cell Biology,* vol. 179, no. 3, pp. 485-500.

Fitzpatrick, A.W.P., Falcon, B., He, S., Murzin, A.G., Murshudov, G., Garringer, H.J., Crowther, R.A., Ghetti, B., Goedert, M. & Scheres, S.H.W. 2017, "Cryo-EM structures of tau filaments from Alzheimer's disease", *Nature,* vol. 547, no. 7662, pp. 185-190.

Flach, K., Hilbrich, I., Schiffmann, A., Gartner, U., Kruger, M., Leonhardt, M., Waschipky, H., Wick, L., Arendt, T. & Holzer, M. 2012, "Tau oligomers impair artificial membrane integrity and cellular viability.", *Journal of Biological Chemistry,* vol. 287, no. 52, pp. 43223-43233.

Flament, S., Delacourte, A., Verny, M., Hauw, J. & Javoy-Agid, F. 1991, "Abnormal Tau proteins in progressive supranuclear palsy. Similarities and differences with the neurofibrillary degeneration of the Alzheimer type.", *Acta Neuropathologica,* vol. 81, no. 6, pp. 591-596.

Forman, M.S., Lal, D., Zhang, B., Dabir, D.V., Swanson, E., Lee, V.M. & Trojanowski, J.Q. 2005, "Transgenic mouse model of tau pathology in astrocytes leading to nervous system degeneration." *Journal of Neuroscience*, vol. 25, no. 14, pp. 3539–50.

Freundt, E.C., Maynard, N., Clancy, E.K., Roy, S., Bousset, L., Sourigues, Y., Covert, M., Melki, R., Kirkegaard, K. & Brahic, M. 2012, "Neuron-to-neuron transmission of alpha-synuclein fibrils through axonal transport", *Annals of Neurology,* vol. 72, no. 4, pp. 517-524.

Friedhoff, P., Schneider, A., Mandelkow, E.M. & Mandelkow, E. 1998a, "Rapid assembly of Alzheimer-like paired helical filaments from microtubule-associated protein tau monitored by fluorescence in solution.", *Biochemistry,* vol. 37, no. 28, pp. 10223-10230.

Friedhoff, P., Von Bergen, M., Mandelkow, E.M., Davies, P. & Mandelkow, E. 1998b, "A nucleated assembly mechanism of Alzheimer paired helical filaments", *Proceedings of the National Academy of Sciences of the United States of America,* vol. 95, no. 26, pp. 15712-15717.

Frost, B., Jacks, R.L. & Diamond, M.I. 2009, "Propagation of Tau misfolding from the outside to the inside of a cell.", *Journal of Biological Chemistry,* vol. 284, no. 19, pp. 12845-12852.

Frost, B. & Diamond, M.I. 2010, "Prion-like mechanisms in neurodegenerative diseases", *Nature Reviews Neuroscience,* vol. 11, no. 3, pp. 155-159.

Furukawa, Y., Kaneko, K., Watanabe, S., Yamanaka, K. & Nukina, N. 2011, "A seeding reaction recapitulates intracellular formation of Sarkosyl-insoluble transactivation response element (TAR) DNA-binding protein-43 inclusions.", *Journal of Biological Chemistry,* vol. 286, no. 21, pp. 18664-18672.

Gamblin, T.C., Berry, R.W. & Binder, L.I. 2003, "Modeling Tau Polymerization in Vitro: A Review and Synthesis.", *Biochemistry,* vol. 42, no. 51, pp. 15009-15017.

Gamblin, T.C., Chen, F., Zambrano, A., Abraha, A., Lagalwar, S., Guillozet, A.L., Lu, M., Fu, Y., Garcia-Sierra, F., LaPointe, N., Miller, R., Berry, R.W., Binder, L.I. & Cryns, V.L. 2003, "Caspase cleavage of tau: Linking amyloid and neurofibrillary tangles in Alzheimer's disease.", *Proceedings of the National Academy of Sciences of the United States of America,* vol. 100, no. 17, pp. 10032-10037.

Gerdes, H.H., Bukoreshtliev, N.V. & Barroso, J.F. 2007, "Tunneling nanotubes: a new route for the exchange of components between animal cells ", *FEBS letters,* vol. 581, no. 11, pp. 2194-2201.

Gerson, J.E. & Kayed, R. 2013, "Formation and propagation of tau oligomeric seeds.", *Frontiers in neurology,* vol. 4, pp. 93.

Ghetti, B., Wszolek, Z.W., Boeve, B.F., Spina, S. & Goedert, M. 2011, "Frontotemporal dementia and parkinsonism linked to chromosome 17", *Neurodegeneration: The Molecular*

Pathology of Dementia and Movement Disorders, eds. D.W. Dickson & R.O. Weller, 2nd edn edn, Wiley-Blackwell, Oxford, pp. 110-134.

Goedert, M. 2015, "Neurodegeneration. Alzheimer's and Parkinson's diseases: The prion concept in relation to assembled Abeta, tau, and alpha-synuclein", *Science,* vol. 349, no. 6248, pp. 1255555.

Goedert, M. 2005, "Tau gene mutations and their effects.", *Movement Disorders,* vol. 20, no. 12, pp. S45-S52.

Goedert, M. & Jakes, R. 2005, "Mutations causing neurodegenerative tauopathies.", *Biochimica et Biophysica Acta - Molecular Basis of Disease,* vol. 1739, no. 2, pp. 240-250.

Goedert, M. & Jakes, R. 1990, "Expression of separate isoforms of human tau protein: correlation with the tau pattern in brain and effects on tubulin polymerization", *The EMBO journal,* vol. 9, no. 13, pp. 4225-4230.

Goedert, M., Jakes, R. & Vanmechelen, E.1995, “Monoclonal antibody AT8 recognises tau protein phosphorylated at both serine 202 and threonine 205”, *Neuroscience Letters,* vol. 189, no. 3, pp. 167–169.

Goedert, M., Jakes, R., Spillantini, M.G., Hasegawa, M., Smith, M.J. & Crowther, R.A. 1996, "Assembly of microtubule-associated protein tau into Alzheimer-like filaments induced by sulphated glycosaminoglycans", *Nature,* vol. 383, no. 6600, pp. 550-553.

Goedert, M., Spillantini, M.G., Cairns, N.J. & Crowther, R.A. 1992, "Tau proteins of Alzheimer paired helical filaments: abnormal phosphorylation of all six brain isoforms", *Neuron,* vol. 8, no. 1, pp. 159-168.

Goedert, M., Spillantini, M.G. & Crowther, R.A. 1992, "Cloning of a big tau microtubule-associated protein characteristic of the peripheral nervous system", *Proceedings of the National Academy of Sciences of the United States of America,* vol. 89, no. 5, pp. 1983-1987.

Goedert, M., Wischik, C.M., Crowther, R.A., Walker, J.E. & Klug, A. 1988, "Cloning and sequencing of the cDNA encoding a core protein of the paired helical filament of Alzheimer disease: Identification as the microtubule-associated protein tau.", *Proceedings of the National Academy of Sciences of the United States of America,* vol. 85, no. 11, pp. 4051-4055.

Goedert, M., Clavaguera, F. & Tolnay, M. 2010, "The propagation of prion-like protein inclusions in neurodegenerative diseases", *Trends in neurosciences,* vol. 33, no. 7, pp. 317-325.

Goedert, M., Hasegawa, M., Jakes, R., Lawer, S., Cuenda, A. & Cohen, P. 1997, “Phosphorylation of microtubule-associated protein tau by stress-activated protein kinases”, *FEBS letters,* vol. 409, no. 1, pp. 57-62.

Gomez-Isla, T., Hollister, R., West, H., Mui, S., Growdon, J.H., Petersen, R.C., Parisi, J.E. & Hyman, B.T. 1997, "Neuronal loss correlates with but exceeds neurofibrillary tangles in Alzheimer's disease", *Annals of Neurology,* vol. 41, no. 1, pp. 17-24.

Gomez-Ramos, A., Diaz-Hernandez, M., Rubio, A., Miras-Portugal, M.T. & Avila, J. 2008, "Extracellular tau promotes intracellular calcium increase through M1 and M3 muscarinic receptors in neuronal cells.", *Molecular and Cellular Neuroscience,* vol. 37, no. 4, pp. 673-681.

Goode, B.L., Denis, P.E., Panda, D., Radeke, M.J., Miller, H.P., Wilson, L. & Feinstein, S.C. 1997, "Functional interactions between the proline-rich and repeat regions of tau enhance microtubule binding and assembly", *Molecular biology of the cell,* vol. 8, no. 2, pp. 353-365.

Goode, B.L. & Feinstein, S.C. 1994, "Identification of a novel microtubule binding and assembly domain in the developmentally regulated inter-repeat region of tau", *The Journal of cell biology,* vol. 124, no. 5, pp. 769-782.

Gordon, C.P., Venn-Brown, B., Robertson, M.J., Young, K.A., Chau, N., Mariana, A., Whiting, A., Chircop, M., Robinson, P.J. & McCluskey, A. 2013, "Development of second-generation indole-based dynamin GTPase inhibitors", *Journal of medicinal chemistry,* vol. 56, no. 1, pp. 46-59.

Gousset, K. & Zurzolo, C. 2009, "Tunnelling nanotubes A highway for prion spreading?", *Prion,* vol. 3, no. 2, pp. 94-98.

Greenberg, S.G. & Davies, P. 1990, "A preparation of Alzheimer paired helical filaments that displays distinct tau proteins by polyacrylamide gel electrophoresis", *Proceedings of the National Academy of Sciences of the United States of America,* vol. 87, no. 15, pp. 5827-5831.

Greenberg, S.G., Davies, P., Schein, J.D. & Binder, L.I. 1992, "Hydrofluoric acid-treated tau PHF proteins display the same biochemical properties as normal tau", *The Journal of biological chemistry,* vol. 267, no. 1, pp. 564-569.

Guo, J.L., Buist, A., Soares, A., Callaerts, K., Calafate, S., Stevenaert, F., Daniels, J.P., Zoll, B.E., Crowe, A., Brunden, K.R., Moechars, D. & Lee, V.M. 2016, "The Dynamics and Turnover of Tau Aggregates in Cultured Cells: Insights into Therapies for Tauopathies", *The Journal of biological chemistry,* vol. 291, no. 25, pp. 13175-13193.

Guo, J.L. & Lee, V.M.Y. 2013, "Neurofibrillary tangle-like tau pathology induced by synthetic tau fibrils in primary neurons over-expressing mutant tau.", *FEBS letters,* vol. 587, no. 6, pp. 717-723.

Guo, J.L. & Lee, V.M. 2011, "Seeding of normal tau by pathological tau conformers drives pathogenesis of Alzheimer-like tangles.", *Journal of Biological Chemistry,* vol. 286, no. 17, pp. 15317-15331.

Guo, J.L., Narasimhan, S., Changolkar, L., He, Z., Stieber, A., Zhang, B., Gathagan, R.J., Iba, M., McBride, J.D., Trojanowski, J.Q. & Lee, V.M. 2016, "Unique pathological tau conformers from Alzheimer's brains transmit tau pathology in nontransgenic mice", *The Journal of experimental medicine,* vol. 213, no. 12, pp. 2635-2654.

Guo, J.L. & Lee, V.M.Y. 2014, "Cell-to-cell transmission of pathogenic proteins in neurodegenerative diseases", *Nature medicine,* vol. 20, no. 2, pp. 130-138.

Guo, T., Noble, W. & Hanger, D.P. 2017, "Roles of tau protein in health and disease", *Acta Neuropathologica,* vol. 133, no. 5, pp. 665-704.

Gurke, S., Barroso, J.F. & Gerdes, H.H. 2008, "The art of cellular communication: tunneling nanotubes bridge the divide ", *Histochemistry and cell biology,* vol. 129, no. 5, pp. 539-550.

Gustke, N., Trinczek, B., Biernat, J., Mandelkow, E.M. & Mandelkow, E. 1994, "Domains of tau protein and interactions with microtubules", *Biochemistry,* vol. 33, no. 32, pp. 9511-9522.

Hall, G.F., Lee, V.M., Lee, G. & Yao, J. 2001, "Staging of neurofibrillary degeneration caused by human tau overexpression in a unique cellular model of human tauopathy.", *American Journal of Pathology,* vol. 158, no. 1, pp. 235-246.

Hansen, C., Angot, E., Bergstrom, A.L., Steiner, J.A., Pieri, L., Paul, G., Outeiro, T.F., Melki, R., Kallunki, P., Fog, K., Li, J.Y. & Brundin, P. 2011, "alpha-Synuclein propagates from mouse brain to grafted dopaminergic neurons and seeds aggregation in cultured human cells.", *Journal of Clinical Investigation,* vol. 121, no. 2, pp. 715-725.

Hasegawa, M., Smith, M.J. & Goedert, M. 1998, "Tau proteins with FTDP-17 mutations have a reduced ability to promote microtubule assembly.", *FEBS letters,* vol. 437, no. 3, pp. 207-210.

Hasegawa, M., Nonaka, T. & Masuda-Suzukake, M. 2017, “Prion-like mechanisms and potential therapeutic targets in neurodegenerative disorders”, *Pharmacology & Therapeutics,* vol. 172, pp. 22-33.

Higuchi, M., Zhang, B., Forman, M.S., Yoshiyama, Y., Trojanowski, J.Q. & Lee, V.M. 2005 “Axonal degeneration induced by targeted expression of mutant human tau in oligodendrocytes of transgenic mice that model glial tauopathies”, *Journal of Neuroscience*, vol. 25, no. 41, pp. 9434–43.

Hodneland, E., Lundervold, A., Gurke, S., Tai, X., Rustom, A. & Gerdes, H. 2006, "Automated detection of tunneling nanotubes in 3D images ", *Cytometry Part A,* vol. 69A, no. 9, pp. 961-972.

Holmes, B., DeVos, S., Kfoury, N., Miller, T., Papy-Garcia, D. & Diamond, M. 2013., "Heparan sulfate proteoglycans mediate internalization and propagation of specific proteopathic seeds.", *Glycobiology,* vol. 23, no. 11, pp. 1409.

Holmes, B.B., DeVos, S.L., Kfoury, N., Li, M., Jacks, R., Yanamandra, K., Ouidja, M.O., Brodsky, F.M., Marasa, J., Bagchi, D.P., Kotzbauer, P.T., Miller, T.M., Papy-Garcia, D. & Diamond, M.I. 2013, "Heparan sulfate proteoglycans mediate internalization and propagation of specific proteopathic seeds.", *Proceedings of the National Academy of Sciences of the United States of America,* vol. 110, no. 33, pp. E3138-E3147.

Holmes, B.B., Furman, J.L., Mahan, T.E., Yamasaki, T.R., Mirbaha, H., Eades, W.C., Belaygorod, L., Cairns, N.J., Holtzman, D.M. & Diamond, M.I. 2014, "Proteopathic tau seeding predicts tauopathy in vivo.", *Proceedings of the National Academy of Sciences of the United States of America,* vol. 111, no. 41, pp. E4376-85.

Hong, M., Zhukareva, V., Vogelsberg-Ragaglia, V., Wszolek, Z., Reed, L., Miller, B.I., Geschwind, D.H., Bird, T.D., McKeel, D., Goate, A., Morris, J.C., Wilhelmsen, K.C., Schellenberg, G.D., Trojanowski, J.Q. & Lee, V.M. 1998, "Mutation-specific functional impairments in distinct tau isoforms of hereditary FTDP-17", *Science,* vol. 282, no. 5395, pp. 1914-1917.

Hoover, B.R., Reed, M.N., Su, J., Penrod, R.D., Kotilinek, L.A., Grant, M.K., Pitstick, R., Carlson, G.A., Lanier, L.M., Yuan, L.L., Ashe, K.H. & Liao, D. 2010, "Tau mislocalization to dendritic spines mediates synaptic dysfunction independently of neurodegeneration", *Neuron,* vol. 68, no. 6, pp. 1067-1081.

Hutton, M., Lendon, C.L., Rizzu, P., Baker, M., Froelich, S., Houlden, H., Pickering-Brown, S., Chakraverty, S., Isaacs, A., Grover, A., Hackett, J., Adamson, J., Lincoln, S., Dickson, D., Davies, P., Petersen, R.C., Stevens, M., De Graaff, E., Wauters, E., Van Baren, J., Hillebrand, M., Joosse, M., Kwon, J.M., Nowotny, P., Che, L.K., Norton, J., Morris, J.C., Reed, L.A., Trojanowski, J., Basun, H., Lannfelt, L., Neystat, M., Fahn, S., Dark, F., Tannenberg, T., Dood, P.R., Hayward, N., Kwok, J.B.J., Schofield, P.R., Andreais, A., Snowden, J., Craufurd, D., Neary, D., Owen, F., Oostra, B.A., Van Swieten, J., Mann, D., Lynch, T. & Heutink, P. 1998, "Association of missense and 5'-splice-site mutations in tau with the inherited dementia FTDP-17", *Nature,* vol. 393, no. 6686, pp. 702-705.

Iba, M., Guo, J.L., McBride, J.D., Zhang, B., Trojanowski, J.Q. & Lee, V.M. 2013, "Synthetic tau fibrils mediate transmission of neurofibrillary tangles in a transgenic mouse model of alzheimer's-like tauopathy.", *Journal of Neuroscience,* vol. 33, no. 3, pp. 1024-1037.

Ittner, L.M., Ke, Y.D., Delerue, F., Bi, M., Gladbach, A., van Eersel, J., Wolfing, H., Chieng, B.C., Christie, M.J., Napier, I.A., Eckert, A., Staufenbiel, M., Hardeman, E. & Gotz, J. 2010, "Dendritic function of tau mediates amyloid-beta toxicity in Alzheimer's disease mouse models", *Cell,* vol. 142, no. 3, pp. 387-397.

Jackson, S.J., Kerridge, C., Cooper, J., Cavallini, A., Falcon, B., Cella, C.V., Landi, A., Szekeres, P.G., Murray, T.K., Ahmed, Z., Goedert, M., Hutton, M., O'Neill, M.J. & Bose, S. 2016, "Short Fibrils Constitute the Major Species of Seed-Competent Tau in the Brains of Mice Transgenic for Human P301S Tau", *The Journal of neuroscience : the official journal of the Society for Neuroscience,* vol. 36, no. 3, pp. 762-772.

Jaworski, T., Dewachter, I., Lechat, B., Croes, S., Termont, A., Demedts, D., Borghgraef, P., Devijver, H., Filipkowski, R.K., Kaczmarek, L., Kugler, S. & Van Leuven, F. 2009, "AAV-tau mediates pyramidal neurodegeneration by cell-cycle re-entry without neurofibrillary tangle formation in wild-type mice.", *PLoS ONE,* vol. 4, no. 10, pp. e7280.

Jaworski, T., Lechat, B., Demedts, D., Gielis, L., Devijver, H., Borghgraef, P., Duimel, H., Verheyen, F., Kgler, S. & Van Leuven, F. 2011, "Dendritic degeneration, neurovascular defects, and inflammation precede neuronal loss in a mouse model for tau-mediated neurodegeneration.", *American Journal of Pathology,* vol. 179, no. 4, pp. 2001-2015.

Jeganathan, S., von Bergen, M., Brutlach, H., Steinhoff, H.J. & Mandelkov, E. 2006, "Global hairpin folding of tau in solution", *Biochemistry,* vol. 45, pp. 2283.

Johnston, J.A., Ward, C.L. & Kopito, R.R. 1998, "Aggresomes: a cellular response to misfolded proteins", *The Journal of cell biology,* vol. 143, no. 7, pp. 1883-1898.

Kampers, T., Friedhoff, P., Biernat, J., Mandelkow, E.M. & Mandelkow, E. 1997, "RNA stimulates the aggregation of microtubule-associated protein tau into Alzheimer-like paired helical filaments", *Molecular biology of the cell,* vol. 8, no. SUPPL, pp. 264A.

Kanmert, D., Cantlon, A., Muratore, C.R., Jin, M., O'Malley, T.T., Lee, G., Young-Pearse, T.L., Selkoe, D.J. & Walsh, D.M. 2015, "C-Terminally Truncated Forms of Tau, But Not Full-Length Tau or Its C-Terminal Fragments, Are Released from Neurons Independently of Cell Death", *The Journal of neuroscience : the official journal of the Society for Neuroscience,* vol. 35, no. 30, pp. 10851-10865.

Karch, C.M., Jeng, A.T. & Goate, A.M. 2012, "Extracellular tau levels are influenced by variability in tau that is associated with tauopathies.", *Journal of Biological Chemistry,* vol. 287, no. 51, pp. 42751-42762.

Kaufman, S.K., Sanders, D.W., Thomas, T.L., Ruchinskas, A.J., Vaquer-Alicea, J., Sharma, A.M., Miller, T.M. & Diamond, M.I. 2016, "Tau Prion Strains Dictate Patterns of Cell Pathology, Progression Rate, and Regional Vulnerability In Vivo", *Neuron,* vol. 92, no. 4, pp. 796-812.

Kerppola, T.K. 2006, "Visualization of molecular interactions by fluorescence complementation.", *Nature Reviews Molecular Cell Biology,* vol. 7, no. 6, pp. 449-456.

Kfoury, N., Holmes, B.B., Jiang, H., Holtzman, D.M. & Diamond, M.I. 2012, "Trans-cellular propagation of Tau aggregation by fibrillar species.", *Journal of Biological Chemistry,* vol. 287, no. 23, pp. 19440-19451.

Khalil, I.A., Kogure, K., Akita, H. & Harashima, H. 2006, "Uptake pathways and subsequent intracellular trafficking in nonviral gene delivery", *Pharmacological reviews,* vol. 58, no. 1, pp. 32-45.

Khlistunova, I., Biernat, J., Wang, Y., Pickhardt, M., von Bergen, M., Gazova, Z., Mandelkow, E. & Mandelkow, E.M. 2006, "Inducible expression of Tau repeat domain in cell models of tauopathy: aggregation is toxic to cells but can be reversed by inhibitor drugs.", *Journal of Biological Chemistry,* vol. 281, no. 2, pp. 1205-1214.

Kidd, M. 1963, "Paired helical filaments in electron microscopy of Alzheimer's disease.", *Nature,* vol. 197, pp. 192-193.

Kim, J.I., Cali, I., Surewicz, K., Kong, Q., Raymond, G.J., Atarashi, R., Race, B., Qing, L., Gambetti, P., Caughey, B. & Surewicz, W.K. 2010, "Mammalian prions generated from bacterially expressed prion protein in the absence of any mammalian cofactors", *Journal of Biological Chemistry,* vol. 285, pp. 14083-14087.

Kim, W., Lee, S. & Hall, G.F. 2010a, "Secretion of human tau fragments resembling CSF-tau in Alzheimer's disease is modulated by the presence of the exon 2 insert", *FEBS letters,* vol. 584, no. 14, pp. 3085-3088.

Kim, W., Lee, S. & Hall, G.F. 2010b, "Secretion of human tau fragments resembling CSF-tau in Alzheimer's disease is modulated by the presence of the exon 2 insert.", *FEBS letters,* vol. 584, no. 14, pp. 3085-3088.

Kim, W., Lee, S., Jung, C., Ahmed, A., Lee, G. & Hall, G.F. 2010, "Interneuronal transfer of human tau between lamprey central neurons in situ.", *Journal of Alzheimer's Disease,* vol. 19, no. 2, pp. 647-664.

Kimura, T., Whitcomb, D.J., Jo, J., Regan, P., Piers, T., Heo, S., Brown, C., Hashikawa, T., Murayama, M., Seok, H., Sotiropoulos, I., Kim, E., Collingridge, G.L., Takashima, A. & Cho, K. 2014, "Microtubule-associated protein tau is essential for long-term depression in the hippocampus.", *Philosophical Transactions of the Royal Society of London - Series B: Biological Sciences,* vol. 369, no. 1633, pp. 20130144.

Kimura, T., Yamashita, S., Fukuda, T., Park, J.M., Murayama, M., Mizoroki, T., Yoshiike, Y., Sahara, N. & Takashima, A. 2007, “Hyperphosphorylated tau in parahippocampal cortex impairs place learning in aged mice expressing wild-type human tau”, *The EMBO Journal*, vol. 26, no. 24, pp. 5143–52.

Klein, R.L., Dayton, R.D., Lin, W.L. & Dickson, D.W. 2005, "Tau gene transfer, but not alpha-synuclein, induces both progressive dopamine neuron degeneration and rotational behavior in the rat.", *Neurobiology of disease,* vol. 20, no. 1, pp. 64-73.

Klein, R.L., Dayton, R.D., Tatom, J.B., Diaczynsky, C.G. & Salvatore, M.F. 2008, "Tau expression levels from various adeno-associated virus vector serotypes produce graded neurodegenerative disease states.", *European Journal of Neuroscience,* vol. 27, no. 7, pp. 1615-1625.

Klein, R.L., Lin, W.L., Dickson, D.W., Lewis, J., Hutton, M., Duff, K., Meyer, E.M. & King, M.A. 2004, "Rapid neurofibrillary tangle formation after localized gene transfer of mutated tau.", *American Journal of Pathology,* vol. 164, no. 1, pp. 347-353.

Kobayashi, T., Vischer, U.M., Rosnoblet, C., Lebrand, C., Lindsay, M., Parton, R.G., Kruithof, E.K.O. & Gruenberg, J. 2000, "The tetraspanin CD63/lamp3 cycles between endocytic and secretory compartments in human endothelial cells", *Molecular biology of the cell,* vol. 11, no. 5, pp. 1829-1843.

Kolarova, M., Garcia-Sierra, F., Bartos, A., Ricny, J. & Ripova, D. 2012, "Structure and pathology of tau protein in Alzheimer disease.", *International Journal of Alzheimer's Disease,* vol. 2012, Article ID 731526, 13 pages.

Komori, T., Shibata, N., Kobayashi, M., Sasaki, S. & Iwata, M. 1998, "Inducible nitric oxide synthase (iNOS)-like immunoreactivity in argyrophilic, tau-positive astrocytes in progressive supranuclear palsy.", *Acta Neuropathologica,* vol. 95, no. 4, pp. 338-344.

Kosik, K.S., Joachim, C.L. & Selkoe, D.J. 1986, "Microtubule-associated protein tau is a major antigenic component of paired helical filaments in Alzheimer disease.", *Proceedings of the National Academy of Sciences of the United States of America,* vol. 83, no. 11, pp. 4044-4048.

Koyanagi, M., Brandes, R.P., Haendeler, J., Zeiher, A.M. & Dimmeler, S. 2005, "Cell-to-cell connection of endothelial progenitor cells with cardiac myocytes by nanotubes: a novel mechanism for cell fate changes? ", *Circulation research,* vol. 96, no. 10, pp. 1039-1041.

Kruger, U., Wang, Y., Kumar, S. & Mandelkow, E.M. 2012, "Autophagic degradation of tau in primary neurons and its enhancement by trehalose.", *Neurobiology of aging,* vol. 33, no. 10, pp. 2291-2305.

Ksiezak-Reding, H., Morgan, K., Mattiace, L.A., Davies, P., Liu, W.K., Yen, S.H., Weidenheim, K. & Dickson, D.W. 1994, "Ultrastructure and biochemical composition of paired helical filaments in corticobasal degeneration", *The American journal of pathology,* vol. 145, no. 6, pp. 1496-1508.

Lasagna-Reeves, C.A., Castillo-Carranza, D.L., Sengupta, U., Clos, A.L., Jackson, G.R. & Kayed, R. 2011, "Tau oligomers impair memory and induce synaptic and mitochondrial dysfunction in wild-type mice.", *Molecular Neurodegeneration,* vol. 6, pp. 39.

Lasagna-Reeves, C.A., Castillo-Carranza, D.L., Sengupta, U., Sarmiento, J., Troncoso, J., Jackson, G.R. & Kayed, R. 2012, "Identification of oligomers at early stages of tau aggregation in Alzheimer's disease.", *FASEB Journal,* vol. 26, no. 5, pp. 1946-1959.

Lee, H., Suk, J., Patrick, C., Bae, E., Cho, J., Rho, S., Hwang, D., Masliah, E. & Lee, S. 2010, "Direct transfer of alpha-synuclein from neuron to astroglia causes inflammatory responses in synucleinopathies.", *Journal of Biological Chemistry,* vol. 285, no. 12, pp. 9262-9272.

Lee, S., Jung, C., Lee, G. & Hall, G.F. 2009, "Exonic point mutations of human tau enhance its toxicity and cause characteristic changes in neuronal morphology, tau distribution and tau phosphorylation in the lamprey cellular model of tauopathy.", *Journal of Alzheimer's Disease,* vol. 16, no. 1, pp. 99-111.

Lee, S.E., Tartaglia, M.C., Yener, G., Genc, S., Seeley, W.W., Sanchez-Juan, P., Moreno, F., Mendez, M.F., Klein, E., Rademakers, R., Lopez de Munain, A., Combarros, O., Kramer, J.H., Kenet, R.O., Boxer, A.L., Geschwind, M.D., Gorno-Tempini, M.L., Karydas, A.M., Rabinovici, G.D., Coppola, G., Geschwind, D.H. & Miller, B.L. 2013, "Neurodegenerative disease phenotypes in carriers of MAPT p.A152T, a risk factor for frontotemporal dementia spectrum disorders and Alzheimer disease", *Alzheimer Disease and Associated Disorders,* vol. 27, no. 4, pp. 302-309.

Lee, V.M., Balin, B.J., Otvos, L.J. & Trojanowski, J.Q. 1991, "A68 a major subunit of paired helical filaments and derivatized forms of normal tau", *Science,* vol. 251, no. 4994, pp. 675-678.

Legname, G., Nguyen, H.O., Baskakov, I.V., Cohen, F.E., Dearmond, S.J. & Prusiner, S.B. 2005, "Strain-specified characteristics of mouse synthetic prions", *Proceedings of the National Academy of Sciences of the United States of America,* vol. 102, no. 6, pp. 2168-2173.

Legname, G., Nguyen, H.O., Peretz, D., Cohen, F.E., DeArmond, S.J. & Prusiner, S.B. 2006, "Continuum of prion protein structures enciphers a multitude of prion isolate-specified phenotypes", *Proceedings of the National Academy of Sciences of the United States of America,* vol. 103, no. 50, pp. 19105-19110.

Lei, P., Ayton, S., Finkelstein, D.I., Spoerri, L., Ciccotosto, G.D., Wright, D.K., Wong, B.X.W., Adlard, P.A., Cherny, R.A., Lam, L.Q., Roberts, B.R., Volitakis, I., Egan, G.F., McLean, C.A., Cappai, R., Duce, J.A. & Bush, A.I. 2012, "Tau deficiency induces parkinsonism with dementia by impairing APP-mediated iron export.", *Nature medicine,* vol. 18, no. 2, pp. 291-295.

Lei, P., Ayton, S., Moon, S., Zhang, Q., Volitakis, I., Finkelstein, D.I. & Bush, A.I. 2014, "Motor and cognitive deficits in aged tau knockout mice in two background strains", *Molecular neurodegeneration,* vol. 9, pp. 29-1326-9-29.

Lewis, J., Dickson, D.W., Lin, W., Chisholm, L., Corral, A., Jones, G., Yen, S., Sahara, N., Skipper, L., Yager, D., Eckman, C., Hardy, J., Hutton, M. & McGowan, E. 2001, "Enhanced neurofibrillary degeneration in transgenic mice expressing mutant tau and APP.", *Science,* vol. 293, no. 5534, pp. 1487-1491.

Li, G., Yin, H. & Kuret, J. 2004, "Casein Kinase 1 Delta Phosphorylates Tau and Disrupts Its Binding to Microtubules.", *Journal of Biological Chemistry,* vol. 279, no. 16, pp. 15938-15945.

Li, J., Englund, E., Holton, J.L., Soulet, D., Hagell, P., Lees, A.J., Lashley, T., Quinn, N.P., Rehncrona, S., Bjorklund, A., Widner, H., Revesz, T., Lindvall, O. & Brundin, P. 2008, "Lewy bodies in grafted neurons in subjects with Parkinson's disease suggest host-to-graft disease propagation", *Nature medicine,* vol. 14, no. 5, pp. 501-503.

Lim, S., Haque, M.M., Kim, D., Kim, D.J. & Kim, Y.K. 2014, "Cell-based Models To Investigate Tau Aggregation", *Computational And Structural Biotechnology Journal,* vol. 12, no. 20-21, pp. 7-13.

Liu, L., Drouet, V., Wu, J.W., Witter, M.P., Small, S.A., Clelland, C. & Duff, K. 2012, "Trans-synaptic spread of tau pathology in vivo.", *PLoS ONE,* vol. 7, no. 2, pp. e31302.

Loeffler, D.A. 2013, "Intravenous immunoglobulin and Alzheimer's disease: what now?", *Journal of neuroinflammation,* vol. 10, no. 70, pp. 853.

Lou, E., Fujisawa, S., Morozov, A., Barlas, A., Romin, Y., Dogan, Y., Gholami, S., Moreira, A.L., Manova-Todorova, K. & Moore, M.A. 2012, "Tunneling nanotubes provide a unique conduit for intercellular transfer of cellular contents in human malignant pleural mesothelioma", *PloS one,* vol. 7, no. 3, pp. e33093.

Lu, M. & Kosik, K.S. 2001, "Competition for microtubule-binding with dual expression of tau missense and splice isoforms.", *Molecular biology of the cell,* vol. 12, no. 1, pp. 171-184.

Lu, B., Nagappan, G., Guan, X., Nathan, P.J. & Wren, P. 2013, "BDNF-based synaptic repair as a disease-modifying strategy for neurodegenerative diseases", *Nature reviews.Neuroscience,* vol. 14, no. 6, pp. 401-416.

Luk, K.C., Kehm, V.M., Zhang, B., O'Brien, P., Trojanowski, J.Q. & Lee, V.M. 2012, "Intracerebral inoculation of pathological alpha-synuclein initiates a rapidly progressive neurodegenerative alpha-synucleinopathy in mice", *The Journal of experimental medicine,* vol. 209, no. 5, pp. 975-986.

Luk, K.C., Song, C., O'Brien, P., Stieber, A., Branch, J.R., Brunden, K.R., Trojanowski, J.Q. & Lee, V.M. 2009, "Exogenous alpha-synuclein fibrils seed the formation of Lewy body-like intracellular inclusions in cultured cells", *Proceedings of the National Academy of Sciences of the United States of America,* vol. 106, no. 47, pp. 20051-20056.

Lyubchenko, T.A., Georjeana, A.W. & Zweifacht, A. 2003, "The actin cytoskeleton and cytotoxic T lymphocytes: evidence for multiple roles that could affect granule exocytosis-dependent target cell killing", *Journal of physiology,* vol. 547, no. 3, pp. 835-847.

Maeda, S., Sahara, N., Saito, Y., Murayama, M., Yoshiike, Y., Kim, H., Miyasaka, T., Murayama, S., Ikai, A. & Takashima, A. 2007, "Granular tau oligomers as intermediates of tau filaments.", *Biochemistry,* vol. 46, no. 12, pp. 3856-3861.

Magalhaes, A.C., Baron, G.S., Lee, K.S., Steele-Mortimer, O., Dorward, D., Prado, M.A.M. & Caughey, B. 2005, "Uptake and neuritic transport of scrapie prion protein coincident with infection of neuronal cells.", *Journal of Neuroscience,* vol. 25, no. 21, pp. 5207-5216.

Magnani, E., Fan, J., Gasparini, L., Golding, M., Williams, M., Schiavo, G., Goedert, M., Amos, L.A. & Spillantini, M.G. 2007, "Interaction of tau protein with the dynactin complex.", *The EMBO Journal,* vol. 26, no. 21, pp. 4546-4554.

Mair, W., Muntel, J., Tepper, K., Tang, S., Biernat, J., Seeley, W.W., Kosik, K.S., Mandelkow, E., Steen, H. & Steen, J.A. 2016, "FLEXITau: Quantifying Post-translational Modifications of Tau Protein in Vitro and in Human Disease", *Analytical Chemistry,* vol. 88, no. 7, pp. 3704-3714.

Maphis, N., Xu, G., Kokiko-Cochran, O.N., Jiang, S., Cardona, A., Ransohoff, R.M., Lamb, B.T. & Bhaskar, K. 2015, "Reactive microglia drive tau pathology and contribute to the spreading of pathological tau in the brain", *Brain : a journal of neurology,* vol. 138, no. Pt 6, pp. 1738-1755.

McEwan, W.A., Falcon, B., Vaysburd, M., Clift, D., Oblak, A.L., Ghetti, B., Goedert, M. & James, L.C. 2017, "Cytosolic Fc receptor TRIM21 inhibits seeded tau aggregation", *Proceedings of the National Academy of Sciences of the United States of America,* vol. 114, no. 3, pp. 574-579.

Mercer, J. & Helenius, A. 2009, "Virus entry by macropinocytosis", *Nature cell biology,* vol. 11, no. 5, pp. 510-520.

Merrick, S.E., Trojanowski, J.Q. & Lee, V.M.Y. 1997, "Selective destruction of stable microtubules and axons by inhibitors of protein serine/threonine phosphatases in cultured human neurons (NT2N cells)", *Journal of Neuroscience,* vol. 17, no. 15, pp. 5726-5737.

Meyer-Luehmann, M., Coomaraswamy, J., Bolmont, T., Kaeser, S., Schaefer, C., Kilger, E., Neuenschwander, A., Abramowski, D., Frey, P., Jaton, A.L., Vigouret, J.M., Paganetti, P., Walsh, D.M., Mathews, P.M., Ghiso, J., Staufenbiel, M., Walker, L.C. & Jucker, M. 2006a, "Exogenous induction of cerebral beta-amyloidogenesis is governed by agent and host", *Science,* vol. 313, no. 5794, pp. 1781-1784.

Meyer-Luehmann, M., Coomaraswamy, J., Bolmont, T., Kaeser, S., Schaefer, C., Kilger, E., Neuenschwander, A., Abramowski, D., Frey, P., Jaton, A.L., Vigouret, J., Paganetti, P., Walsh, D.M., Mathews, P.M., Ghiso, J., Staufenbiel, M., Walker, L.C. & Jucker, M. 2006b, "Exogenous induction of cerebral beta-amyloidogenesis is governed by agent and host", *Science,* vol. 313, no. 5794, pp. 1781-1784.

Millecamps, S. & Julien, J.P. 2013, "Axonal transport deficits and neurodegenerative diseases", *Nature reviews.Neuroscience,* vol. 14, no. 3, pp. 161-176.

Mirbaha, H., Holmes, B.B., Sanders, D.W., Bieschke, J. & Diamond, M.I. 2015, "Tau Trimers Are the Minimal Propagation Unit Spontaneously Internalized to Seed Intracellular Aggregation", *The Journal of biological chemistry,* vol. 290, no. 24, pp. 14893-14903.

Mocanu, M.M., Nissen, A., Eckermann, K., Khlistunova, I., Biernat, J., Drexler, D., Petrova, O., Schonig, K., Bujard, H., Mandelkow, E., Zhou, L., Rune, G. & Mandelkow, E.M. 2008, “The potential for beta-structure in the repeat domain of tau protein determines aggregation, synaptic decay, neuronal loss, and coassembly with endogenous tau in inducible mouse models of tauopathy.”, *Journal of Neuroscience*, vol. 28, no. 3, pp. 737–48.

Mollenhauer, B., Trautmann, E., Taylor, P., Manninger, P., Sixel-Doring, F., Ebentheuer, J., Trenkwalder, C. & Schlossmacher, M.G. 2013, "Total CSF alpha-synuclein is lower in de novo Parkinson patients than in healthy subjects.", *Neuroscience letters,* vol. 532, pp. 44-48.

Morozova, O.A., March, Z.M., Robinson, A.S. & Colby, D.W. 2013, "Conformational features of tau fibrils from alzheimer's disease brain are faithfully propagated by unmodified recombinant protein.", *Biochemistry,* vol. 52, no. 40, pp. 6960-6967.

Morris, M., Maeda, S., Vossel, K. & Mucke, L. 2011, "The Many Faces of Tau.", *Neuron,* vol. 70, no. 3, pp. 410-426.

Morsch, R., Simon, W. & Coleman, P.D. 1999, "Neurons may live for decades with neurofibrillary tangles", *Journal of neuropathology and experimental neurology,* vol. 58, no. 2, pp. 188-197.

Munch, C., O'Brien, J. & Bertolotti, A. 2011, "Prion-like propagation of mutant superoxide dismutase-1 misfolding in neuronal cells.", *Proceedings of the National Academy of Sciences of the United States of America,* vol. 108, no. 9, pp. 3548-3553.

Murray, M.E., Kouri, N., Lin, W.L., Jack, C.R.Jr, Dickson, D.W. & Vemuri, P. 2014, "Clinicopathologic assessment and imaging of tauopathies in neurodegenerative dementias", *Alzheimer's Research & Therapy,* vol. 6, no. 1, pp. 1.

Nacharaju, P., Lewis, J., Easson, C., Yen, S., Hackett, J., Hutton, M. & Yen, S. 1999, "Accelerated filament formation from tau protein with specific FTDP-17 missense mutations", *FEBS letters,* vol. 447, no. 2-3, pp. 195-199.

Nave, K.A. & Werner, H.B. 2014, "Myelination of the nervous system: mechanisms and functions", *Annual Review of Cell and Developmental Biology,* vol. 30, pp. 503-533.

Neve, R.L., Harris, P., Kosik, K.S., Kurnit, D.M. & Donlon, T.A. 1986, "Identification of cDNA clones for the human microtubule-associated protein tau and chromosomal localization of the genes for tau and microtubule-associated protein 2.", *Brain research,* vol. 387, no. 3, pp. 271-280.

Nishimura, M., Namba, Y., Ikeda, K. & Oda, M. 1992, "Glial fibrillary tangles with straight tubules in the brains of patients with progressive supranuclear palsy.", *Neuroscience letters,* vol. 143, no. 1-2, pp. 35-38.

Nixon, R.A. & Yang, D. 2011, "Autophagy failure in Alzheimer's disease-locating the primary defect", *Neurobiology of disease,* vol. 43, no. 1, pp. 38-45.

Nobuhara, C.K., DeVos, S.L., Commins, C., Wegmann, S., Moore, B.D., Roe, A.D., Costantino, I., Frosch, M.P., Pitstick, R., Carlson, G.A., Hock, C., Nitsch, R.M., Montrasio, F., Grimm, J., Cheung, A.E., Dunah, A.W., Wittmann, M., Bussiere, T., Weinreb, P.H., Hyman, B.T. & Takeda, S. 2017, "Tau Antibody Targeting Pathological Species Blocks Neuronal Uptake and Interneuron Propagation of Tau in Vitro", *The American journal of pathology,* vol. 187, no. 6, pp. 1399-1412.

Noda, K., Sasaki, K., Fujimi, K., Wakisaka, Y., Tanizaki, Y., Wakugawa, Y., Kiyohara, Y., Iida, M., Aizawa, H. & Iwaki, T. 2006, "Quantitative analysis of neurofibrillary pathology in a general population to reappraise neuropathological criteria for senile dementia of the neurofibrillary tangle type (tangle-only dementia): The Hisayama study.", *Neuropathology,* vol. 26, no. 6, pp. 508-518.

Nonaka, T., Watanabe, S.T., Iwatsubo, T. & Hasegawa, M. 2010, "Seeded Aggregation and Toxicity of alpha-Synuclein and Tau in Cellular models of neurodegenerative diseases", *Journal of Biological Chemistry,* vol. 285, no. 45, pp. 34885-34898.

Oddo, S., Caccamo, A., Kitazawa, M., Tseng, B.P. & LaFerla, F.M. 2003a, "Amyloid deposition precedes tangle formation in a triple transgenic model of Alzheimer's disease", *Neurobiology of aging,* vol. 24, no. 8, pp. 1063-1070.

Oddo, S., Caccamo, A., Shepherd, J.D., Murphy, M.P., Golde, T.E., Kayed, R., Metherate, R., Mattson, M.P., Akbari, Y. & LaFerla, F.M. 2003b, "Triple-transgenic model of Alzheimer's disease with plaques and tangles: intracellular Abeta and synaptic dysfunction", *Neuron,* vol. 39, no. 3, pp. 409-421.

Onfelt, B., Nedvetzki, S., Benninger, R.K., Purbhoo, M.A., Sowinski, S., Hume, A.N., Seabra, M.C., Neil, M.A., French, P.M. & Davis, D.M. 2006, "Structurally distinct membrane nanotubes

between human macrophages support long-distance vesicular traffic or surfing of bacteria ", *Journal of immunology,* vol. 177, no. 12, pp. 8476-8483.

Onfelt, B., Nedvetzki, S., Yanagi, K. & Davis, D.M. 2004, "Cutting edge: Membrane nanotubes connect immune cells ", *Journal of immunology,* vol. 173, no. 3, pp. 1511-1513.

Outeiro, T.F., Putcha, P., Tetzlaff, J.E., Spoelgen, R., Koker, M., Carvalho, F., Hyman, B.T. & McLean, P.J. 2008, "Formation of toxic oligomeric alpha-synuclein species in living cells.", *PLoS ONE,* vol. 3, no.4, pp. e1867.

Perez, M., Moran, M.A., Ferrer, I., Avila, J. & Gomez-Ramos, P. 2008, "Phosphorylated tau in neuritic plaques of APP(sw)/tau(vlw) transgenic mice and Alzheimer disease.", *Acta Neuropathologica,* vol.116, no. 4, pp. 409–18.

Perez, M., Ribe, E., Rubio, A., Lim, F., Moran, M.A., Ramos, P.G., Ferrer, I., Isla, M.T. & Avila, J. 2005, "Characterization of a double (amyloid precursor protein-tau) transgenic: tau phosphorylation and aggregation.", *Neuroscience,* vol. 130, no. 2, pp. 339–47.

Peterson, D.W., Zhou, H., Dahlquist, F.W. & Lew, J. 2008, "A soluble oligomer of tau associated with fiber formation analyzed by NMR", *Biochemistry,* vol. 47, no. 28, pp. 7393-7404.

Plouffe, V., Mohamed, N.V., Rivest-McGraw, J., Bertrand, J., Lauzon, M. & Leclerc, N. 2012, "Hyperphosphorylation and cleavage at D421 enhance tau secretion", *PloS one,* vol. 7, no. 5, pp. e36873.

Pollock, N.J., Mirra, S.S. & Binder, L.I. 1986, "Filamentous aggregates in Pick's disease, progressive supranuclear palsy, and Alzheimer's disease share antigenic determinants with microtubule-associated protein, tau.", *Lancet,* vol. 2, no. 8517, pp. 1211.

Polydoro, M., Acker, C.M., Duff, K., Castillo, P.E. & Davies, P. 2009, "Age-dependent impairment of cognitive and synaptic function in the htau mouse model of tau pathology", *Journal of Neuroscience,* vol. 29, no. 34, pp. 10741–9.

Pooler, A.M., Phillips, E.C., Lau, D.H.W., Noble, W. & Hanger, D.P. 2013, "Physiological release of endogenous tau is stimulated by neuronal activity", *EMBO reports,* vol. 14, no. 4, pp. 389-394.

Probst, A., Langui, D., Lautenschlager, C., Ulrich, J., Brion, J.P. & Anderton, B.H. 1988, "Progressive supranuclear palsy: Extensive neuropil threads in addition to neurofibrillary tangles. Very similar antigenicity of subcortial neuronal pathology in progressive supranuclear palsy and Alzheimer's disease.", *Acta Neuropathologica,* vol. 77, no. 1, pp. 61-68.

Probst, A., Tolnay, M., Langui, D., Goedert, M. & Spillantini, M.G. 1996, "Pick's disease: Hyperphosphorylated tau protein segregates to the somatoaxonal compartment.", *Acta Neuropathologica,* vol. 92, no. 6, pp. 588-596.

Probst, A., Gotz, J., Wiederhold, K.H., Tolnay, M., Mistl, C., Jaton, A.L., Hong, M., Ishihara, T., Lee, V.M., Trojanowski, J.Q., Jakes, R., Crowther, R.A., Spillantini, M.G., Burki, K. & Goedert, M,. 2000, "Axonopathy and amyotrophy in mice transgenic for human four-repeat tau protein." *Acta Neuropathoogica*, vol.99, no. 5, pp. 469–81.

Prusiner, S.B. 2013, "Biology and genetics of prions causing neurodegeneration.", *Annual Review of Genetics,* vol. 47, pp. 601-623.

Pul, R., Dodel, R. & Stangel, M. 2011, "Antibody-based therapy in Alzheimer's disease", *Expert opinion on biological therapy,* vol. 11, no. 3, pp. 343-357.

Ramachandran, G. & Udgaonkar, J.B. 2011, "Understanding the kinetic roles of the inducer heparin and of rod-like protofibrils during amyloid fibril formation by tau protein.", *Journal of Biological Chemistry,* vol. 286, no. 45, pp. 38948-38959.

Ramirez, J.J., Poulton, W.E., Knelson, E., Barton, C., King, M.A. & Klein, R.L. 2011, "Focal expression of mutated tau in entorhinal cortex neurons of rats impairs spatial working memory.", *Behavioural brain research,* vol. 216, no. 1, pp. 332-340.

Ramsden, M., Kotilinek, L., Forster, C., Paulson, J., McGowan, E., SantaCruz, K., Guimaraes, A., Yue, M., Lewis, J., Carlson, G., Hutton, M. & Ashe, K.H. 2005 “Age-dependent neurofibrillary tangle formation, neuron loss, and memory impairment in a mouse model of human tauopathy (P301L)”, *Journal of Neuroscience,* vol. 25, no. 46, pp. 10637–47.

Reilly, P., Winston, C.N., Baron, K.R., Trejo, M., Rockenstein, E.M., Akers, J.C., Kfoury, N., Diamond, M., Masliah, E., Rissman, R.A. & Yuan, S.H. 2017, "Novel human neuronal tau model exhibiting neurofibrillary tangles and transcellular propagation", *Neurobiology of disease,* vol. 106, pp. 222-234.

Ren, P.H., Lauckner, J.E., Kachirskaia, I., Heuser, J.E., Melki, R. & Kopito, R.R. 2009, "Cytoplasmic penetration and persistent infection of mammalian cells by polyglutamine aggregates ", *Nature cell biology,* vol. 11, no. 2, pp. 219-225.

Ribe, E.M., Perez, M., Puig, B., Gich, I., Lim, F., Cuadrado, M., Sesma, T., Catena, S., Sanchez, B., Nieto, M., Gomez-Ramos, P., Moran, M.A., Cabodevilla, F., Samaranch, L., Ortiz, L., Perez, A., Ferrer, I., Avila, J. & Gomez-Isla, T. 2005 “Accelerated amyloid deposition, neurofibrillary degeneration and neuronal loss in double mutant APP/tau transgenic mice.” *Neurobiology of Disease,* vol. 20, no. 3, pp. 814–22.

Rizzo, M.A., Springer, G.H., Granada, B. & Piston, D.W. 2004, "An improved cyan fluorescent protein variant useful for FRET.", *Nature biotechnology,* vol. 22, no. 4, pp. 445-449.

Rizzu, P., Van Swieten, J.C., Joosse, M., Hasegawa, M., Stevens, M., Tibben, A., Niermeijer, M.F., Hillebrand, M., Ravid, R., Oostra, B.A., Goedert, M., van Duijn, C.M. & Heutink, P. 1999, "High prevalence of mutations in the microtubule-associated protein tau in a population study of frontotemporal dementia in the Netherlands", *American Journal of Human Genetics,* vol. 64, no. 2, pp. 414-421.

Roberson, E.D., Scearce-Levie, K., Palop, J.J., Yan, F., Cheng, I.H., Wu, T., Gerstein, H., Yu, G.Q. & Mucke, L. 2007, "Reducing endogenous tau ameliorates amyloid beta-induced deficits in an Alzheimer's disease mouse model", *Science,* vol. 316, no. 5825, pp. 750-754.

Rustom, A., Saffrich, R., Markovic, I., Walther, P. & Gerdes, H. 2004, "Nanotubular highways for intercellular organelle transport.", *Science,* vol. 303, no. 5660, pp. 1007-1010.

Safavi, A., Langevin, M., Vandenberg, P., Novokhatny, V., Scuderi, P., Mohn, G. & Petteway, S. 2016, "Comparison of several human immunoglobulin products for anti Abeta1-42 titer", *10th international conference on Alzheimer's disease and related disorders*, 2016.

Saito, Y., Ruberu, N.N., Sawabe, M., Arai, T., Tanaka, N., Kakuta, Y., Yamanouchi, H. & Murayama, S. 2004, "Staging of argyrophilic grains: an age-associated tauopathy.", *Journal of Neuropathology & Experimental Neurology,* vol. 63, no. 9, pp. 911-918.

Saman, S., Kim, W., Raya, M., Visnick, Y., Miro, S., Saman, S., Jackson, B., McKee, A.C., Alvarez, V.E., Lee, N.C.Y. & Hall, G.F. 2012, "Exosome-associated Tau Is Secreted in Tauopathy Models and Is Selectively Phosphorylated in Cerebrospinal Fluid in Early Alzheimer Disease", *Journal of Biological Chemistry,* vol. 287, no. 6, pp. 3842-3849.

Sanders, D.W., Kaufman, S.K., DeVos, S.L., Sharma, A., Barker, S.J., Mirbaha, H., Li, A., Miller, T.M., Foley, A., Thorpe, J.R., Maina, M.B., Serpell, L., Grinberg, L.T., Seeley, W.W. & Diamond, M.I. 2014., "Distinct tau prion strains propagate in cells and mice and define different tauopathies.", *Prion,* vol. 8, pp. 18-19.

Sanders, D.W., Kaufman, S.K., DeVos, S.L., Sharma, A.M., Mirbaha, H., Li, A., Barker, S.J., Foley, A.C., Thorpe, J.R., Serpell, L.C., Miller, T.M., Grinberg, L.T., Seeley, W.W. & Diamond, M.I. 2014, "Distinct tau prion strains propagate in cells and mice and define different tauopathies.", *Neuron,* vol. 82, no. 6, pp. 1271-1288.

Sankaranarayanan, S., Barten, D.M., Vana, L., Devidze, N., Yang, L., Cadelina, G., Hoque, N., DeCarr, L., Keenan, S., Lin, A., Cao, Y., Snyder, B., Zhang, B., Nitla, M., Hirschfeld, G., Barrezueta, N., Polson, C., Wes, P., Rangan, V.S., Cacace, A., Albright, C.F., Meredith, J.,Jr, Trojanowski, J.Q., Lee, V.M., Brunden, K.R. & Ahlijanian, M. 2015, "Passive immunization with phospho-tau antibodies reduces tau pathology and functional deficits in two distinct mouse tauopathy models", *PloS one,* vol. 10, no. 5, pp. e0125614.

Santacruz, K., Lewis, J., Spires, T., Paulson, J., Kotilinek, L., Ingelsson, M., Guimaraes, A., DeTure, M., Ramsden, M., McGowan, E., Forster, C., Yue, M., Orne, J., Janus, C., Mariash, A., Kuskowski, M., Hyman, B., Hutton, M. & Ashe, K.H. 2005, "Tau suppression in a neurodegenerative mouse model improves memory function", *Science,* vol. 309, no. 5733, pp. 476-481.

Santa-Maria, I., Varghese, M., Ksiezak-Reding, H., Dzhun, A., Wang, J. & Pasinetti, G.M. 2012, "Paired helical filaments from Alzheimer disease brain induce intracellular accumulation of tau protein in aggresomes.", *Journal of Biological Chemistry,* vol. 287, no. 24, pp. 20522-20533.

Sato, S., Tatebayashi, Y., Akagi, T., Chui, D., Murayama, M., Miyasaka, T., Planel, E., Tanemura, K., Sun, X., Hashikawa, T., Yoshioka, K., Ishiguro, K. & Takashima, A. 2002, "Aberrant tau phosphorylation by glycogen synthase kinase-3beta and JNK3 induces oligomeric tau fibrils in COS-7 cells.", *Journal of Biological Chemistry,* vol. 277, no. 44, pp. 42060-42065.

Scattoni, M.L., Gasparini, L., Alleva, E., Goedert, M., Calamandrei, G. & Spillantini, M.G. 2010, "Early behavioural markers of disease in P301S tau transgenic mice.", *Behavioural brain research,* vol. 208, no. 1, pp. 250-257.

Scheinfeld, N.S. 2017, "Intravenous immunoglobulin", *Medscape,* [Online], .

Schneider, A., Biernat, J., von Bergen, M., Mandelkow, E. & Mandelkow, E.M. 1999, "Phosphorylation that detaches tau protein from microtubules (Ser262, Ser214) also protects it against aggregation into Alzheimer paired helical filaments", *Biochemistry,* vol. 38, no. 12, pp. 3549-3558.

Scott, M., Groth, D., Foster, D., Torchia, M., Yang, S., Dearmond, S.J. & Prusiner, S.B. 1993, "Propagation of prions with artificial properties in transgenic mice expressing chimeric PrP genes", *Cell,* vol. 73, no. 5, pp. 979-988.

Seitz, A., Kojima, H., Oiwa, K., Mandelkow, E.M., Song, Y.H. & Mandelkow, E. 2002, "Single-molecule investigation of the interference between kinesin, tau and MAP2c", *The EMBO journal,* vol. 21, no. 18, pp. 4896-4905.

Selkoe, D.J. 2002, "Alzheimer's disease is a synaptic failure", *Science,* vol. 298, no. 5594, pp. 789-791.

Serrano-Pozo, A., Frosch, M.P., Masliah, E. & Hyman, B.T. 2011, "Neuropathological alterations in Alzheimer disease", *Cold Spring Harbor perspectives in medicine,* vol. 1, no. 1, pp. a006189.

Simon, D., Garcia-Garcia, E., Royo, F., Falcon-Perez, J.M. & Avila, J. 2012, "Proteostasis of tau. Tau overexpression results in its secretion via membrane vesicles", *FEBS letters,* vol. 586, no. 1, pp. 47-54.

Smith, L.M., Coffey, M.P., Klaver, A.C. & Loeffler, D.A. 2013, "Intravenous immunoglobulin products contain specific antibodies to recombinant human tau protein", *International immunopharmacology,* vol. 16, no. 4, pp. 424-428.

Spillantini, M.G., Murrell, J.R., Goedert, M., Farlow, M.R., Klug, A. & Ghetti, B. 1998, "Mutation in the tau gene in familial multiple system tauopathy with presenile dementia", *Proceedings of the National Academy of Sciences of the United States of America,* vol. 95, no. 13, pp. 7737-7741.

Spillantini, M.G., Bird, T.D. & Ghetti, B. 1998, "Frontotemporal dementia and Parkinsonism linked to chromosome 17: A new group of tauopathies.", *Brain Pathology,* vol. 8, no. 2, pp. 387-402.

Spillantini, M.G., Murrell, J.R., Goedert, M., Farlow, M.R., Klug, A. & Ghetti, B. 1998, "Mutation in the tau gene in familial multiple system tauopathy with presenile dementia", *Proceedings of the National Academy of Sciences of the United States of America,* vol. 95, no. 13, pp. 7737-7741.

Spires-Jones, T.L., de Calignon, A., Matsui, T., Zehr, C., Pitstick, R., Wu, H.Y., Osetek, J.D., Jones, P.B., Bacskai, B.J., Feany, M.B., Carlson, G.A., Ashe, K.H., Lewis, J. & Hyman, B.T. 2008, "In vivo imaging reveals dissociation between caspase activation and acute neuronal death in tangle-bearing neurons", *The Journal of neuroscience : the official journal of the Society for Neuroscience,* vol. 28, no. 4, pp. 862-867.

Spires-Jones, T.L. & Hyman, B.T. 2014, "The intersection of amyloid beta and tau at synapses in Alzheimer's disease", *Neuron,* vol. 82, no. 4, pp. 756-771.

Sterniczuk, R., Antle, M.C., Laferla, F.M. & Dyck, R.H. 2010, “Characterization of the 3xTg-AD mouse model of Alzheimer’s disease: part 2. Behavioral and cognitive changes.” *Brain Research,* vol. 1348, pp. 149–55.

Stöhr, J., Watts, J.C., Mensinger, Z.L., Oehler, A., Grillo, S.K., DeArmond, S.J., Prusiner, S.B. & Giles, K. 2012, "Purified and synthetic Alzheimer's amyloid beta prions", *Proceedings of the National Academy of Sciences of the United States of America ,* vol. 109, pp. 11025-11030.

Stohr, J., Wu, H., Nick, M., Wu, Y., Bhate, M., Condello, C., Johnson, N., Rodgers, J., Lemmin, T., Acharya, S., Becker, J., Robinson, K., Kelly, M.J.S., Gai, F., Stubbs, G., Prusiner, S.B. & DeGrado, W.F. 2017, "A 31-residue peptide induces aggregation of tau's microtubule-binding region in cells", *Nature Chemistry, v*ol. 9, no. 9, pp. 874-881.

Sultan, A., Nesslany, F., Violet, M., Begard, S., Loyens, A., Talahari, S., Mansuroglu, Z., Marzin, D., Sergeant, N., Humez, S., Colin, M., Bonnefoy, E., Buee, L. & Galas, M.C. 2011, "Nuclear tau, a key player in neuronal DNA protection", *The Journal of biological chemistry,* vol. 286, no. 6, pp. 4566-4575.

Sydow, A., Van der Jeugd, A., Zheng, F., Ahmed, T., Balschun, D., Petrova, O., Drexler, D., Zhou, L., Rune, G., Mandelkow, E., D’Hooge, R., Alzheimer, C. & Mandelkow, E.M. 2011, “Tau-induced defects in synaptic plasticity, learning, and memory are reversible in transgenic mice after switching off the toxic tau mutant.”, *Journal of Neuroscience,* vol. 31, no. 7, pp. 2511–25.

Tai, H.C., Wang, B.Y., Serrano-Pozo, A., Frosch, M.P., Spires-Jones, T.L. & Hyman, B.T. 2014, "Frequent and symmetric deposition of misfolded tau oligomers within presynaptic and postsynaptic terminals in Alzheimer's disease", *Acta neuropathologica communications,* vol. 2, pp. 146.

Tak, H., Haque, M.M., Kim, M.J., Lee, J.H., Baik, J.H., Kim, Y., Kim, D.J., Grailhe, R. & Kim, Y.K. 2013, "Bimolecular fluorescence complementation; lighting-up tau-tau interaction in living cells.", *PLoS ONE,* vol. 8, no. 12, pp. e81682.

Tanaka, M., Collins, S.R., Toyama, B.H. & Weissman, J.S. 2006, "The physical basis of how prion conformations determine strain phenotypes", *Nature,* vol. 442, no. 7102, pp. 585-589.

Tapiola, T., Alafuzoff, I., Herukka, S., Parkkinen, L., Hartikainen, P., Soininen, H. & Pirttila, T. 2009, "Cerebrospinal fluid -amyloid 42 and tau proteins as biomarkers of Alzheimer-type pathologic changes in the brain.", *Archives of Neurology,* vol. 66, no. 3, pp. 382-389.

Tardivel, M., Begard, S., Bousset, L., Dujardin, S., Coens, A., Melki, R., Buee, L. & Colin, M. 2016, "Tunneling nanotube (TNT)-mediated neuron-to neuron transfer of pathological Tau protein assemblies", *Acta neuropathologica communications,* vol. 4, no. 1, pp. 117.

Thies, E. & Mandelkow, E.M. 2007, "Missorting of tau in neurons causes degeneration of synapses that can be rescued by the kinase MARK2/Par-1", *The Journal of neuroscience : the official journal of the Society for Neuroscience,* vol. 27, no. 11, pp. 2896-2907.

Togo, T., Sahara, N., Yen, S., Cookson, N., Ishizawa, T., Hutton, M., De Silva, R., Lees, A. & Dickson, D.W. 2002, "Argyrophilic grain disease is a sporadic 4-repeat tauopathy.", *Journal of neuropathology and experimental neurology,* vol. 61, no. 6, pp. 547-556.

Tolnay, M. & Clavaguera, F. 2004, "Argyrophilic grain disease: A late-onset dementia with distinctive features among tauopathies.", *Neuropathology,* vol. 24, no. 4, pp. 269-283.

Tolnay, M. & Probst, A. 2002, "Frontotemporal lobar degeneration - Tau as a pied piper?.", *Neurogenetics,* vol. 4, no. 2, pp. 63-75.

Tolnay, M., Sergeant, N., Ghestem, A., Chalbot, S., de Vos, R.A.I., Jansen Steur, E.N.H., Probst, A. & Delacourte, A. 2002, "Argyrophilic grain disease and Alzheimer's disease are distinguished by their different distribution of tau protein isoforms.", *Acta Neuropathologica,* vol. 104, no. 4, pp. 425-434.

Trabzuni, D., Wray, S., Vandrovcova, J., Ramasamy, A., Walker, R., Smith, C., Luk, C., Gibbs, J.R., Dillman, A., Hernandez, D.G., Arepalli, S., Singleton, A.B., Cookson, M.R., Pittman, A.M., De silva, R., Weale, M.E., Hardy, J. & Ryten, M. 2012, "MAPT expression and splicing is differentially regulated by brain region: Relation to genotype and implication for tauopathies.", *Human molecular genetics,* vol. 21, no. 18, pp. 4094-4103.

Umeda, T., Eguchi, H., Kunori, Y., Matsumoto, Y., Taniguchi, T., Mori, H. & Tomiyama, T. 2015, "Passive immunotherapy of tauopathy targeting pSer413-tau: a pilot study in mice", *Annals of clinical and translational neurology,* vol. 2, no. 3, pp. 241-255.

Urrutia, R., Henley, J.R., Cook, T. & McNiven, M.A. 1997, "The dynamins: redundant or distinct functions for an expanding family of related GTPases?", *Proceedings of the National Academy of Sciences of the United States of America,* vol. 94, no. 2, pp. 377-384.

van Dijk, K.D., Bidinosti, M., Weiss, A., Raijmakers, P., Berendse, H.W. & van de Berg, W.D.J. Mar 2014, "Reduced -synuclein levels in cerebrospinal fluid in Parkinson's disease are unrelated to clinical and imaging measures of disease severity.", *European Journal of Neurology,* vol. 21, no. 3, pp. 388-394.

Varghese, M., Santa-Maria, I., Ho, L., Ward, L., Yemul, S., Dubner, L., Księżak-Reding, A. & Pasinetti, G.M. 2016, " Extracellular Tau Paired Helical Filaments Differentially Affect Tau Pathogenic Mechanisms in Mitotic and Post-Mitotic Cells: Implications for Mechanisms of Tau Propagation in the Brain ", *Journal of Alzheimer's Disease,* vol. 54, no. 2, pp. 477.

Vasconcelos, B., Stancu, I.C., Buist, A., Bird, M., Wang, P., Vanoosthuyse, A., Van Kolen, K., Verheyen, A., Kienlen-Campard, P., Octave, J.N., Baatsen, P., Moechars, D. & Dewachter, I. 2016, "Heterotypic seeding of Tau fibrillization by pre-aggregated Abeta provides potent seeds for prion-like seeding and propagation of Tau-pathology in vivo", *Acta Neuropathologica,* vol. 131, no. 4, pp. 549-569.

Vella, L.J., Sharples, R.A., Lawson, V.A., Masters, C.L., Cappai, R. & Hill, A.F. 2007, "Packaging of prions into exosomes is associated with a novel pathway of PrP processing", *Journal of Pathology,* vol. 211, no. 5, pp. 582-590.

Verheyen, A., Diels, A., Dijkmans, J., Oyelami, T., Meneghello, G., Mertens, L., Versweyveld, S., Borgers, M., Buist, A., Peeters, P. & Cik, M. 2015, "Using Human iPSC-Derived Neurons to Model TAU Aggregation", *PloS one,* vol. 10, no. 12, pp. e0146127.

Vogelsberg-Ragaglia, V., Bruce, J., Richter-Landsberg, C., Zhang, B., Hong, M., Trojanowski, J.Q. & Lee, V.M. 2000, "Distinct FTDP-17 missense mutations in tau produce tau aggregates and other pathological phenotypes in transfected CHO cells", *Molecular biology of the cell,* vol. 11, no. 12, pp. 4093-4104.

Volpicelli-Daley, L.A., Luk, K.C., Patel, T.P., Tanik, S.A., Riddle, D.M., Stieber, A., Meaney, D.F., Trojanowski, J.Q. & Lee, V.M. 2011, "Exogenous alpha-synuclein fibrils induce Lewy body pathology leading to synaptic dysfunction and neuron death", *Neuron,* vol. 72, no. 1, pp. 57-71.

von Bergen, M., Friedhoff, P., Biernat, J., Heberle, J., Mandelkow, E.M. & Mandelkow, E. 2000, "Assembly of tau protein into Alzheimer paired helical filaments depends on a local sequence motif ((306)VQIVYK(311)) forming beta structure", *Proceedings of the National Academy of Sciences of the United States of America,* vol. 97, no. 10, pp. 5129-5134.

von Bergen, M., Barghorn, S., Li, L., Marx, A., Biernat, J., Mandelkow, E.M. & Mandelkow, E. 2001, "Mutations of tau protein in frontotemporal dementia promote aggregation of paired helical filaments by enhancing local beta-structure", *Journal of Biological Chemistry,* vol. 276, no. 51, pp. 48165-48174.

Wagner, U., Utton, M., Gallo, J. & Miller, C.C.J. 1996, "Cellular phosphorylation of tau by GSK-3-beta influences tau binding to microtubules and microtubule organisation", *Journal of cell science,* vol. 109, no. 6, pp. 1537-1543.

Walsh D.M. & Selkoe, D.J. 2016, "A critical appraisal of the pathogenic protein spread hypothesis of neurodegeneration.", *Nature Reviews Neuroscience,* vol. 17, no. 4, pp. 251-260.

Wang, Y., Balaji, V., Kaniyappan, S., Kruger, L., Irsen, S., Tepper, K., Chandupatla, R., Maetzler, W., Schneider, A., Mandelkow, E. & Mandelkow, E.M. 2017, "The release and trans-synaptic transmission of Tau via exosomes", *Molecular neurodegeneration,* vol. 12, no. 5.

Wang, Y. & Mandelkow, E. 2012, "Degradation of tau protein by autophagy and proteasomal pathways.", *Biochemical Society transactions,* vol. 40, no. 4, pp. 644-652.

Wang, Y., Martinez-Vicente, M., Kruger, U., Kaushik, S., Wong, E., Mandelkow, E.M., Cuervo, A.M. & Mandelkow, E. 2009, "Tau fragmentation, aggregation and clearance: the dual role of lysosomal processing", *Human molecular genetics,* vol. 18, no. 21, pp. 4153-4170.

Wang, Y.P., Biernat, J., Pickhardt, M., Mandelkow, E. & Mandelkow, E. 2007, "Stepwise proteolysis liberates tau fragments that nucleate the Alzheimer-like aggregation of full-length tau in a neuronal cell model.", *Proceedings of the National Academy of Sciences of the United States of America,* vol. 104, no. 24, pp. 10252-10257.

Weksler, M.E., Relkin, N., Turkenich, R., LaRusse, S., Zhou, L. & Szabo, P. 2002, "Patients with Alzheimer disease have lower levels of serum anti-amyloid peptide antibodies than healthy elderly individuals", *Experimental gerontology,* vol. 37, no. 7, pp. 943-948.

Wilcock, G.K. & Esiri, M.M. 1982, "Plaques, tangles and dementia. A quantitative study.", *Journal of the neurological sciences,* vol. 56, no. 2-3, pp. 343-356.

Wille, H., Drewes, G., Biernat, J., Mandelkow, E.M. & Mandelkow, E. 1992, "Alzheimer-like paired helical filaments and anitparallel dimers formed from microtubule-associated protein tau in vitro", *Journal of Cell Biology,* vol. 118, no. 3, pp. 573-584.

Witman, G.B., Cleveland, D.W., Weingarten, M.D. & Kirschner, M.W. 1976, "Tubulin requires tau for growth into microtubule initiating sites.", *Proceedings of the National Academy of Sciences of the United States of America,* vol. 73, no. 11, pp. 4070-4074.

Wood, S.J., Wypych, J., Steavenson, S., Louis, J.C., Citron, M. & Biere, A.L. 1999, "alpha-synuclein fibrillogenesis is nucleation-dependent. Implications for the pathogenesis of Parkinson's disease", *The Journal of biological chemistry,* vol. 274, no. 28, pp. 19509-19512.

Wu, J.W., Hussaini, S.A., Bastille, I.M., Rodriguez, G.A., Mrejeru, A., Rilett, K., Sanders, D.W., Cook, C., Fu, H., Boonen, R.A., Herman, M., Nahmani, E., Emrani, S., Figueroa, Y.H., Diamond, M.I., Clelland, C.L., Wray, S. & Duff, K.E. 2016, "Neuronal activity enhances tau propagation and tau pathology in vivo", *Nature neuroscience,* vol. 19, no. 8, pp. 1085-1092.

Wu, J.W., Herman, M., Liu, L., Simoes, S., Acker, C.M., Figueroa, H., Steinberg, J.I., Margittai, M., Kayed, R., Zurzolo, C., Di Paolo, G. & Duff, K.E. 2013, "Small Misfolded Tau Species Are Internalized via Bulk Endocytosis and Anterogradely and Retrogradely Transported in Neurons", *Journal of Biological Chemistry,* vol. 288, no. 3, pp. 1856-1870.

Yamada, K., Cirrito, J.R., Stewart, F.R., Jiang, H., Finn, M.B., Holmes, B.B., Binder, L.I., Mandelkow, E.M., Diamond, M.I., Lee, V.M. & Holtzman, D.M. 2011, "In vivo microdialysis reveals age-dependent decrease of brain interstitial fluid tau levels in P301S human tau transgenic mice.", *Journal of Neuroscience,* vol. 31, no. 37, pp. 13110-13117.

Yamada, K., Holth, J.K., Liao, F., Stewart, F.R., Mahan, T.E., Jiang, H., Cirrito, J.R., Patel, T.K., Hochgrafe, K., Mandelkow, E.M. & Holtzman, D.M. 2014, "Neuronal activity regulates extracellular tau in vivo.", *Journal of Experimental Medicine,* vol. 211, no. 3, pp. 387-393.

Yamada, T., McGeer, P.L. & McGeer, E.G. 1992, "Appearance of paired nucleated, Tau-positive glia in patients with progressive supranuclear palsy brain tissue.", *Neuroscience letters,* vol. 135, no. 1, pp. 99-102.

Yan, M.H., Wang, X. & Zhu, X. 2013, "Mitochondrial defects and oxidative stress in Alzheimer disease and Parkinson disease", *Free radical biology & medicine,* vol. 62, pp. 90-101.

Yanamandra, K., Kfoury, N., Jiang, H., Mahan, T.E., Ma, S., Maloney, S.E., Wozniak, D.F., Diamond, M.I. & Holtzman, D.M. 2013a, "Anti-tau antibodies that block tau aggregate seeding in vitro markedly decrease pathology and improve cognition in vivo", *Neuron,* vol. 80, pp. 402-414.

Yanamandra, K., Kfoury, N., Jiang, H., Mahan, T.E., Ma, S., Maloney, S.E., Wozniak, D.F., Diamond, M.I. & Holtzman, D.M. 2013b, "Anti-tau antibodies that block tau aggregate seeding invitro markedly decrease pathology and improve cognition in vivo.", *Neuron,* vol. 80, no. 2, pp. 402-414.

Yang, W., Dunlap, J.R., Andrews, R.B. & Wetzel, R. 2002, "Aggregated polyglutamine peptides delivered to nuclei are toxic to mammalian cells", *Human molecular genetics,* vol. 11, no. 23, pp. 2905-2917.

Yerbury, J.J. 2016, "Protein aggregates stimulate macropinocytosis facilitating their propagation", *Prion,* vol. 10, no. 2, pp. 119-126.

Yoshida, M. & Goedert, M. 2006, “Sequential phosphorylation of tau protein by cAMP-dependent protein kinase and SAPK4/p38δ or JNK2 in the presence of heparin generates the AT100 epitope”, *Journal of Neurochemistry*, vol. 99, no. 1, pp. 165-164.

Yoshiyama, Y., Higuchi, M., Zhang, B., Huang, S.M., Iwata, N., Saido, T.C., Maeda, J., Suhara, T., Trojanowski, J.Q. & Lee, V.M. 2007, “Synapse loss and microglial activation precede tangles in a P301S tauopathy mouse model”, *Neuron,* vol. 53, no. 3, pp. 337–51.

Zeineddine, R., Pundavela, J.F., Corcoran, L., Stewart, E.M., Do-Ha, D., Bax, M., Guillemin, G., Vine, K.L., Hatters, D.M., Ecroyd, H., Dobson, C.M., Turner, B.J., Ooi, L., Wilson, M.R., Cashman, N.R. & Yerbury, J.J. 2015, "SOD1 protein aggregates stimulate macropinocytosis in neurons to facilitate their propagation", *Molecular neurodegeneration,* vol. 10, no. 57.

Zempel, H., Luedtke, J., Kumar, Y., Biernat, J., Dawson, H., Mandelkow, E. & Mandelkow, E.M. 2013, "Amyloid-beta oligomers induce synaptic damage via Tau-dependent microtubule severing by TTLL6 and spastin ", *The EMBO journal,* vol. 32, no. 22, pp. 2920-2937.

Zhang, Z., Song, M., Liu, X., Kang, S.S., Kwon, I.S., Duong, D.M., Seyfried, N.T., Hu, W.T., Liu, Z., Wang, J.Z., Cheng, L., Sun, Y.E., Yu, S.P., Levey, A.I. & Ye, K. 2014, "Cleavage of tau by asparagine endopeptidase mediates the neurofibrillary pathology in Alzheimer's disease.", *Nature medicine,* vol. 20, no. 11, pp. 1254-1262.

Zhang, B., Higuchi, M., Yoshiyama, Y., Ishihara, T., Forman, M.S., Martinez, D., Joyce, S., Trojanowski, J.Q. & Lee, V.M. 2004, “Retarded axonal transport of R406W mutant tau in transgenic mice with a neurodegenerative tauopathy”, *Journal of Neuroscience*, vol. 24, no. 19, pp. 4657–67.

Zhong, Q., Congdon, E.E., Nagaraja, H.N. & Kuret, J. 2012, "Tau isoform composition influences rate and extent of filament formation.", *Journal of Biological Chemistry,* vol. 287, no. 24, pp. 20711-20719.

Zhou, L., McInnes, J., Wierda, K., Holt, M., Herrmann, A.G., Jackson, R.J., Wang, Y.C., Swerts, J., Beyens, J., Miskiewicz, K., Vilain, S., Dewachter, I., Moechars, D., De Strooper, B., Spires-Jones, T.L., De Wit, J. & Verstreken, P. 2017, "Tau association with synaptic vesicles causes presynaptic dysfunction", *Nature communications,* vol. 8, pp. 15295.